A genomics-based discovery pipeline for *Pseudomonas* derived antifungals effective against the wheat pathogen *Zymoseptoria tritici*

George Lund BSc (Hons)

Thesis submitted to the University of Nottingham for the degree of Doctor of Philosophy

June 2021

Rothamsted Research

Harpenden

Hertfordshire

UK

Acknowledgements

Firstly, I would like to thank my supervisors Jason Rudd, Tim Mauchline, and Matt Dickinson for their advice, encouragement, and the interesting discussions throughout this project. This project has been a lot of fun!

I would like to thank past and present colleagues in the Microbial Molecular Ecology Group, and Wheat Pathogenomics Team, for their advice and making the lab an amusing place to work!

I would like to thank Marnix Medema, and the members of the Bioinformatics Department at Wageningen University, for their hospitality during my placement. Dankjewel!

I would also like to thank the Nottingham BBSRC DTP and Lawes Agricultural Trust for the funding to conduct this project.

I'm grateful to Gareth Thomas, for the rigorous scientific discussions on the regular walks to Sainsbury's. I'm thankful for the support from friends, namely Ajit, Kevin, and Emily.

I would particularly like to thank Carolina Alves, for her constant support. Foram o teu amor e compreensão que me guiaram nos momentos mais difíceis. Obrigado por me incentivares e por acreditares em mim.

Finally, I would like to thank my family, particularly my Mum, Dad and my brother Frank, for their encouragement throughout.

Abstract

Zymoseptoria tritici, the causal agent of Septoria tritici blotch, is an economically important foliar fungal pathogen of wheat. Resistance to all known classes of fungicides has arisen over the last 30 years, and new chemical control strategies are urgently needed. Environmental bacterial isolates are a potential untapped source of naturally derived novel antifungal compounds effective against *Z. tritici*. *Pseudomonas* bacteria have shown great promise as a source of novel antifungal secondary metabolites, with a proven ability to antagonise many fungal plant pathogens both in *in vitro* and *in planta* settings.

A high throughput screening methodology using the blastospore growth form of *Z. tritici* was used to screen a wheat-associated *Pseudomonas* collection containing 534 isolates. In total, 52 isolates were found to exhibit an antagonistic phenotype *in vitro*.

A subset of 88 *Pseudomonas* isolates from the initial 534 isolates (17 antagonistic and 71 non-antagonistic) were genome sequenced and phylogenetically assigned to three *Pseudomonas* species groupings, namely *P. koreensis*, *P. lurida* and *P. fluorescens,* with each group possessing both antagonistic and non-antagonistic isolates. Furthermore, statistically significant differences in the mean sizes of zones of inhibition produced by antagonistic *Pseudomonas* isolates were found between genetically diverse *Z. tritici* isolates.

Significant diversity in predicted secondary metabolite biosynthetic gene clusters (BGCs) was found from the genome assemblies of the *Pseudomonas* isolates. BGCs of the known antifungal compound 2,4-diacetylphloroglucinol (2,4-DAPG) was predicted from genome assemblies of 6 antagonistic *Pseudomonas* isolates, whilst 11 antagonistic *Pseudomonas* isolates were found to have no significant hit with known antifungal BGCs. 2,4-DAPG was found to be present in agar extracts of zones of inhibition produced by *Pseudomonas* isolate Roth 112 in the *Z. tritici* blastospore confrontation assay. An authentic chemical standard of 2,4-DAPG was also used to confirm antifungal activity against *Z. tritici* blastospores *in vitro*.

Transcriptomic responses of predicted BGCs to confrontation with *Z. tritici* blastospores were found for both antagonistic and non-antagonistic *Pseudomonas* isolates. The highly significant (Padj < 0.01) upregulation of a currently unknown gene cluster was observed by antagonistic *Pseudomonas* isolate Roth 16, potentially encoding a yet uncharacterised siderophore.

The findings of this study contribute to the understanding of *Pseudomonas*-*Zymoseptoria* interactions, and the potential of bio-prospecting to identify novel bacterial secondary metabolites implicated in fungal antagonism, which could ultimately lead to future crop protection products. More broadly, these combined approaches could be utilised to identify bacterial secondary metabolites with other functions.

Table of Contents

Acknowledgements ii

Abstract iii

List of Abbreviations xiii

List of Figures xv

List of Tables xviii

List of Supplementary Figures xviii

List of Supplementary Tables xix

Chapter 1. General Introduction 1

1.1. Overarching introduction 1

1.1.1. Global population rising 1

1.1.2. Wheat is a globally important food crop 1

1.1.3. Increases in wheat yield are insufficient, as there is also a need to reduce losses due to pests and pathogens 2

1.1.4. Fungal Diseases of Wheat 3

1.1.5. Control of fungal plant pathogens and problems with Fungicide resistance 3

1.1.6. Life cycle of *Z. tritici* 4

1.1.7. Control of *Zymoseptoria tritici* and the evolution of fungicide resistance 7

1.1.8. Bacteria as a potential source of new solutions for *Z. tritici* control 8

1.1.9. The genus *Pseudomonas* 9

1.1.10. Bacterially mediated antifungal secreted secondary metabolites . 11

1.1.11. Non-ribosomal peptide synthetases (NRPSs). 11

1.1.12. Polyketide Synthases (PKS) 11

1.1.13. Post-Ribosomal Peptide Synthesis (PRPS) 11

1.1.14. The genomics age of natural product discovery 13

1.1.15. Predictive Bioinformatics 13
1.2. Aims of this Project 14

Chapter 2. Development of a high throughput *in vitro* assay for the identification of *Pseudomonas* isolates with the ability to antagonise *Z. tritici* 16

2.1. Introduction 16

2.2. Chapter specific Methods 18

2.2.1. *Pseudomonas* isolate collection 18
2.2.2. Culturing of *Z. tritici* blastospores 18
2.2.3. Culturing of *Pseudomonas* isolates 19
2.2.4. Storage of isolates 19
2.2.5. High throughput *in vitro* screen for fungal antagonism of *Z. tritici* by *Pseudomonas* isolates 19
2.2.6. Hyphal inhibition assays 20
2.2.7. Preparation of bacterial cells for *in planta* disease assessment 20
2.2.8. Preparation of *Z. tritici* spores for *in planta* disease assessment 20
2.2.9. *In planta* assessment of *Pseudomonas* biocontrol potential 20
2.2.10. Quantification of *Z. tritici* pycnidiospore formation 21
2.2.11. Statistical analyses 21
2.3. Results 22

2.3.1. Development of a high throughput *in vitro* assay to qualitatively identify *Pseudomonas* isolates exhibiting an antagonistic phenotype against *Z. tritici in vitro*. 22
2.3.2. Assessment of *Z. tritici* blastospore antagonism by *Pseudomonas* isolates derived from rhizosphere and endosphere samples 23
2.3.3. Inhibition of *Z. tritici* hyphae by *Pseudomonas* isolates 24
2.3.4. *In planta* assessment of the biocontrol potential of *Pseudomonas* isolates against *Z. tritici* 27
2.3.5. Assessment of *Pseudomonas* inoculation on *Z. tritici* pycnidia formation and pycnidiospore production *in planta* 30
2.4. Discussion 33

2.4.1. *Z. tritici* blastospores can be utilised in a qualitative high throughput assay for fungal antagonism by *Pseudomonas* isolates.....34
2.4.2. No statistically significant association between *Pseudomonas* isolation niche and *in vitro Z. tritici* blastospore antagonism phenotype....36
2.4.3. Both antagonistic and non-antagonistic *Pseudomonas* isolates from the blastospore assay antagonise hyphal formation of *Z. tritici*.....37
2.4.4. Inoculation of wheat leaves with *Z. tritici* antagonistic *Pseudomonas* isolates did not affect disease severity.....39
2.4.5. Inoculation of wheat leaves with *Pseudomonas* isolates before subsequent infection with *Z. tritici* did not alter pycnidia formation or pycnidiospore production 41
2.5. Conclusions.....42

Chapter 3. Quality assessment and phylogenetic analysis of generated *Pseudomonas* genome assemblies.....43

3.1. Introduction.....43

3.2. Chapter specific methods 45

3.2.1. DNA extraction 45
3.2.2. DNA quantification.....45
3.2.3. DNA sequencing and genome assembly construction 45
3.2.4. BUSCO (Benchmarking Universal Single-Copy Orthologs) analysis 46
3.2.5. Phylogenetic tree construction 46
3.2.6. Construction of Sankey diagram 46
3.3. Results 47

3.3.1. Initial quality control assessment of environmental *Pseudomonas* genome assemblies 47
3.3.2. Assessment of the phylogenetic distribution of *Pseudomonas* isolates 51
3.4. Discussion 54

3.4.1. Contamination of genome assemblies detected using BUSCO....54

3.4.2. *G*enome assemblies generated through 250bp Illumina MiSeq are sufficient to compare bacterial phylogenies 55
3.4.3. *Zymoseptoria tritici* blastospore antagonistic *Pseudomonas* isolates are distributed throughout the *P. fluorescens*, *P. lurida* and *P. koreensis* subclades of a phylogeny 56
3.5. Conclusions 58
Chapter 4. Predictive Bioinformatics and chemical analysis of *Pseudomonas* secondary metabolism 59
4.1. Introduction 59
4.2. Chapter specific methods 60
4.2.1. Secondary Metabolite Biosynthetic Gene Cluster Prediction 60
4.2.2. Sequence similarity network analysis of predicted Secondary Metabolite Gene Clusters 61
4.2.3. Chemical analysis of secreted secondary metabolites produced by *Pseudomonas* isolates 61
4.2.4. Microscopic and macroscopic analysis of the effect of 2,4-DAPG on *Z. tritici* blastospore growth *in vitro* 63
4.3. Results 63
4.3.1. Prediction of secondary metabolite biosynthetic gene clusters from *Pseudomonas* genome sequences 63
4.3.2. Network analysis of predicted secondary metabolite biosynthetic gene clusters 64
4.3.3. Assessment of the predicted secondary metabolite biosynthetic gene cluster diversity within a *Pseudomonas* phylogeny 65
4.3.4. Assessment of secondary metabolite GCFs associated with *Z. tritici* blastospore antagonism phenotype in *Pseudomonas* isolates 74
4.3.5. Identification of known secondary metabolite biosynthetic gene clusters through BiGSCAPE 75
4.3.6. Chemical analysis of agar extracts in *Pseudomonas* confrontation with *Z. tritici* blastospores *in vitro* 78

4.3.7. Preliminary assessment of susceptibility of *Z. tritici* blastospores to antagonism by 2,4-DAPG *in vitro* 79
4.4. Discussion 81
4.4.1. Similarities in the number of predicted secondary metabolite BGCs from antagonistic and non-antagonistic *Pseudomonas* isolates 81
4.4.2. Predicted BGCs are correlated with a *Z. tritici* blastospore antagonistic phenotype in *Pseudomonas* isolates 82
4.4.3. Identification of phylogenetic relationships with secondary metabolite BGCs prediction 85
4.4.4. Identification of predicted secondary metabolite BGCs with high sequence similarity to known antifungal secondary metabolite BGCs 85
4.4.5. *Z. tritici* blastospore antagonism by *Pseudomonas* isolates cannot be explained through the identification of known antifungal BGCs within genome assemblies 89
4.4.6. Identification of 2,4-DAPG in agar extracts of *Z. tritici* blastospore antagonistic *Pseudomonas* isolate Roth112 90
4.4.7. Confirmation of antifungal activity of 2,4-DAPG against *Z. tritici* blastospore growth *in vitro* 90
4.5. Conclusions 91
Chapter 5. Variation in susceptibility of *Z. tritici* isolates to antagonism by *Pseudomonas* bacteria 93
5.1. Introduction 93
5.2. Chapter specific methods 94
5.2.1. Culturing of *Z. tritici* blastospores 94
5.2.2. Culturing of *Pseudomonas* isolates 94
5.2.3. Storage of isolates 95
5.2.4. *In vitro* screen for fungal antagonism of *Z. tritici* by *Pseudomonas* isolates 95
5.2.5. Quantification of zones of inhibition 95
5.2.6. Statistical analysis 96

5.3 Results 96

5.3.1. Significant variation exists in the *in vitro* sensitivity of genetically diverse *Z. tritici* isolates to antagonism by *Pseudomonas* isolates 96

5.4. Discussion 108

5.4.1. Quantitative assessment of *in vitro Z. tritici* blastospore antagonism by *Pseudomonas* isolates 109

5.4.2. Variation in the *in vitro* sensitivity of *Z. tritici* isolates to antagonistic pseudomonads 110

5.4.3. Implications for the development of bio-fungicides 111

5.5. Conclusions 112

Chapter 6. Transcriptomics of predicted secondary metabolite biosynthetic gene clusters of antagonistic and non-antagonistic *Pseudomonas* isolates 113

6.1. Introduction 113

6.2. Chapter specific methods 115

6.2.1. Storage of isolates 115

6.2.2. Preparation of *Z. tritici* blastospores for confrontation with *Pseudomonas* isolates in liquid culture 115

6.2.3. Preparation of *Pseudomonas* cells for confrontation with *Z. tritici* blastospores in liquid culture 115

6.2.4. Confrontation of *Pseudomonas* cells with *Z. tritici* blastospores in liquid culture 116

6.2.5. RNA extraction 117

6.2.6. RNA quality assessment 117

6.2.7. RNA sequencing 118

6.2.8. Processing of sequencing reads for downstream analysis 118

6.2.9. Principal component analysis 119

6.2.10. Differential gene expression analysis 119

6.2.11. BGC Prediction and amino acid alignments 119

6.3. Results 120

6.3.1. Principal component analysis reveals transcriptomic changes in both pseudomonads isolates tested as a consequence of confrontation with *Z. tritici*. 120
6.3.2. Validation of expression for predicted gene models of *Pseudomonas* isolates Roth16 and Roth105 122
6.3.3. Amino acid alignments reveal common and unique predicted BGCs from *Pseudomonas* isolates Roth 16 and Roth 105 122
6.3.4. Differential expression analysis reveals significant changes for genes within predicted secondary metabolite BGCs 123
6.3.5. Upregulation of a unique predicted BGC of unknown function by antagonistic *Pseudomonas* isolate Roth 16 in confrontation with *Z. tritici* 125
6.3.6. Concordant and discordant responses in BGC expression between antagonistic and non-antagonistic *Pseudomonas* isolates in confrontation with *Z. tritici* blastospores 126
6.4. Discussion 132
6.4.1. Common genes within predicted secondary metabolite BGCs from antagonistic and non-antagonistic *Pseudomonas* isolates undergo concordant and discordant regulatory changes in response to confrontation with *Z. tritici* blastospores in liquid culture 133
6.4.2. A unique BGC encoding an unknown secondary metabolite is significantly upregulated in response to *Z. tritici* confrontation by antagonistic *Pseudomonas* isolate Roth 16 135
6.5. Conclusions 138
Chapter 7. General Discussion 140
7.1. The future challenges faced by fungicide resistant pathogens to agriculture 141
7.2. The selection of *Zymoseptoria tritici* as the initial target for the discovery pipeline 141
7.3. Bacteria as an underexploited source of novel fungicides? 143

7.4. How to identify novel natural products with potential antifungal activities? 144
7.5. The search for microbial natural products versus biological control agents 145
7.6. Applications of natural product discovery pipelines beyond this study . 150
Bibliography 153
Appendix 177
Supplementary Figures 177
Supplementary Tables 179

List of Abbreviations

2,4-DAPG	2,4-diacetylphloroglucinol
ANOVA	Analysis of Variance
antiSMASH	antibiotics and secondary metabolite analysis shell
BGC	Biosynthetic Gene Cluster
BiG-SCAPE	Biosynthetic gene similarity clustering and prospecting engine
BUSCO	Benchmarking Universal Single Copy Orthologs
c.v.	Cultivar
DNA	Deoxyribonucleic acid
GCF	Gene Cluster Family
GWAS	Genome Wide Association Study
HCN	Hydrogen Cyanide
HMM	Hidden Markov Model
kDA	Kilodalton
LC-MS	Liquid chromatography–mass spectrometry
MBC	Methyl benzimidazole carbamate
MiBIG	Minimum Information about a Biosynthetic Gene cluster
mRNA	messenger Ribonucleic Acid
NCBI	National Center for Biotechnology Information

NGS	Next Generation Sequencing
nm	nanometre
NRP	Non-ribosomal peptide
NRPS	Non-ribosomal
OD	Optical Density
PCR	Polymerase Chain Reaction
PDA	Potato Dextrose Agar
PDB	Potato Dextrose Broth
PKS	Polyketide synthase
PRPS	Post-Ribosomal Peptide Synthesis
QOI	Quinone Outside Inhibitors
RiPPs	Ribosomally synthesized and post-translationally modified peptides
RNA	Ribonucleic acid
s.e.d.	standard error of the difference
SDHI	Succinate Dehydrogenase Inhibitors
spp.	several species
STB	Septoria Tritici Blotch
UPLC	Ultra Performance Liquid Chromatography

List of Figures

Figure 1.1 Production share of wheat by world region. 2

Figure 2.1 High throughput *in vitro* assay for *Z. tritici* blastospore antagonism. . 23

Figure 2.2 Hyphal *Z. tritici in vitro* antagonism assay. 26

Figure 2.3 *In planta* assessment of biocontrol capability of *Pseudomonas* isolates. 29

Figure 2.4 Assessment of *Z. tritici* pycnidia formation. 32

Figure 2.5 Pycnidiospores recovered from wheat leaves infected with *Z. tritici* after inoculation with *Pseudomonas* isolates. 33

Figure 3.1. Overview of genome assembly quality control process. 49

Figure 3.2. Status of 124 single copy orthologous genes within 129 *Pseudomonas* genome assemblies assessed by BUSCO. 50

Figure 3.3 Phylogenetic distribution of *Z. tritici* blastospore antagonistic and non-antagonistic *Pseudomonas* isolates. 53

Figure 4.1 Predictive bioinformatics network analysis of secondary metabolite biosynthetic gene clusters. 65

Figure 4.2 Distribution of predicted secondary metabolite BGCs forming (RiPP) class Gene Cluster Families, for 17 *Z. tritici* blastospore antagonistic and 71 non-antagonistic *Pseudomonas* isolates, within a phylogeny. 70

Figure 4.3 Distribution of predicted secondary metabolite BGCs forming (NRPS) class Gene Cluster Families, for 17 *Z. tritici* blastospore antagonistic and 71 non-antagonistic *Pseudomonas* isolates, within a phylogeny. 71

Figure 4.4 Distribution of predicted secondary metabolite BGCs forming 'Other' class Gene Cluster Families, for 17 *Z. tritici* blastospore antagonistic and 71 non-antagonistic *Pseudomonas* isolates, within a phylogeny. 72

Figure 4.5 Distribution of predicted secondary metabolite BGCs forming PKS Other (PKSOther), PKS Type 1 (PKS1), Terpene, and Saccharide class Gene Cluster Families, for 17 *Z. tritici* blastospore antagonistic and 71 non-antagonistic *Pseudomonas* isolates, within a phylogeny. 73

Figure 4.6 Chemical analysis of agar extracts of antagonistic *Pseudomonas* isolate Roth112. 79

Figure 4.7 Microscopic and macroscopic changes in the growth of *Z. tritici* blastospores *in vitro*, in response to 2,4-DAPG. 80

Figure 5.1 A phylogeny of *Z. tritici* isolates from across Europe. 101

Figure 5.2 *In vitro* fungal antagonism assays involving bacterial species. 102

Figure 5.3 Inhibition of *Z. tritici* blastospores by *Pseudomonas* isolates *in vitro*. 103

Figure 5.4 Zones of inhibition produced by *Pseudomonas* isolate BFR20 in confrontation with genetically diverse *Z. tritici* blastospores *in vitro*. 104

Figure 5.5 Zones of inhibition produced by *Pseudomonas* isolate BFB20 in confrontation with genetically diverse *Z. tritici* blastospores *in vitro*. 105

Figure 5.6 Zones of inhibition produced by *Pseudomonas* isolate Roth 82 in confrontation with genetically diverse *Z. tritici* blastospores *in vitro*. 106

Figure 5.7 Zones of inhibition produced by *Pseudomonas* isolate Roth 107 in confrontation with genetically diverse *Z. tritici* blastospores *in vitro*. 107

Figure 5.8 Zones of inhibition produced by *Pseudomonas* isolate Roth 112 in confrontation with genetically diverse *Z. tritici* blastospores *in vitro*. 108

Figure 6.1 Principal components analysis of RNA reads for *Pseudomonas* isolates in confrontation with *Z. tritici* blastospores. 121

Figure 6.2 Amino acid alignments of *Pseudomonas* predicted secondary metabolite biosynthetic gene clusters. 127

Figure 6.3 Volcano plots indicating differentially expressed predicted secondary metabolite genes from *Pseudomonas* isolates in confrontation with *Z. tritici*. ... 128

Figure 6.4 A heatmap indicating expression of predicted secondary metabolite core biosynthesis genes for *Pseudomonas* isolate Roth 16 in confrontation with *Z. tritici* blastospores. 129

Figure 6.5 A heatmap indicating expression of predicted secondary metabolite core biosynthesis genes for *Pseudomonas* isolate Roth 105 in confrontation with *Z. tritici* blastospores. 130

Figure 6.6 Amino acid alignments of *Pseudomonas* predicted secondary metabolite biosynthetic gene clusters annotated with differential expression data. 131

Figure 7.1 An overview of the bio-prospecting pipeline for naturally derived antifungal compounds generated by this project. 152

List of Tables

Table 2.1 The antagonism phenotype of *Pseudomonas* isolates screened against both the hyphal and blastospore growth forms of *Z. tritici in vitro* (1 indicates observed antagonism, 0 indicates no observed antagonism). 27

Table 2.2 *Z. tritici* blastospore antagonism data (1 indicates antagonism observed, 0 indicates no antagonism observed) for *Pseudomonas* isolates screened in the *in planta* assessment of biocontrol potential. 30

Table 4.1 GCF networks containing predicted BGCs solely derived from *Pseudomonas* isolates exhibiting *Z. tritici* blastospore antagonism *in vitro*. 75

Table 4.2 GCFs containing reference secondary metabolite BGC sequences from MiBIG. 77

Table 5.1 A list of *Pseudomonas* isolates screened for antagonism in confrontation with genetically diverse *Z. tritici* isolates within this study, with previously described antagonism phenotype (Chapter 2) indicated. 102

List of Supplementary Figures

Supplementary Figure 1. Assessment to determine the viability of *Pseudomonas* inoculum prepared as described in Methods. 177

Supplementary Figure 2. Images of control plates of the hyphal *Z. tritici in vitro* antagonism assay. 178

List of Supplementary Tables

Supplementary Table 1. Inhibition data (1 or a 0) for environmental bacterial isolates that were screened using the *in vitro Z. tritici* blastospore assay, alongside the field conditions and niche from which they were isolated. 179

Supplementary Table 2. One-way Analysis of Variance of recovered pycnidiospore count data after treatment with *Pseudomonas* inoculum. 201

Supplementary Table 3. Genome assembly information, taxonomic prediction, gyrB copy status, and BUSCO scores of 129 bacterial isolates. 202

Supplementary Table 4. One-way Analysis of Variance of the radius of zones of inhibition produced by *Pseudomonas* isolate BFR20 in confrontation with genetically diverse *Z. tritici* isolates in the blastospore antagonism assay *in vitro*. 210

Supplementary Table 5. Tukey's test for multiple comparisons at the 5% level of significance, comparing zones of inhibition produced by *Pseudomonas* isolate BFR20 in confrontation with different *Z. tritici* genotypes *in vitro*. 210

Supplementary Table 6. One-way Analysis of Variance of the radius of zones of inhibition produced by *Pseudomonas* isolate BFB20 in confrontation with genetically diverse *Z. tritici* isolates in the blastospore antagonism assay *in vitro*. 212

Supplementary Table 7. Tukey's test for multiple comparisons at the 5% level of significance, comparing zones of inhibition produced by *Pseudomonas* isolate BFB20 in confrontation with different *Z. tritici* genotypes *in vitro*. 212

Supplementary Table 8. One-way Analysis of Variance of the radius of zones of inhibition produced by *Pseudomonas* isolate Roth 82 in confrontation with genetically diverse *Z. tritici* isolates in the blastospore antagonism assay *in vitro*. 214

Supplementary Table 9. Tukey's test for multiple comparisons at the 5% level of significance, comparing zones of inhibition produced by *Pseudomonas* isolate Roth 82 in confrontation with different *Z. tritici* genotypes *in vitro*. 214

Supplementary Table 10. One-way Analysis of Variance of the radius of zones of inhibition produced by *Pseudomonas* isolate Roth 107 in confrontation with genetically diverse *Z. tritici* isolates in the blastospore antagonism assay *in vitro*. 216

Supplementary Table 11. Tukey's test for multiple comparisons at the 5% level of significance, comparing zones of inhibition produced by *Pseudomonas* isolate Roth 107 in confrontation with different *Z. tritici* genotypes *in vitro*. 216

Supplementary Table 12. One-way Analysis of Variance of the radius of zones of inhibition produced by *Pseudomonas* isolate Roth 112 in confrontation with genetically diverse *Z. tritici* isolates in the blastospore antagonism assay *in vitro*. 218

Supplementary Table 13. Tukey's test for multiple comparisons at the 5% level of significance, comparing zones of inhibition produced by *Pseudomonas* isolate Roth 112 in confrontation with different *Z. tritici* genotypes *in vitro*. 219

Supplementary Table 14. Sequencing depth of coverage. 221

Supplementary Table 15. A table indicating the log2fold change and Benjamini-Hochberg adjusted p-values from differential expression analysis for genes within Roth 16 predicted secondary metabolite BGCs. 222

Supplementary Table 16. A table indicating the log2fold change and Benjamini-Hochberg adjusted p-values from differential expression analysis for genes within Roth 105 predicted secondary metabolite BGCs. 233

Supplementary Table 17. A table indicating the log2fold change and Benjamini-Hochberg adjusted p-values from differential expression analysis for core biosynthetic genes within Roth 16 predicted secondary metabolite BGCs. 241

Supplementary Table 18. A table indicating the log2fold change and Benjamini-Hochberg adjusted p-values from differential expression analysis for core biosynthetic genes within Roth 105 predicted secondary metabolite BGCs. 243

Chapter 1. General Introduction

1.1. Overarching introduction

This review examines the importance of the plant pathogenic fungus *Zymoseptoria tritici* in agricultural systems and discusses methods that are available for its control. This project is concerned *Pseudomonas fluorescens* derived control of *Z. tritici*. I will be studying the mode of action for the suppression of *Z. tritici* and will utilise a combination of *in vitro*, *in planta* as well as bioinformatic approaches including genomics as well as transcriptomics.

1.1.1. Global population rising

The global human population is predicted to grow to around 8.5 billion by 2030, and 9.7 billion by 2050, from around 7.7 billion in mid-2019 (United Nations Department of Economic and Social Affairs Population Division, 2019). A major challenge facing humanity is how agricultural systems will be able to rapidly increase food production, in line with increasing demand from the rising population.

1.1.2. Wheat is a globally important food crop

Wheat is an important staple crop within global food production systems. It is the most widely cultivated cereal in the world, with more than 220 million hectares planted annually (Shiferaw et al., 2013) and the consumption of wheat accounts for around 20% of total calories consumed globally (Trnka et al., 2019).

The global production of wheat is mainly distributed throughout temperate climates, with Asia and Europe producing the majority of wheat worldwide (Figure 1.1). Within Europe, France and Germany are the biggest wheat producers, harvesting around 26% and 17% of the total respectively, with the UK producing around 8.5% (Fones and Gurr, 2015).The future required production of wheat to satisfy a larger global population is difficult to accurately predict, with studies

indicating that an increase of approximately 25%–70% above current production levels could be required to meet 2050 wheat demand (Hunter et al., 2017).

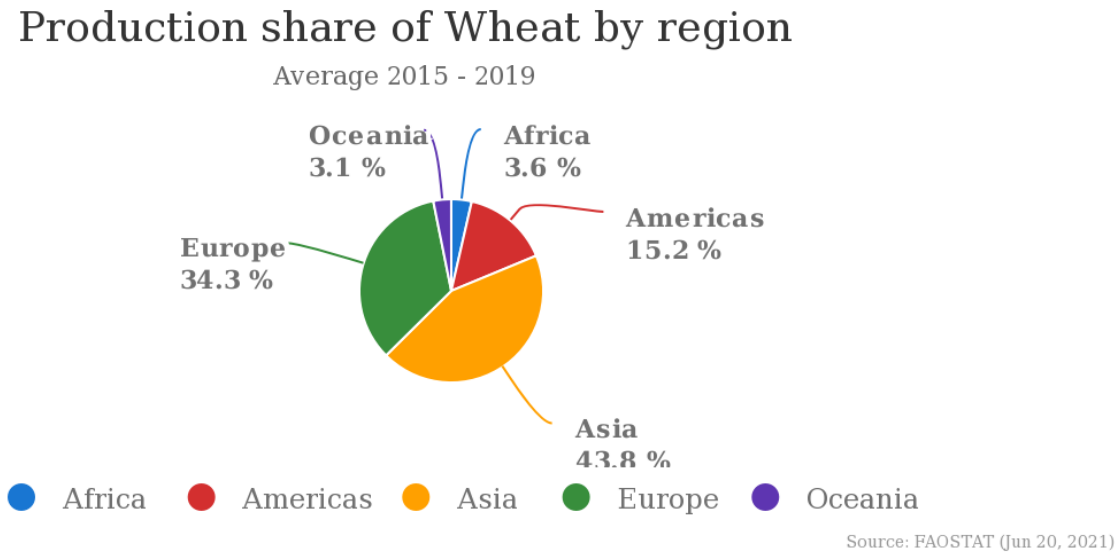


Figure 1.1 Production share of wheat by world region.
The average share of wheat production for regions between 2015 and 2019 (http://www.fao.org/faostat/en/#data/QC/visualize).

1.1.3. Increases in wheat yield are insufficient, as there is also a need to reduce losses due to pests and pathogens

Increases in wheat yield, through means such as genetics and conventional breeding, have traditionally been responsible for agricultural yield gains, though these have stagnated in recent years (Schauberger et al., 2018). However, wheat yields can also be enhanced by reducing crop losses. For example, mitigation or reduction of the effects of abiotic and biotic stresses to crops is an alternative strategy to reduce yield losses. Fungal pathogens are a major contributor to the wheat 'yield gap', the difference between the potential yield of crops and the actual yield harvested, with current estimates suggesting wheat yield losses of around 21.5% exist due to pathogens and pests (Savary et al., 2019; Simón et al., 2021). Reducing wheat yield losses due to pests and pathogens could contribute significantly towards future wheat production.

1.1.4. Fungal Diseases of Wheat

Many fungal diseases of wheat have been identified, affecting a diverse range of host tissues.

For example, Fusarium head blight caused by *Fusarium graminearum*, and Wheat blast, caused by *Magnaporthe oryzae pathotype triticum*, mainly affect floral tissues of wheat (Ceresini et al., 2018; Yang et al., 2013), whereas take-all disease is a root borne fungus of wheat caused by *Gaeumannomyces graminis var tritici* (Mac Nish et al., 1973).

In addition, a number of fungal diseases affecting foliar tissues exist, including Yellow rust, caused by *Puccinia striiformis* f. sp. *tritici*, Stagonospora Nodorum blotch caused by *Parastagonospora nodorum,* although the most economically important disease of wheat in Western Europe is currently Septoria tritici blotch caused by the ascomycete fungus *Zymoseptoria tritici* (Dean et al., 2012; Kettles and Kanyuka, 2016; Rudd, 2015). The pathogen is well adapted to the intensification of wheat production (i.e., dense planting of monocultures), and the climates of this region.

1.1.5. Control of fungal plant pathogens and problems with Fungicide resistance

Control of fungal diseases in agriculture is commonly achieved by breeding for genetic resistance of the host (Figlan et al., 2020; Zetzsche et al., 2020), application of chemical fungicides (Wiik, 2009), or management strategies to reduce inoculum/disease severity (Cotterill and Sivasithamparam, 1988). Fungicides are currently the main control strategy employed against many foliar fungal plant pathogens of wheat. The market for cereal fungicides in Europe is worth over $2.4bn (€1.8bn; at farm level 2014), with $1.7bn (€1.3bn) used on wheat, 70% ($1.2bn, €1bn) of which is primarily targeted towards the management of *Z. tritici* (Torriani, 2015). The emergence of fungicide resistant plant pathogens is a major threat to future food security and agricultural production, with resistance

to chemical control strategies having already arisen in many fungal plant pathogens (Fisher et al., 2018, 2012). The emergence of insensitivity to all known fungicides over the last 40 years has made *Z. tritici* a particular concern (Blake et al., 2018; Kildea et al., 2019).

1.1.6. Life cycle of *Z. tritici*

Z. tritici remains extracellular for its entire life cycle, and has a long latent period between infection and symptom development (Orton et al., 2017). The infection process of *Z. tritici* begins with sexual airborne ascospores or rain splash propagated asexual pycnidiospores landing on the host leaf (Stage 1, Figure 1.2), then germinating to form hyphae under high humidity conditions (Stage 2, Figure 1.2)(Shaw, 1991), before the hyphae then enter the leaf through stomatal openings (Palmer and Skinner, 2002)(Stage 3, Figure 1.2).

After entering the leaf, hyphae colonise the intercellular space of the mesophyll tissue, during the symptomless phase of infection (Stage 4, Figure 1.2). The type of growth during this latent phase has been described as biotrophic (in association with living plant cells), although there is no evidence of feeding and no presence of specialized structures associated with other biotrophic pathogens such as haustoria or arbuscules (Keon et al., 2007; Orton et al., 2011; Shetty et al., 2007).

After a period of around 10 days post-inoculation under optimum conditions (20-25°C and high humidity), a switch in the fungal lifestyle occurs, resulting in necrosis of the host leaf (Kema et al., 1996; Lucas et al., 1999; Palmer and Skinner, 2002) and a switch to necrotrophic colonisation of dead leaf tissue (Stage 5, Figure 1.2). Hyphae then colonise the substomatal cavities around the infection site and initiate formation of the asexual sporulation structures, pycnidia (Eyal et al., 1987; Palmer and Skinner, 2002; Steinberg, 2015). These structures are responsible for the production of asexual pycnidiospores.

In high humidity conditions, or during rainfall, mature pycnidiospores are exuded into an extracellular matrix to protrude out of the leaf (Palmer and Skinner, 2002),

before spores are dispersed through rain splash to other local leaves/wheat plants (Stage 6, Figure 1.2). *Zymoseptoria* isolates can also reproduce sexually, forming ascospores. This process requires the two isolates to have opposing mating types, and usually occurs in field conditions on dead leaf tissue, before dispersal via wind.

Zymoseptoria tritici is somewhat unique for an ascomycete filamentous fungus as it exhibits an environmentally regulated, and inducible, growth dimorphism. Both pycnidiospores and ascospores undergo blastosporulation when grown on rich nutrient agar, analogous to 'yeast-like' growth (Dean et al., 2012; Francisco et al., 2019; Rudd, 2015; Steinberg, 2015). Whilst this is the most predominant growth form of *Z. tritici* on most agars (Francisco et al., 2019). Conversely, when any of the spore morphologies of *Z. tritici* are placed under nutrient limiting conditions, they differentiate to form hyphae, required for stomatal penetration within natural settings. The fungus has recently emerged as a model system for the study of fungal genomics, owing to its tractability *in vitro*, ease of mutagenesis and availability of a 'complete' reference genome (Goodwin et al., 2011; Testa et al., 2015).

As outlined above, *Z. tritici* blastospores are morphologically and transcriptomically identical to pycnidiospores; the only difference being the mechanism and tissue from which the spores are derived. Pycnidiospores are derived from a pycnidium; the asexual fruiting body of *Z. tritici*. Blastospores are formed from blastosporulation, or budding, from other spore types. Under laboratory conditions, on all but very limiting agar, all spore types of *Z. tritici* will undergo 'yeast-like' cell division forming blastospores, or undergo hyphal germination and extension on low nutrient agar, such as tap water agar (Kema et al., 1996; Mehrabi and Kema, 2006) (Figure 1.3). For this reason, the blastospore growth form of *Z. tritici* has been fundamental in the discovery of fungicide insensitivity (Blake et al., 2018), the preparation of inoculum for *in planta* disease assessment (Keon et al., 2007), the identification of plant resistance genes such as *Stb6* (Saintenac et al., 2018, p. 6), and published standard laboratory workflows including high throughput mutagenesis and stable transformation (Fagundes et al., 2020).

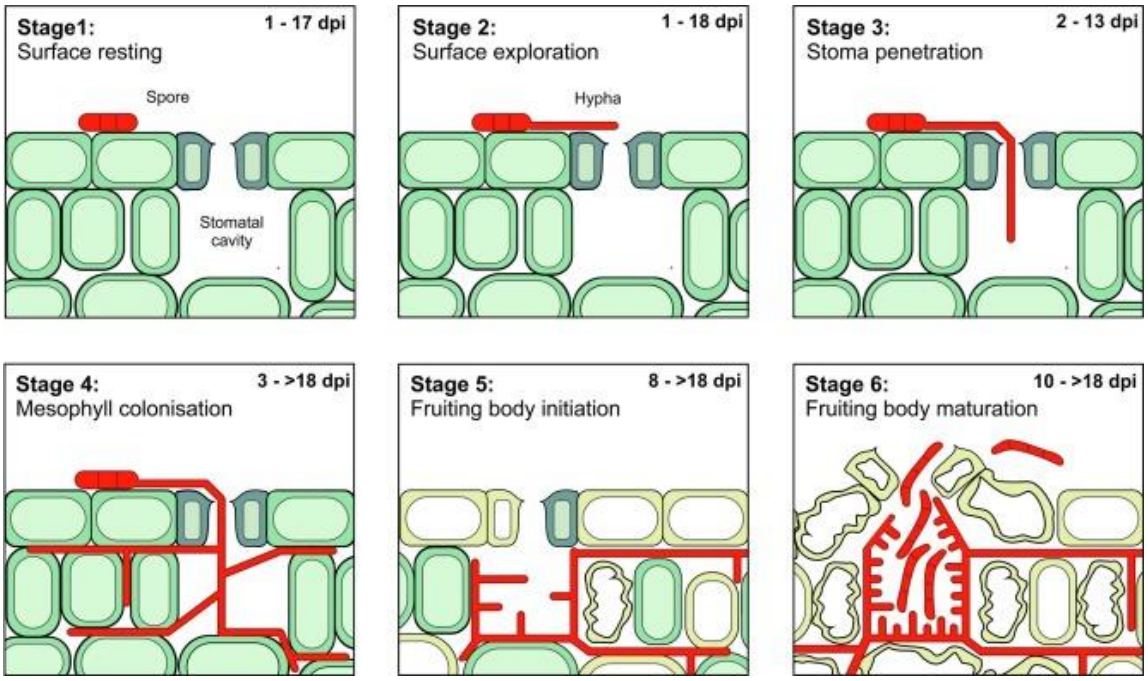


Figure 1.2. Overview of the wheat leaf infection cycle of *Z. tritici*.
An illustration depicting the approximate timings of the wheat leaf infection cycle of *Z. tritici*, adapted from (Fantozzi et al., 2021).

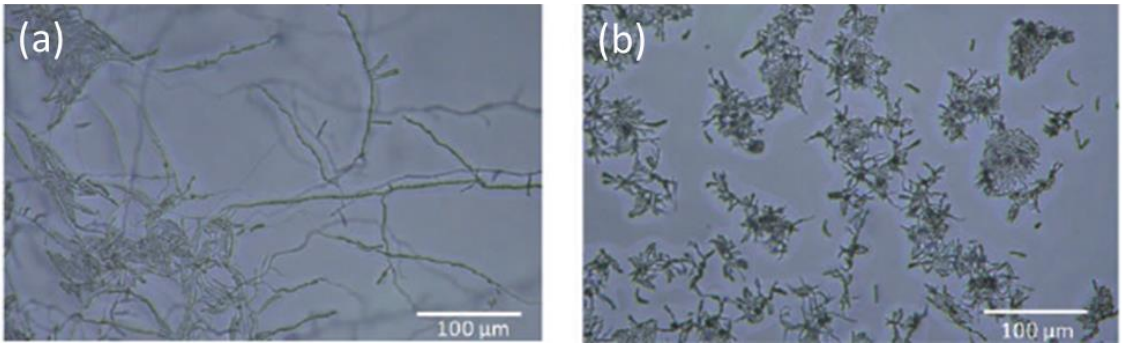


Figure 1.3 Inducible growth dimorphism of *Z. tritici*.
Light microscope images showing the two growth morphologies of *Z. tritici*. (a) The plant pathogenic hyphal growth form of *Z. tritici*. (b) The 'yeast-like' growth form of *Z. tritici* blastospores (adapted from (Motteram et al., 2011)).

1.1.7. Control of *Zymoseptoria tritici* and the evolution of fungicide resistance

There are currently limited control strategies effective against *Z. tritici*. Control through durable host genetic resistance is not possible (Torriani, 2015), due to *Z. tritici* populations having high genetic diversity compared to other fungal plant pathogens and high genomic instability (Möller et al., 2018). Several genes have been identified that are implicated in providing partial resistance to Septoria Tritici Blotch (STB) in wheat, and are incorporated into wheat breeding programmes (Brown et al., 2015), restricting or delaying pathogen development (Nelson and Marshall, 1990; Palmer and Skinner, 2002). For this reason, fungicides are the main control strategy employed by farmers in the control of *Z. tritici* (Torriani, 2015).

Over the last 40 years, *Z. tritici* has become insensitive to every class of fungicides currently available. These fungicides were developed to interfere with essential cellular processes such as respiration and ergosterol biosynthesis. Multiple mechanisms by which pathogenic fungi such as *Z. tritici* can become resistant have been identified: target site resistance, overexpression of target protein, or efflux pumps and degradation of the fungicide by metabolic enzymes (Lucas et al., 2015). Resistance to methyl benzimidazoles (MBCs) and quinone outside inhibitors (QOIs) has evolved in *Z. tritici*, mostly though point mutations at codon 198 (E198A) (Lucas and Fraaije, 2008) and 143 (G143A), respectively (Lucas et al., 2015) which reside within the chemistry binding pocket. Azoles (demethylation inhibitors that block ergosterol biosynthesis) will most likely remain the basis of cereal fungicide sprays for the foreseeable future (Cools et al., 2013). To prolong the effectiveness of fungicides, modern treatment programmes include multiple compounds, such as a mix of triazoles and succinate dehydrogenase inhibitors (SDHIs), targeting multiple cellular functions. Our reliance on chemical fungicides in the control of STB mean that it is only a matter of time before resistance to current fungicide programmes arise and become widespread. For this reason the discovery of novel antifungal compounds that can be utilised in multi-site fungicide strategies or alternative solutions based on biologicals and/or natural chemistries

are urgently required in order to maintain wheat production across Europe (O'Driscoll et al., 2014).

1.1.8. Bacteria as a potential source of new solutions for *Z. tritici* control

Bacteria have the potential to be utilised in crop protection solutions against fungal plant pathogens as biological control agents, or as a source of novel antifungal compounds. Antagonism can be caused by a number of described mechanisms, such as outcompeting pathogens for rate limiting nutrients or resources (Elad, 2003) , the secretion of antagonistic molecules (Raaijmakers et al., 2002) release of volatile compounds (Schmidt et al., 2016, 2015), induction or priming of plant defences (van Loon et al., 1998), and hyperparasitism (Boosalis, 1964). Biocontrol agents may use one or a combination of these mechanisms as a means of directly or indirectly competing with pathogens.

Several bacterial biocontrol agents, effective against *Z. tritici,* have been investigated. Recent work has shown the ability of *Paenibacillus polymyxa*, an endophyte capable of inducing systemic resistance in wheat, as a promising candidate in biocontrol of STB (Samain et al., 2017). *Bacillus megaterium* has also been shown to reduce STB severity *in planta* (Kildea et al., 2008). In the same study using bacteria isolated from Irish soils, two *P. fluorescens* isolates (MKB21 and MKB91) exhibited an ability to inhibit STB in controlled conditions, but this did not translate to a field setting (Kildea et al., 2008). However, the addition of *Bacillus subtilis* QST 713 (aka Serenade ASO®) to a chemical spray programme reduced control of STB compared to the same treatment without *B. subtilis* inoculum (Heick et al., 2017).

Robust biocontrol of fungal plant pathogens using living microbial inoculants has still not been achieved commercially or practically at field scale. However, in addition to being directly applied to counter fungal pathogens, bacterial isolates can also be utilised as a source of novel natural products, as part of a 'bio-prospecting' approach. This approach may offer the potential to isolate antifungal

compounds from microbial species that do not demonstrate *in planta* pathogen suppression. Bioprospecting is a term given to the exploration of natural sources of small molecules, with the aim to utilise and harness the functions and/or properties of these molecules in a wide range of applications. Secreted secondary metabolites, identified from biocontrol agents, have previously been used as 'templates' to produce chemical control strategies. For example, pyrrolnitrin is an antifungal compound produced by pseudomonads and other soil bacteria (Howell and Stipamnovic, 1979; Pfender et al., 1993). Subsequently, the chemical structure of pyrrolnitrin was used as the lead structure in the development of phenylpyrrole agricultural fungicides (Ligon et al., 2000).

1.1.9. The genus *Pseudomonas*

The *Pseudomonas* genus is extremely complex, owing to the large number of species described within the genus (Gomila et al., 2015) although *Pseudomonas* themselves do not possess any notable features that make them more evolvable than other bacteria (Spiers et al., 2000). Species within the *Pseudomonas* genus have a wide range of ecological roles, including opportunistic human pathogenic *Pseudomonas aeruginosa* (Kerr and Snelling, 2009), plant pathogenic *Pseudomonas syringae* (Morris et al., 2013), and plant growth promoting activities.

Pseudomonas were first described in 1894, where taxonomic classifications of bacteria were based on observable macro and microscopic morphologies (Peix et al 2018, Miguela et al 1894). Throughout the 20th and early 21st century, methods used to classify *Pseudomonas* have changed as new approaches became available. *Pseudomonas* taxonomy was based on carbon utilisation ability (Den Dooren de Jong, 1926), GC content and DNA-DNA hybridisation (Colwell et al., 1965; Johnson and Palleroni, 1989; Peix et al., 2018) as well as 16S rRNA gene sequences (Scarpellini et al., 2004) before Average Nucleotide Identity (ANI), calculated with the BLAST algorithm (ANI-b), became the gold standard to define prokaryotic species boundaries for whole genomes (Richter and Rosselló-Móra, 2009), fuelled by the ongoing reduction in sequencing costs since the mid-2000s.

Whilst ANI-b is still utilised to distinguish *Pseudomonas* whole-genome similarity, comparative phylogenetic methods to ascribe *Pseudomonas* isolates to known species based on alignments of 'house-keeping' genes, ubiquitous and conserved protein encoding genes have commonly been used (Ogier et al., 2019). Whole genome-based approaches to estimate phylogeny from alignments of Clusters of Orthologous Groups (COGs)(Tatusov, 2001), using FastTree2 (Price et al., 2010), also allow for the identification of closest-neighbours from the National Center for Biotechnology Information (NCBI) database to large alignments of query isolates.

A multilocus sequence alignment (MLSA) of partial sequences of four core 'housekeeping' genes (16S rRNA, *gyrB*, *rpoB* and *rpoD*) of 107 *Pseudomonas* type strains was shown to discriminate *P. aeruginosa* and *P. fluorescens* groups of type strains, into three and six subgroups respectively (Mulet et al., 2010). The authors proposed the use of a MLSA-based approach for ascribing novel *Pseudomonas* strains to known species. In 2016, Garrido-sans et al sought to unify *Pseudomonas* taxonomy, and phylogenomic analyses through paired MLSA of 16S rRNA, *gyrB*, *rpoD* and *rpoB* housekeeping genes, and whole-genome based analyses, to distinguish 9 distinct clades of *P. fluorescens* sub-species (Garrido-Sanz et al., 2016). This was followed by the identification of 9 markers that allow for the classification of an unknown *Pseudomonas* isolate into 8 of the *P.fluorescens* sub-species, with 98.34% accuracy, using a PCR based system (Garrido-Sanz et al., 2017).

In 2015, 144 *Pseudomonas* species were recognised in the List of Prokaryotic Names with Standing in Nomenclature (LPSN) (Gomila et al., 2015; Parte, 2014). Between 2009 to 2018, more than 70 new species of *Pseudomonas* were described (Peix et al., 2018), with isolation and sequencing efforts increasing this number considerably since. Owing to this, the current *Pseudomonas* taxonomy remains in a state of flux, and will seemingly do so for the foreseeable future, due to reclassification events, changing definitions of species boundaries based on experimental evidence, and the identification of yet undescribed novel species of *Pseudomonas*.

1.1.10. Bacterially mediated antifungal secreted secondary metabolites

The biosynthesis of secreted secondary metabolites can take place through several mechanisms.

1.1.11. Non-ribosomal peptide synthetases (NRPSs).

Non-ribosomal peptide synthetases are large, multi-enzyme machineries that assemble peptides independently of ribosomes and mRNA, encoding the biosynthesis of non-ribosomal peptides (NRPs) (Süssmuth and Mainz, 2017). NRPs can have a diverse range of properties, some being directly antimicrobial, for example *P. fluorescens* strain SS101 suppresses the oomycete *Phytophthora infestans* through the production of NRP massetolide A, whereas other strains produce metal chelating siderophores and compete for nutrients (Bonneau et al., 2020). For example, pyoverdines are siderophores produced by many *Pseudomonas* isolates with antifungal ability against *Aspergillus fumigatus* (Sass et al., 2019, 2018).

1.1.12. Polyketide Synthases (PKS)

Polyketide Synthases (PKSs) are enzyme complexes encoding the production of a large number of secondary metabolite products. Three types of PKS are described, with type I and type II PKSs existing as large protein complexes, and type III PKSs as small homodimeric proteins (~45 kDa monomer) (Weng and Noel, 2012). For example, the antifungal metabolite 2,4-Diacetylphloroglucinol (DAPG), which is implicated in the antagonism of many plant pathogenic fungi (Levy et al., 1992b; Raaijmakers and Weller, 1998) is synthesised through a type III PKS (Bangera and Thomashow, 1999; Moynihan et al., 2009).

1.1.13. Post-Ribosomal Peptide Synthesis (PRPS)

Ribosomally synthesized and post-translationally modified peptides (RiPPs), are secondary metabolites produced through Post-Ribosomal Peptide Synthesis

(PRPS). The post-translational modification usually includes a proteolytic step that cleaves the precursor peptide into a smaller, active fragment that forms the secondary metabolite product (McIntosh et al., 2009). Pinensins A and B, produced by *Chitinophaga pinensis* DSM 28390, are the first described antifungal lanthipeptide RiPPs, shown to have broad spectrum antifungal activity against both yeasts, and filamentous fungi (Mohr et al., 2015).

Bacterial species, such as *Streptomyces* and *Bacillus*, have been identified as preferential sources of natural product discovery due to their diverse secondary metabolism, and ability to be easily cultured through spores. In addition, *Pseudomonas* bacteria also have a highly diverse secondary metabolism (Gross and Loper, 2009), but are relatively unexplored in terms of being exploited for natural product discovery. A potential advantage of working with *Pseudomonas* spp. over other bacteria, such as *Streptomyces*, is that their secondary metabolite catalogue is less complex. This can facilitate the identification of candidate suppressive molecules and biosynthetic gene clusters.

Nevertheless, a handful of previous studies have identified plant pathogenic fungal antagonism by *Pseudomonas* bacteria, which demonstrates their potential use as a source of natural products. Studies investigating the antagonism of *Z. tritici* by *Pseudomonas aeruginosa* isolate LEC1 *in vitro*, found the siderophore pyocyanin (Flaishman et al., 1990) and 1-hydroxyphenazine (Levy et al., 1992a, 1989) to partially contribute towards antagonism. *Pseudomonas fluorescens* PMF2 was found to antagonise *Z. tritici* through the production of 2,4-diacetylphloroglucinol (DAPG) and 2 further antifungal compounds could not be identified within the study (Levy et al., 1992b). Tropolone, produced by *Pseudomonas lindbergii*, was found to inhibit the growth of *Z. tritici in vitro* (Levy et al., 1988; Lindberg et al., 1980). *Pseudomonas* isolates have also previously been shown to antagonise *Z. tritici* through the production of volatile compounds. *Pseudomonas putida* BK8661 was found to antagonise *Z. tritici in vitro*, through the production of hydrogen cyanide (HCN) (Flaishman, 1996).

1.1.14. The genomics age of natural product discovery

The last decade has seen the development of affordable, high throughput next generation sequencing (NGS). This, coupled with advances in sequencing quality, has led to the so-called ‘genomics age’. The large volume of high-quality sequencing data allows us to ask questions that were not possible previously. The use of statistical modelling, alongside functional assays and genomics data now allow us to rapidly predict functions from genomic data, all of which were not previously possible.

1.1.15. Predictive Bioinformatics

Predictive bioinformatics has emerged as a rapidly expanding area of research, facilitated by the large reduction in cost of whole genome sequencing, and public repositories such as the National Center for Biotechnology Information (NCBI).

Genes implicated in the biosynthesis of secondary metabolites are often clustered together spatially. Predictive bioinformatic tools allow us to explore the diversity of secondary metabolite gene clusters within genome sequences. Use of such tools can rapidly speed up the identification of both known and unknown secondary metabolite gene clusters that may be implicated in a phenotype.

The biosynthesis of secondary metabolites takes place in localised clusters of genes, referred to as biosynthetic gene clusters (BGCs). The spatial clustering of genes involved in the biosynthesis of secondary metabolites within bacterial genome sequences has given rise to algorithms such as Clusterfinder (Cimermancic et al., 2014), based on hidden Markov models (HMMs) (Baum and Petrie, 1966), to identify spatial clusters of genes within bacterial genome sequences that could potentially encode BGCs of both known and unknown classes. The antibiotics and secondary metabolite analysis shell (antiSMASH), is a predictive bioinformatic tool, integrating detection algorithms such as Clusterfinder, with rule based detection and prediction of known BGC classes from bacterial genomes (Blin et al., 2019). The Minimum information about a

Biosynthetic Gene Cluster (MiBIG) database is a standardised repository for the deposition of BGC sequences, to allow for comparison of BGC sequences described in literature, with query sequences (Kautsar et al., 2019). Comparative tools for secondary metabolite BGCs have been developed, such as 'Biosynthetic Gene Similarity Clustering and Prospecting Engine' (BiG-SCAPE), enabling the comparison of BGCs through the generation of sequence similarity networks (Navarro-Muñoz et al., 2020). This allows the comparison of targets for functional characterisation in a database of secondary metabolites and identification of potentially novel secondary metabolite BGCs, which could be exploited to direct fungicide production.

1.2. Aims of this Project

To summarise, at present, there is a need to discover novel mechanisms to provide STB control into the future, as *Z. tritici* continuously evolves resistance to conventional fungicides. Advances in genome sequencing and mutagenesis of both *Z. tritici* and *P. fluorescens* provide an exciting opportunity to better understand the interactions between inhibitory *P. fluorescens* isolates and *Z. tritici*. This information, coupled with chemical analysis, could identify compounds on which to base novel fungicides and/or reveal novel fungal genes which make them susceptible to nature's fungicides.

The aim of this project is to develop a high-throughput functional assay and predictive bioinformatics driven pipeline, for the discovery of antifungal compounds, effective against *Z. tritici*, that are produced by *Pseudomonas* isolates.

More specifically this project aims to:

1. Develop a high throughput phenotypic screen for *Z. tritici* antagonism by *Pseudomonas* bacteria.

2. Assess genetic diversity of *Pseudomonas* isolates and discover if this can be linked to fungal antagonism.

3. Use predictive bioinformatics to assess whether there is a link between *Z. tritici* antagonism and presence of predicted secondary metabolite BGCs in *Pseudomonas* isolates.

4. Assess whether a relationship exists between *Z. tritici* genetic diversity and *Pseudomonas* antagonism.

5. Assess transcriptomic response of *Pseudomonas* isolates to confrontation with *Z. tritici* in co-culture.

Chapter 2. Development of a high throughput *in vitro* assay for the identification of *Pseudomonas* isolates with the ability to antagonise *Z. tritici*

2.1. Introduction

The discovery of novel bacterial biocontrol agents effective against pathogenic fungi, relies on the screening of bacterial candidates for an antagonistic phenotype against fungal pathogens in confrontation assays in *in vitro* or *in planta* settings. *In vitro* assays are most commonly used, as they offer reduced costs, and are less labour intensive when compared to *in planta* screening. Currently, a lack of high throughput screening procedures to identify microbial agents capable of antagonising fungal plant pathogens exist, with most described screening systems being low throughput (Kjeldgaard et al., 2022). High throughput screens are not practically feasible against many fungal plant pathogens, due to the hyphal growth morphology of most plant pathogenic fungi. The discovery of new antifungal compounds is urgently required, and screening microbial collections in a high throughput manner *in vitro*, may assist in natural product discovery efforts. *Z. tritici in vitro* confrontation assays currently described in literature are carried out in low throughput formats (Kildea et al., 2008; Lynch et al., 2016). By developing a high throughput *in vitro* confrontation assay, microbial collections could be more easily screened for *Z. tritici* antagonism, generating leads for natural product discovery efforts.

Z. tritici exhibits an environmentally regulated growth dimorphism, a unique trait among Ascomycete filamentous fungi, consisting of a ‘yeast-like’ growth form of blastospores, and a hyphal growth form (Figure 2.1). This dimorphism is inducible under laboratory conditions, with ‘yeast-like’ growth of blastospores induced under high nutrient and lower temperature conditions, the hyphal growth form occurs under nutrient limited conditions and higher temperature conditions (Francisco et al., 2019). *Z. tritici* blastospores have been utilised *in vitro* to investigate the effect

of drug synergies of isolated natural products in a high throughput manner, in a liquid culture system (Augostine and Avery, 2022). In this system, optical density measurements are used to assess inhibition at OD_{600}, which make this system impractical to assess co-cultures of *Pseudomonas* isolates and *Z. tritici* blastospores together in liquid culture, as the growth of *Pseudomonas* isolates also produce an optical density signal at OD_{600} (Ionescu et al., 2015).

Pseudomonas bacteria have previously described biocontrol abilities against many fungal plant pathogens (Couillerot et al., 2011; Duffy and Défago, 1997; Huang et al., 2004; Keel et al., 1992). However, studies screening large numbers of *Pseudomonas* isolates for antagonism of *Z. tritici* have not been conducted, owing to the low-throughput nature of currently employed techniques (Kildea et al., 2008; Zwiers et al., 2003).

Previous studies investigating the ability of *Pseudomonas* isolates to antagonise *Z. tritici* identified a number of secreted secondary metabolites contributing to *in vitro* antagonism, including 2,4-DAPG (Levy et al., 1992b), pyocyanin (Flaishman et al., 1990) and 1-hydroxyphenazine (Levy et al., 1989). A previous study sought to investigate the biocontrol potential of two *Pseudomonas* isolates against *Z. tritici in planta*, though *in vitro* biocontrol ability *in planta* against blastospores did not translate to effective *Z. tritici* control in a field setting with the application of live *Pseudomonas* inoculum (Kildea et al., 2008).

There is no rapid and high throughput *in vitro* screen available to assess the antagonistic potential of bacterial isolates against *Z. tritici*, or plant pathogenic fungi more broadly, although a high throughput methodology to screen putative antifungal compounds against the hyphal pathogenic fungus *Aspergillus flavus* has been described (Medina et al., 2012). The development of a high throughput *in vitro* screen for bacterial antagonism of *Z. tritici* blastospores would enable the screening of bacterial isolate collections for fungal antagonism phenotypes, to identify candidate isolates for further investigation and characterisation. This would, in turn, increase the speed at which molecular discovery efforts to identify

bacterially derived *Z. tritici* antagonistic compounds (potentially novel natural fungicides), could be made, forming an initial step in a microbial natural product discovery pipeline.

Hypotheses:

(1) *Z. tritici* blastospores be exploited to develop a high throughput *in vitro* screen for *Pseudomonas* bacterial antagonists, in a qualitative manner.
(2) Application of antagonistic *Pseudomonas* inoculum to wheat leaves alters disease progression and disrupts pycnidia (asexual sporulation) formation in *Z. tritici.*

2.2. Chapter specific Methods

2.2.1. *Pseudomonas* isolate collection

The library of *Pseudomonas* isolates utilised in this chapter were generated in two previous projects. One experiment contributed 480 isolates from the rhizosphere and endosphere of wheat roots in a take-all infested field at Rothamsted (BBSRC funded ISP: "Optimization of nutrients in soil-plant systems: How can we control nitrogen cycling in soil?" BBS/E/C/00005196)(Mauchline et al., 2015), and another 54 were obtained from bulk soil and wheat roots from the Rothamsted Highfield experiment (Heather Ruscoe, personal communication)(NERC PhD project, Heather Ruscoe "Rhizosphere bacteria promote sustainable plant growth" Project reference: 1641948).

2.2.2. Culturing of *Z. tritici* blastospores

Z. tritici blastospores were cultured from glycerol stocks stored at -80°C, by spreading 30µl of glycerol stock on potato dextrose agar (PDA, Formedium) plates, before inverting and placing in darkness at 16°C for 5 days. Blastospores were harvested using a sterile loop after 5 days of growth. *Z. tritici* isolate IPO323 was

used throughout this study, as it is a well characterised reference strain, with a complete genome sequence.

2.2.3. Culturing of *Pseudomonas* isolates

Pseudomonas isolates were cultured from glycerol stocks stored at -80°C, by inoculating 10ml of LB Miller Broth (Formedium), with a chip of frozen glycerol stock. The inoculated broth was placed in a shaking incubator at 180 rpm and 25°C overnight (~18hours).

2.2.4. Storage of isolates

Both bacterial and fungal isolates were stored as glycerol stocks at -80°C. *Z. tritici* glycerol stocks were prepared by suspending blastospores, cultured as described above, into sterilised 80% glycerol. Stocks were left at room temperature for 20 minutes, before snap freezing in liquid nitrogen. Aliquots were made so that stocks were not repeatedly freeze-thawed during this study. Bacterial glycerol stocks were prepared by mixing 370µl of overnight LB (Formedium) culture, as described above, with 630µl of sterilised 80% glycerol.

2.2.5. High throughput *in vitro* screen for fungal antagonism of *Z. tritici* by *Pseudomonas* isolates

Z. tritici blastospores were cultured from glycerol stocks as described above for 5 days preceding the antagonism assay, and *Pseudomonas* isolates were cultured from glycerol stocks as described above, the evening before. A blastospore suspension was prepared from a 20µl loop of harvested *Z. tritici* blastospores and 5ml of distilled water, containing approximately $1x10^6$ blastospores per ml (Hongxin Chen, personal communication). The solution was vortexed to homogenise the solution. 800µl of spore suspension was added to each 120mm x 120mm Petri dish containing 50ml PDA (Formedium). The plates were tilted to achieve a confluent lawn of blastospore suspension across the plate before excess spore suspension was removed by pipetting. Plates were air-dried for 20 minutes in a laminar flow

hood, before 1µl of *Pseudomonas* overnight culture was applied. Plates were sealed and inverted, before being stored in darkness at 16 °C for 12 days. *Z. tritici* blastospore antagonism assays were carried out in triplicate.

2.2.6. Hyphal inhibition assays

Hyphal inhibition assays were conducted using *Z. tritici* blastospores and *Pseudomonas* cultures grown as described above. 50% strength PDA (Formedium) plates were prepared with 16g of Agar-Agar (Fisher-Bioreagents) added. 2µl aliquots of *Z. tritici* blastospore suspension (as previously described) and *Pseudomonas* overnight culture were spotted onto the 50% PDA (Formedium) plates 10mm apart. Plates were sealed and inverted, before being left in darkness at room temperature for 21 days.

2.2.7. Preparation of bacterial cells for *in planta* disease assessment

Pseudomonas inoculum was prepared by pelleting 40ml of overnight LB (Formedium) culture at 4000rpm. Cells were washed twice by resuspending in sterile tap water, before centrifugation. The final pellet was resuspended in 5ml of 0.01% tween solution for application to the leaf surface. The suspension was vortexed immediately before application to the leaf surface using an atomiser.

2.2.8. Preparation of *Z. tritici* spores for *in planta* disease assessment

Z. tritici inoculum was prepared by suspending five 20µl loops of blastospores grown as described above, in 5ml of 0.01% Tween-20 (Fisher-Bioreagents) solution (approximately 200µl of 1 x 10^6 blastospores per ml). The suspension was vortexed immediately before application to the leaf surface using an atomiser.

2.2.9. *In planta* assessment of *Pseudomonas* biocontrol potential

Wheat seeds (c.v. Riband) were sown and grown for 21 days in a growth cabinet (Sanyo MLR-350) under a 18/6 light/dark cycle and at 19 °C. After 21 days the

second true leaves were fixed to a metal platform for inoculation, as described in (Saintenac et al., 2018). *Pseudomonas* inoculum was prepared as described above and applied using an atomiser spray bottle (approximately 200µl of 1 x 10^8 cells per ml) to 3 wheat leaves (in triplicate), before the plants were placed in a humidity dome for 24 hours. *Z. tritici* inoculum was prepared as described above and was then applied to the wheat leaves using an atomiser spray bottle (approximately 200µl of 1 x 10^6 blastospores per ml). The plants were then covered with a humidity dome for 48 hours before being placed in a plant growth cabinet under a 18/6 light/dark cycle and ambient temperature for a further 19 days before images were taken. Pycnidia formation was induced on excised leaves by placing in a 15ml falcon tube with wetted tissue paper for 24 hours at room temperature, before images were taken. 0.01% Tween-20 solution was used as a control treatment for both *Pseudomonas* inoculum and *Z. tritici* inoculum, and applied to the wheat leaves at the same time points using an atomiser. Wheat cultivar Riband was utilised in this study to assess *Z. tritici* disease progression *in planta*, as previous studies have used this cultivar for *in planta* disease progression assessment (Saintenac et al., 2018).

2.2.10. Quantification of *Z. tritici* pycnidiospore formation

Pycnidiospore formation was quantified by washing *Z. tritici* infected leaves (n=3) with induced pycnidia formation as described in 2.2.9., with 2ml of 0.01% Tween-20 solution, followed by vortexing for 30 seconds. Spores of resulting suspensions were then counted using a haemocytometer, before being converted to spores/ml as described previously (Stephens et al., 2021).

2.2.11. Statistical analyses

Statistical analysis of *Pseudomonas* isolation niche and observed *in vitro* qualitative *Z. tritici* blastospore antagonism phenotype was conducted using Pearson's Chi-squared test of independence. One-way analysis of variance (ANOVA) was used to determine if there was a significant difference in the number

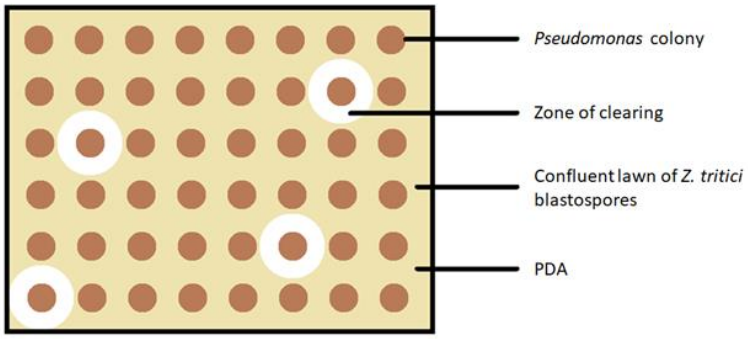
of recovered pycnidiospores (2.2.10) after treatment with *Pseudomonas* isolates (outlined in Section 2.3.4), and induction of pycnidia formation (2.2.9). All statistical analyses were carried out in RStudio (Build 461, R version 4.1.3), using packages stats, emmeans, multcomp, multcompView, ggpubR and ggplot2.

2.3. Results

2.3.1. Development of a high throughput *in vitro* assay to qualitatively identify *Pseudomonas* isolates exhibiting an antagonistic phenotype against *Z. tritici in vitro*.

To investigate the ability of *Pseudomonas* isolates to antagonise *Z. tritici* blastospores, an *in vitro* assay was developed. The growth of a confluent blastospore lawn of *Z. tritici* was induced across the plate through the use of nutrient rich PDA, and 48 individual *Pseudomonas* isolates were distributed across each plate as separate colonies (Figure 2.2a). A total of 534 *Pseudomonas* isolates were screened for antagonism of *Z. tritici* blastospores, from two *Pseudomonas* libraries from previous projects (480 isolates were generated in a previous BBSRC funded ISP: “Optimization of nutrients in soil-plant systems: How can we control nitrogen cycling in soil?” (BBS/E/C/00005196), 54 isolates from NERC PhD project, Heather Ruscoe “Rhizosphere bacteria promote sustainable plant growth” Project reference: 1641948)(Supplementary Table 1.). A positive antagonistic phenotype of *Pseudomonas* isolates was defined as the presence of a visible zone of clearing/zone of inhibition of the confluent lawn of *Z. tritici* blastospores immediately surrounding the *Pseudomonas* colony (Figure 2.2b). Of 534 *Pseudomonas* isolates studied, 52 were identified as exhibiting an antagonistic interaction towards *Z. tritici* blastospores (Supplementary Table 1.).

(a)



(b)



Figure 2.1 High throughput *in vitro* assay for *Z. tritici* blastospore antagonism.
(a) A diagram indicating the components of the *Z. tritici* blastopore antagonism assay. **(b)** A photograph taken of the *Z. tritici* blastospore antagonism assay, with 48 *Pseudomonas* colonies on one assay plate.

2.3.2. Assessment of *Z. tritici* blastospore antagonism by *Pseudomonas* isolates derived from rhizosphere and endosphere samples

To assess the relative proportion of antagonistic *Pseudomonas* isolates derived from the rhizosphere and endosphere, antagonism data generated from the *Pseudomonas* library isolated from a Take-all infested wheat field were analysed. The *Pseudomonas* library consisting of 480 *Pseudomonas* isolates was derived from the rhizosphere and endosphere of wheat plants grown in the Take-all infested field at Rothamsted in a previous project (Mauchline et al., 2015) ("Optimization of nutrients in soil-plant systems: How can we control nitrogen cycling in soil?" (BBS/E/C/00005196). Only *Pseudomonas* isolated as part of the Take-all infested wheat field trial were analysed, due to differences in sampling

methodologies in the generation of this *Pseudomonas* isolate collection, and the 54 *Pseudomonas* isolated as part of the NERC project (Heather Ruscoe "Rhizosphere bacteria promote sustainable plant growth" Project reference: 1641948), making comparison between isolation niche of the different experiments not possible. A total of 41 *Pseudomonas* isolates from the Take-all experiment collection showed antagonistic activity against *Z. tritici* blastospores *in vitro*. Of the 192 *Pseudomonas* isolates derived from endosphere samples, 15 exhibited an antagonistic phenotype in the blastospore antagonism assay. A total of 26 *Pseudomonas* isolates derived from the wheat rhizosphere, were determined to be antagonistic towards *Z. tritici* blastospores *in vitro,* out of the 288 screened. These results indicate that 7.81% and 9.02% of *Pseudomonas* isolates screened from the endosphere and rhizosphere compartments, respectively, exhibited antagonism of *Z. tritici* blastospores (Supplementary Table 1.).

To determine if there was a significant association between *Pseudomonas* isolation niche and *in vitro Z. tritici* blastospore antagonism, Pearson's Chi-squared test of independence was used. No significant association between isolation niche and *in vitro Z. tritici* blastospore antagonism phenotype was found, $X^2(1, N = 480) = 0.22$, $p = 0.64$.

2.3.3. Inhibition of *Z. tritici* hyphae by *Pseudomonas* isolates

To determine the ability of *Pseudomonas* isolates to antagonise the hyphal growth form of *Z. tritici*, confrontation assays were conducted *in vitro*. The hyphal growth form of *Z. tritici* was induced by the use of ½ strength PDA (Formedium) plates, with 2µl aliquots of *Z. tritici* blastospores and *Pseudomonas* overnight culture placed 10mm apart (Figure 2.3a). A random subset of 10 *Pseudomonas* isolates from project BBS/E/C/00005196 (Take-all experiment), exhibiting antagonistic (4) and non-antagonistic (6) phenotypes against *Z. tritici* blastospores was studied (Table 2.2) in a preliminary investigation.

Confrontation plates were photographed after 21 days, with all 10 *Pseudomonas* isolates seen to antagonise the hyphal growth form of *Z. tritici in vitro*, irrespective of the antagonistic phenotype identified in the blastospore antagonism assay (Table 2.2). For all confrontation plates observed, successful hyphal extension of *Z. tritici* was observed on the edge of the *Z. tritici* colony, with an absence of hyphal growth observed on the edge of the *Z. tritici* colony closest to the *Pseudomonas* colony. Control plates of *Z. tritici* grown alone on ½ PDA show successful hyphal extension in all directions (Supplementary Figure 2a). *Pseudomonas* isolate Roth 16 can also be observed to exhibit swarming motility in both confrontation with *Z. tritici* hyphae (Figure 2.2c) and grown alone (Supplementary Figure 2b) on ½ PDA agar.

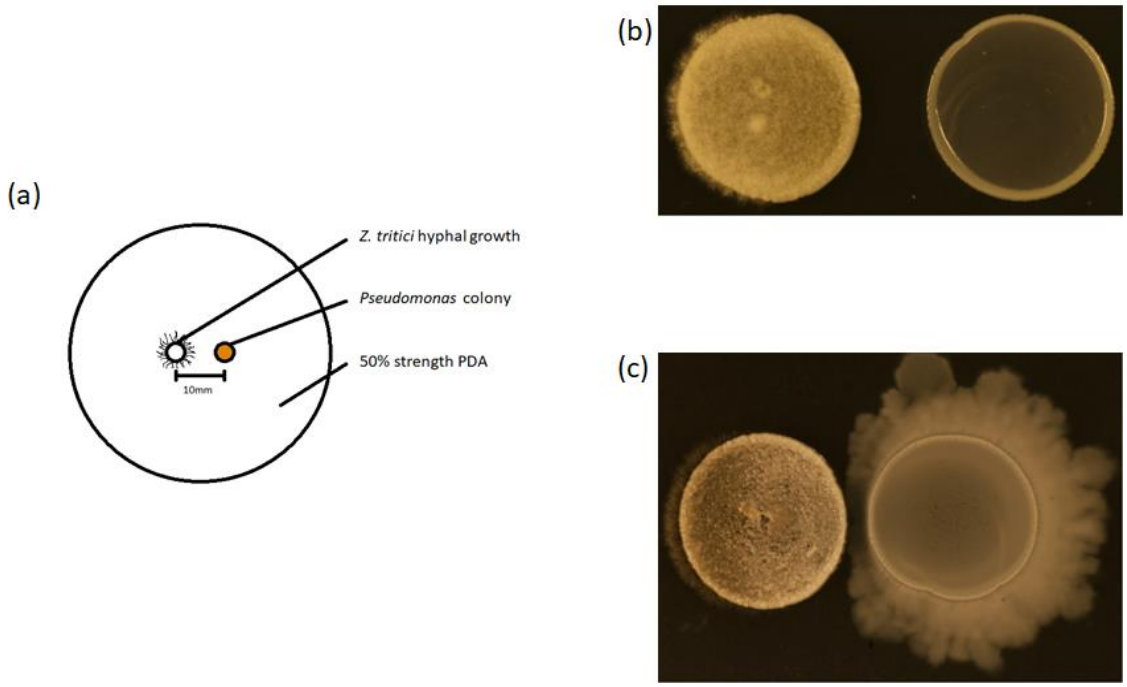


Figure 2.2 Hyphal *Z. tritici in vitro* antagonism assay.
(a) A diagram indicating the components utilised in the antagonism assay involving the hyphal growth form of *Z. tritici*. **(b)** A photograph of a hyphal antagonism assay after 21 days, *Z. tritici* isolate IPO323 (left) and *Z. tritici* blastospore non-antagonistic *Pseudomonas* isolate Roth 42 (right). The *Z. tritici* colony exhibits disrupted hyphal growth closest to the *Pseudomonas* colony (centre of image), with hyphal extension of *Z. tritici* visible furthest away from the *Pseudomonas* colony (left of image). **(c)** A photograph of a hyphal antagonism assay after 21 days, *Z. tritici* isolate IPO323 (left) and *Z. tritici* blastospore antagonistic *Pseudomonas* isolate Roth 16 (right). The *Z. tritici* colony exhibits disrupted hyphal growth closest to the *Pseudomonas* colony (centre of image), with hyphal extension of *Z. tritici* visible furthest away from the *Pseudomonas* colony (left of image).

Table 2.1 The antagonism phenotype of *Pseudomonas* isolates screened against both the hyphal and blastospore growth forms of *Z. tritici in vitro* (1 indicates observed antagonism, 0 indicates no observed antagonism).

***Pseudomonas* isolate**	***Z. tritici* blastospore antagonism phenotype**	***Z. tritici* hyphal antagonism phenotype**
Roth26	1	1
Roth3	0	1
Roth36	1	1
Roth40	1	1
Roth42	0	1
Roth53	0	1
Roth56	0	1
Roth71	0	1
Roth73	0	1
Roth75	1	1

2.3.4. *In planta* assessment of the biocontrol potential of *Pseudomonas* isolates against *Z. tritici*

To assess the effect of *Pseudomonas* inoculum application to wheat leaves, *in planta* experiments were conducted on wheat plants (cv. Riband) through the application of *Pseudomonas* inoculum to the wheat leaf surface. The application of bacterial inoculum took place 24 hours before subsequent inoculation with *Z. tritici* inoculum or 0.01% Tween-20 control (Figure. 2.4a). Four *Pseudomonas* isolates previously observed to exhibit a *Z. tritici* blastospore antagonistic phenotype *in vitro*, and one *Pseudomonas* isolate observed to exhibit a non-antagonistic phenotype against *Z. tritici* blastospore *in vitro* were utilised in this study (Table 2.3).

The viability of *Pseudomonas* inoculum prepared as described in Methods, was determined by inoculating LB agar plates with *Pseudomonas* inoculum using an atomiser. LB plates were incubated at 25°C overnight. Viable *Pseudomonas* colonies and macroscopic growth were observed for all isolates tested after 18 hours incubation (Supplementary Figure 1.). Experimental controls for

Pseudomonas inoculum and *Z. tritici* inoculum consisted of 0.01% Tween-20 solution, applied to the wheat leaf surface at the same time point using the same methodology. Wheat leaves treated with *Pseudomonas* inoculum, before subsequent application of 0.01% Tween-20 solution, showed no observable effect on the wheat leaves compared to Tween-20 control (Fig. 2.4b). Wheat leaves treated with *Pseudomonas* inoculum, before subsequent application of *Z. tritici* inoculum, showed no observable difference in disease severity at 21 days post *Z. tritici* inoculation, for both antagonistic and non-antagonistic *Pseudomonas* isolates (Fig. 2.4c), when compared to 0.01% Tween-20 control.

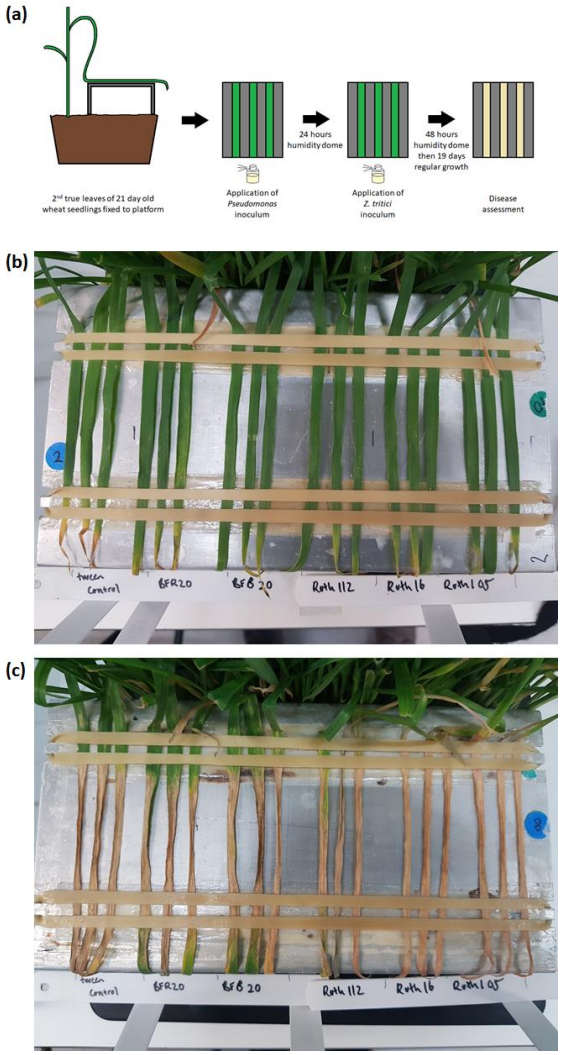


Figure 2.3 *In planta* assessment of biocontrol capability of *Pseudomonas* isolates.
(a) A diagram outlining the methodology and timings used in the *in planta* assessment. **(b)** A photograph of wheat leaves at 21 days post inoculation with 0.01% Tween-20 as a *Z. tritici* inoculum control. Three wheat leaves were treated with bacterial inoculum as described, with *Pseudomonas* isolates labelled under the wheat leaves (from the left: 0.01% Tween-20 control, BFR20, BFB20, Roth 112, Roth 16 and Roth 105). No leaves show signs of necrosis or yellowing. (c) A photograph of wheat leaves at 21 days post inoculation with *Z. tritici*. Three wheat leaves were treated with bacterial inoculum as described, with *Pseudomonas* isolates labelled under the wheat leaves (from the left: 0.01% Tween-20 control, BFR20, BFB20, Roth 112, Roth 16 and Roth 105). All leaves show substantial necrosis and yellowing.

Table 2.2 *Z. tritici* blastospore antagonism data (1 indicates antagonism observed, 0 indicates no antagonism observed) for *Pseudomonas* isolates screened in the *in planta* assessment of biocontrol potential.

***Pseudomonas* isolate**	**Blastospore Inhibition**
BF-R-20	1
BF-B-20	1
Roth112	1
Roth16	1
Roth105	0

2.3.5. Assessment of *Pseudomonas* inoculation on *Z. tritici* pycnidia formation and pycnidiospore production *in planta*

To examine the effect of *Pseudomonas* inoculum application on the formation of *Z. tritici* pycnidia, pycnidia formation was induced on excised wheat leaves that were studied in the *in planta* assessment of biocontrol potential (Section 2.3.4). After 24 hours incubation in a high humidity environment, images of wheat leaves were taken from a standardised height (Figure 2.5a). For all wheat leaves inoculated with *Pseudomonas* isolates before subsequent application of Tween-20 as a *Z. tritici* inoculum control, no visible pycnidia were detected (Figure 2.5b). For all wheat leaves inoculated with *Pseudomonas* isolates before subsequent inoculation with *Z. tritici* inoculum, pycnidia formation was observed (Figure 2.5c). No difference in abundance of visible pycnidia could be seen for wheat leaves inoculated with *Z. tritici*, for 0.01% Tween-20 bacterial control treatment (left), inoculation with antagonistic *Pseudomonas* isolate Roth 16 (centre), or inoculation with non-antagonistic *Pseudomonas* isolate Roth 105 (right) (Figure 2.5c).

To quantitatively assess the effect of *Pseudomonas* inoculum on *Z. tritici* pycnidiospore formation, the three wheat leaves from each treatment were then pooled, and pycnidiospores were recovered by vortexing the leaves with 2ml 0.01% Tween-20 solution. The recovered pycnidiospores were then pelleted by centrifugation at 14,000rpm for 10 minutes, before resuspension in 100µl 0.01% Tween-20 solution. Pycnidiospores within this suspension were counted (n=4), as

described in 2.2.10, using a haemocytometer. One-way analysis of variance (ANOVA) was performed, to assess if significant differences in the mean number of recovered pycnidiospores from *Z. tritici* infected wheat leaves after treatment with *Pseudomonas* inoculum. One-way ANOVA revealed no statistically significant difference in the mean number of recovered pycnidiospores ($F(5, 18) = 0.05856$) (Supplementary Table 2.).

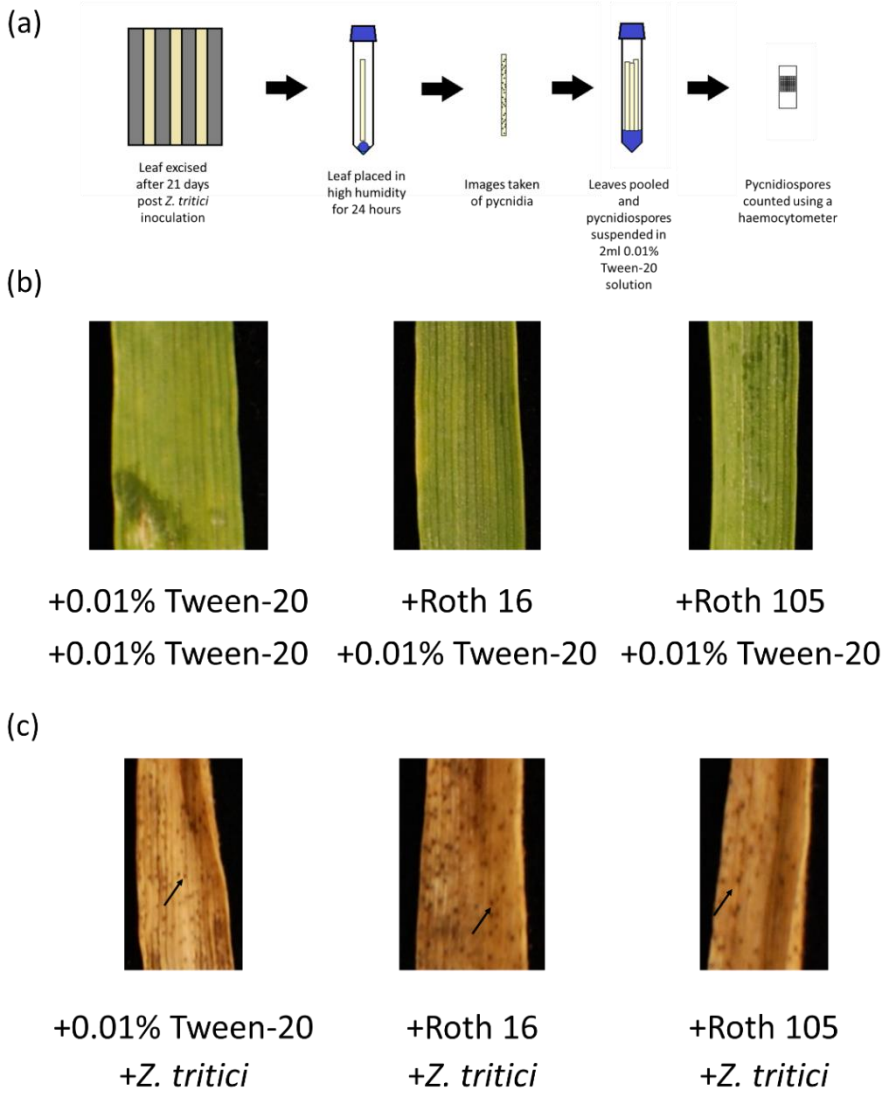


Figure 2.4 Assessment of *Z. tritici* pycnidia formation.
(a) A diagram summarising the methodology used to induce *Z. tritici* pycnidia formation on wheat leaves, before quantification of pycnidiospores using a haemocytometer. **(b)** A photograph of wheat leaves inoculated with 0.01% Tween-20 as a *Z. tritici* inoculation control. No visible pycnidia are present on leaves inoculated with 0.01% Tween-20 (left), antagonistic *Pseudomonas* isolate Roth 16 (centre), or non-antagonistic *Pseudomonas* isolate Roth 105 (right) at the bacterial inoculation stage. **(c)** A photograph of wheat leaves inoculated with *Z. tritici* at the fungal inoculation stage. Visible pycnidia (dark spots indicated by black arrows) are present on leaves inoculated with 0.01% Tween-20 (left), antagonistic *Pseudomonas* isolate Roth 16 (centre), or non-antagonistic *Pseudomonas* isolate Roth 105 (right) at the bacterial inoculation stage.

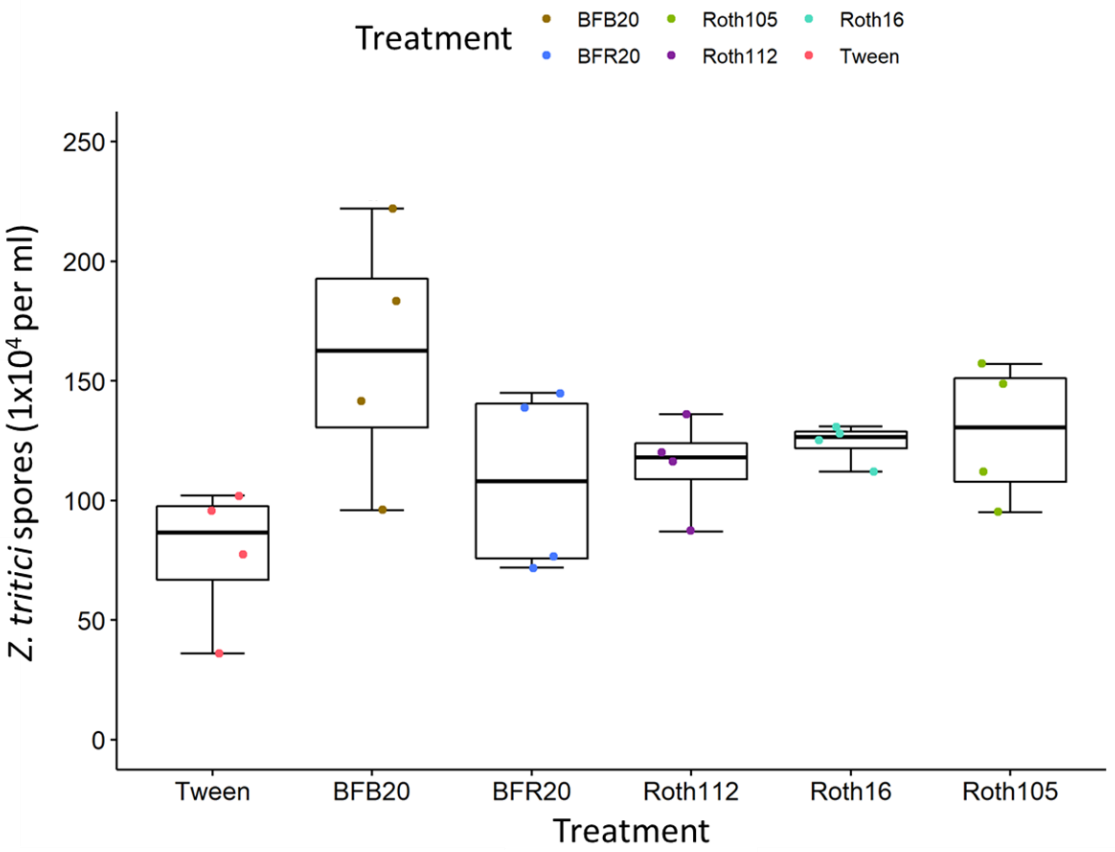


Figure 2.5 Pycnidiospores recovered from wheat leaves infected with *Z. tritici* after inoculation with *Pseudomonas* isolates.
Pycnidiospores were counted using a haemocytometer (n=4), with no significant differences found between treatments (one-way ANOVA ,($F(5, 18) = 0.05856$)).

2.4. Discussion

The results described in this chapter indicate that some *Pseudomonas* isolates have the potential to antagonise *Z. tritici* blastospores through as yet unknown mechanisms. The results also indicate the complexity of assessing antagonistic potential of biocontrol agents against a pathogenic fungus with a complex life cycle

and multiple growth morphologies, and the difficulties in translating *in vitro* antagonism data to more natural systems.

2.4.1. *Z. tritici* blastospores can be utilised in a qualitative high throughput assay for fungal antagonism by *Pseudomonas* isolates

The results from this chapter indicate that some *Pseudomonas* isolates possess the ability to antagonise *Z. tritici* blastospores *in vitro*. Of 534 bacterial isolates within the *Pseudomonas* libraries that were assessed in the initial screen, 52 exhibited an antagonistic phenotype against *Z. tritici* blastospores *in vitro*. These results indicate that the 'yeast-like' growth form of *Z. tritici* blastospores can be utilised in a high throughput antagonism screen of environmental bacterial isolates for fungal antagonism. Zones of clearing observed in the assay are indicative of the secretion of fungistatic or fungicidal compounds produced by the pseudomonads *in vitro*. An alternative explanation for this effect, e.g. competition for resources, would not create a clear, radial zone of clearing around the bacterial colony. The production of a volatile compound cannot be ruled out, as the agar plates were inverted, although the radial shape of the zones of clearing are more likely to indicate a diffusion of secreted compounds through the agar. For this reason, a positive result in the *Z. tritici* blastospore antagonism assay can be interpreted as that the *Pseudomonas* isolate possesses the biosynthetic potential to antagonise *Z. tritici* through the production of secreted compounds. The method developed and described here is simple to conduct, using common laboratory reagents and enables the assessment of 48 bacterial isolates per agar plate in a qualitative manner. The increase in throughput in screening bacterial isolates for fungal antagonism could speed up the discovery of bacterial biocontrol agents and/or biocontrol compounds of bacterial origin effective against *Z. tritici*. This screen could help prioritise antagonistic bacterial isolates for low-throughput screening against other plant pathogenic fungi, such as *Fusarium graminearum* or *Gaeumannomyces var. tritici*. An *in vitro* screen used to identify antagonistic

actinomycete bacteria effective against *Magnoportha oryzae* consisted of the dual culture of single bacterial isolates per plate (Xu et al., 2017). The work in that study screened 482 actinomycete strains over 482 plates. Using the blastospore assay methodology described in this chapter the same number of bacteria could be assessed using just 11 agar plates (per replicate), a clear increase in assay throughput. Due to the close spacing of the *Pseudomonas* isolates within the blastospore antagonism assay at this throughput (48 isolates per plate), there may be interaction effects between bacterial isolates. For this reason, data collected at this stage is qualitative, with concentric zones of inhibition indicating a positive antagonism phenotype as an initial screen. This result should be interpreted as the bacterial isolate possessing the biosynthetic potential to antagonise *Z. tritici in vitro*. Quantitative assessment of *Z. tritici* blastospore antagonism *in vitro*, a lower throughput (12 isolates per plate) is addressed in Chapter 5. The *in vitro* 'yeast-like' growth of *Z. tritici* has previously been referred to as macropycnidiospores (Steinberg, 2015), and later blastospores (Francisco et al., 2019), in reference to the mechanism by which the cells asexually reproduce, blastosporulation. Pycnidiospores, consisting of micro and macropycnidiospores, form a major part of the natural *Z. tritici* infection cycle, being dispersed from pycnidia- the fruiting bodies of *Z. tritici*, by rain splash, before germinating to form hyphae on the leaf surface (Steinberg, 2015; Wiese, 1987). Whilst blastospores and macropycnidiospores differ in their nomenclature, due to the mechanism by which the cells are derived, they are morphologically and transcriptomically identical, and were both referred to as macropycnidiospores (Steinberg, 2015), prior to Francisco et al in 2019. All publications studying the infection of wheat plants have utilised blastospores. Whilst the environmental conditions within the *in vitro Z. tritici* blastospore antagonism assay differ from the *in planta* conditions in the natural infection cycle of *Z. tritici*, the mechanisms by which blastospore growth is inhibited *in vitro* may have potential applications to control pycnidiospores in the natural infection cycle of *Z. tritici in planta*. Other spore types of *Z. tritici*, such as

ascospores, are technically infeasible to screen for antagonism *in vitro*, as ascospores would differentiate to form blastospores on rich media, and germinate to form hyphae under nutrient poor media (Morais et al., 2015; Steinberg, 2015; Suffert et al., 2011). *Z. tritici* isolate IPO323 was utilised in all assays within this chapter, as it a well characterised reference strain, with a complete genome sequence. IPO323 was first isolated in the Netherlands in 1984 (Goodwin et al., 2011). Within natural agricultural systems, *Z. tritici* populations have significant genetic diversity (Chen and McDonald, 1996). It will be important to screen multiple *Z. tritici* genotypes through this system, to investigate if antagonism is observed across *Z. tritici* genotypes, including strains isolated after observed resistance to multiple fungicide classes (Blake et al., 2018; Cheval et al., 2017), have arisen since the isolation of IPO323. It will be interesting to investigate if resistance to conventional fungicides, and the mechanisms by which resistance is achieved, correlate with resistance to microbial antagonism *in vitro* and *in planta*.

2.4.2. No statistically significant association between *Pseudomonas* isolation niche and *in vitro Z. tritici* blastospore antagonism phenotype

These results indicate that there is no significant association between the isolation niche and observed proportion isolates observed to antagonise *Z. tritici* blastospores qualitatively *in vitro*.

However, *Pseudomonas* isolates derived from rhizosphere samples are not necessarily incapable of colonising the wheat endosphere. Likewise, *Pseudomonas* isolates derived from endosphere samples may also exist within the wheat rhizosphere. For these reasons, it is not possible to truly distinguish endosphere competent *Pseudomonas* isolates from isolates that solely exist within the rhizosphere compartment. This highlights an important distinction between niche isolation source, and niche competence ability of a bacterial isolate. Whilst

these results indicate that preliminary analysis indicates no statistically significant association between *Z. tritici* blastospore antagonism ability *in vitro* and isolation niche, further experiments to determine endosphere competence of isolates, and how this relates to *Z. tritici* blastospore antagonism, or fungal antagonism more generally, may yield differing results. Previous studies have indicated pathogen-induced activation of the endophytic microbial consortia within *Beta vulgaris subsp. vulgaris* (Sugar Beet) roots and associated secondary metabolite biosynthetic gene clusters (BGCs), were found to be essential for disease suppression of *Rhizoctonia solanii*. It will be interesting to investigate whether similar disease suppressive endophytic microbial consortia exist within natural systems that are able to suppress *Z. tritici*.

Further investigations in the proportion of *Pseudomonas* isolates derived from other wheat plant compartments would be interesting to investigate, particularly the phyllosphere or phylloplane, to ascertain whether there are similar proportions of antagonistic *Pseudomonas* isolates across all compartments, or there is a greater evolutionary selection pressure for the ability to antagonise fungi within certain compartments.

2.4.3. Both antagonistic and non-antagonistic *Pseudomonas* isolates from the blastospore assay antagonise hyphal formation of *Z. tritici*

The observed antagonism of the hyphal growth form of *Z. tritici* by all *Pseudomonas* isolates tested did not correlate with the *Z. tritici* blastospore antagonism phenotype observed *in vitro*.

The hyphal antagonism assay incorporates a developmental switch between the ‘yeast-like’ blastospore suspension of *Z. tritici* that is applied to the plates, and the hyphal growth form, in response to the environmental conditions. It is possible that the *Pseudomonas* isolates screened in this assay were able to antagonise *Z. tritici* through disabling the ability of the *Z. tritici* blastospores to form hyphae in the area

closest to the *Pseudomonas* colony. This could be through the disruption of proteins that are essential for the formation of hyphae but are non-essential for the blastospore growth form of *Z. tritici*, by the *Pseudomonas* isolates through a yet unknown mechanism. A number of proteins essential for the successful development of *Z. tritici* hyphae have been described, such as *MgAlg2* (Motteram et al., 2011) or *ZtGT2* (King et al., 2017), that are involved in glycosylation. Disruption of both *MgAlg2* and *ZtGT2* separately result in an ability of *Z. tritici* to form hyphae yet have no discernible effect on the blastospore growth form. These results indicate the possibility of differing importance of gene targets within *Z. tritici* for the hyphal and blastospore growth forms and raise the prospect of differing sensitivity of these growth morphologies to antagonists. The hyphal antagonism assay described in this chapter does induce limited, although not extensive, hyphal growth of *Z. tritici,* that can be observed on the side of the *Z. tritici* colony furthest away from the *Pseudomonas* colony in Figure 2.3 (b&c). The hyphal confrontation assay was conducted on ½ strength PDA, to balance nutritional requirements of the *Pseudomonas* colony and induce the hyphal growth form of *Z. tritici*. True hyphal growth of *Z. tritici* is usually studied on water agar containing no dextrose. This highlights a constraint in the design of confrontation assays with the hyphal growth form of *Z. tritici*, as the environmental conditions required to induce hyphal growth must be balanced with nutritional needs of *Pseudomonas* isolates. Another potential explanation for the observation that *Pseudomonas* isolates, previously observed to be antagonistic and non-antagonistic towards *Z. tritici* blastospores *in vitro*, all appeared to antagonise the hyphal growth form of *Z. tritici in vitro*, could be due to the environmentally regulated growth dimorphism of *Z. tritici*. Whilst the experiment was conducted at temperatures conducive to the hyphal growth form of the fungus, the nutrient status of the area surrounding the *Z. tritici* hyphae may have been altered through the solubilisation and accumulation of nutrients by the nearby *Pseudomonas* colony. These conditions may have been conducive to blastopore growth of *Z. tritici*, and repress hyphal formation. The dimorphic switch

of *Z. tritici* is not absolute, with intermediate nutrient availability and temperatures shown to produce both hyphal and blastospore growth *in vitro* (Steinberg 2015). Further experiments will be necessary to deduce whether the apparent lack of *Z. tritici* hyphal growth close to the *Pseudomonas* colony is direct antagonism, or repression of the hyphal growth form of the fungus. This highlights a potential key difficulty in the screening of microbial isolates for *Z. tritici* hyphal antagonistic *in vitro*, and more generally, as similar difficulties in differentiating direct antagonism from repression of the hyphal growth form of *Z. tritici* may be similarly seen when screening cell-filtrates against the hyphal growth form of the fungus *in planta,* which has been routinely carried out in a number of studies (Lynch et al., 2016), and may explain the observed antagonism of hyphae *in planta*, yet absence of antagonism of blastospores *in vitro* in another study (Kildea et al., 2008). These provisional observations indicate that the *Z. tritici* hyphal antagonism assay described within this chapter requires further optimization and experimentation to further understand the mechanisms by which the hyphae are antagonised and/or repressed by the presence of *Pseudomonas* isolates *in vitro*.

2.4.4. Inoculation of wheat leaves with *Z. tritici* antagonistic *Pseudomonas* isolates did not affect disease severity

The results indicate that the application of *Pseudomonas* inoculum to wheat leaves did not visibly alter leaf disease symptoms at 21 days post inoculation when compared to the 0.01% Tween-20 control. The antagonistic phenotype observed by *Pseudomonas* against *Z. tritici* blastospores *in vitro* did not correlate with an observable reduction in the disease progression or severity of *Z. tritici* at 21 days compared to a 0.01% Tween-20 control. The difference in antagonism could be due to the environmental differences between the *in vitro* blastospore antagonism assay, and the *in planta* biocontrol assay. The blastospore antagonism assay was conducted on PDA, which is considered a rich growth medium, containing nutrients and macronutrients, alongside dextrose as a source of carbon. The phyllosphere

of wheat plants is a comparatively nutrient poor environment (Vorholt, 2012), with markedly lower levels of available nutrients and sugars compared to rich nutrient agars such as PDA. It has been found that the population size of *P. fluorescens* A506 was limited by the availability of carbon sources on the leaf surface of bean plants (Phaseolus vulgaris L. cv. Bush Blue Lake) (Mercier and Lindow, 2000). Further experiments to investigate the number of colony forming units (CFUs) of the inoculated *Pseudomonas* bacteria, throughout the time course of *Z. tritici* inoculation and disease progression, will shed light on if the *Pseudomonas* bacteria are able to persist upon and within the wheat leaf surface after initial inoculation.

Another factor that could reduce the ability of *Pseudomonas* isolates to antagonise *Z. tritici in planta*, is the colonisation of the wheat leaf tissue during inoculation. The phyllosphere, whilst a relatively nutrient-poor environment compared to PDA, will harbour a microbiome before inoculation with *Pseudomonas*. The phyllosphere microbiome may contain microbes that themselves are antagonistic towards *Pseudomonas* isolates or are perhaps better able to compete for scarce nutrients in the phyllosphere. The ability of *Pseudomonas* isolates to successfully colonise the phyllosphere may vary between isolates, and the ability of antagonistic *Pseudomonas* isolates to antagonise *Z. tritici* in nutrient-poor environments may similarly vary depending on the underlying mechanisms of antagonism. This complex interaction between *Pseudomonas* inoculum, *Z. tritici* inoculum, the wheat leaf and potential leaf microbiome could explain why the deployment of biocontrol agents in some settings can be effective, and ineffective in others. It should also be noted that the *in planta* disease assessment was conducted using a single cultivar of bread wheat, Riband, and a single genotype of *Z. tritici* as fungal inoculum, IPO323. In agricultural settings, other elite varieties of bread wheat are commonly grown, and infection with *Z. tritici* commonly takes place with many genotypes of *Z. tritici* simultaneously (Chen and McDonald, 1996). If a promising *Z. tritici* biocontrol agent, effective *in planta*, is identified in future experiments, it will be important to screen against multiple genotypes of *Z. tritici*, on multiple wheat

cultivars to gain a better understanding of how consistently biocontrol is achieved, and if this effect better translates to a field setting from controlled environments.

2.4.5. Inoculation of wheat leaves with *Pseudomonas* isolates before subsequent infection with *Z. tritici* did not alter pycnidia formation or pycnidiospore production

The results indicate that the application of *Pseudomonas* inoculum alone to wheat leaves did not produce a visible effect compared to 0.01% Tween-20 controls. The results indicate that the application of *Pseudomonas* inoculum prior to infection with *Z. tritici* did not significantly alter pycnidiospore production. Pycnidia formation (asexual sporulation), leading to pycnidiospore production is the most important and essential step in the spread of *Z. tritici* infection throughout wheat fields by rain splash (Sanderson et al., 1985; Steinberg, 2015). The results may indicate that curative (late) application of antagonistic *Pseudomonas* isolates would have little to no effect on the local transmission of *Z. tritici* conidiospores within a wheat field setting, as this is the stage of *Z. tritici* infection where blastospores are most prevalent on the wheat leaf surface. The finding that *Pseudomonas* isolates previously identified as exhibiting both antagonistic, and non-antagonistic phenotypes *in vitro* showed no statistically significant difference in the number of recovered pycnidiospores could be indicative of the environmental conditions within the *in planta* experiment as being unconducive to the *Z. tritici* antagonism. This could be due to environmental cues, such as reduced carbon availability on the leaf surface compared to PDA, causing the repression of antifungal molecules (Shanahan et al., 1992). A statistically significant reduction in the pycnidial coverage of *Z. tritici* on wheat leaves has been reported, after application with *Pseudomonas putida* inoculum hours prior to subsequent inoculation with *Z. tritici* blastospores (Flaishman, 1996). Other studies have reporting varying success with the use of *Pseudomonas* isolates as biocontrol agents, with wheat cultivar and field season seeming to play an important role in outcomes (Kildea et al., 2008; Lynch

et al., 2016). It will be important to investigate if differences in the success of *in planta* inhibition in different environmental conditions, with different wheat cultivars, or with mixed genotypic *Z. tritici* inoculum more representative of natural systems, as part of future *in planta* experiments. *In planta* experiments are important to carry out, as it is possible to observed other mechanisms of biocontrol such as inducing plant systemic resistance or priming plant defences that are not possible to screen for *in vitro* (Choudhary et al., 2007).

These findings, within the context of my PhD project, led me to focus on *Z. tritici* inhibition by *Pseudomonas* within the *in vitro* antagonism system, as a means to first identify *Pseudomonas* isolates with the genetic and/or biosynthetic capability to antagonise *Z. tritici* blastospores. By first identifying mechanisms of *Z. tritici* antagonism within a simplified *in vitro* system, it is hoped that more directed *in planta* antagonism assays will be conducted in the future.

2.5. Conclusions

Pseudomonas isolates can be screened in a rapid, high-throughput manner for antagonism of *Z. tritici in vitro*.

Z. tritici hyphae appear to be inhibited by both antagonistic and non-antagonistic *Pseudomonas* isolates *in vitro*.

Antagonistic *Pseudomonas* isolates, identified through the *Z. tritici* blastospore screen, do not appear to alter STB disease symptoms or severity *in planta*, and did not significantly alter pycnidiospore production.

Chapter 3. Quality assessment and phylogenetic analysis of generated *Pseudomonas* genome assemblies

3.1. Introduction

This chapter describes the investigation into links between taxonomy and *Pseudomonas* isolates observed to exhibit an antagonistic and non-antagonistic phenotype towards *Z. tritici* blastospores *in vitro*, as described previously in Chapter 2. This chapter will also investigate taxonomic enrichments in *Pseudomonas* isolated from specific environments.

The *Pseudomonas* genus contains 144 distinct species, which is the largest number of species within a genus for gram-negative bacteria (Gomila et al., 2015). *Pseudomonas fluorescens* species are themselves said to exist within a species complex, comprising 9 distinct subgroups (Garrido-Sanz et al., 2016; Mulet et al., 2010). As described in Chapter 2, the *Pseudomonas* library used in the *in vitro* blastospore antagonism assay was derived from endospheric and rhizospheric samples of wheat, and bulk soil samples (Mauchline et al., 2015). A taxonomic comparison and classification of *Pseudomonas* isolates exhibiting a fungal antagonistic phenotype against *Z. tritici* has not been conducted, due to the relatively low number of antagonistic *Pseudomonas* isolates previously described as exhibiting a fungal antagonistic phenotype.

Taxonomic classification and phylogenetic analysis allow the comparison of bacterial isolates and their relation to each other. Taxonomic assessment of environmental bacterial isolates would traditionally be carried out through observation of physical characteristics. Modern taxonomic classification of environmental bacterial isolates relies on DNA sequencing-based techniques. The advent of Sanger-based DNA sequencing technologies and polymerase chain reaction (PCR) enabled species to be taxonomically classified by genetic

elements. This would be conducted using DNA sequences of ‘housekeeping’ genes involved in core cellular processes, that exist as single copy homeologues or 16S rRNA gene sequences from the bacterial isolate. The concatenation of multiple ‘housekeeping’ gene sequences would allow for greater resolution when comparing bacterial isolates through multiple sequence alignments, and has routinely been used as a method to determine phylogeny (Gomila et al., 2015).

Recent reductions in the cost of DNA sequencing approaches, have made ‘whole genome’ sequencing for taxonomic classification and phylogenetic assessment economically feasible, using bioinformatic tools. New approaches allow taxonomic classification at the level of individual sequencing reads, through bioinformatic software such as Kraken (Wood and Salzberg, 2014), and at the genome assembly level, through the construction of phylogenetic trees using software such as FastTree2 (Price et al., 2010). FastTree2 is a bioinformatic software that allows the construction of phylogenetic trees from whole genome sequence data, through the concatenation and subsequent multiple sequence alignment of a set of orthologous genes. These tools allow for a greater resolution when assigning taxonomy to bacterial isolates and allow the comparison of genome assemblies with publicly available reference genomes. Identification of contamination within genome assemblies, and the assessment of genome annotation completeness, is possible through analysis of single copy orthologous genes within the genome assembly, using bioinformatic software such as Benchmarking Universal Single Copy Orthologs (BUSCO) (Simão et al., 2015).

The phylogenetic distribution of *Z. tritici* blastospore antagonistic and non-antagonistic *Pseudomonas* isolates within the *Pseudomonas* genus is currently unknown. This chapter describes the quality assessment of *Pseudomonas* genome assemblies generated as part of this project, and phylogenetic assessment of *Z. tritici* blastospore antagonistic and non-antagonistic *Pseudomonas* isolates through ‘whole-genome’ based bioinformatic approaches.

Hypothesis:

(1) *Pseudomonas* isolates exhibiting a *Z. tritici* blastospore antagonism phenotype *in vitro* form a distinct clade within a constructed phylogeny.

3.2. Chapter specific methods

3.2.1. DNA extraction

Genomic DNA was extracted from 500ul of LB overnight bacterial cultures, using a GenElute™ Bacterial Genomic DNA Kit according to manufacturer's instructions, except for eluting in 200ul nuclease free water in the final elution step (ThermoFisher Scientific). *Pseudomonas* isolates were cultured from glycerol stocks stored at -80°C, by inoculating 10ml of LB Miller Broth (Formedium), with a chip of frozen glycerol stock. The inoculated broth was placed in a shaking incubator at 180 rpm and 25°C overnight (~18hours).

3.2.2. DNA quantification

DNA was quantified using Qubit Fluorometric Quantification (Life Technologies), according to the manufacturer's instructions, to ensure that genomic DNA samples met the minimum criteria for genome sequencing at MicrobesNG (1ng/ul). DNA samples for all 129 isolates met the minimum criteria required.

3.2.3. DNA sequencing and genome assembly construction

Draft genome assemblies were constructed for a subset of *Pseudomonas* isolates screened for *Z. tritici* blastospore antagonism in Chapter 2. Genome assemblies were constructed for a total of 129 *Pseudomonas* isolates, comprising of 38 *Z. tritici* blastospore antagonistic and 91 non-antagonistic *Pseudomonas* isolates.

Genome sequencing was undertaken by MicrobesNG, using 250bp paired end Illumina MiSeq. Sequences were passed through a bioinformatic pipeline consisting of Kraken, BWA mem, before genomes were assembled *de novo* using SPAdes and annotated using Prodigal by MicrobesNG. A total of 129 genome assemblies were generated.

3.2.4. BUSCO (Benchmarking Universal Single-Copy Orthologs) analysis

BUSCO analysis of genomes was carried out on a local server using BUSCO version 4.0.12, using the odb11 reference single copy orthologous genes dataset for bacterial species.

3.2.5. Phylogenetic tree construction

A phylogenetic tree based on whole genomes was constructed using FastTree2 (Price et al., 2010), using the app developed and deployed by Roman Sutormin on KBase (version 2.2.0) (Arkin et al., 2018). 20 of the closest publicly available genomes were included in the multiple sequence alignment and phylogenetic tree construction. Phylogenetic trees and annotations were edited using International Tree Of Life (Letunic and Bork, 2019).

3.2.6. Construction of Sankey diagram

Sankey diagram was constructed using SankeyMATIC.

3.3. Results

3.3.1. Initial quality control assessment of environmental *Pseudomonas* genome assemblies

To assess the quality of *Pseudomonas* genome assemblies generated by MicrobesNG, genome assemblies were subjected to a multi-step quality control pipeline (Figure 3.1).

To first assess the completeness of core genes within the generated genome assemblies and identify chimeric genome assemblies containing genes from multiple bacterial sources, analysis of single copy orthologous genes within genome annotations was conducted. This analysis was carried out using Benchmarking Universal Single-Copy Orthologs (BUSCO) software. BUSCO analysis was conducted on 129 genome assemblies, consisting of 38 *Z. tritici* blastospore antagonistic and 91 non-antagonistic genome assemblies identified in Chapter 1 (Figure 3.2). BUSCO analysis revealed 31 genome assemblies, consisting of 15 antagonistic and 16 non-antagonistic *Pseudomonas* isolates, were found to contain a significant number of multiple copies of single copy orthologous genes, defined as a BUSCO score lower than < 95, and were omitted from further downstream analysis. 98 genome assemblies were found to have good annotation completeness, as defined by a BUSCO score > 95, with 23 antagonistic and 75 non-antagonistic isolates passing this step (Supplementary Table 3).

Secondly, genome assemblies were taxonomically classified by MicrobesNG with Kraken (Supplementary Table 3). Of the genome assemblies passing the BUSCO QC step, 3 were identified as containing Enterobacteriaceae as the most frequent family, with *Serratia proteamaculans* as the most frequent species present within the assembly (Supplementary Table 3). To assist with downstream comparative analyses, these genome assemblies were omitted from downstream analyses.

Thirdly, the gene copy number status of single-copy orthologous gene, *gyrB*, was assessed in the 95 genome assemblies passing the two previous QC steps. Six *Pseudomonas* genome assemblies were found to contain multiple copies of *gyrB* and were omitted from further analyses (Supplementary Table 3.).

One *Pseudomonas* isolate, Roth 22, was unrecoverable from the glycerol stock within the collection, and was omitted from further analyses.

A total of 88 *Pseudomonas* genome assemblies passed the QC steps outlined, corresponding to 17 *Z. tritici* blastospore antagonistic and 71 non-antagonistic isolates (Figure 3.1).

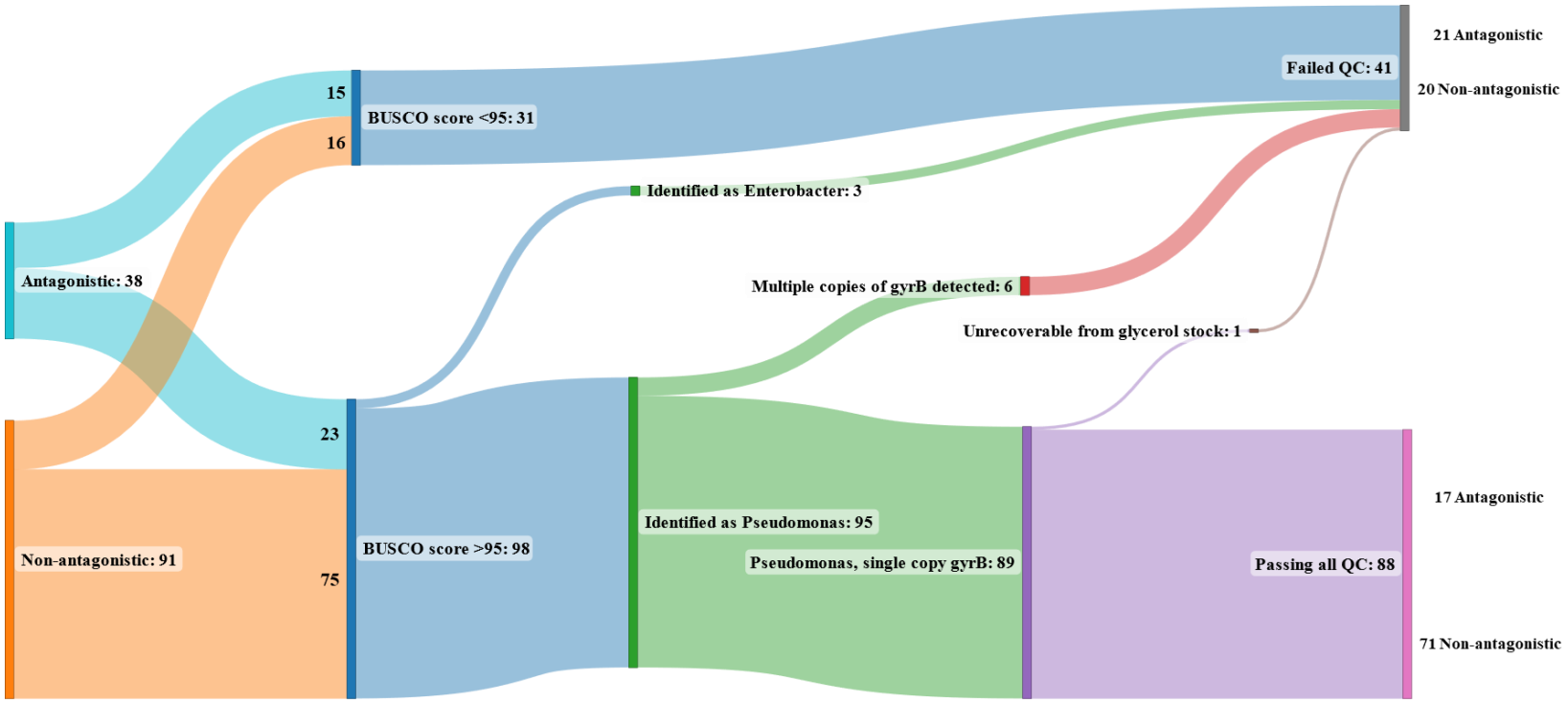


Figure 3.1. Overview of genome assembly quality control process.
A Sankey diagram illustrating the number of *Pseudomonas* genome assemblies passing quality control thresholds. Genome assemblies with a BUSCO score of < 95, identified as *Enterobacter* using Kraken by MicrobesNG, were unrecoverable from glycerol stocks, or containing multiple copies of *gyrB* were removed from downstream comparative analysis.



Figure 3.2. Status of 124 single copy orthologous genes within 129 *Pseudomonas* genome assemblies assessed by BUSCO.
A chart indicating the status of 124 single copy orthologous genes within genome assemblies indicated by BUSCO analysis (Complete single copy BUSCO genes are indicated by blue bars, duplicated as orange bars, fragmented genes as grey bars, and BUSCO genes missing from genome assemblies are indicated as yellow bars).

3.3.2. Assessment of the phylogenetic distribution of *Pseudomonas* isolates

To assess the phylogenetic distribution of the 17 antagonistic and 71 non-antagonistic single *Pseudomonas* isolates, a phylogenetic tree was constructed. The phylogenetic tree was constructed using the FastTree2 app on KBase, and the closest 20 publicly available reference genomes were automatically identified and incorporated into the phylogenetic tree (Figure 3.2). To examine the distribution of the *Z. tritici* blastospore antagonism phenotype within the phylogenetic tree, blastospore antagonism data was overlaid onto the phylogenetic tree using Interactive Tree Of Life (ITOL) (Letunic and Bork, 2019). To investigate correlations between sampling location with *Z. tritici* blastospore antagonism phenotype and phylogeny, sampling metadata was also overlaid onto the phylogenetic tree (red, yellow and green coloured leaf labels indicating rhizosphere, bulk soil, and endosphere isolation source respectively).

It was found that the 88 *Pseudomonas* isolates formed 3 distinct clades with reference isolates, within the overall phylogeny. Seven *Pseudomonas* isolates formed a distinct clade with reference isolate *P. fluorescens* F113 (turquoise highlighted branches), 34 *Pseudomonas* isolates formed a clade with reference isolate *P. lurida* L228 (pink highlighted branches), and 47 *Pseudomonas* isolates formed a clade with *P. koreensis* D26 (purple highlighted branches). All 7 *Pseudomonas* isolates forming a clade with reference isolate *P. fluorescens* F113 were isolated from the endosphere, with 6 out of 7 *Pseudomonas* isolates within this clade previously shown to exhibit an antagonistic phenotype against *Z. tritici* blastospores *in vitro*. Of the 34 *Pseudomonas* isolates forming a clade with reference isolate *P. lurida* L228, 24 were isolated from rhizospheric samples, and 10 were isolated from endospheric samples. It was found that 5 of the 34 *Pseudomonas* isolates within this clade were previously observed to antagonise *Z. tritici* blastospores *in vitro*. A total of 47 *Pseudomonas* isolates formed a clade with

reference isolate *P. koreensis* D26, consisting of 14 *Pseudomonas* isolates derived from rhizosphere samples, 20 from endosphere samples, and 13 from bulk soil samples. Of these 47 isolates, 6 were observed to exhibit an antagonistic phenotype against *Z. tritici* blastospores *in vitro*.

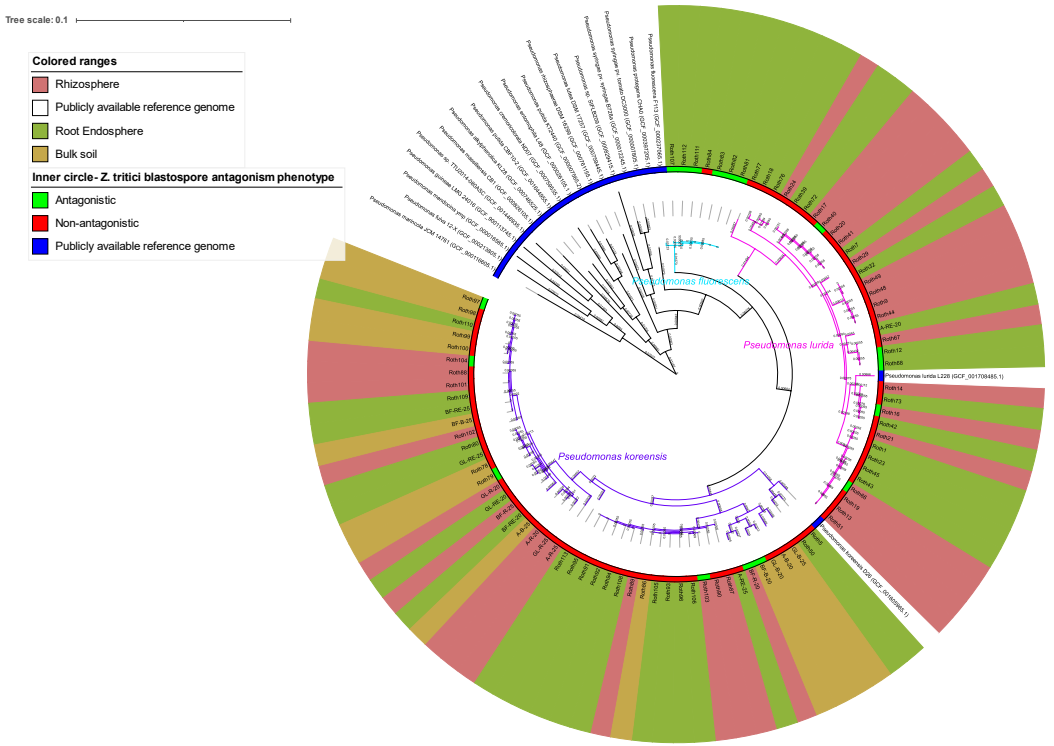


Figure 3.3 Phylogenetic distribution of *Z. tritici* blastospore antagonistic and non-antagonistic *Pseudomonas* isolates.

A phylogenetic tree based on 108 *Pseudomonas* genome assemblies was constructed using FastTree2 in KBase, consisting of 17 antagonistic *Pseudomonas* isolates (green inner circle), 71 non-antagonistic *Pseudomonas* isolates (red inner circle), and 20 of the closest publicly available reference genomes (blue inner circle). The isolation source of *Pseudomonas* isolates is indicated with brown (bulk soil), red (rhizosphere) and green (endosphere) coloured labels. The 3 distinct clades formed with publicly available reference isolates are highlighted, *P. koreensis* D26 (purple), *P. lurida* L228 (pink), and *P. fluorescens* F113 (turquoise). This figure is a scalable graphics vector, with all detail visible if magnification is increased.

3.4. Discussion

The results described in this Chapter indicate that the library of 88 single *Pseudomonas* isolates consist of *P. fluorescens*, *P. lurida*, and *P. koreensis* bacterial species. Of these taxonomic groups, the *P. fluorescens* group contains the highest proportion of *Z. tritici* blastospores antagonistic isolates. The *Z. tritici* blastospore antagonism phenotype does not form a single distinct clade within the phylogeny, indicating that *P. fluorescens*, *P. lurida*, and *P. koreensis* isolates are capable of antagonising *Z. tritici* blastospores *in vitro*.

3.4.1. Contamination of genome assemblies detected using BUSCO

The presence of genome assemblies predicted to be *Serratia proteamaculans* at the species level, and as a potential source of contamination of *Pseudomonas* genome assemblies, is most likely due to co-isolation of *S. proteamaculans* as part of initial isolation efforts, where *Pseudomonas* selective agar containing CFC (Cetrimide 10mg/l, Fucidin 10mg/l, Cephalosporin 50mg/l) antibiotics was used to select colonies, before streaking to extinction 3 times (Tim Mauchline, personal communication). In future studies, it may be beneficial to include a quality control step before DNA samples are sent for genome sequencing, consisting of the sequencing a gene or genomic region that is divergent between *Pseudomonas* isolates and Enterobacter species, to reduce the potential of chimeric assemblies consisting of a mixture of the two species. A recent study isolating *Pseudomonas* species from Salmon processing environments, also utilised *Pseudomonas* selective agar containing CFC antibiotics, and classified some isolates as Serratia by 16S rRNAand *rpoD* gene sequencing (Thomassen et al., 2022), among members of other genuses, indicating that the media is not completely selective for pseudomonads. Where genome assemblies were found to contain duplicate BUSCO genes, the most likely cause for contamination is due to incomplete separation of isolates through streaking to extinction. To avoid this, sequencing of

PCR fragments of single copy, polymorphic genes such as 16S rRna or *gyrB* genes could be used as a diagnostic for colonies- with low quality sequencing of the region indicating the presence of multiple variants of the single gene locus within the sample, suggesting the presence of two distinct microbes and incomplete separation of single colonies. 16S rRNA or *rpoD* gene sequencing could also be used prior to genome sequencing to classify *Pseudomonas* isolates, as described in (Thomassen et al., 2022), using bioinformatic tools such as Kraken 2 (Lu), or QIIME 2 (Bolyen et al., 2019). An alternative approach could include a include a modification to *Pseudomonas* selective (CFC) agar, to distinguish between pseudomonads and Enterobacteriaceae, through the addition of arginine and phenol red producing a pink colouration around only pseudomonad colonies (Stanbridge and Board, 1994). Distinguishing between closely associated environmental *Pseudomonas* isolates at an early stage may prove challenging, as isolates may be closely related and be of the same sub-species. In this case, additional rounds of streaking cultures to extinction would reduce the potential of generating *Pseudomonas*-only chimeric genome assemblies.

3.4.2. *G*enome assemblies generated through 250bp Illumina MiSeq are sufficient to compare bacterial phylogenies

Genome assemblies were constructed from 250bp Illumina MiSeq sequencing by MicrobesNG. All 88 *Pseudomonas* genome assemblies examined through BUSCO analysis, and determined to show no evidence of contamination, were shown to have BUSCO scores > 95, which indicates a high level of genome annotation completeness for core genes. These results indicate that short read sequencing can generate good quality bacterial genome assemblies, for further downstream analysis, including taxonomic classification.

3.4.3. *Zymoseptoria tritici* blastospore antagonistic *Pseudomonas* isolates are distributed throughout the *P. fluorescens*, *P. lurida* and *P. koreensis* subclades of a phylogeny

The results from this Chapter indicate that the library of 88 single *Pseudomonas* isolates form 3 distinct clades within a phylogeny built with the closest publicly available reference isolates. 7 *Pseudomonas* isolates form a clade with *P. fluorescens* isolate F113, 34 form a clade with *P. lurida* isolate L228, and 47 isolates form a clade with *P. koreensis* isolate D26. There appears to be an enrichment for *Z. tritici* blastospore antagonistic *Pseudomonas* isolates within the *P. fluorescens* clade, compared to the *P. lurida* and *P. koreensis* clade. Over 85% of *P. fluorescens* isolates within the library exhibited an antagonistic phenotype, compared to 14% and 12% within the *P. lurida* and *P. koreensis* clades respectively. However, a lower number of *P. fluorescens* isolates were observed compared to *P. lurida* and *P. koreensis* isolates. *P. fluorescens* isolates Roth81, Roth82, Roth83, and Roth111 appear to be closely related, or potentially clonal, with branch lengths of 0 indicated on the phylogenetic tree. This result is indicative of no differences in the multiple sequence alignments of 49 concatenated orthologous genes used to construct the phylogenetic tree. Interestingly, Roth84 exhibits a non-antagonistic phenotype against *Z. tritici* blastospores, yet is highly similar, in the multiple sequence alignment of 49 COG genes, to Roth81, Roth82, Roth83, and Roth111, that all exhibit an antagonistic phenotype. Further investigations into similarities and differences in other regions of the genomes of these genetically similar isolates could uncover potential mechanisms underlying the fungal antagonism phenotype. The results also indicate an enrichment for *P. koreensis* isolates within bulk soil samples, with all 13 bulk soil derived isolates assessed to be within this clade. The sub-species *P. koreensis* was first described in 2003, with type strain Ps 9-14T isolated from agricultural soil from the Umsong region of South Korea using P1 agar (Kwon et al., 2003). *P. fluorescens* have previously been shown to be efficient colonisers of soil (Varivarn et al., 2013), yet

no isolates derived from bulk soil samples were predicted to be *P. fluorescens* at the species level. Similarly, there appears to be a selection for *P. lurida* isolates within the endosphere and rhizosphere associated *Pseudomonas* isolates, compared to bulk soil associated *Pseudomonas* isolates. This is an interesting result, as *P. lurida* isolates have previously been shown to be associated with the phyllosphere of grass species (Behrendt et al., 2007). The phylogenetic tree indicated that the *Z. tritici* blastospore antagonism phenotype was dispersed throughout the phylogenetic tree and did not appear to form a distinct single clade within genome sequences analysed. These results indicate that whilst there appears to be an enrichment for *Z. tritici* blastospore antagonism in the *P. fluorescens* clade, some *P. lurida* and *P. koreensis* isolates also exhibit an antagonistic phenotype.

Pseudomonas koreensis isolate S150, isolated from the tobacco rhizosphere, has previously been shown to exhibit *in vitro* antifungal activity against *Phytophthora nicotianae* and *Rhizoctonia solani,* with Lokisin-encoding genes within a predicted NRPS associated with anti-fungal capacity (Gu et al., 2020). Our results suggest that *P. koreensis* strains isolated from the wheat rhizosphere exhibit the ability to antagonise pathogenic fungi from the phyllosphere *in vitro*. It will be interesting to investigate if some sub-species of *Pseudomonas* are found to more commonly exhibit fungal antagonism than others, by performing high throughput antagonism screening against collections of *Pseudomonas* sub-species, and whether fungal antagonism is achieved by different *Pseudomonas* subspecies by different mechanisms.

My results indicate that *Z. tritici* blastospore antagonism is not a monophyletic trait, as antagonistic *Pseudomonas* isolates appear throughout the constructed phylogeny. This may be indicative of multiple mechanisms by which environmental *Pseudomonas* isolates achieve *Z. tritici* blastospore *antagonism in vitro*. It should be noted that the environmental *Pseudomonas* isolates utilised in this study were

isolated from bulk soil, wheat rhizosphere and endosphere compartments, and that these compartments are not previously described as containing *Z. tritici* blastospores. Therefore, the presence of a *Z. tritici* blastospore antagonistic phenotype *in vitro* may be indicative of broad-spectrum fungal antagonism ability, as previously described in many studies involving fungal root pathogens of wheat (Mauchline et al., 2015). In an evolutionary context, our results indicate that *in vitro Z. tritici* blastospore antagonism has not arisen as a single evolutionary event within the *Pseudomonas* phylogeny constructed, and that horizontal transfer of genetic elements could be a mechanism by which this trait is distributed between environmental *Pseudomonas* isolates. Further investigations into the mechanisms by which the *Z. tritici* blastospore antagonism trait is achieved by the *Pseudomonas* isolates may be able to further resolve evolutionary questions arising around *Z. tritici* blastospore antagonism with greater resolution, as some mechanisms may indicate horizontal transfer, vertical transmission, or a mixture of both.

3.5. Conclusions

P. fluorescens, *P. lurida*, and *P. koreensis* isolates are capable of antagonising *Z. tritici* blastospores *in vitro*.

Over 85% of *Pseudomonas* isolates classified as *P. fluorescens* exhibited an antagonistic phenotype against *Z. tritici* blastospores *in vitro*.

Pseudomonas genome assemblies constructed from short-read sequencing are sufficiently complete in annotation to assess bacterial phylogeny through bioinformatic tools.

Chapter 4. Predictive Bioinformatics and chemical analysis of *Pseudomonas* secondary metabolism

4.1. Introduction

Bacterial secondary metabolism is a potentially underutilized source of novel compounds with important functions, such as antibiotics and antifungal compounds (Gross and Loper, 2009). Previous studies have described the involvement of bacterial secondary metabolites in the antagonism of *Z. tritici* (Levy et al., 1992, 1989), and many other fungal plant pathogens (Raaijmakers et al., 2002) by *Pseudomonas* isolates. Low throughput analytical chemistry approaches were previously employed to elucidate the secondary metabolites, produced by biocontrol bacteria, antagonistic towards fungal plant pathogens *in vitro* (Levy et al., 1992, 1989; Omoboye et al., 2019). Individual biocontrol bacteria can produce multiple secondary metabolites (Levy et al., 1992), which can slow discovery rate through analytical chemistry approaches.

Improvements in genetic sequencing technologies are revolutionising discovery platforms through the ability to now sequence whole genomes at high throughput and low cost. These can then be interrogated to identify the likely basis of physiological traits. New predictive bioinformatic tools, such as antiSMASH, enable the prediction of secondary metabolite biosynthetic gene clusters (BGCs) from genome assemblies (Blin et al., 2019) and network analysis of BGCs based on sequence similarity through BiG-SCAPE (Navarro-Muñoz et al., 2020). The Minimum Information about a Biosynthetic Gene Cluster (MiBIG) repository is a standardised database of known biosynthetic gene clusters and annotations, enabling the integration of previously described BGCs into comparative approaches (Kautsar et al., 2019; Medema et al., 2015). Together, these new bioinformatic tools and resources could enable rapid, low-cost, and high throughput analysis of the secondary metabolite potential of bacterial species,

through the analysis of genome assemblies. This increase in throughput could, in turn, permit the application of comparative genomic approaches to identify predicted secondary metabolite BGCs within genome assemblies that are associated with a phenotype, which has not been possible with the conventional approach of analytical chemistry, due to throughput limitations.

The application of these approaches and resources to investigate the potential involvement of secondary metabolites in a fungal antagonistic phenotype of *Pseudomonas* species has not been conducted. This Chapter describes an integrated approach, combining predictive bioinformatics, network analysis and comparative genomics to elucidate the potential involvement of secondary metabolism in the antagonism of *Z. tritici* blastospores by *Pseudomonas* isolates *in vitro*. Specifically, I aimed to determine whether antagonistic bacteria were enriched for predicted secondary metabolite clusters compared to non-antagonistic, and whether any particular known (or unknown) clusters could be found to associate with the antagonism phenotype. Finally, I sought to assess the *in vitro* activity of a well characterised antifungal secondary metabolite, 2,4-DAPG.

Hypothesis:

(1) Genome assemblies of *Z. tritici* antagonistic *Pseudomonas* isolates contain predicted antifungal secondary metabolite biosynthetic gene clusters.

4.2. Chapter specific methods

4.2.1. Secondary Metabolite Biosynthetic Gene Cluster Prediction

Secondary metabolite gene clusters were predicted using antiSMASH 5.2 on a local server for 17 antagonistic and 71 non-antagonistic *Pseudomonas* genome sequences.

4.2.2. Sequence similarity network analysis of predicted Secondary Metabolite Gene Clusters

Sequence similarity networks were constructed from the antiSMASH output of 17 antagonistic and 71 non-antagonistic *Pseudomonas* genome sequences, using BiG-SCAPE on a local server. A cut-off value of 0.2 was used, and 1808 reference sequences from the MiBIG database were included in the construction of Gene Cluster Family (GCF) networks based on sequence similarity.

4.2.3. Chemical analysis of secreted secondary metabolites produced by *Pseudomonas* isolates

PDA (Formedium) plates were inoculated with 1ul bacterial overnight culture (prepared as described in chapter 2) of *Pseudomonas* isolate Roth112 alone, and in confrontation with *Z. tritici* blastospores as part of a *Z. tritici* blastospore *in vitro* antagonism assay (conducted as described in chapter 2). Plates were sealed and inverted, before being stored in darkness at 16 °C for 14 days. A 10mm diameter section of agar surrounding the *Pseudomonas* colony edge was excised from both treatments. Chemical extracts were prepared by macerating agar sections in 1ml MeOH, with resulting solutions centrifuged at >13000rpm for 10 minutes. Supernatant was collected for analysis by liquid chromatography-mass spectrometry (LC-MS).

Zymoseptoria tritici blastospore antagonism assays, followed by methanol extractions, were conducted by me. Total Ion Chromatograms (positive mode) were generated from methanol extracts by Dr David Withall, and peaks associated with the presence of 2,4-diacetylphloroglucinol (2,4-DAPG) identified by Dr David Withall (personal communication) through analysis of the MS, MS/MS fragmentation using Waters MassLynx data analysis software and comparison with an authentic standard.

Ultraperformance liquid chromatography-mass spectrometry (UPLC) methodology was adapted from Dr David Withall (personal communication) and Callum Williams (Williams, 2020). UPLC was conducted on agar extracts using an ACQUITY UPLC® system, consisting of an autosampler and binary pump (Waters, USA). Column separation was achieved using an AQUITY BEH C18 (1.7 µm, 2.1 x 50 mm) analytical column (Waters, USA), with extractions eluted over 38 minutes. Up to 95% organic (mobile phase used: UPLC grade water + 0.1% formic acid and methanol + 0.1% formic acid). The flow rate was 0.21 mL minute^{-1} with an injection volume of 4 µl. The UPLC system was coupled with Quantitative Time-of-Flight mass spectrometer SYNAPT G2-Si (Waters, USA), with electrospray ion source run in negative [M-H]- and positive [M+H]+ ionisation mode and data acquired over 50-1200 m/z range. The following optimised parameters were used for negative control: capillary voltage (2 kV); cone voltage (30 V); source offset (80 V); source temperature (100 °C); desolvation temperature (300°C); desolvation gas (800 L/h); cone gas (57 L/h); nebuliser pressure (6.5 bar); LM resolution (4.7); HM resolution (15.00); ion energy (1.8); collision gas flow (2 mL/min). The parameters used for positive control were: capillary voltage (3 kV); cone voltage (30 V); source offset (80 V); source temperature (100 °C); desolvation temperature (300 °C); desolvation gas (800 L/h); cone gas (57 L/h); nebuliser pressure (6.5 bar); LM resolution (4.7); HM resolution (15.00); ion energy (1.0); collision gas flow (2 mL/min). Time of flight MS settings were: scan time (0.1 seconds); interscan time (0.014 seconds); data format (centroid). The lock mass solution consisted of Leucine Enkephalin (200 pg/µL). The lockspray was acquired during UPLC-MS acquisition and corrected for ([M+H]+ m/z 556.2771 & [M-H]- m/z 554.2615). Instrument control and data acquisition was carried out in MassLynx (Waters, USA).

4.2.4. Microscopic and macroscopic analysis of the effect of 2,4-DAPG on *Z. tritici* blastospore growth *in vitro*

PDA (Formedium) plates were prepared, amended with 2,4-DAPG (Sigma-Aldrich) solubilized in DMSO, to achieve final concentrations of 0.5µg/ml, 2µg/ml, 10µg/ml, 50µg/ml,100µg/ml, and 200µg/ml. A *Z. tritici* blastospore suspension was prepared (as described in Chapter 2), containing approximately $1x10^6$ blastospore per ml (Hongxin Chen, personal communication). Control plates were prepared containing the respective volume of DMSO. For microscopic observation, 20µl of *Z. tritici* blastospore suspension was distributed across plates using a spreader, before being sealed and inverted. Microscopic images were taken after 2 days of incubation at 16 °C in darkness. Plates prepared for macroscopic observation were inoculated with 2ul of *Z. tritici* blastospore suspension, spotted as serial dilutions, before being inverted and sealed. Macroscopic images were taken after 6 days of incubation at 16 °C in darkness. 3 replicate plates were prepared for each treatment.

4.3. Results

4.3.1. Prediction of secondary metabolite biosynthetic gene clusters from *Pseudomonas* genome sequences

To investigate the secondary metabolite biosynthetic potential of the 17 antagonistic and 71 non-antagonistic *Pseudomonas* isolates, predictive bioinformatic approaches were used. Secondary metabolite BGCs were predicted for each genome sequence using antiSMASH 5.2. A total of 747 secondary metabolite BGCs were predicted from all 88 *Pseudomonas* genome sequences. 140 BGCs were predicted from the 17 antagonistic single *Pseudomonas* isolates, and 607 BGCs were predicted from 71 non-antagonistic single *Pseudomonas* isolates. This equates to an average of 8.24 BGCs per antagonistic *Pseudomonas* isolate, and 8.55 BGCs per non-antagonistic *Pseudomonas* isolate. The 747 BGCs

predicted from the 88 *Pseudomonas* isolates were classified as 175 RiPP BGCs, 227 NRPS BGCs, 307 'Other' BGCs, 3 PKS1 BGCs, 7 PKSOther BGCs, 27 Terpene BGCs and 1 Saccharide BGC.

4.3.2. Network analysis of predicted secondary metabolite biosynthetic gene clusters

To identify homologous BGCs between *Pseudomonas* genome assemblies, BGC sequence similarity networks were constructed. Sequence similarity networks were constructed using BiG-SCAPE, with a cut-off value of 0.2, to construct networks of predicted BGCs from genome sequences that showed high levels of similarity. Reference sequences of 1808 BGCs from MiBIG were included in construction of GCF networks, to identify reference BGC sequences with a high sequence similarity to predicted BGCs (Figure 4.1), to identify clusters producing known compounds.

Of 747 predicted BGCs from 88 *Pseudomonas* genome sequences, 129 Gene Cluster Families (GCFs) were formed. The 129 predicted GCFs were classified as 42 non-ribosomal peptide synthetases (NRPS) GCFs, 12 Terpene GCFs, 24 Ribosomally synthesized and post-translationally modified peptide (RiPP) GCFs, 1 Polyketide Synthase Type 1 (PKS1) GCF, 1 Polyketide synthase - Other (PKSOther) GCF , 48 Other GCFs, and 1 Saccharide GCF.

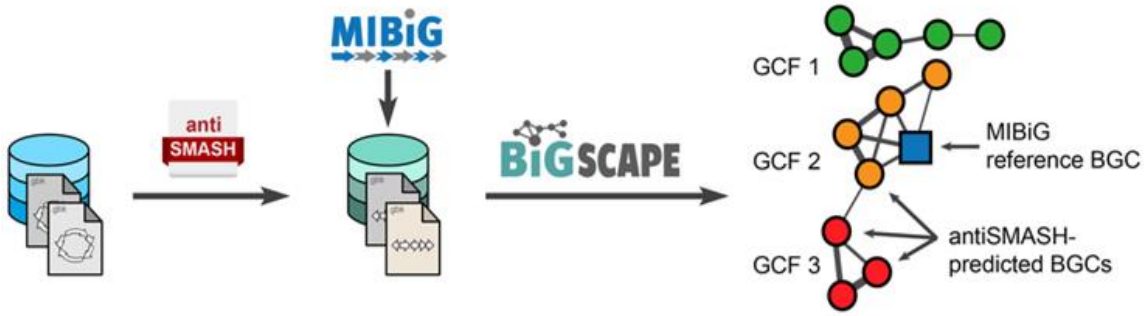


Figure 4.1 Predictive bioinformatics network analysis of secondary metabolite biosynthetic gene clusters.
A diagram indicating the process of secondary metabolite BGC prediction from genome sequences using antiSMASH, and subsequent sequence similarity network analysis of predicted secondary metabolite BGCs with reference BGC sequences from the MiBIG database into Gene Cluster Family Networks (GCFs), adapted from (Navarro-Muñoz et al., 2020).

4.3.3. Assessment of the predicted secondary metabolite biosynthetic gene cluster diversity within a *Pseudomonas* phylogeny

To investigate the predicted secondary metabolite biosynthetic gene cluster diversity and distribution within the *Pseudomonas* collection, a phylogenetic tree was constructed from 17 antagonistic and 71 non-antagonistic *Pseudomonas* isolates using FastTree2, as previously described in Chapter 3. Generated BiGSCAPE GCF network files were converted to BGC presence/absence data for constructed GCFs. BGC presence/absence data was added to the constructed phylogeny for each class of GCF/BGC (Figures 4.2-4.5).

A total of 24 GCF networks of RiPP BGCs were predicted from the 88 *Pseudomonas* genome assemblies. Within the *P. fluorescens* subclade, BGCs that were part of GCF network RiPP_2431 (tan squares, Figure 4.2), were predicted from all 7 genome assemblies. Two distinct groups within the phylogeny were formed from BGCs within this GCF, that were predicted from 6 *P. koreensis* genome assemblies. No other RiPP class BGCs were predicted from *P. fluorescens* genome assemblies. Within the *P. lurida* subclade, predicted RiPP

BGCs were found within a total of 11 distinct GCF networks. From all 34 P.lurida genome assemblies, BGCs contained within GCF network RiPP_2301 (tan triangle, Figure 4.2) were predicted, with no BGCs predicted from *P. fluorescens* or *P. koreensis* isolates found to be similar at the 0.2 cut off value in BiG-SCAPE. BGCs within GCF RiPP_2303 (purple circle, Figure 4.2) were predicted from 33 out of 34 *P. lurida* genome assemblies, and also predicted from 4 *P. koreensis* genome assemblies phylogenetically closest to the *P. lurida* subclade. Predicted BGCs from the 47 *P. koreensis* genome assemblies were found in a total of 14 GCFs networks. Ten *P. koreensis* genome assemblies were predicted to contain BGCs found within GCF RiPP_2494 (olive star, Figure 4.2), were found to group distinctly within the phylogenetic tree. Eight *Pseudomonas* genome assemblies predicted to contain BGCs within GCF RiPP_2495 (orange square, Figure 4.2), fall solely within the *P. koreensis* subclade. Similarly, 4 genome assemblies with predicted BGCs within the RiPP_2398 (olive triangle, Figure 4.2) GCF network were found to form a group within the *P. koreensis* subclade. BGCs that formed GCF RiPP_2520 (tan star, Figure 4.2) were predicted from 18 *P. koreensis* isolates, distributed more loosely throughout the *P. koreensis* subclade. Nine RiPP GCF networks were made up of singleton BGCs predicted from single *Pseudomonas* isolates within the collection, found to have no similarity to any other predicted RiPP BGCs from within the *Pseudomonas* collection or MiBIG repository. Nine out of 24 RiPP GCF networks were formed from singleton predicted BGCs from genome assemblies within the *Pseudomonas* collection.

A total of 42 GCF networks were formed of NRPS BGCs were predicted from the 88 *Pseudomonas* genome assemblies (Figure 4.3). From 7 *P. fluorescens* genome assemblies, 22 predicted NRPS BGCs formed 5 distinct GCF networks. For all 7 *P. fluorescens* genome assemblies within the collection, BGCs were predicted that formed GCF networks NRPS_2425 (orange square, Figure 4.3) and NRPS_2428 (orange star, Figure 4.3). GCF NRPS_2007 (purple triangle, Figure 4.3) was constituted of 7 predicted BGCs; 6 predicted from *P. fluorescens* genome

assemblies and 1 from *P. koreensis* isolate Roth 91. 121 predicted NRPS BGCs from the 34 *P. lurida* genome assemblies were found in a total of 28 distinct GCF networks. BGCs that formed GCFs NRPS_ 2174 (blue circle, Figure 4.3), NRPS_2333 (dark pink square), NRPS_2335 (dark pink circle, Figure 4.3), NRPS_2390 (light pink star, Figure 4.3) were predicted from the same 7 closely grouped *P. lurida* isolates. Distinct groups within the *P. lurida* phylogeny could also be observed for GCFs NRPS_2028 (olive star, Figure 4.3), NRPS_2171 (blue star, Figure 4.3), NRPS_2208 (pink square, Figure 4.3), NRPS_2317 (green circle), NRPS_2319 (green star), and NRPS_2348 (dark pink star). Two distinct groups of genome assemblies within the *P. lurida* clade contain predicted BGCs that form GCF NRPS_2042 (olive triangle, Figure 4.3). Predicted NRPS BGCs found within GCFs NRPS_31 (tan circle, Figure 4.3) and NRPS_2130 (orange square) all originate from *P. lurida* genome assemblies loosely formed a group within the subclade. 13 GCF networks were formed from a total of 84 NRPS BGCs predicted from the 47 *P. koreensis* isolates from the collection. BGCs in GCF network NRPS_2498 (turquoise square, Figure 4.3) were predicted from 23 genome assemblies distributed throughout the *P. koreensis* subclade. GCF NRPS_2516 (brown triangle, Figure 4.3) contained predicted BGCs from genome assemblies from across the constructed phylogeny, derived from 18 *P. koreensis* isolates, 1 *P. fluorescens* isolate, Roth 83, and 1 *P. lurida* isolate, Roth 77. 13 *P. koreensis* genome assemblies were predicted to contain BGCs that formed GCF NRPS_2497 (brown circle, Figure 4.3) and grouped closely with phylogenetic distance. GCF NRPS_1906 (purple circle, Figure 4.3) was constructed from 16 predicted NRPS BGCs derived from genome assemblies from across half of the *P. koreensis* subclade. 14 predicted NRPS BGCs were found to form GCF networks as singletons, with each BGC predicted from a single *Pseudomonas* genome assembly from the collection.

Forty-eight GCF networks were formed from 307 predicted BGCs classified as ‘Other’ by antiSMASH, derived from the 88 *Pseudomonas* genome assemblies. All

7 *P. fluorescens* genome assemblies were found to contain predicted BGCs within the GCF networks Other_2004 (orange square, Figure 4.4) and Other_2008 (orange triangle, Figure 4.4), and Other_2427 (light pink star, Figure 4.4). BGCs found in GCF network Other_2047 (pink triangle, Figure 4.4) were predicted from 4 closely grouped *P. lurida* isolates. 34 *P. lurida* genome assemblies contain a predicted BGC that formed GCF Other_2045 (blue triangle), with BGCs predicted from the genome assemblies of *P. koreensis* isolates Roth 108 and Roth 103 also contained within this GCF network. GCFs Other_2029 (blue circle, Figure 4.4), Other_2103 (pink circle, Figure 4.4), Other_2171 (green square, Figure 4.4), Other_2394 (light pink square, Figure 4.4), Other_2175 (turquoise square, Figure 4.4), and Other_2302 (coral triangle, Figure 4.4) were found to contain predicted BGCs from genome assemblies within the *P. lurida* subclade that group loosely with the phylogenetic distribution of the isolates. Genome assemblies that were found to contain predicted BGCs within GCFs Other_1919 (orange circle, Figure 4.4) and Other_2462 (dark pink triangle, Figure 4.4) group clearly within the *P. koreensis* phylogeny. GCF networks Other_2482 (dark pink circle, Figure 4.4), Other_2515 (green circle, Other_1900 (olive triangle, Figure 4.4), Other_1886 (olive square, Figure 4.4), and Other_2292 (coral circle, Figure 4.4) were constructed from predicted BGCs that originated from across the *P. koreensis* phylogeny. A total of 16 'Other' GCFs contained single predicted BGCs, derived from single *Pseudomonas* genome assemblies. These were distributed across the constructed phylogeny, with 5 singleton GCFs derived from *P. lurida* and 11 GCFs from *P. koreensis* genome assemblies.

A single PKS Type 1 GCF, PKS1_01887 (dark pink circle, Figure 4.5), was formed of a single predicted BGC from the genome assembly of *P. koreensis* isolate GLB25. GCF PKSOther_2429 (orange star, Figure 4.5) was formed from 7 predicted BGCs from *P. fluorescens* genome assemblies. A total of 12 Terpene GCF networks were constructed from 27 predicted Terpene BGCs. Saccharide GCF Saccharide_1908 (orange square, Figure 4.5) was found to contain a single

saccharide BGC, predicted from the genome assembly of *P. koreensis* isolate GLRE20. *P. lurida* genome assemblies from which predicted BGCs constituting GCF networks Terpene_2032 (green star, Figure 4.5), Terpene_2102 (dark pink star, Figure 4.5), Terpene_2031 (light pink circle, Figure 4.5), and Terpene_2353 (light pink star, Figure 4.5) can be seen to group clearly within the phylogeny. Eight of the 12 Terpene GCF networks contain a single BGC, predicted from single *Pseudomonas* genome assemblies. Five of these singleton Terpene BGCs were derived from the genome assemblies of *P. koreensis* isolates, and 3 from *P. lurida* genome assemblies.

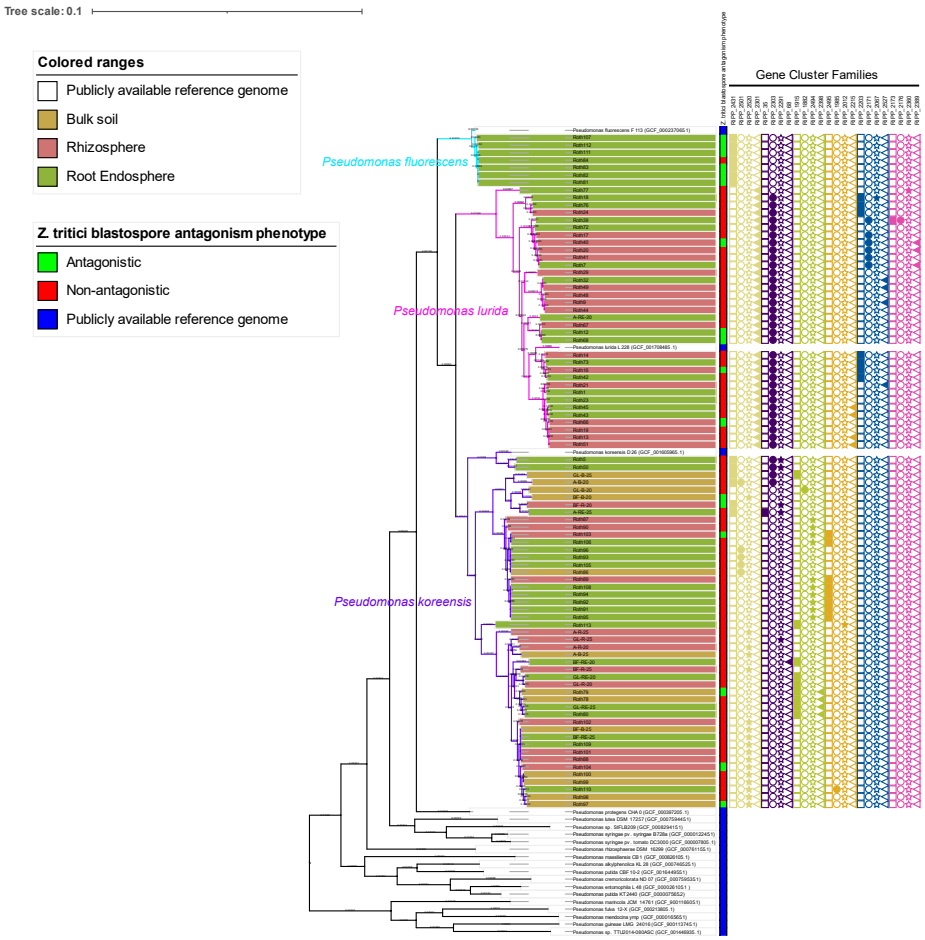


Figure 4.2 Distribution of predicted secondary metabolite BGCs forming (RiPP) class Gene Cluster Families, for 17 *Z. tritici* blastospore antagonistic and 71 non-antagonistic *Pseudomonas* isolates, within a phylogeny.
A phylogenetic tree of 108 *Pseudomonas* isolates was constructed using FastTree2 in KBase, consisting of 17 antagonistic *Pseudomonas* isolates (green square in relevant column), 71 non-antagonistic *Pseudomonas* isolates (red square in relevant column), and 20 of the closest publicly available reference genomes (blue square in relevant column, white leaf label). The isolation source of *Pseudomonas* isolates is indicated with brown (bulk soil), red (rhizosphere) and green (endosphere) coloured labels. The 3 distinct clades formed with publicly available reference isolates are highlighted, *P. koreensis* D26 (purple), *P. lurida* L228 (pink), and *P. fluorescens* F113 (turquoise). Unique shape and colour combinations are used to depict BGCs within a GCF network, to allow for referencing within text. Presence of a predicted BGC within a GCF network for each *Pseudomonas* isolate is indicated with a filled coloured shape. Absence of a predicted BGC within a GCF network is indicated by an empty coloured shape. For each GCF network, reference BGCs from the MiBIG database within the GCF network are indicated in brackets. This figure is a scalable graphics vector, with all detail visible if magnification is increased.

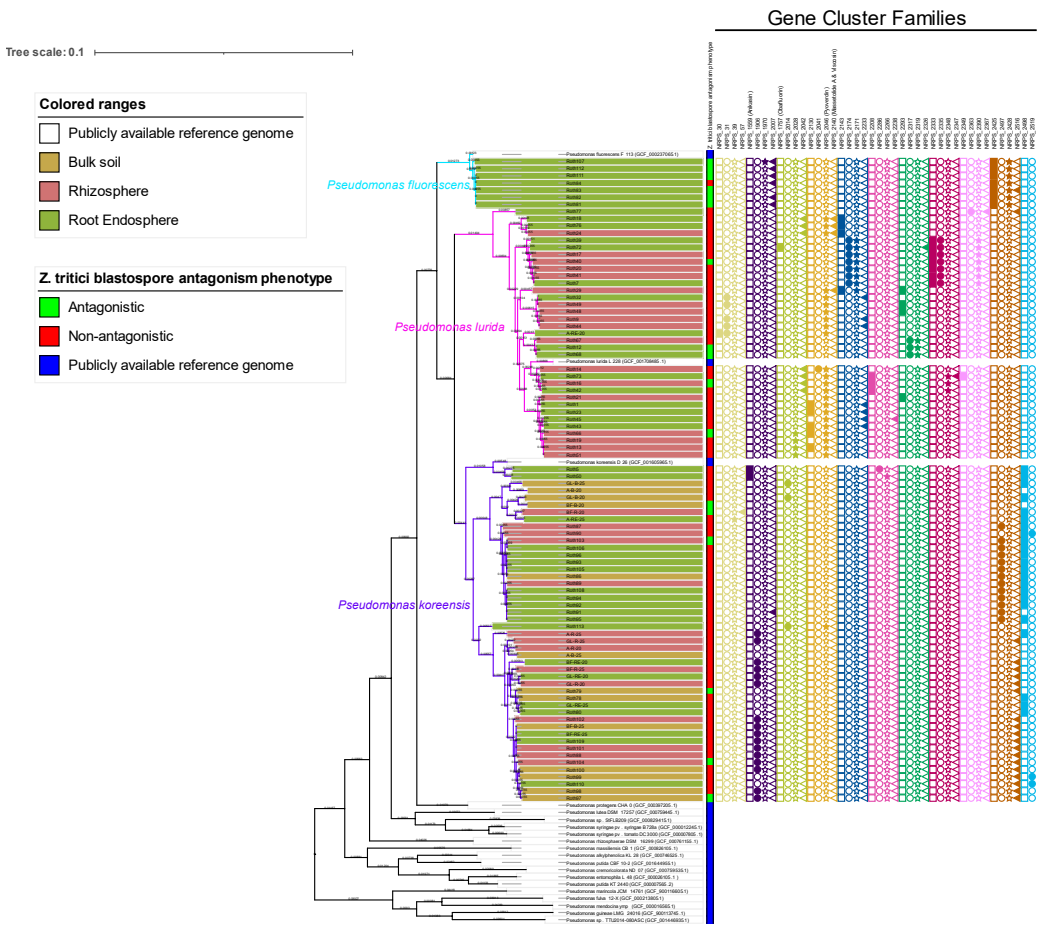


Figure 4.3 Distribution of predicted secondary metabolite BGCs forming (NRPS) class Gene Cluster Families, for 17 *Z. tritici* blastospore antagonistic and 71 non-antagonistic *Pseudomonas* isolates, within a phylogeny.
A phylogenetic tree of 108 *Pseudomonas* isolates was constructed using FastTree2 in KBase, consisting of 17 antagonistic *Pseudomonas* isolates (green square in relevant column), 71 non-antagonistic *Pseudomonas* isolates (red square in relevant column), and 20 of the closest publicly available reference genomes (blue square in relevant column, white leaf label). The isolation source of *Pseudomonas* isolates is indicated with brown (bulk soil), red (rhizosphere) and green (endosphere) coloured labels. The 3 distinct clades formed with publicly available reference isolates are highlighted, *P. koreensis* D26 (purple), *P. lurida* L228 (pink), and *P. fluorescens* F113 (turquoise). Unique shape and colour combinations are used to depict BGCs within a GCF network, to allow for referencing within text. Presence of a predicted BGC within a GCF network for each *Pseudomonas* isolate is indicated with a filled coloured shape. Absence of a predicted BGC within a GCF network is indicated by an empty coloured shape. For each GCF network, reference BGCs from the MiBIG database within the GCF network are indicated in brackets. This figure is a scalable graphics vector, with all detail visible if magnification is increased.

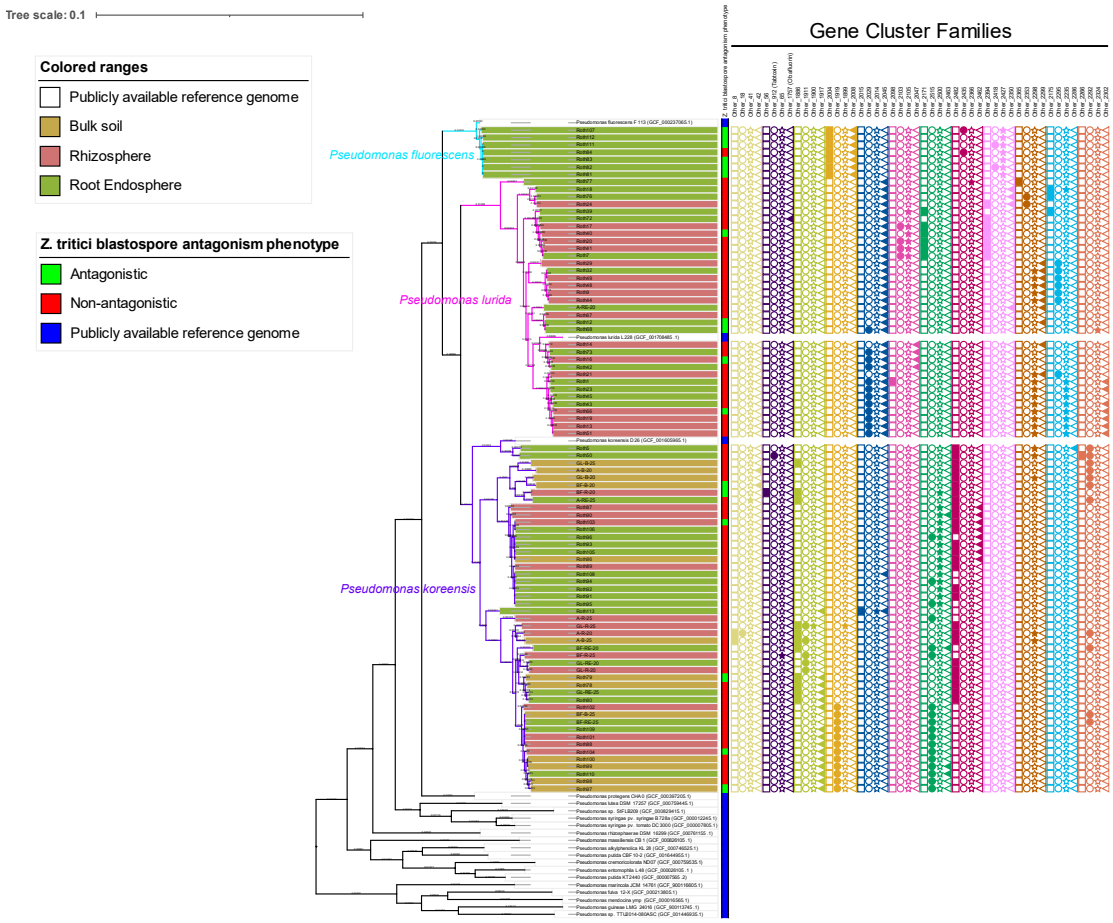


Figure 4.4 Distribution of predicted secondary metabolite BGCs forming 'Other' class Gene Cluster Families, for 17 *Z. tritici* blastospore antagonistic and 71 non-antagonistic *Pseudomonas* isolates, within a phylogeny.
A phylogenetic tree of 108 *Pseudomonas* isolates was constructed using FastTree2 in KBase, consisting of 17 antagonistic *Pseudomonas* isolates (green square in relevant column), 71 non-antagonistic *Pseudomonas* isolates (red square in relevant column), and 20 of the closest publicly available reference genomes (blue square in relevant column, white leaf label). The isolation source of *Pseudomonas* isolates is indicated with brown (bulk soil), red (rhizosphere) and green (endosphere) coloured labels. The 3 distinct clades formed with publicly available reference isolates are highlighted, *P. koreensis* D26 (purple), *P. lurida* L228 (pink), and *P. fluorescens* F113 (turquoise). Unique shape and colour combinations are used to depict BGCs within a GCF network, to allow for referencing within text. Presence of a predicted BGC within a GCF network for each *Pseudomonas* isolate is indicated with a filled coloured shape. Absence of a predicted BGC within a GCF network is indicated by an empty coloured shape. For each GCF network, reference BGCs from the MiBIG database within the GCF network are indicated in brackets. This figure is a scalable graphics vector, with all detail visible if magnification is increased.



Figure 4.5 Distribution of predicted secondary metabolite BGCs forming PKS Other (PKSOther), PKS Type 1 (PKS1), Terpene, and Saccharide class Gene Cluster Families, for 17 *Z. tritici* blastospore antagonistic and 71 non-antagonistic *Pseudomonas* isolates, within a phylogeny.

A phylogenetic tree of 108 *Pseudomonas* isolates was constructed using FastTree2 in KBase, consisting of 17 antagonistic *Pseudomonas* isolates (green square in relevant column), 71 non-antagonistic *Pseudomonas* isolates (red square in relevant column), and 20 of the closest publicly available reference genomes (blue square in relevant column, white leaf label). The isolation source of *Pseudomonas* isolates is indicated with brown (bulk soil), red (rhizosphere) and green (endosphere) coloured labels. The 3 distinct clades formed with publicly available reference isolates are highlighted, *P. koreensis* D26 (purple), *P. lurida* L228 (pink), and *P. fluorescens* F113 (turquoise). Unique shape and colour combinations are used to depict BGCs within a GCF network, to allow for referencing within text. Presence of a predicted BGC within a network for each *Pseudomonas* isolate is indicated with a filled coloured shape. Absence of a predicted BGC within a GCF network is indicated by an empty coloured shape. For each GCF network, reference BGCs from the MiBIG database within the GCF network are indicated in brackets. This figure is a scalable graphics vector, with all detail visible if magnification is increased.

4.3.4. Assessment of secondary metabolite GCFs associated with *Z. tritici* blastospore antagonism phenotype in *Pseudomonas* isolates

To examine whether the observed *in vitro Z. tritici* blastospore antagonism phenotype of *Pseudomonas* isolates correlated with a single known or unknown predicted BGC, GCF networks were analysed. No single BGC of any class was predicted from the genome assemblies of all *Z. tritici* blastospore antagonistic *Pseudomonas* isolates within the collection.

To identify potential candidate unknown BGCs associated with the observed *in vitro* antagonism of *Z. tritici* blastopores, predicted GCF networks were analysed. Two GCF networks consisted of singleton predicted NRPS BGCs were derived from only *Z. tritici* blastospore antagonistic *Pseudomonas* genome assemblies (Table 4.1). GCF network NRPS_57 (tan triangle, Figure 4.3), was found to contain a single predicted BGC derived from *Z. tritici* blastospore antagonistic *P. koreensis* isolate BFR20. GCF network NRPS_1970 (purple star, Figure 4.3), consisted of a single predicted BGC from the genome assembly of *P. fluorescens* isolate Roth107, which was found to be antagonistic towards *Z. tritici* blastospores *in vitro*. Three GCF networks were found to contain 'Other' BGCs that were predicted from the genome assemblies of only *Z. tritici* antagonistic *Pseudomonas* isolates. Two of these GCF networks, Other_56 (purple square, Figure 4.4) and Other_2324 (coral star, Figure 4.4), were found to contain singleton BGCs, predicted from the genome assemblies of antagonistic *P. lurida* isolate Roth 68 and antagonistic *P. koreensis* isolate BFR20 respectively (Table 4.1). GCF network Other_2418 (light pink circle, Figure 4.4), was found to consist of two BGCs predicted from the genome assemblies of two antagonistic *P. fluorescens* isolates, Roth 111 and Roth82 (Table 4.1). Two singleton Terpene GCF networks contained predicted BGCs derived from *Z. tritici* antagonistic *Pseudomonas* isolates, Terpene_45 (green square, Figure 4.5) and Terpene_2380 (light pink triangle, Figure 4.5)

contain BGCs from *P. koreensis* isolates BFB20 and Roth 79 respectively (Table 4.1).

Table 4.1 GCF networks containing predicted BGCs solely derived from *Pseudomonas* isolates exhibiting *Z. tritici* blastospore antagonism *in vitro*. BGC GCF networks originating exclusively from *Z. tritici* blastospore antagonistic *Pseudomonas* isolates.

GCF ID	Number of predicted BGCs in GCF network	*Pseudomonas* isolate
NRPS_57	1	BF-R-20
NRPS_1970	1	Roth107
Other_56	1	BF-R-20
Other_2418	2	Roth111 & Roth82
Other_2324	1	Roth68
Terpene_45	1	BF-B-20
Terpene_2380	1	Roth79

4.3.5. Identification of known secondary metabolite biosynthetic gene clusters through BiGSCAPE

To identify the presence of predicted BGCs encoding the biosynthesis of known secondary metabolites within the collection of *Pseudomonas* genome assemblies, GCF networks were analysed. 1808 reference BGCs from the MiBIG repository were included in the construction of sequence similarity networks (GCFs), with predicted BGCs from the 88 *Pseudomonas* genome assemblies within the collection using BiGSCAPE. A total of 11 reference BGCs from MiBIG were found to form 7 GCF networks with predicted BGCs from the *Pseudomonas* collection (Table 4.2). A total of 4 NRPS GCF networks were found to be positive ‘hits’ for MiBIG reference BGCs. NRPS_02046 (orange star, Figure 4.3) was found to contain 24 predicted BGCs and a reference BGC for pyoverdine (BGC0000413). The reference BGCs encoding the production of massetolide A (BGC0000389) and Viscosin (BGC0001312) were included in GCF network NRPS_02140 (orange

triangle, Figure 4.3), alongside 4 predicted BGCs from 4 *P. lurida* genome assemblies. Two reference BGCs within the MiBIG repository, encoding the biosynthesis of Obafluorin (BGC0001437 & BGC0001710), were found to form GCF networks NRPS_1757 (olive square, Figure 4.3) and Other_1757 (purple triangle, Figure 4.4) with a predicted BGC from *P. koreensis* isolate Roth 72. GCF network NRPS_01559 (purple square, Figure 4.3) was found to contain predicted BGCs from *P. lurida* isolates Roth 5 and Roth 50, and MiBIG reference BGC0001509, encoding the production of anikasin (Table 4.2). The reference BGC from the MiBIG repository encoding the biosynthesis of Tabtoxin (BGC0000846) was found to be similar to single BGCs predicted from the genome assembly of *P. lurida* isolate Roth 50 and formed GCF networks Other_912 (purple circle, Figure 4.4) (Table 4.2). GCF PKSOther_2429 (orange star, Figure 4.5) was found to contain two reference BGCs from the MiBIG repository, BGC0000280.1 & BGC0000281.1, both encoding the biosynthesis of 2,4-diacetylphloroglucinol (Table 4.2). No RiPP GCF networks were found to contain reference RiPP BGCs from the MiBIG database.

To examine the level of similarity of predicted BGCs with reference MiBIG BGC sequences, antiSMASH outputs were analysed. 100% of genes within reference MiBIG sequences for massetolide A, obafluorin, anikasin and 2,4-DAPG were found to have significant BLAST hits to genes within all predicted BGCs within the respective GCF networks. Predicted BGCs showing high levels of similarity to MiBIG reference BGC sequences for pyoverdine, viscosin, and tabtoxin, were found to contain varying partial BGC sequences.

Table 4.2 GCFs containing reference secondary metabolite BGC sequences from MiBIG.

BGC/GCF class	GCF ID	MiBIG reference BGC ID/s	Secondary metabolite product of reference BGC	Source of reference BGC sequence
NRPS	FAM_02046	BGC0000413.1	Pyoverdine	*Pseudomonas protegens Pf-5*
NRPS	FAM_02140	BGC0000389.1	Massetolide A	*Pseudomonas fluorescens SS101*
NRPS	FAM_02140	BGC0001312.1	Viscosin	*Pseudomonas fluorescens SBW25*
NRPS	FAM_01757	BGC0001437.1 & BGC0001710.1	Obafluorin	*Pseudomonas fluorescens ATCC 39502*
NRPS	FAM_01559	BGC0001509.1	Anikasin	*Pseudomonas fluorescens HKI0770*
Other	FAM_00912	BGC0000846.1	Tabtoxin	*Pseudomonas syringae BR2*
Other	FAM_01757	BGC0001437.1 & BGC0001710.1	Obafluorin	*Pseudomonas fluorescens ATCC 39502*
PKSOther	FAM_02429	BGC0000280.1 & BGC0000281.1	2,4-diacetylphloroglucinol	*Pseudomonas fluorescens Q2-87*

4.3.6. Chemical analysis of agar extracts in *Pseudomonas* confrontation with *Z. tritici* blastospores *in vitro*

To gather further support for the predictive pipeline, the secreted secondary metabolites present in the agar interaction zone between antagonistic *Pseudomonas* isolates and *Z. tritici* blastospores were analysed. Specifically, for this preliminary work, we sought to determine whether the prediction of 2,4-DAPG BGCs could be validated through detection of this known antifungal compound.

Chemical extraction was performed on agar sections surrounding antagonistic *Pseudomonas* isolate Roth112, both as part of the *in vitro Z. tritici* blastospore antagonism assay, and alone on PDA. LC-MS of chemical extracts, conducted by Dr David Withall, indicated the presence of a peak associated with 2,4-DAPG, in agar sections from *Pseudomonas* isolate Roth112 grown alone, and in confrontation with *Z. tritici* blastospores *in vitro* (Figure 4.6). This data strongly indicates that *Pseudomonas* isolate Roth112 can biosynthesise a compound likely to be 2,4-DAPG, within the *Z. tritici* blastospore confrontation assay. The identity of the compound associated with this peak was later confirmed through co-injection of the sample with an authentic chemical standard of 2,4-DAPG (Sigma-Aldrich) (David Withall, personal communication).

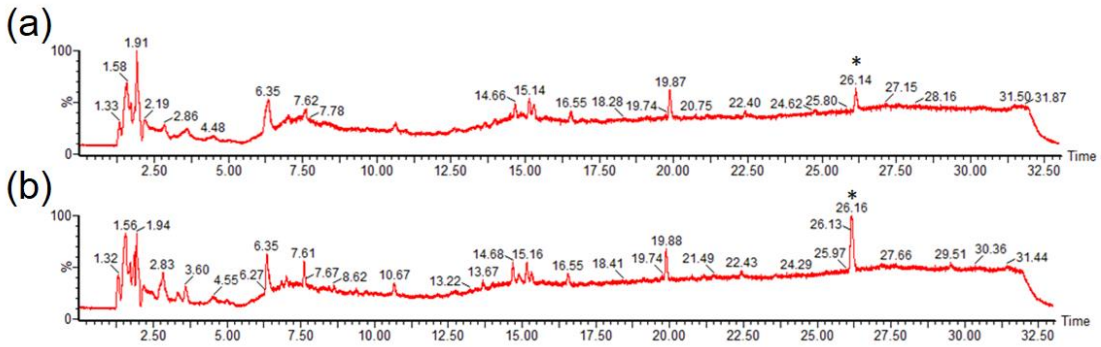


Figure 4.6 Chemical analysis of agar extracts of antagonistic *Pseudomonas* isolate Roth112.
Total Ion Chromatogram (TIC; positive mode) of agar extracts of Roth112 alone **(a)**, and in confrontation with *Z. tritici* blastospores. **(b)** Peak indicative of 2,4-DAPG is indicated by *.

4.3.7. Preliminary assessment of susceptibility of *Z. tritici* blastospores to antagonism by 2,4-DAPG *in vitro*

To confirm 2,4-DAPG as a causative agent in the antagonism of *Z. tritici* blastospores on PDA plates *in vitro*, and to determine the susceptibility of *Z. tritici* IPO323 blastospores to antagonism by 2,4-DAPG, growth of *Z. tritici* blastospores was measured in response to exposure to the commercially authentic chemical standard of 2,4-DAPG (Sigma-Aldrich). PDA (Formedium) plates were prepared as described in Methods 4.2.4., with the addition 2,4-DAPG (Sigma-Aldrich) solubilised in DMSO. Control PDA plates were amended with the volume of DMSO used to solubilise 2,4-DAPG for each given concentration. This experiment was carried out in triplicate.

Microscope images were taken after 2 days of growth of *Z. tritici* blastospores on PDA plates containing varying concentrations of 2,4-DAPG. A clear reduction blastosporulation can be observed in *Z. tritici* blastospore growth on PDA plates containing 50µg/ml, 100µg/ml, and 200µg/ml 2,4-DAPG, compared to control plates (Figure 4.7a).

Similarly, macroscopic images of *Z. tritici* colonies taken after 6 days of growth, grown on PDA amended with a range of 2,4-DAPG concentrations, show a strong inhibitory effect of 2,4-DAPG at concentrations of 100µg/ml and 200µg/ml, compared to control plates (Figure 4.7b). Concentrations of 2,4-DAPG at 50µg/ml do not appear to completely inhibit the growth *Z. tritici* blastospore growth *in vitro* macroscopically (Figure 4.7b), despite observed reductions in budding of blastospores microscopically (Figure 4.7a). These data demonstrate that 2,4-DAPG is indeed effective at inhibiting the growth of *Z. tritici* blastospores *in vitro*.

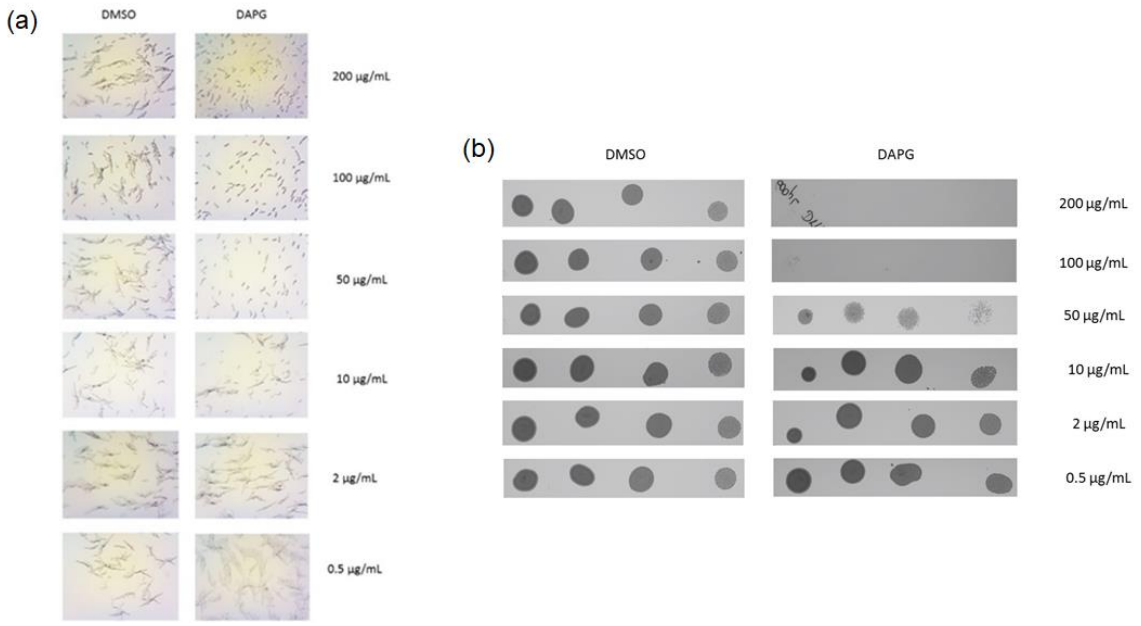


Figure 4.7 Microscopic and macroscopic changes in the growth of *Z. tritici* blastospores *in vitro*, in response to 2,4-DAPG.
(a) Microscope images of *Z. tritici* blastospores grown on PDA plates amended with a range of 2,4-DAPG concentrations after 2 days of growth. A clear reduction in blastosporulation can be observed in *Z. tritici* blastospore growth on PDA plates containing 50µg/ml, 100µg/ml, and 200µg/ml DAPG. **(b)** Macroscopic images of *Z. tritici* blastospore colonies grown on PDA plates amended with a range of 2,4-DAPG concentrations after 6 days of growth. Clear inhibition of macroscopic growth of *Z. tritici* blastospores can be observed at 2,4-DAPG concentrations of 100µg/ml and 200µg/ml.

4.4. Discussion

The results described in this Chapter indicate that *Pseudomonas* isolates within the test library are predicted to contain known secondary metabolite BGCs with previously described antifungal activity, alongside unknown secondary metabolite BGCs that correlate with an *in vitro Z. tritici* blastospore antagonism phenotype. These results highlight the potential of predictive bioinformatic techniques and network analysis in secondary metabolite BGC association studies, to uncover secondary metabolite BGCs underpinning a phenotype or function. More broadly, the results show the diversity of predicted secondary metabolite BGCs within *Pseudomonas* genome assemblies with currently unknown function, as most GCFs do not contain reference BGCs from the MiBIG repository.

4.4.1. Similarities in the number of predicted secondary metabolite BGCs from antagonistic and non-antagonistic *Pseudomonas* isolates

These results indicate that the number of predicted BGCs for antagonistic and non-antagonistic *Pseudomonas* isolates within this study, broadly fall within the lower than expected ranges within the linear trend between genome size and predicted BGC count previously described (Cimermancic et al., 2014) (average genome assembly size ~6.5Mb described in Chapter 3). These results could more broadly explain the comparatively small number of studies characterising secondary metabolite BGCs predicted from bacterial species, such as pseudomonads, falling within the linear trend of predicted BGCs count and genome size, compared to studies characterising secondary metabolite BGCs of bacterial species such as *Streptomyces*, harbouring approximately double the number of BGCs than expected based on the linear trend.

4.4.2. Predicted BGCs are correlated with a *Z. tritici* blastospore antagonistic phenotype in *Pseudomonas* isolates

The results presented highlight predicted BGC candidates, encoding the biosynthesis of potentially novel secondary metabolites, may be causative of the observed antagonism of *Z. tritici* blastospores *in vitro* by *Pseudomonas* isolates. These candidate BGCs require further investigation and characterisation, as no previously published reference BGCs from the MiBIG database were found to have high sequence similarity. It will be interesting to investigate the expression levels of these candidate BGCs in *Pseudomonas* isolates confronted with *Z. tritici* blastospores, through RNA sequencing or qPCR analysis, alongside chemical analysis of secreted secondary metabolites produced by *Pseudomonas* isolates containing these BGCs within their genomes.

Characterisation of the contribution of these predicted BGCs to the *Z. tritici* blastospore antagonism phenotype, if evidence of expression is observed, could be conducted through the generation of loss-of-function *Pseudomonas* mutants, similar to parallel studies (Sass et al., 2018). These loss of function mutants could be rescreened in the *in vitro Z. tritici* blastospore antagonism assay and compared to wild-type. Previous studies have characterised unknown BGCs and their biosynthetic products through the generation of loss-of-function mutants paired with chemical analyses (Mullins et al., 2021). Agar extracts of wild-type and loss-of-function mutant strains can be analysed with LC-MS, and peaks associated with the functioning BGC identified, that are absent in the LC-MS traces of the mutant strain. This approach can give indications into the types or molecular weights of BGC products, before chemical structure elucidation using Nuclear magnetic resonance spectroscopy (NMR).

An alternative strategy could be to ectopically express the BGC of interest in bacterial isolates amenable to transformation, such as *Escherichia coli*, before

characterising the secondary metabolite products (Bangera and Thomashow, 1999).

Comparative studies and network analysis of predicted BGCs to investigate underlying mechanisms of fungal antagonism at this scale have not previously been conducted. The only published study utilizing BGC similarity networks to investigate secondary metabolite BGCs involved in antifungal activity, consisted of a comparison of 5 *Pseudomonas koreensis* genomes (Gu et al., 2020). The work in this Chapter is, to my knowledge, the first to identify predicted BGCs associated with an antifungal phenotype through a secondary metabolite BGC association, and is similar to Genome Wide Association Studies (GWAS) approaches utilised to determine the genetic basis of complex traits in plants (Hall et al., 2010).

The GCF networks that are associated with the *in vitro Z. tritici* blastospore antagonism phenotype are small, mostly containing single predicted BGCs. It will be interesting to expand the network analysis of predicted BGCs to include more *Pseudomonas* isolates screened for *Z. tritici* blastospore antagonism *in vitro* and observe if more predicted BGCs form networks with the GCFs associated with antagonism.

A limitation of this approach is that presence of a predicted BGC within a genome assembly does guarantee expression or production of the secondary metabolite under specific environmental conditions. This could lead to false negative results within our analysis, as BGCs that are instrumental in the antagonism of *Z. tritici* blastospores by *Pseudomonas* bacteria but are present within the genome sequences of non-antagonistic *Pseudomonas* isolates, in which they are not expressed, would not be identified as associating with the antagonism phenotype, warranting further investigation. Rare BGCs that form singleton or small GCF networks could also be identified as false positive results within this analysis.

The associations between *Z. tritici* blastopore antagonism phenotype and identified GCF networks should be considered preliminary, and as BGC candidates warranting further investigation and characterisation. Formal statistical assessment of the association between *Z. tritici* antagonism and GCF presence/absence will be investigated as part of a future project. It may be possible to employ statistical approaches that are used in association statistics of genes within pangenomes with binary traits, such as Scoary (Brynildsrud et al., 2016). However, with approaches such as this, a correction for multiple comparisons, such as a Bonferroni correction as part of Fisher's exact test, would need to be employed, given the large number of predicted GCF families compared. This would reduce the power of the statistical test, potentially increasing the rate of Type II errors to unacceptable levels (Nakagawa, 2004). Recent studies have utilised another approach, analysing phylogenetic distance and antagonistic phenotype of *Bacillus* species, to predict the contribution of each predicted BGC to antagonism (Xia et al., 2022), although this type of analysis was conducted on data where antagonism is closely associated with phylogeny, unlike the data presented within this study. Further investigation into the correct statistical approach to conduct on data of this type, considering Type II error rates, and potential redundancy of GCFs with respect to the antagonism phenotype are necessary. Another used Pearson's rank coefficient to associate predicted BGCs with *in vitro* antagonism of *Streptomyces scabies*, the causative agent of potato common scab, by *Pseudomonas* isolates (Pacheco-Moreno et al., 2021). It was not possible to conduct Pearson's rank correlation coefficient on the data presented within this Chapter, as the *Z. tritici* blastospore antagonism data is qualitative in nature. It will be interesting to utilise this approach in combination with large scale quantitative assessment of *Z. tritici* antagonism as part of a future experiment.

4.4.3. Identification of phylogenetic relationships with secondary metabolite BGCs prediction

These results indicate that the distribution of many BGCs forming GCF networks appear to group with the constructed *Pseudomonas* species phylogeny, with many GCFs appearing to be specific to *Pseudomonas* subspecies within the collection. The *Pseudomonas* phylogeny was constructed using genes from the 'core genome' (Price et al., 2010), whereas secondary metabolite BGCs are found most commonly in the 'flexible' genome (Gross and Loper, 2009). Predicted BGCs forming GCF networks strongly correlating with a phylogeny based on 'core' genes, could indicate that vertical transmission of the BGC is the most likely mechanism of transmission. Similarly, the presence of predicted BGCs from across the phylogeny forming GCF networks could be indicative of horizontal transfer events of the BGC. However, these hypotheses should be tested with wider comparison amongst *Pseudomonas* genome sequences, as the presence of predicted cluster PKSOther_2429, corresponding to the BGC encoding the biosynthesis of 2,4-DAPG, also appears to group with phylogeny. However, previous studies have indicated multiple independent acquisition events of the 2,4-DAPG gene cluster within *Pseudomonas* spp. as opposed to a single event followed by vertical inheritance (Almario et al., 2017). It will be interesting to compare constructed GCF networks from this study to the Biosynthetic Gene Cluster Family database 'BiG-FAM' (Kautsar et al., 2021), to further investigate the distribution of similar clusters within other subspecies of *Pseudomonas*, and other taxa more broadly.

4.4.4. Identification of predicted secondary metabolite BGCs with high sequence similarity to known antifungal secondary metabolite BGCs

These results indicate the presence of previously described secondary metabolite BGCs within the test *Pseudomonas* library. A number of reference BGC sequences

forming GCF networks with predicted secondary metabolite BGCs have previously been described as exhibiting antifungal activity against fungal plant pathogens.

Secondary metabolite 2,4-DAPG has previously described antifungal activity against a range of fungal plant pathogens, including *Thielaviopsis basicola* (Keel et al., 1992), *Pythium ultimum* (Shanahan et al., 1992), *Rhizoctonia solani* (Howell and Stipamnovic, 1979), *Gaeumannomyces var. tritici* (Bangera and Thomashow, 1999; Keel et al., 1992; Raaijmakers and Weller, 2001; Vincent et al., 1991), *Fusarium oxysporum* (Duffy and Défago, 1997) and *Z. tritici* (Levy et al., 1992b). Interestingly, all 7 *Pseudomonas* isolates within the *Pseudomonas fluorescens* clade, originating from the endosphere, contain a predicted BGC showing high sequence similarity with the reference BGC for 2,4-DAPG production from the MiBIG database, with significant BLAST hits for all genes within the reference BGC sequence. Of the 7 *Pseudomonas fluorescens* isolates found to contain a predicted BGC forming a GCF network with the reference BGC for 2,4-DAPG, 6 isolates showed an antagonistic phenotype against *Z. tritici* blastospores *in vitro*. Roth84 was predicted to contain a BGC showing high sequence similarity to the 2,4-DAPG cluster but did not show an antagonistic phenotype against *Z. tritici in vitro*. This result could be due to differences in expression levels of the BGC, as presence of a predicted BGC within a genome assembly does not confirm expression of the BGC. BGC sequences may exist as artefacts within bacterial genomes, or may only be expressed under specific environmental conditions (Buijs et al., 2020). This will be investigated as part of future work. Similarly, differences in promoter sequences, or expression dependent upon external conditions or cues, may mean that there is variation between *Pseudomonas* isolates found to contain a BGC highly similar to 2,4-DAPG. It will be interesting to investigate if differences in upstream promoter regions exist within the *P. fluorescens* isolates found to contain BGCs predicted to encode 2,4-DAPG biosynthesis yet exhibit differing *Z. tritici* blastospore antagonism phenotypes.

Generation of loss-of-function mutants in 2,4-DAPG biosynthesis would be useful, both as an alternative approach to confirm 2,4-DAPG as the causative agent of *in vitro Z. tritici* blastospore antagonism, and to also examine the relative contribution of this gene cluster to the observed phenotype. Loss-of-function mutants in 2,4-DAPG biosynthesis that retain the antagonistic phenotype against *Z. tritici* blastospores would indicate that multiple, possibly cryptic, mechanisms of antagonism are present, warranting further investigation into the other unknown BGCs present within the genome assembly. Loss-of-function mutants in 2,4-DAPG biosynthesis have previously been generated through transposon mutagenesis in *phlD*, found to be essential for the synthesis of the precursor of 2,4-DAPG (Bangera and Thomashow, 1999; Yang and Cao, 2012), or through allelic replacement of *phlACBD* (Hansen et al., 2021).

Other identified BGCs from *Pseudomonas* isolate genome assemblies were predicted to encode the biosynthesis of a previously described antifungal secondary metabolite.

Predicted BGCs from *Pseudomonas* isolate genome assemblies were found to contain significant BLAST hits with all genes in the MiBIG reference BGCs encoding the biosynthesis of massetolide A, obafluorin, and anikasin.

All predicted BGCs forming a GCF network with the MiBIG reference BGC for the biosynthesis of massetolide A, were also found to contain significant BLAST hits for all genes present in the reference sequence. Massetolide A has previously described antifungal activity against *Phytophthora infestans* by *P. fluorescens* SS101 (Tran et al., 2007), but does not play a significant role in the suppression of *Pythium* spp. *in vitro* (Mazzola et al., 2007). All 4 *P. lurida* isolates within my test library were predicted to contain the BGC for the production of massetolide A, however, all exhibited a non- antagonistic phenotype against *Z. tritici* blastospores *in vitro*. These results could be indicative of massetolide A functioning as a narrow-spectrum antifungal compound or could indicate that under the environmental

conditions in the *Z. tritici* blastospore antagonism assay, expression of the BGC is not induced.

Predicted BGC sequences forming a GCF network with MiBIG reference BGC encoding the biosynthesis of pyoverdine, were found to contain part of the BGC sequence. Pyoverdine has previously been described as the causative agent in the *in vitro* inhibition of *Aspergillus fumigatus* by *Pseudomonas aeruginosa* PA14 (Sass et al., 2019, 2018). However, it was found that the partial BGC sequence for pyoverdine biosynthesis did not usually correlate with *Z. tritici* blastospore antagonism. Only 2 out of 34 *Pseudomonas* isolates predicted to contain a partial sequence of a pyoverdine BGC were found to be antagonistic towards *Z. tritici* blastospores *in vitro*, with 32 *Pseudomonas* isolates found to be non-antagonistic. It will be interesting to investigate if *Z. tritici* blastospores are resistant to the inhibition by pyoverdine, as these results may suggest. However, it could also be the case that these isolates are not pyoverdine producers.

The reference BGC for pyoverdine consists of 4 core biosynthesis genes, spanning a genomic region of 175,054bp as described in the MiBIG database. The identification of partial predicted pyoverdine BGC sequences could be due to the short-read sequencing technology employed in the generation of *Pseudomonas* genome assemblies, resulting in contig lengths shorter than the length of the pyoverdine reference BGC. It will be interesting to see if the generation of *Pseudomonas* genome assemblies using long-read sequencing approaches, such as PacBIO, would allow the identification of complete sequences of large secondary metabolite BGCs such as pyoverdine as described in previous studies (Guo et al., 2021). Coupling this approach with a chemical identification of pyoverdine production would inform on how widespread the production of this metabolite is by pseudomonads, and whether this can be accurately predicted by bioinformatics.

Other complete BGC sequences, corresponding to MiBIG reference BGC sequences encoding the biosynthesis of anikasin and obafluorin, were found in predicted BGCs from pseudomonads within the pseudomonad library. Anikasin has previously been described as a niche amoebicide, and enabling swarming motility in *P. fluorescens* HKI0770 (Götze et al., 2017). Obafluorin is an antibiotic, produced by *P. fluorescens* (ATCC 39502), showing weak antibiotic activity against a range of bacteria (Wells et al., 1984). These results highlight the ability of network analysis of predicted secondary metabolite BGCs and MiBIG reference BGC sequences to identify previously described BGCs with a range of functions.

4.4.5. *Z. tritici* blastospore antagonism by *Pseudomonas* isolates cannot be explained through the identification of known antifungal BGCs within genome assemblies

The previous section highlighted the use of bioinformatic tools and confrontation assays to predict the presence and production of known antifungal metabolites by *Pseudomonas* bacteria against *Z. tritici*. In addition, these tools can also be used to determine whether the *in vitro Z. tritici* blastospore antagonistic phenotype exhibited by *Pseudomonas* isolates within the library cannot be wholly explained through the identification of previously described BGC sequences within the MiBIG repository. These results could indicate that predicted secondary metabolite BGCs of yet unknown function are conducive to *Z. tritici* blastospores antagonism *in vitro*, or that a differing underlying mechanism of antagonism is present. It will be interesting to investigate the expression levels of these BGCs of unknown function present in *Pseudomonas* isolates in confrontation with *Z. tritici* and characterise their effect on antagonism and secreted metabolites as previously outlined.

These results could also indicate that *Z. tritici* blastospore antagonism by *Pseudomonas* isolates, previously described, takes place through a mechanism different to the secretion of secondary metabolites. However, the formation of

zones of clearing by antagonistic *Pseudomonas* species on confluent lawns of *Z. tritici* blastospores as part of the antagonism assay are indicative of secreted compounds produced by the *Pseudomonas* colonies.

4.4.6. Identification of 2,4-DAPG in agar extracts of *Z. tritici* blastospore antagonistic *Pseudomonas* isolate Roth112

These results are indicative of the biosynthesis and secretion of 2,4-DAPG by *Z. tritici* blastospore antagonistic *Pseudomonas* isolate Roth112 *in vitro*. A study describing a whole-cell biosensor for the detection of 2,4-DAPG producing bacteria similarly used LC-MS to detect 2,4-DAPG from agar extracts of a number of *Pseudomonas* species, to confirm the effectiveness of the biosensor (Hansen et al., 2021). The finding of a total ion chromatogram peak associated with 2,4-DAPG from agar extracts surrounding Roth112 both in confrontation with *Z. tritici* blastospores, and alone, could be indicative of the stimulation of 2,4-DAPG production by dextrose contained within the PDA growth medium, which has previously been found to be strain dependent (Duffy and Défago, 1999). Fungal metabolites produced by *F. oxysporum f. sp. radicis-lycopersici* have previously been shown to repress the production of 2,4-DAPG by *P. fluorescens* isolate CHA0, both *in vitro*, and on tomato roots (Schnider-Keel et al., 2000). It will be interesting to investigate whether fungal metabolites produced by *Z. tritici* could also repress the production of antifungal secondary metabolites by *Pseudomonas* isolates.

4.4.7. Confirmation of antifungal activity of 2,4-DAPG against *Z. tritici* blastospore growth *in vitro*

These results indicate that 2,4-DAPG can inhibit the growth of *Z. tritici* blastospores *in vitro* at 50ug/ml-100ug/ml, adding to previous studies that have shown 2,4-DAPG to inhibit the growth of *Z. tritici* hyphae *in vitro* (Levy et al., 1992b). This result could further support the hypothesis that Roth 84, whilst containing a

predicted BGC encoding the biosynthesis of 2,4-DAPG, may show an altered or no expression of the BGC *in vitro*, compared to other isolates containing the same predicted BGC. The application of transcriptomic approaches will be necessary to further investigate the perceived antagonism differences between *Pseudomonas* isolates predicted to possess the biosynthetic ability to produce 2,4-DAPG. Variation in fungicide sensitivity (Lendenmann et al., 2015) and abiotic stress tolerance (Lendenmann et al., 2016) within *Z. tritici* populations has been shown previously. A liquid culture optical density-based system could be used to calculate *in vitro* half maximal effective concentration EC_{50} values for 2,4-DAPG, utilised by previous studies to quantify insensitivity to azoles (Cools et al., 2012) and DMI fungicides (Blake et al., 2018). This would be particularly useful to compare EC_{50} values between genetically diverse *Z. tritici* isolates in response to 2,4-DAPG.

A study investigating the cellular targets and mode-of-action of 2,4-DAPG in *Saccharomyces cerevisiae* found that 2,4-DAPG acts as a proton ionophore, uncoupling respiration and ATP synthesis by dissipating the proton gradient across the mitochondrial membrane (Troppens et al., 2013). The authors described a *ydc1* mutant, with altered sphingolipid homeostasis, that displayed increased tolerance to 2,4-DAPG *in vitro*. It will be interesting to investigate if a mutant in an orthologous gene of *ydc1* within *Z. tritici* similarly confers increased tolerance to 2,4-DAPG *in vitro*, and if similar mutations in sphingolipid homeostasis are found within natural populations of *Z. tritici*, conferring resistance to conventional fungicides or providing biotic stress tolerance.

4.5. Conclusions

Secondary metabolite biosynthetic gene cluster prediction reveals many predicted BGCs of currently unknown function within the *Pseudomonas* collection.
The distribution of numerous BGCs within the *Pseudomonas* collection appear to be *Pseudomonas* subspecies specific.

Zymoseptoria tritici blastospore antagonism cannot be explained by phylogeny or through the prediction of previously described antifungal BGCs from *Pseudomonas*, raising the prospect that BGCs of currently unknown function may contribute to the observed phenotype.

Chapter 5. Variation in susceptibility of *Z. tritici* isolates to antagonism by *Pseudomonas* bacteria

5.1. Introduction

This Chapter describes the screening of genetically diverse *Z. tritici* isolates against a subset of the *Pseudomonas* isolate collection, to identify if there is any variation in sensitivity to antagonism by *Pseudomonas* isolates. This Chapter will utilise the *Z. tritici* blastospore antagonism assay described in Chapter 2 in a lower throughput format and combine image analysis to quantitatively assess differences in the antagonism of *Z. tritici* blastospores of different genotypes, by *Pseudomonas* isolates *in vitro*.

Previous studies have identified that in natural field settings, high levels of genetic diversity are observed in *Z. tritici* populations. For example, over 600 different genotypes of *Z. tritici* were isolated from a single field over a 3 month period (Chen and McDonald, 1996), around 90% of global gene diversity was found to be distributed within a wheat field (Zhan et al., 2003), and individual leaf lesions were found to harbour 2-5 different genotypes (Linde et al., 2002).

Previous studies investigating the antagonistic potential of bacterial isolates against fungal plant pathogens *in vitro*, including *Z. tritici*, have mostly consisted of single genotypes of the fungal plant pathogen (Flaishman et al., 1990; Flaishman, 1996; Levy et al., 1992a, 1992b, 1989, 1988). Quantification of *in vitro* antagonism of fungal pathogens by bacterial isolates is difficult, owing to the hyphal growth of most fungal pathogens, and has commonly taken place through qualitative, rather than quantitative assessments (Figure 5.2). The radial zones of clearing produced by antagonistic *Pseudomonas* isolates, in the *Z. tritici* blastospore antagonism assay developed in Chapter 2, on confluent lawns of *Z. tritici* blastospores offer the potential to quantitatively assess antagonism of *Z. tritici* blastospores *in vitro*,

through image analysis. These quantitative assessments could facilitate the comparison of the sensitivity of genetically diverse *Z. tritici* isolates to antagonistic *Pseudomonas* isolates and facilitate the identification of subtle differences in sensitivity. This could be important for selection of novel antifungal compounds for further study and potential commercial use, as compounds that control all fungal pathogen variants could offer greater value than those which only selectively inhibit a subset of the population.

No previous studies have investigated potential variation in the response of genetically diverse *Z. tritici* isolates to bacterial antagonism. This Chapter describes the screening of 5 antagonistic and 6 non-antagonistic *Pseudomonas* isolates (when tested against IPO323), confronted with 11 genetically diverse *Z. tritici* isolates *in vitro*.

Hypothesis:

(1) Zones of inhibition produced by a given *Pseudomonas* bacterial strain in confrontation with genetically diverse *Z. tritici* isolates differ significantly.

5.2. Chapter specific methods

5.2.1. Culturing of *Z. tritici* blastospores

Zymoseptoria tritici blastospores were cultured from glycerol stocks as described in Chapter 2, *Z. tritici* isolates were collected from across Europe in 2015 and 2016 (Chen et al., manuscript under revision).

5.2.2. Culturing of *Pseudomonas* isolates

Pseudomonas isolates were cultured from glycerol stocks as described in Chapter 2.

5.2.3. Storage of isolates

Both *Pseudomonas*, and *Z. tritici* isolates were stored as glycerol stocks, as described in Chapter 2.

5.2.4. *In vitro* screen for fungal antagonism of *Z. tritici* by *Pseudomonas* isolates

Zymoseptoria tritici blastospore antagonism assays were conducted as previously described in Chapter 2, with the number of *Pseudomonas* isolates screened per plate reduced to 11, to increase the spacing between isolates, and enable quantitative data collection. A total of 11 *Pseudomonas* isolates alongside an overnight LB Miller Broth (Formedium) negative control were screened on each plate. A total of four replicate confrontation assay plates were set up for each *Z. tritici* isolate, as part of the same factorial experimental design.

5.2.5. Quantification of zones of inhibition

Zones of clearing were quantified by taking photographs using a Nikon D80 digital camera with a Sigma 70mm F2.8 DG Macro lens (settings ISO 400, RAW image quality, large image size) of each plate, from a standardised height of 78.5cm after 12 days of growth. Measurements were taken from the edge of the bacterial colony to the edge of the zone of clearing of *Z. tritici* blastospores, in a radial manner from the centre of the bacterial colony, using FIJI/ImageJ (version 2.1.0/1.53c) to quantify the number of pixels (2253 pixels= 1mm). A total of 3 measurements were taken for each bacterial colony in the *Z. tritici* blastospore confrontation assay, using a random angle of measurement from the colony centre for each measurement. This was achieved through the use of a random integer generator between 0 and 359.

5.2.6. Statistical analysis

Analysis of Variance (ANOVA) was used to determine if there was a significant difference in the size of zones of inhibition produced by antagonistic *Pseudomonas* isolates in confrontation with genetically diverse *Z. tritici* isolates. Tukey's multiple comparison post-hoc test was used to examine pairwise data comparisons between *Z. tritici* genotypes at the 5% level of significance. All statistical analyses were carried out in RStudio (Build 461, R version 4.1.3), using packages stats, emmeans, multcomp, multcompView, ggpubR and ggplot2.

5.3 Results

5.3.1. Significant variation exists in the *in vitro* sensitivity of genetically diverse *Z. tritici* isolates to antagonism by *Pseudomonas* isolates

To examine variation in the sensitivity of *Z. tritici* isolates to antagonism by *Pseudomonas* isolates *in vitro*, a genetically diverse library of 11 *Z. tritici* isolates isolated from across Europe in 2015/16 in a previous project (Chen et al, manuscript under revision)(Figure 5.1), were screened for antagonism by a library of 11 *Pseudomonas* isolates – 5 antagonistic and 6 non-antagonistic isolates described in Chapter 2 (Table 5.1), where screening was conducted against *Z. tritici* isolate IPO323, the common reference isolate first collected in the Netherlands in 1984. The antagonistic isolates were selected to represent a range of predicted antagonistic mechanisms identified in Chapter 4, where secondary metabolite BGC indicated the presence of a BGC with a 100% similarity score using antiSMASH 5.2, to 2,4-DAPG within the genome assemblies of antagonistic *Pseudomonas* isolates Roth107, Roth111 and Roth112. No significant BGC hit to previously known BGCs was found for antagonistic *Pseudomonas* isolates BF-R-20 and BF-B-20 through the same analysis in chapter 4.

Antagonism screening was conducted using the *Z. tritici* blastospore antagonism assay described in Chapter 2, with the number of *Pseudomonas* isolates screened per plate reduced to 11, to increase the spacing between isolates (Figure 5.2). A phylogenetic tree was constructed from a concatenation of 6 housekeeping genes (18S (1799bp, full length), EF1alpha (1-1309bp trimmed from potential full length of 1389), ITS1 (141bp), ITS2 (161bp), RPB1 (RNA polymerase II largest subunit 5322bp, full length), RPB2 (RNA polymerase II second largest subunit 3759bp, full length)) by Hongxin Chen, which demonstrated that there was a link between sample location and genotypes, evidencing that the *Z. tritici* strain set is highly diverse (Figure 5.1).

All 6 *Pseudomonas* isolates previously determined to be non-antagonistic towards *Z. tritici* IPO323 blastospores *in vitro*, did not produce an observable zone of clearing when confronted with any of the other *Z. tritici* isolates screened within this study, indicating that IPO323 is a good test system. In addition, the application of 1ul of LB Miller Broth (Formedium) did not result in any observable zone of clearing for any *Z. tritici* isolates screened, indicating that the medium itself is not inhibitory to *Z. tritici* growth. All 5 *Pseudomonas* isolates previously determined to be antagonistic towards *Z. tritici* IPO323 *in vitro*, also produced an observable zone of clearing when confronted with all *Z. tritici* isolates screened within our study (Figure 5.3).

To compare differences in the size of zones of inhibition produced by antagonistic *Pseudomonas* isolates in confrontation with genetically diverse *Z. tritici* isolates, statistical methods were employed. Zones of inhibition data of *Z. tritici* isolates in confrontation with *Pseudomonas* isolate BFR20 were log transformed, to fulfil the requirement of analysis of variance (ANOVA) for data to be approximately normally distributed. Zones of inhibition data for all other antagonistic *Pseudomonas* isolates were found to be approximately normally distributed without a transformation.

Significant differences in the mean zones of inhibition produced by *Pseudomonas* isolate BFR20 in confrontation with genetically diverse *Z. tritici* isolates were determined using one-way analysis of variance (ANOVA). A statistically significant difference in the mean zones of inhibition was detected between genetically diverse *Z. tritici* isolates between at least two groups, confronted with *Pseudomonas* isolate BFR20 ($F(11, 36) = 11.48$, $p < 0.001$) (Supplementary Table 4.). To further investigate differences in the mean zones of inhibition produced by *Pseudomonas* isolate BFR20, against individual *Z. tritici* genotypes, Tukey's multiple comparison post-hoc test was used (results summarised in Figure 5.4). Pairwise comparisons between the mean zones of inhibition revealed significant differences between some *Z. tritici* genotypes (Supplementary Table 5.). Mean values of zones of inhibition not sharing any letter are significantly different by Tukey's test for multiple comparisons at the 5% level of significance (Figure 5.4).

To assess if significant differences in the mean zones of inhibition produced by *Pseudomonas* isolate BFB20 in confrontation with genetically diverse *Z. tritici* isolates were found, a one-way analysis of variance (ANOVA) was performed. One-way ANOVA revealed a statistically significant difference in the mean zones of inhibition produced by *Pseudomonas* isolate BFB20 between genetically diverse *Z. tritici* isolates between at least two groups ($F(11, 36) = 10.97$, $p < 0.001$) (Supplementary Table 6.). To examine the differences in the mean zones of inhibition produced by *Pseudomonas* isolate BFB20, between individual *Z. tritici* genotypes, Tukey's multiple comparison post-hoc test was used (results summarised in Figure 5.5). Pairwise comparisons between the mean zones of inhibition revealed significant differences between some *Z. tritici* genotypes (Supplementary Table 7.). Mean values of zones of inhibition not sharing any letter are significantly different by Tukey's test for multiple comparisons at the 5% level of significance (Figure 5.5).

To identify if significant differences in the mean zones of inhibition produced by *Pseudomonas* isolate Roth 82 in confrontation with genetically diverse *Z. tritici* isolates were found, one-way analysis of variance (ANOVA) was used. One-way ANOVA revealed a statistically significant difference in the mean zones of inhibition between genetically diverse *Z. tritici* isolates between at least two groups ($F(11, 36) = 4.455$, $p < 0.001$) (Supplementary Table 8.). Tukey's multiple comparison post-hoc test was used to further examine the differences in the mean zones of inhibition produced by *Pseudomonas* isolate Roth 82 between individual *Z. tritici* genotypes (results summarised in Figure 5.6). Significant differences in the mean zones of inhibition produced by Roth 82 were found between some *Z. tritici* genotypes through pairwise comparisons (Supplementary Table 9.). Mean values of zones of inhibition not sharing any letter are significantly different by Tukey's test for multiple comparisons at the 5% level of significance (Figure 5.6).

One-way analysis of variance (ANOVA) was performed, to assess if significant differences in the mean zones of inhibition produced by *Pseudomonas* isolate Roth 107 in confrontation with genetically diverse *Z. tritici* isolates existed. One-way ANOVA revealed a statistically significant difference in the mean zones of inhibition between genetically diverse *Z. tritici* isolates between at least two groups ($F(11, 36) = 5.567$, $p < 0.001$) (Supplementary Table 10.). To identify significant differences in the mean zones of inhibition produced by *Pseudomonas* isolate Roth 107, between individual *Z. tritici* genotypes, Tukey's multiple comparison post-hoc test was used (results summarised in Figure 5.7). Pairwise comparisons between the mean zones of inhibition revealed significant differences between some *Z. tritici* genotypes in confrontation with Roth 107 (Supplementary Table 11.). Mean values of zones of inhibition not sharing any letter are significantly different by Tukey's test for multiple comparisons at the 5% level of significance (Figure 5.7).

To test whether significant differences in the mean zones of inhibition produced by *Pseudomonas* isolate Roth 112 in confrontation with genetically diverse *Z. tritici*

isolates were found, a one-way analysis of variance (ANOVA) was performed. One-way ANOVA revealed statistically significant difference in the zones of inhibition between genetically diverse *Z. tritici* isolates was found between at least two groups ($F(11, 36) = 8.11$, $p < 0.001$) (Supplementary Table 12.). To examine the differences in the mean zones of inhibition produced by *Pseudomonas* isolate Roth 112, between individual *Z. tritici* genotypes, Tukey's multiple comparison post-hoc test was used (results summarised in Figure 5.8). Pairwise comparisons between the mean zones of inhibition revealed significant differences between some *Z. tritici* genotypes (Supplementary Table 13.). Mean values of zones of inhibition not sharing any letter are significantly different by Tukey's test for multiple comparisons at the 5% level of significance (Figure 5.8).

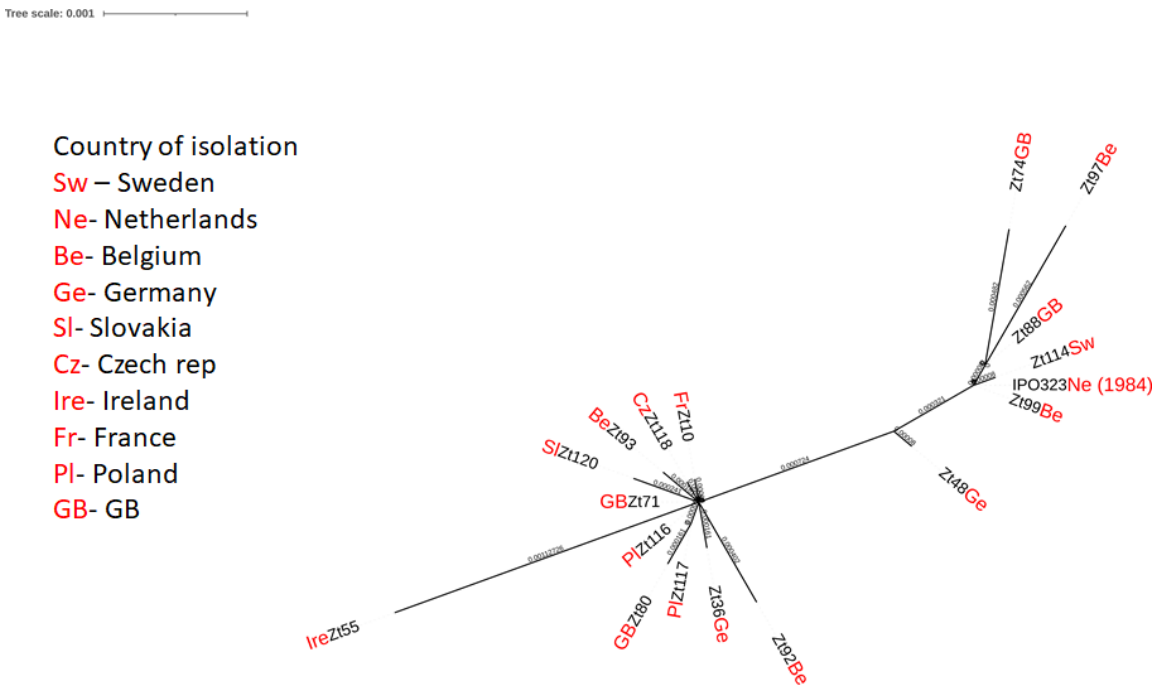


Figure 5.1 A phylogeny of *Z. tritici* isolates from across Europe.
A phylogenetic tree constructed by Hongxin Chen, from a concatenation of 6 housekeeping genes of genetically diverse *Z. tritici* isolates isolated from across Europe, with the country of isolation indicated (personal communication, Hongxin Chen 2021). *Z. tritici* isolates IPO323, Zt10, Zt114, Zt116, Zt118, Zt120, Zt120, Zt36, Zt55, Zt74, Zt80, and Zt92 were screened for variation in response to *Pseudomonas* isolates in this study.

Table 5.1 A list of *Pseudomonas* isolates screened for antagonism in confrontation with genetically diverse *Z. tritici* isolates within this study, with previously described antagonism phenotype (Chapter 2) indicated.

***Pseudomonas* isolate**	***Z. tritici* blastospore antagonism phenotype**
B-F-R20	antagonistic
B-F-B20	antagonistic
Roth17	non-antagonistic
Roth40	non-antagonistic
Roth79	non-antagonistic
Roth82	antagonistic
Roth97	non-antagonistic
Roth105	non-antagonistic
Roth107	antagonistic
Roth112	antagonistic

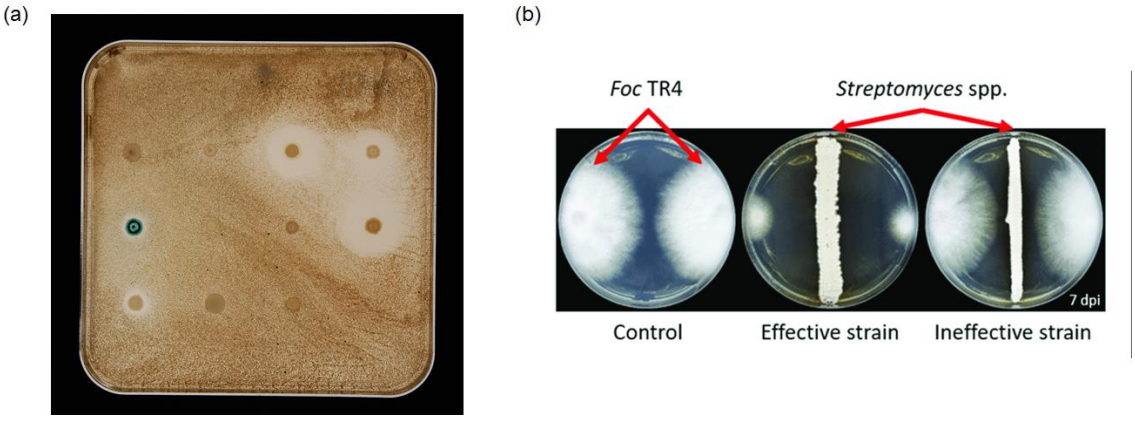


Figure 5.2 *In vitro* fungal antagonism assays involving bacterial species. **(a)** A figure showing the high throughput *Z. tritici* blastospore antagonism assay screening 11 *Pseudomonas* isolates against *Z. tritici* isolate Zt92. **(b)** A conventional fungal antagonism screen involving *Fusarium oxysporum f. sp. cubense* and *Streptomyces* spp., adapted from (Bubici, 2019)**.**

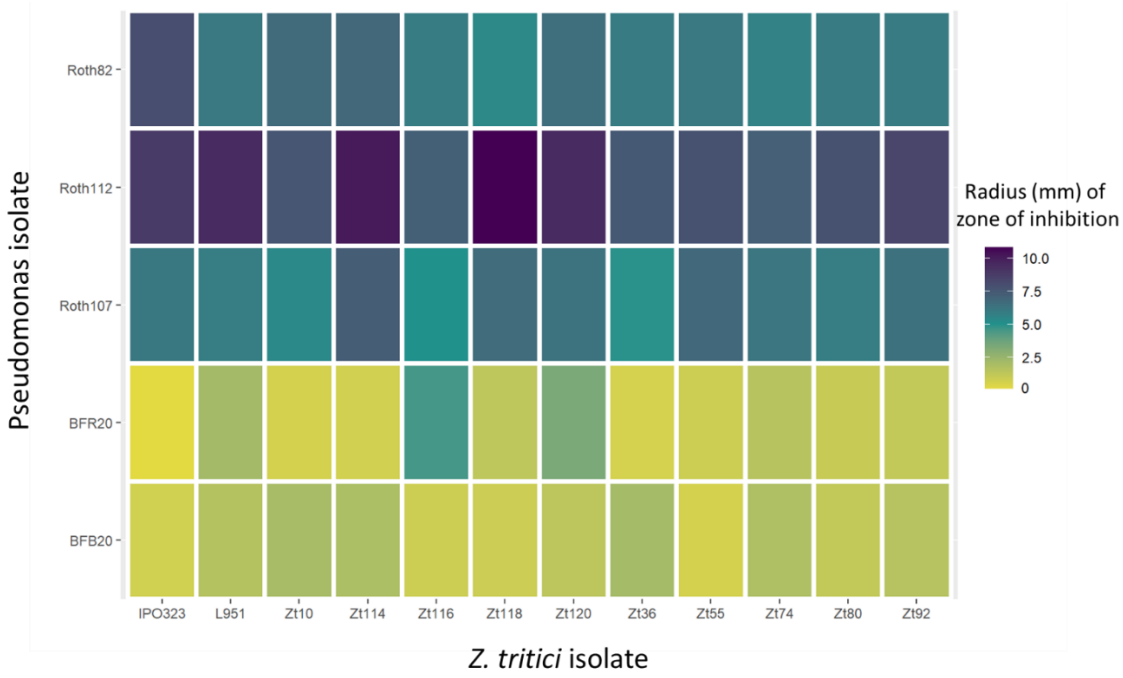


Figure 5.3 Inhibition of *Z. tritici* blastospores by *Pseudomonas* isolates *in vitro*.
Average radius of the zones of inhibition (mm) produced by *Pseudomonas* against different *Z. tritici* strains after 12 days grown on PDA (n=4).

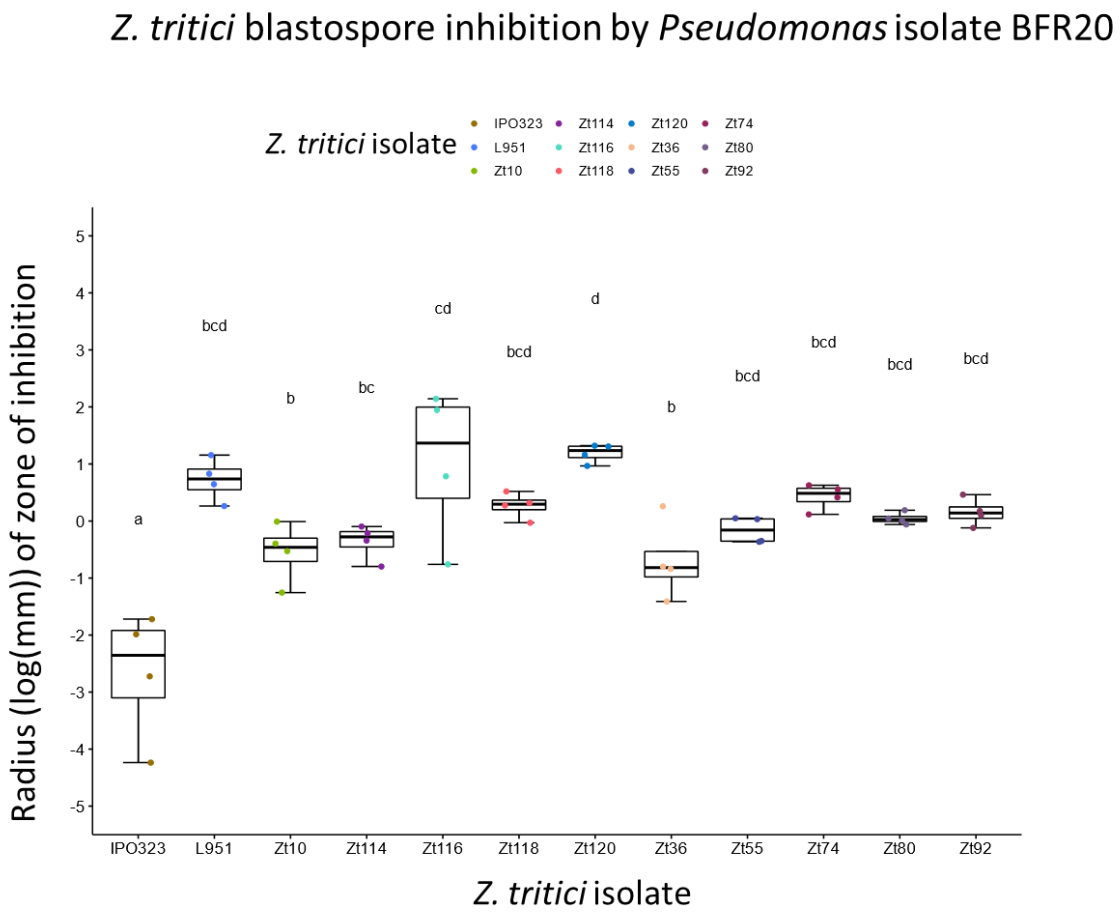


Figure 5.4 Zones of inhibition produced by *Pseudomonas* isolate BFR20 in confrontation with genetically diverse *Z. tritici* blastospores *in vitro*.
Log(Radius) (mm) of the zones of inhibition produced by *Pseudomonas* isolate BFR20 in confrontation with 12 genetically distinct *Z. tritici* isolates within the *Z. tritici* blastospore *in vitro* antagonism assay. Mean values of zones of inhibition not sharing any letter are significantly different by Tukey's test for multiple comparisons at the 5% level of significance (Supplementary Table 6.).

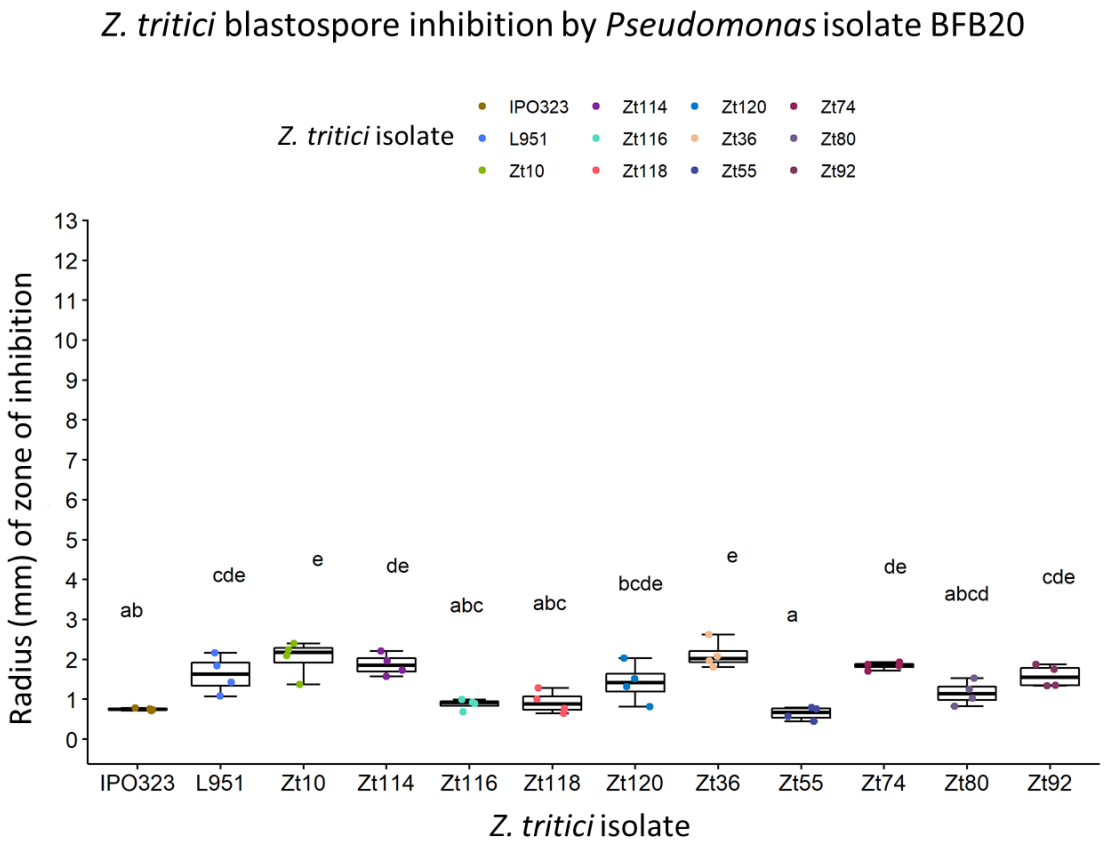


Figure 5.5 Zones of inhibition produced by *Pseudomonas* isolate BFB20 in confrontation with genetically diverse *Z. tritici* blastospores *in vitro*.
Log(Radius) (mm) of the zones of inhibition produced by *Pseudomonas* isolate BFB20 in confrontation with 12 genetically distinct *Z. tritici* isolates within the *Z. tritici* blastospore *in vitro* antagonism assay. Mean values of zones of inhibition not sharing any letter are significantly different by Tukey's test for multiple comparisons at the 5% level of significance (Supplementary Table 8).

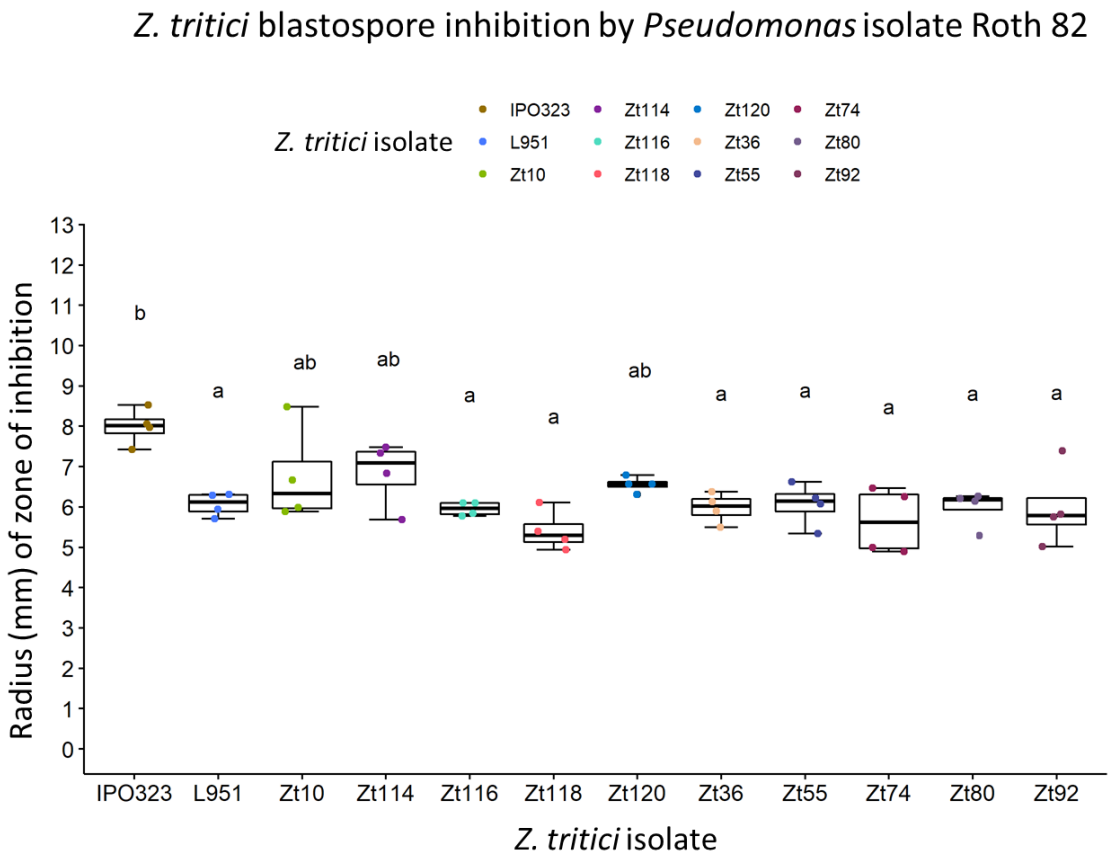


Figure 5.6 Zones of inhibition produced by *Pseudomonas* isolate Roth 82 in confrontation with genetically diverse *Z. tritici* blastospores *in vitro*.
Radius (mm) of the zones of inhibition produced by *Pseudomonas* isolate Roth 82 in confrontation with 12 genetically distinct *Z. tritici* isolates within the *Z. tritici* blastospore *in vitro* antagonism assay. Mean values of zones of inhibition not sharing any letter are significantly different by Tukey's test for multiple comparisons at the 5% level of significance (Supplementary Table 10).

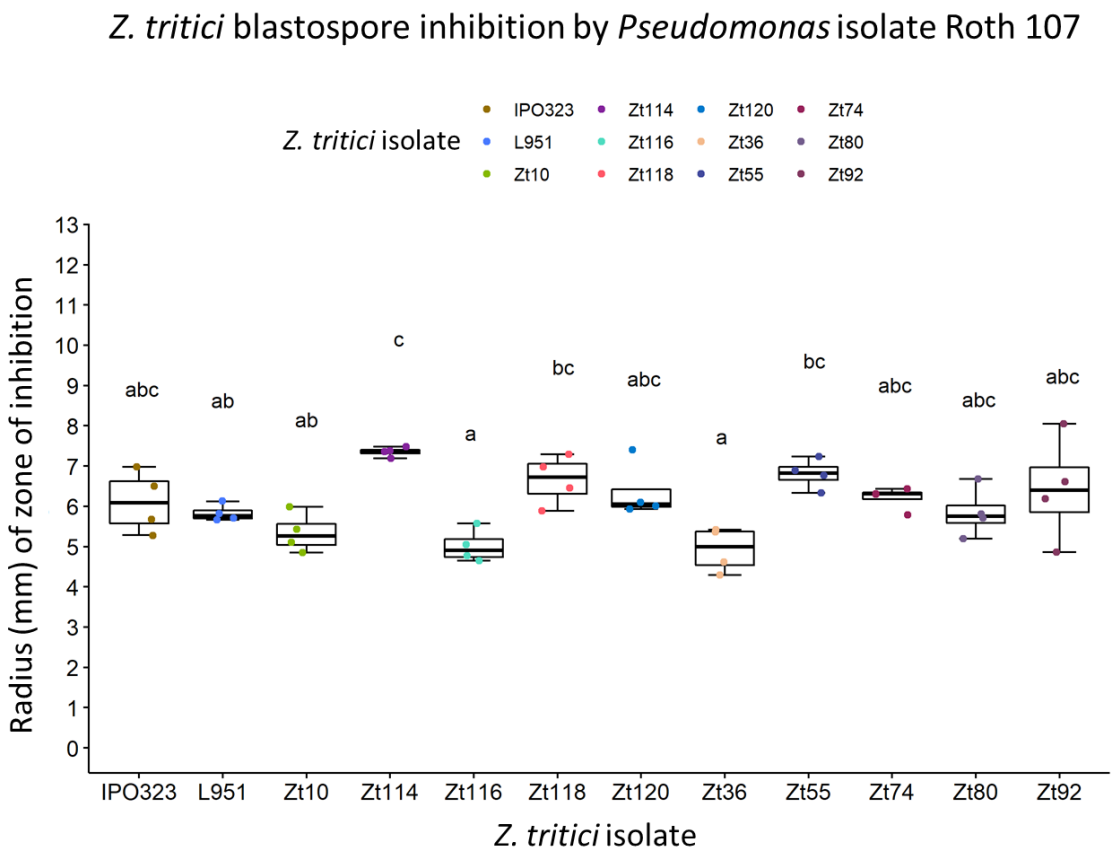


Figure 5.7 Zones of inhibition produced by *Pseudomonas* isolate Roth 107 in confrontation with genetically diverse *Z. tritici* blastospores *in vitro*.
Radius (mm) of the zones of inhibition produced by *Pseudomonas* isolate Roth 107 in confrontation with 12 genetically distinct *Z. tritici* isolates within the *Z. tritici* blastospore *in vitro* antagonism assay. Mean values of zones of inhibition not sharing any letter are significantly different by Tukey's test for multiple comparisons at the 5% level of significance (Supplementary Table 12).

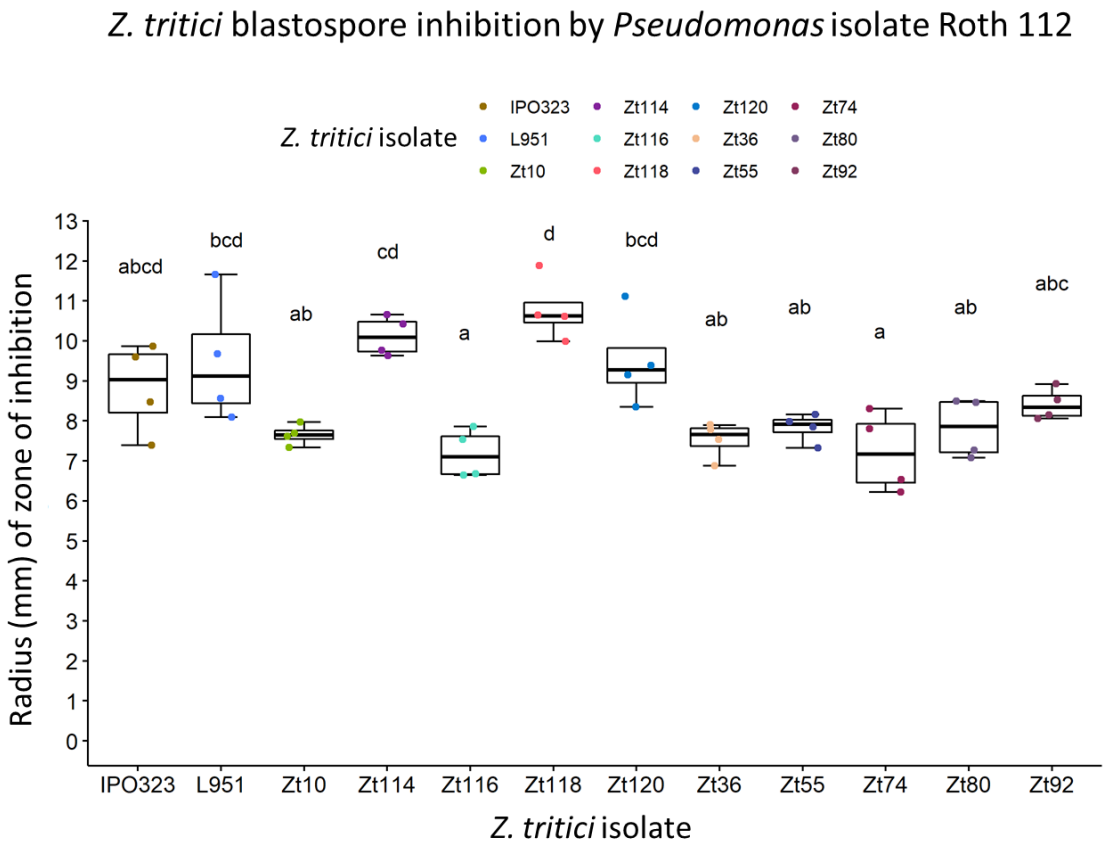


Figure 5.8 Zones of inhibition produced by *Pseudomonas* isolate Roth 112 in confrontation with genetically diverse *Z. tritici* blastospores *in vitro*.
Radius (mm) of the zones of inhibition produced by *Pseudomonas* isolate Roth 112 in confrontation with 12 genetically distinct *Z. tritici* isolates within the *Z. tritici* blastospore *in vitro* antagonism assay. Mean values of zones of inhibition not sharing any letter are significantly different by Tukey's test for multiple comparisons at the 5% level of significance (Supplementary Table 14).

5.4. Discussion

The results described within this Chapter indicate natural variation within *Z. tritici* populations in sensitivity/resistance to antagonism by *Pseudomonas* bacteria *in vitro*, but that complete resistance to previously described antagonistic *Pseudomonas* isolates was not observed in the *Z. tritici* isolates tested. The methodology described in this Chapter enables the generation of quantitative data

of *Z. tritici* blastospore antagonism, through image analysis. In a wider context, these results highlight the potential need for multiple genotypes of fungal pathogen to be assessed in biocontrol studies, particularly for highly genetically diverse species such as *Z. tritici*, as resistance to bacterial antagonism may exist as a quantitative trait within natural populations.

5.4.1. Quantitative assessment of *in vitro Z. tritici* blastospore antagonism by *Pseudomonas* isolates

These results indicate the ability to quantitatively assess antagonism of *Z. tritici* by *Pseudomonas* isolates *in vitro*, using a combination of image analysis and the *Z. tritici* blastospore antagonism assay previously described. Assessment of fungal antagonism by bacterial isolates is commonly conducted qualitatively, owing to the difficulty in quantifying antagonism of hyphae *in vitro*. A high throughput semi-solid medium based screen has been described elsewhere, using spectrophotometer measurements (OD_{600}) and turbidimetric measurements to quantify growth of the pathogenic fungi *Aspergillus* when exposed to chemical libraries, to screen for antagonism of the fungus through a reduction in growth rate compared to control (Medina et al., 2012). However, the application of this technique is limited, due to overlapping spectra commonly used to quantify the growth of bacteria (OD_{500}) and *Z. tritici* (OD_{600}), the screening of bacterial isolates for fungal antagonism using this approach would not be feasible. However, a limitation of the approach employed in this study, is that the observed zones of clearing produced by antagonistic *Pseudomonas* isolates are potentially constrained by the diffusibility of secreted compounds involved in antagonism through the agar medium. This could limit the ability of this screen to identify subtle changes in sensitivity of *Z. tritici* isolates to classes of high-molecular weight secreted compounds with described antifungal activity, such as lipopeptides (Berry, 2010; Geudens and Martins, 2018; Mejri et al., 2018).

The ability to identify subtle changes in the antagonism of *Z. tritici* blastospores by *Pseudomonas* isolates *in vitro*, as described in this Chapter, could also be useful in the characterisation of secondary metabolite BGCs implicated in the *Z. tritici* blastospores antagonism phenotype observed in *Pseudomonas* isolates. It will be interesting to investigate the relative contribution of predicted secondary metabolite BGCs to the *Z. tritici* antagonism phenotype, through the quantification of *Z. tritici* antagonism in loss-of-function *Pseudomonas* mutants.

5.4.2. Variation in the *in vitro* sensitivity of *Z. tritici* isolates to antagonistic pseudomonads

Our results indicate that there is some natural variation in sensitivity or resistance to bacterial antagonists amongst *Z. tritici* isolates obtained from across Europe. This is the first study to investigate variation in the response to bacterial antagonists in a library of genetically diverse isolates of a fungal plant pathogen. This study highlights the possibility of sensitivity to bacterial antagonism by *Pseudomonas* isolates *in vitro*, existing as a quantitative trait within natural *Z. tritici* populations. One clear observation was that there was no significant difference in the variability of inhibition between the “old” reference isolate IPO323 and the more recently isolated strains. This suggests that no obvious selection for broad spectrum insensitivity has occurred across this period. Although this would require more comparisons with additional “old” strains to validate this observation.

A number of quantitative traits have been identified in *Z. tritici* populations, for traits such as temperature tolerance (Lendenmann et al., 2016), and fungicide resistance (Lendenmann et al., 2015). The results presented within this Chapter highlight the possibility of sensitivity to bacterial antagonism existing as a quantitative trait within natural *Z. tritici* populations. The patterns of sensitivity of *Z. tritici* isolates to antagonism by *Pseudomonas* isolates show that no *Z. tritici* isolate tested was consistently the most sensitive or resistant towards all antagonistic

Pseudomonas isolates screened. This could indicate differing underlying mechanisms of antagonism by *Pseudomonas* isolates, and potentially differing genetic targets for antagonism in *Z. tritici* blastospores, or differing levels of tolerance to antifungal metabolites in the *Z. tritici* test set. It will be interesting to generate mapping populations of sexual crosses between *Z. tritici* isolates resistant and sensitive to particular bacterial antagonists, to identify possible 'modes-of-action' of bacterial antagonists. This could be achieved through the screening of the mapping population in the assay described in this chapter, and the use of Genome-Wide Association Study (GWAS) approaches to identify genomic regions associated with heightened sensitivity or resistance to antagonism by the bacterial antagonist.

5.4.3. Implications for the development of bio-fungicides

The results indicating variation in sensitivity to bacterial antagonists by natural *Z. tritici* isolates are relevant for the development of bacterial biocontrol agents effective against fungal plant pathogens, or 'bio-fungicides'. Resistance to conventional fungicides is monitored in natural populations of *Z. tritici* (Cools and Fraaije, 2012). A number of studies have found effective biocontrol agents, effective against single isolates of *Z. tritici*, such as including *Bacillus* spp. (Allioui et al., 2021; Mejri et al., 2018), and *Trichoderma* spp. (Perelló et al., 2009). It will be interesting to assess whether the observed natural variation in the response of *Z. tritici* to antagonism by *Pseudomonas* in this study, is also observed for antagonism by other biocontrol agents. A recent study investigating *in vitro* antagonism of 8 *Pseudomonas* strains against *Ralstonia solanacearum* found differences in the sizes zones of inhibition produced, based on both *Pseudomonas* genotype and *R. solanacearum* genotype (Clough et al., 2022). Monitoring of natural *Z. tritici* populations for variation in response to biological control agents and fungicides could enable more effective deployment of combined control strategies in the future. It will be interesting to examine whether previously

described mechanisms of fungicide resistance that have been observed in *Z. tritici* populations, such as overexpression of efflux pumps (Omrane et al., 2015), also confer resistance to antagonism by biological agents.

5.5. Conclusions

No complete resistance to antagonism by *Pseudomonas* isolates, *in vitro*, exists within the genetically diverse *Z. tritici* library screened in this study.

No obvious pattern of sensitivity was apparent among the *Z. tritici* isolates screened against *Pseudomonas* isolates within this study.

Significant variation in the sensitivity to antagonism by *Pseudomonas* isolates *in vitro* exists within the genetically diverse *Z. tritici* library screened within this study.

Chapter 6. Transcriptomics of predicted secondary metabolite biosynthetic gene clusters of antagonistic and non-antagonistic *Pseudomonas* isolates

6.1. Introduction

This Chapter describes an investigation into the transcriptomic responses of antagonistic and non-antagonistic *Pseudomonas* isolates when confronted with *Z. tritici* blastospores as well as when cultured independently in an *in vitro* set up. This Chapter will also investigate the expression profiles of secondary metabolite BGCs predicted in Chapter 4.

The use of predictive bioinformatic software, such as antiSMASH (Blin et al., 2019), can offer useful insights into the presence of putative secondary metabolite BGCs within bacterial genome assemblies, as outlined in Chapter 4. However, the identification of the presence of a putative secondary metabolite BGC within a bacterial genome assembly does not confirm transcription and expression of the BGC by the cell. Validation of transcription and expression of secondary metabolite BGCs through experimental approaches are required, to further assess their potential implication in observed phenotypes. Transcriptomic analysis is commonly used to identify expression of genes in particular contexts or environmental conditions (Lim et al., 2012; Wu et al., 2011). Such experiments can also be utilised to identify differentially expressed genes between treatment conditions. Comparative transcriptomics has previously been utilised to identify the predicted secondary metabolite BGC associated with the production of salinipostins by *Salinispora* spp. (Amos et al., 2017), and to identify differential gene expression of *Pseudomonas* isolate Pf0-1 confronted with bacterial competitors (Garbeva et al., 2011). Transcriptomic experiments investigating the

underlying transcriptional response of *Pseudomonas* isolates to confrontation with *Z. tritici* isolates have not been conducted. The expression of predicted secondary metabolite BGCs by *Pseudomonas* isolates in relation to observed fungal antagonism phenotypes is currently unknown. This Chapter describes the use of RNA-sequencing to investigate secondary metabolite gene expression of antagonistic *Pseudomonas* isolate Roth16, and non-antagonistic *Pseudomonas* isolate Roth105 after 4 hours of confrontation with *Z. tritici* blastospores *in vitro*. RNA-sequencing was chosen, as this can simultaneously report on the expression of all genes, within all secondary metabolite BGCs in a single sample and step, and thus supersedes determining gene expression through other conventional methods such as single gene qPCR. *Z. tritici* blastospore antagonistic *Pseudomonas* isolate Roth16 was chosen as prediction of secondary metabolite BGCs from the genome assembly, using antiSMASH, and network analysis using BiG-SCAPE with reference BGCs from the MiBIG repository in Chapter 4, indicated that none of the predicted secondary metabolite BGCs were previously known/characterised. *Pseudomonas* isolate Roth 105 was chosen as it was found to be non-antagonistic against all genetically diverse *Z. tritici* isolates tested in Chapter 5 in the *in vitro* blastospore antagonism assay. *Zymoseptoria tritici* isolate IPO323 was used in this study, as this is a model strain and was used in the blastospore antagonism *in vitro* assay used to determine the antagonism phenotype of Roth 16 and Roth 105 in Chapter 2. *Zymoseptoria tritici* isolate IPO323 also has a 'complete' genome sequence with high quality annotations, enabling analysis of the response of *Z. tritici* to confrontation of *Pseudomonas* isolates, as part of a future project.

<u>Hypothesis:</u>

(1) Both constitutive and differential gene expression of *Pseudomonas* predicted secondary metabolite genes can be observed when confronted with *Z. tritici* blastospores.

6.2. Chapter specific methods

6.2.1. Storage of isolates

Both *Pseudomonas*, and *Z. tritici* isolates were stored as glycerol stocks, as described in Chapter 2.

6.2.2. Preparation of *Z. tritici* blastospores for confrontation with *Pseudomonas* isolates in liquid culture

Z. tritici IPO323 blastospores were cultured from glycerol stocks stored at -80°C, by spreading 30µl of glycerol stock on potato dextrose agar (PDA, Formedium) plates, before inverting and placing in darkness at 16°C for 5 days. Blastospores were harvested using a sterile loop after 5 days of growth. A blastospore suspension was prepared using a 20µl loop of *Z. tritici* blastospores and 5ml of distilled water. The suspension was vortexed before optical density measurements were taken at 600nm using a spectrophotometer. A dilution was made to achieve a final optical density of 0.6 at 600nm using distilled water. A 1 ml blastospore suspension at an OD_{600} of 0.6, equating to approximately $1x10^6$ blastospores (Hongxin Chen, personal communication), was used to inoculate 50ml of PDB (Formedium) in conical flasks that were pre-chilled to 16°C for 24 hours. Inoculated flasks were placed into a shaking incubator at 160rpm, 16°C, in darkness for 96 hours before confrontation assays were initiated. *Zymoseptoria tritici* isolate IPO323 was utilised in this study.

6.2.3. Preparation of *Pseudomonas* cells for confrontation with *Z. tritici* blastospores in liquid culture

Pseudomonas cells were prepared by streaking glycerol stocks to extinction on PDA (Formedium) plates, before being placed in an incubator at 25°C in darkness for 48 hours.

Flasks containing 10ml of PDB (Formedium) were inoculated with a single colony picked from the streaked glycerol stocks using a sterile toothpick. The 10ml PDB liquid cultures were placed in a shaking incubator at 160rpm, 16°C for 24 hours, before optical density readings were taken at 500nm a spectrophotometer. Liquid cultures were diluted to achieve a final OD_{500} reading of 0.5 using fresh PDB. 1ml of bacterial culture at an OD_{500} of 0.5 was used to inoculate 100ml of PDB (Formedium) in conical flasks that were pre-chilled to 16°C for 24 hours (approximately 1x 10^7 cells per ml, Heather Ruscoe, personal communication). Inoculated flasks were placed into a shaking incubator at 160rpm, 16°C, in darkness for 16 hours before confrontation assays were initiated.

6.2.4. Confrontation of *Pseudomonas* cells with *Z. tritici* blastospores in liquid culture

For each *Pseudomonas* isolate studied, 50ml of 100ml *Pseudomonas* culture (prepared as described above) was transferred to a sterile 50ml Falcon tube, in a laminar flow hood, after agitation. The remaining 50ml of *Pseudomonas* culture was placed in a shaking incubator at 160rpm, 16°C, in darkness for 4 hours, and were used as control treatments in the experiment. The 50ml aliquot of *Pseudomonas* culture in a sterile 50ml Falcon tube was then added to 50ml conical flasks containing *Z. tritici* blastospores (prepared as above) before placing in a shaking incubator at 160rpm, 16°C, in darkness for 4 hours. Conical flasks containing 50ml of *Z. tritici* blastospores (prepared as described above), with no addition of *Pseudomonas* cells were also used as control treatments in the experiment. Each treatment consisted of 3 replicates.

After the 4-hour co-culture and control treatments, conical flasks were agitated, before 40ml of liquid culture/co-culture were transferred to a sterile Falcon tube. The cells were pelleted by centrifugation at 4000rpm for 10 minutes in an ultracentrifuge (Beckman Coulter Avanti J-301), pre-chilled to 16°C. After

centrifugation, supernatant was removed, before the resulting pellet of cells was flash frozen in liquid nitrogen. Samples were stored at -80°C before extraction of RNA took place.

6.2.5. RNA extraction

RNA extractions were performed using a modification of the TRIZOL procedure (Invitrogen, San Diego, CA, U.S.A.) outlined in (Keon et al., 2007).

RNA was extracted from the samples prepared and stored at -80°C as described above, using 3 ml Trizol (Invitrogen) and disrupted using a homogeniser (Cole-Parmer LabGEN). The Trizol suspension was then separated into two 2ml Eppendorf tubes for further processing. The solution was centrifuged for 10 minutes at 12,000g, 10°C. The supernatant was then transferred into a sterile 2 ml eppendorf tube, before 150 µl of BCP Phase separation reagent (Sigma-Aldrich) was added to each tube. The solution was vortexed, before centrifugation for 10 minutes at 12,000g, 10°C. The upper aqueous phase was transferred to a sterile 2ml Eppendorf tube, before 750 µl isopropanol was added. The solution was then vortexed and placed at room temperature for 10 minutes to precipitate RNA. RNA was then pelleted by centrifugation at 12,000g, 10°C for 10 minutes. Supernatant was discarded, before 1ml of 99.9% ethanol was added to each tube. The solution was vortexed and centrifuged for 10 minutes at 12,000g, 10°C. This ethanol wash step was carried out a further two times for each sample. The RNA pellets were left to dry at room temperature for 7 minutes before being re-suspended in 100µl nuclease-free water. Samples were stored at -80°C before delivery to Novogene on dry ice.

6.2.6. RNA quality assessment

RNA quality was measured using a Nanodrop Microvolume UV spectrophotometer (Thermo Fisher Scientific Inc), measuring the ratios of spectrophotometer readings

at 260 and 280nm. All total RNA samples met the minimum criteria for library preparation, ribosomal depletion and sequencing at Novogene UK (260/230 ratio > 1.8, 260/280 ratio > 1.95). Samples were delivered to Novogene UK, where further quality checks using a Bioanalyser took place prior to downstream processing and sequencing.

6.2.7. RNA sequencing

RNA library preparation, eukaryotic and prokaryotic ribosomal depletion, and sequencing was carried out by Novogene UK. Sequencing was conducted using NovaSeq 6000 PE150, generating between 42-54 million reads per sample.

6.2.8. Processing of sequencing reads for downstream analysis

To determine perform initial quality control of raw sequencing reads received from Novogene UK, FastQC (v was used. FastQC issued a warning for ‘Per base sequence content’ in the first 9bp of reads, which were trimmed at the later mapping stage. No contamination of reads with adapter sequences were found, and zero sequences were flagged as low quality. To generate general feature format (.gff) annotation files from genome assemblies generated by MicrobesNG, EMBOSS (v6.6.0) Seqret was used. To generate FASTA files from genome assemblies for Roth 16 and Roth 105, Bio.SeqIO within Biopython (v1.78) was used. Genomes of Roth 16 and Roth 105 were indexed, and subsequently forward and reverse paired-end reads for each sample were mapped to the respective indexed genomes using HISAT2 (v2.2.1), with 9bp trimmed from both the 5’ and 3’ for each paired read. Resulting sequence alignment files (SAM) were converted to binary alignment files (BAM) using Samtools (v1.12). To calculate read depth from the (BAM) files generated by HISAT2, Samtools was used. Coverage depths were found to be sufficient for differential expression analysis for all samples (Supplementary Table 14.). Quantification of sequencing reads mapping to genomic features within genome assemblies was carried out using Subread (1.6.2)

subpackage FeatureCounts (Liao et al., 2014). The number of reads mapping to genomic features were collated for each of the three biological replicates, for each treatment condition and *Pseudomonas* strain, for differential expression analysis.

6.2.9. Principal component analysis

Principal component analysis was carried out on read counts mapping to genomic features for each sample, using R version 4.0.3, Rstudio version 1.3.1093, and software package ggplot2 v3.3.3.

6.2.10. Differential gene expression analysis

Differential gene expression analysis was carried out using R version 4.0.3 and RStudio version 1.3.1093, using software package DESeq2 version 1.30.0 (Love et al., 2014). Genes with an adjusted p-value < 0.05 were determined to be differentially expressed.

6.2.11. BGC Prediction and amino acid alignments

Prediction of secondary metabolite BGCs from *Pseudomonas* genome assemblies was conducted using antiSMASH 5.2 as described in Chapter 4. Amino acid alignments of predicted BGCs were generated, and figures visualising BGCs generated using clinker (Gilchrist and Chooi, 2021). Amino acid alignments were conducted using a cut-off value of 80% amino acid identity to identify common genes between predicted BGCs.

6.3. Results

6.3.1. Principal component analysis reveals transcriptomic changes in both pseudomonads isolates tested as a consequence of confrontation with *Z. tritici*.

To examine the variation between replicates and treatments, read counts mapping to genomic features for all *Pseudomonas* isolates and treatment conditions, a principal component analysis was conducted. Read counts mapping to genomic features were determined by processing raw sequencing reads as described in Section 6.2.8. It was found that the main source of observed variation was due to treatment, with clear separation of replicate samples within treatments for both Roth 16 (Figure 6.1a) and Roth 105 (Figure 6.1b). Whilst some variation can be observed between biological replicates for both Roth 16 and Roth 105, treatment and control samples are clearly distinguishable. Please note differing scales and differing contributions of principal components to total observed variation. Variation within treatments accounts for up to 13% of the variation for Roth 16, whilst variation between treatments accounts for up to 75% of the total variance. Similarly, variation between biological replicates accounts for 11% of the total variance, whilst variation between treatments accounts for up to 81% of the total variance observed.

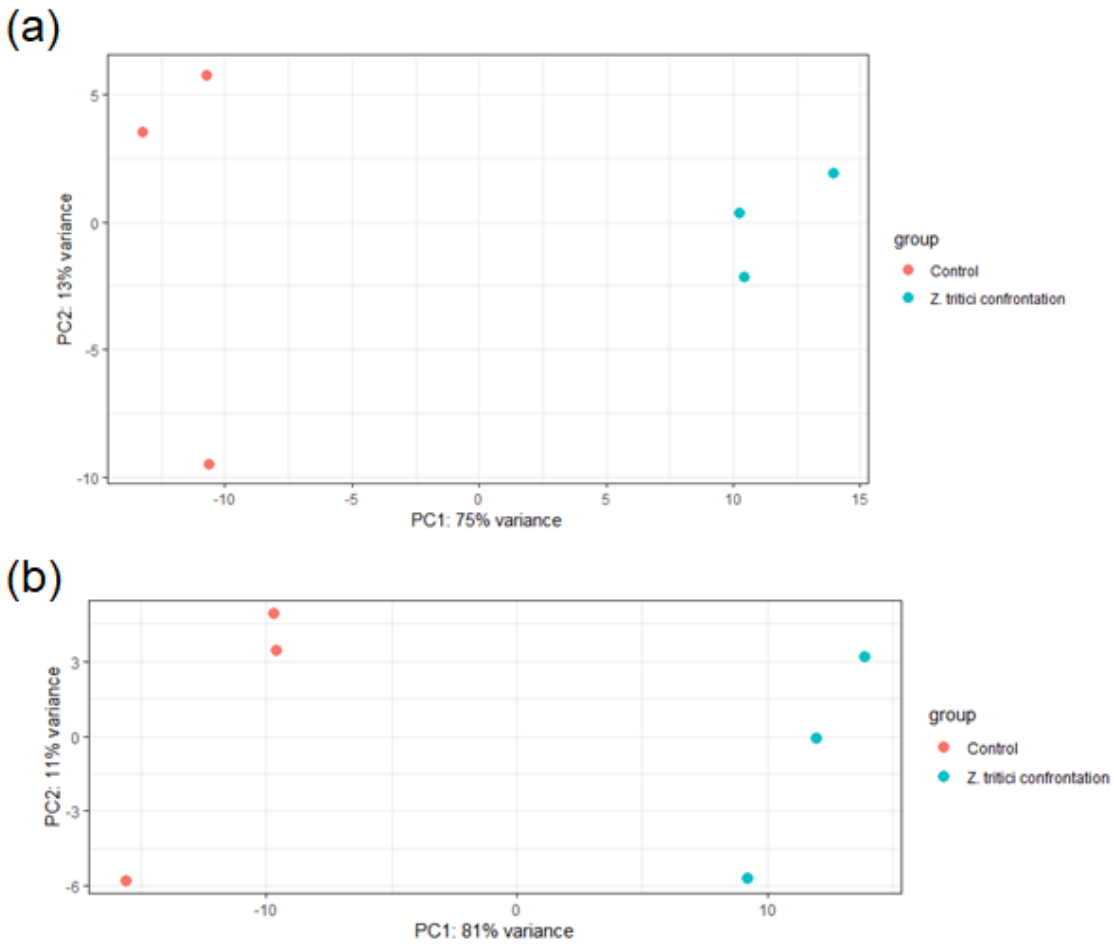


Figure 6.1 Principal components analysis of RNA reads for *Pseudomonas* isolates in confrontation with *Z. tritici* blastospores.
Plots derived from principal components analysis (PCA) of samples relating to antagonistic *Pseudomonas* isolate Roth16 **(a)**, and non-antagonistic *Pseudomonas* isolate Roth105 **(b)**, indicating the variance due to confrontation with *Z. tritici* blastospores.

6.3.2. Validation of expression for predicted gene models of *Pseudomonas* isolates Roth16 and Roth105

To examine the expression of genes predicted in the genome assemblies of *Pseudomonas* isolates, RNA sequencing reads were mapped to *Pseudomonas* genome assemblies using HISAT2 (Kim et al., 2019), and read counts assigned to genomic features were quantified using featureCounts (Liao et al., 2014). Gene expression was detected for 5811 out of 5815 genes (99.93%) predicted from the genome assembly of Roth16 across treatments. Gene expression was detected for all 5975 genes (100%) predicted from the genome assembly of Roth105.

6.3.3. Amino acid alignments reveal common and unique predicted BGCs from *Pseudomonas* isolates Roth 16 and Roth 105

Secondary metabolite BGCs were predicted from *Pseudomonas* genome sequences using antiSMASH 5.2 as described in chapter 4. Thirteen secondary metabolite BGCs were predicted from the genome assembly of Roth 16 and 8 BGCs were predicted from the Roth 105 genome assembly (Figure 6.2).

To compare antiSMASH 5.2 predicted secondary metabolite BGCs between *Pseudomonas* isolates, protein alignments were generated. Amino acid alignments of BGCs were generated using clinker (Gilchrist and Chooi, 2021), with antiSMASH predictions of function highlighted for each BGC (Figure 6.2). It was found that *Pseudomonas* isolate Roth 16 and Roth 105 appear to have both common and unique predicted secondary metabolite BGCs, and genes with high levels of amino acid identity (> 80%). Genes within predicted BGCs Roth 16 BGC 5.1 and Roth 105 BGC 25.1 show significant similarly, with 19 genes predicted to have >80% amino acid identity, with core biosynthetic and additional biosynthetic predicted functions. Roth 16 BGC 8.2 and Roth 105.1 BGC 13 show significant similarity, with 13 genes found to have >80% amino acid identity, including all predicted core biosynthetic genes within the predicted BGCs. Roth BGC 1.2 and Roth 105 BGC

71.1 were found to have 8 common genes, including core biosynthetic and additional biosynthetic functions. Two BGCs from both Roth 16 and Roth 105 were found to share a single common gene, with no predicted function by antiSMASH. A total of 9 BGCs predicted from Roth 16 and Roth 105 appear to be unique, with no genes within the 9 BGCs found to have >80% amino acid identity with any other BGC predicted from either genome.

6.3.4. Differential expression analysis reveals significant changes for genes within predicted secondary metabolite BGCs

To calculate read depth from the binary alignment map (BAM) files generated with HISAT2, Samtools was used. Coverage depths were found to be sufficient for differential expression analysis for all samples (Supplementary Table 15.), with the minimum depth of coverage for an individual sample found to be 185x.

To examine whether genes within predicted secondary metabolite BGCs were found to be differentially expressed when *Pseudomonas* isolate Roth 16 or Roth 105 were in confrontation with *Z. tritici* compared to control treatments, differential expression analysis was conducted. Differential expression was calculated using DESeq2 within Rstudio. Reads mapping to all genomic features were used as input into differential expression analysis, to calculate gene dispersion estimates and to estimate size factors across all genes. The Benjamini-Hochberg adjusted p-values were used to determine significantly differentially expressed genes. A total of 44 out of 281 genes within predicted Roth 16 BGCs were found to be significantly differentially expressed (Benjamini-Hochberg adjusted p-value < 0.05) (Supplementary Table 15). From Roth 105 predicted BGCs, 36 out of 173 genes were found to be significantly differentially expressed (Benjamini-Hochberg adjusted p-value < 0.05) (Supplementary Table 16.). Significantly differentially expressed secondary metabolite genes for Roth 16 consisted of 26 upregulated and 18 downregulated genes, whereas for Roth 105, 18 genes were found to be

upregulated and 18 downregulated. To visualise the log2fold change and Benjamini-Hochberg adjusted p-values for each predicted secondary metabolite gene, volcano plots were generated (Figure 6.3.). Please note the difference in y axis scale between Figure 6.3a and Figure 6.3b. These results indicate that many genes within Roth 16 predicted secondary metabolite BGCs appear to undergo higher log2fold changes, with lower Benjamini-Hochberg adjusted p-values compared to Roth 105 BGC associated genes. This data suggests strong upregulation of some secondary metabolite genes within predicted BGCs for antagonistic *Pseudomonas* isolate Roth 16. Interestingly, all genes found within the circled region in Figure 6.3a were derived from a single predicted BGC, Roth 16 22.1, indicating strong upregulation of 13 genes within this BGC in confrontation with *Z. tritici* blastospores in liquid culture.

antiSMASH BGC detection rules are based on the identification of genes predicted to be involved in core biosynthesis of secondary metabolites. These genes from both *Pseudomonas* isolates were found to be differentially expressed in response to *Z. tritici* confrontation. This analysis revealed a highly significant (Padj < 0.01) upregulation of 3 core biosynthesis genes within BGC 22.1 predicted from the genome assembly of antagonistic *Pseudomonas* isolate Roth 16 (Supplementary Table 17.), in response to *Z. tritici* blastospore confrontation. Additionally, a significant (Padj < 0.05) upregulation of core biosynthesis genes within BGC 45.1 was also observed under this condition, whereas significant (Padj <0.05) and highly significant (Padj < 0.01) downregulation of core biosynthesis genes within BGC 8.1 were also observed in response to *Z. tritici* blastospore confrontation for Roth16. Core biosynthesis genes within the 10 additional predicted secondary metabolite BGCs from the Roth 16 genome assembly were found to not be significantly differentially expressed between treatments (Padj < 0.05).

Differential gene expression analysis on BGCs of non-antagonistic *Pseudomonas* isolate Roth 105 indicated the highly significant downregulation (Padj < 0.01) of

core biosynthesis genes within predicted BGC 99.1, in response to *Z. tritici* blastospore confrontation (Supplementary Table 18.). Core biosynthesis genes within the 7 additional predicted secondary metabolite BGCs from the Roth 105 genome assembly were found to not be significantly differentially expressed between treatments (Padj < 0.05).

To visualise the expression profiles of predicted core biosynthetic genes, for each biological replicate and treatment, heatmaps were generated. Heatmaps were plotted using log transformed count data for Roth 16 (Figure 6.4) and Roth 105 (Figure 6.5), using R package pheatmap. Please note the differing order of treatments in Figure 6.6, based on clustering of treatments based on similarity. It was found that variation in expression profiles appears to be more pronounced for core biosynthetic genes of some BGCs compared to others. Core biosynthetic genes of Roth 16 BGC 22.1 found to be most consistent between control and *Z. tritici* confrontation treatments (Figure 6.4), with other predicted core biosynthetic genes from Roth 16 and Roth 105 found to be less consistent between biological replicates (Figure 6.4 & 6.5). Gene expression was observed for all core biosynthesis genes within secondary metabolite BGCs predicted from the genome assemblies of antagonistic *Pseudomonas* isolate Roth16 and non-antagonistic *Pseudomonas* isolate Roth105.

6.3.5. Upregulation of a unique predicted BGC of unknown function by antagonistic *Pseudomonas* isolate Roth 16 in confrontation with *Z. tritici*

To visualise the generated differential expression data within the genomic context of predicted secondary metabolite BGCs, genomic regions were annotated with differential expression analysis results using clinker (Gilchrist and Chooi, 2021).

The results indicate the significant upregulation of 19 contiguous genes within Roth 16 BGC 22.1 in confrontation with *Z. tritici* blastospores compared to control

treatments (Figure 6.6). The 3 predicted core biosynthesis genes within BGC 22.1 were found to be highly significantly upregulated in response to confrontation with *Z. tritici* (Padj < 0.01). No similarity (>80% amino acid identity) was found between predicted genes within Roth 16 BGC 22.1 and genes predicted from any other BGCs from either *Pseudomonas* strain.

6.3.6. Concordant and discordant responses in BGC expression between antagonistic and non-antagonistic *Pseudomonas* isolates in confrontation with *Z. tritici* blastospores

Interestingly, genes found to have significant amino acid identity between predicted BGCs from both *Pseudomonas* isolates were found to have common and differing expression changes in response to *Z. tritici* confrontation. Concordant downregulation of predicted additional biosynthetic genes *ephD*_1 and *ephD*, within Roth 16 BGC 8.1 and Roth 105 6.1 respectively, and 'other' genes *polC_1* and *polC_3* within Roth 16 BGC 8.2 and Roth 105 BGC 14.1 respectively, were observed in response to *Z. tritici* confrontation between pseudomonads (red links, Figure 6.6). A total of 12 genes were found to be discordantly differentially expressed, between *Pseudomonas* isolates in treatment compared to control (indicated by a blue link, Figure 6.6). Of particular note are genes within Roth16 BGC 8.1, and Roth 105 BGC 6.1, with 4 out of 8 common genes found to be discordantly differentially expressed between isolates. Roth 16 BGC 1.2 and Roth 105 BGC 71.1, containing common genes *bbsG* and *pcp_R*, predicted to have additional biosynthetic and regulatory functions respectively, were found to be significantly upregulated in Roth 16 and significantly downregulated in Roth 105 in response to *Z. tritici* confrontation. Common genes found to not be differentially expressed in either *Pseudomonas* isolate in response to confrontation with *Z. tritici* are indicated with a grey link (Figure 6.6).

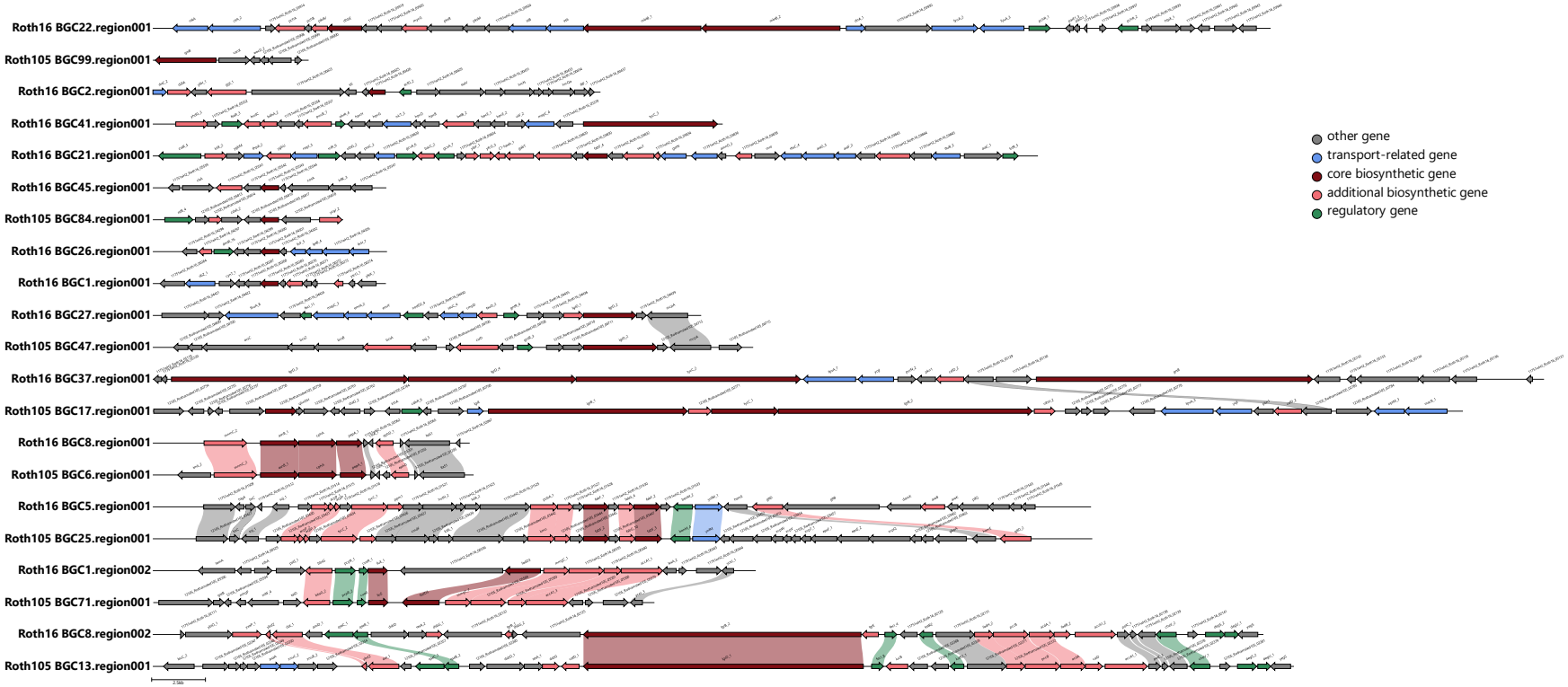
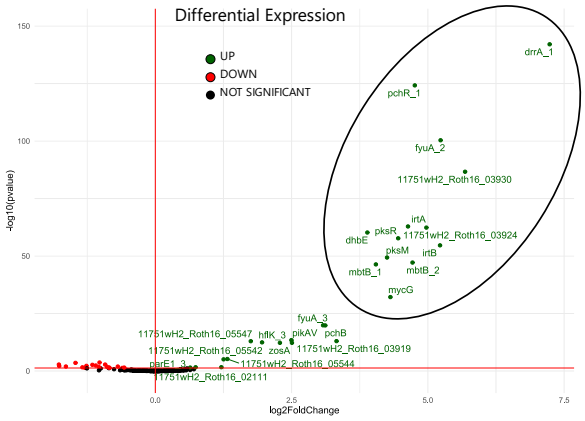


Figure 6.2 Amino acid alignments of *Pseudomonas* predicted secondary metabolite biosynthetic gene clusters. Amino acid alignments of Roth 16 and Roth 105 secondary metabolite BGCs predicted using antiSMASH 5.2. generated using clinker. Genes are coloured based on functional predictions from antiSMASH 5.2. Genes found to have high amino acid identity (> 80%) with a gene within another predicted secondary metabolite BGC are indicated with a coloured link. Links are coloured according to the antiSMASH 5.2 predicted function of the genes. This figure is a scalable graphics vector, with all detail visible if magnification is increased.

a



b

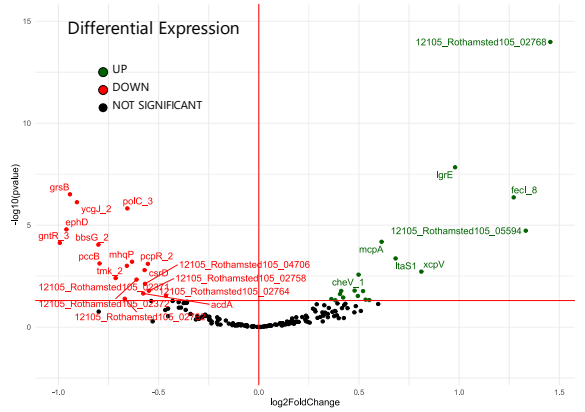


Figure 6.3 Volcano plots indicating differentially expressed predicted secondary metabolite genes from *Pseudomonas* isolates in confrontation with *Z. tritici*.

Volcano plots of genes within secondary metabolite BGCs predicted by antiSMASH 5.2 for Roth 16 (a) and Roth 105 (b). Each dot represents a gene within secondary metabolite BGCs predicted by antiSMASH 5.2. Black dots indicate genes where no significant difference in expression was found between *Z. tritici* confrontation treatments and control (Padj > 0.05). Dots coloured red indicate genes identified as significantly down-regulated in confrontation with *Z. tritici* compared to control (Padj > 0.05), and green dots represent genes that were found to be up-regulated in confrontation with *Z. tritici* compared to control (Padj < 0.05). No fold-change threshold was used to define differential expression. Upregulated genes circled in (a) related to genes within Roth 16 BGC 22.1. The horizontal red line represents a Benjamini-Hochberg adjusted p-value of 0.05, with genes above this line determined to be significantly differentially expressed. Please note differences in scale between (a) and (b). This figure is a scalable graphics vector, with all detail visible if magnification is increased.

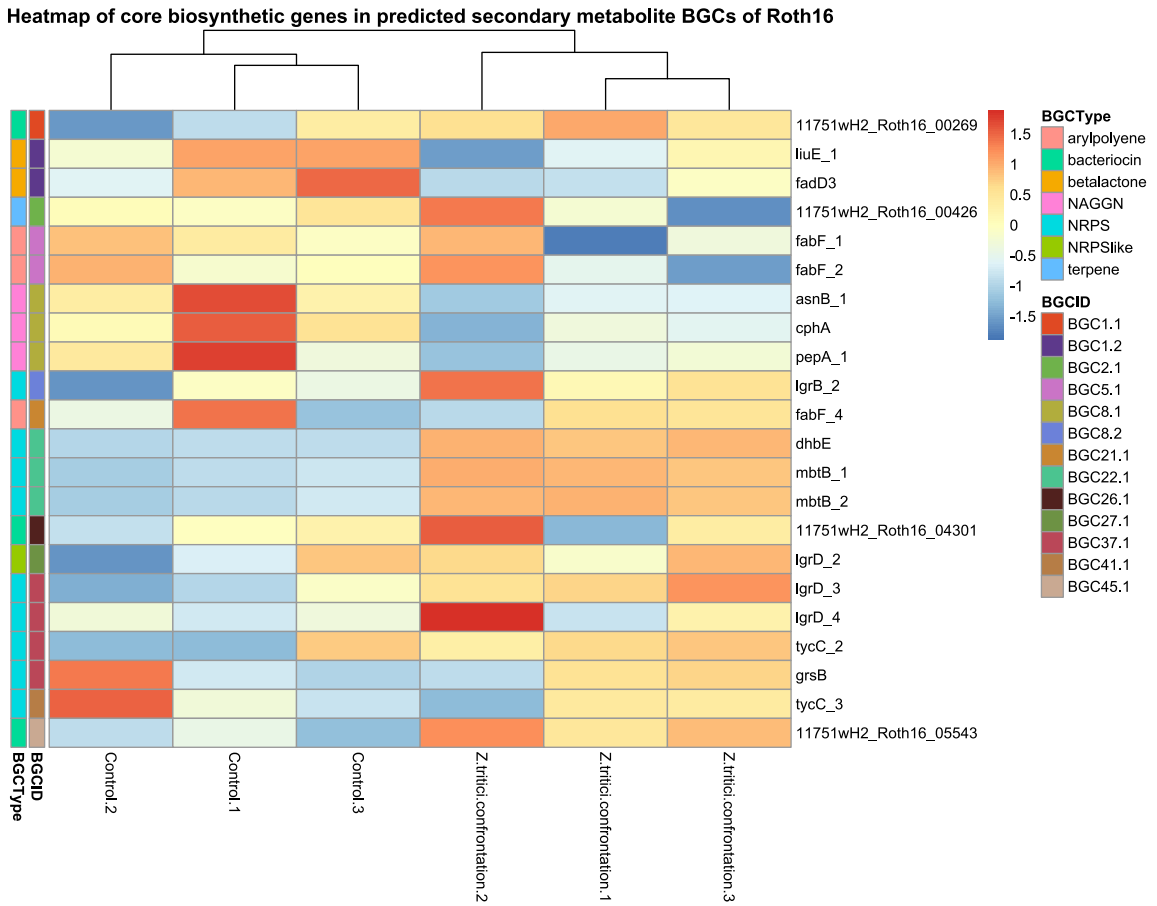


Figure 6.4 A heatmap indicating expression of predicted secondary metabolite core biosynthesis genes for *Pseudomonas* isolate Roth 16 in confrontation with *Z. tritici* blastospores.

A heatmap indicating the expression levels of predicted secondary metabolite 'core-biosynthesis' genes of Roth 16, under control conditions and in confrontation with *Z. tritici* blastospores in liquid culture (n=3). The class of predicted BGC, and BGC ID from which the predicted core biosynthesis genes are derived, are indicated.

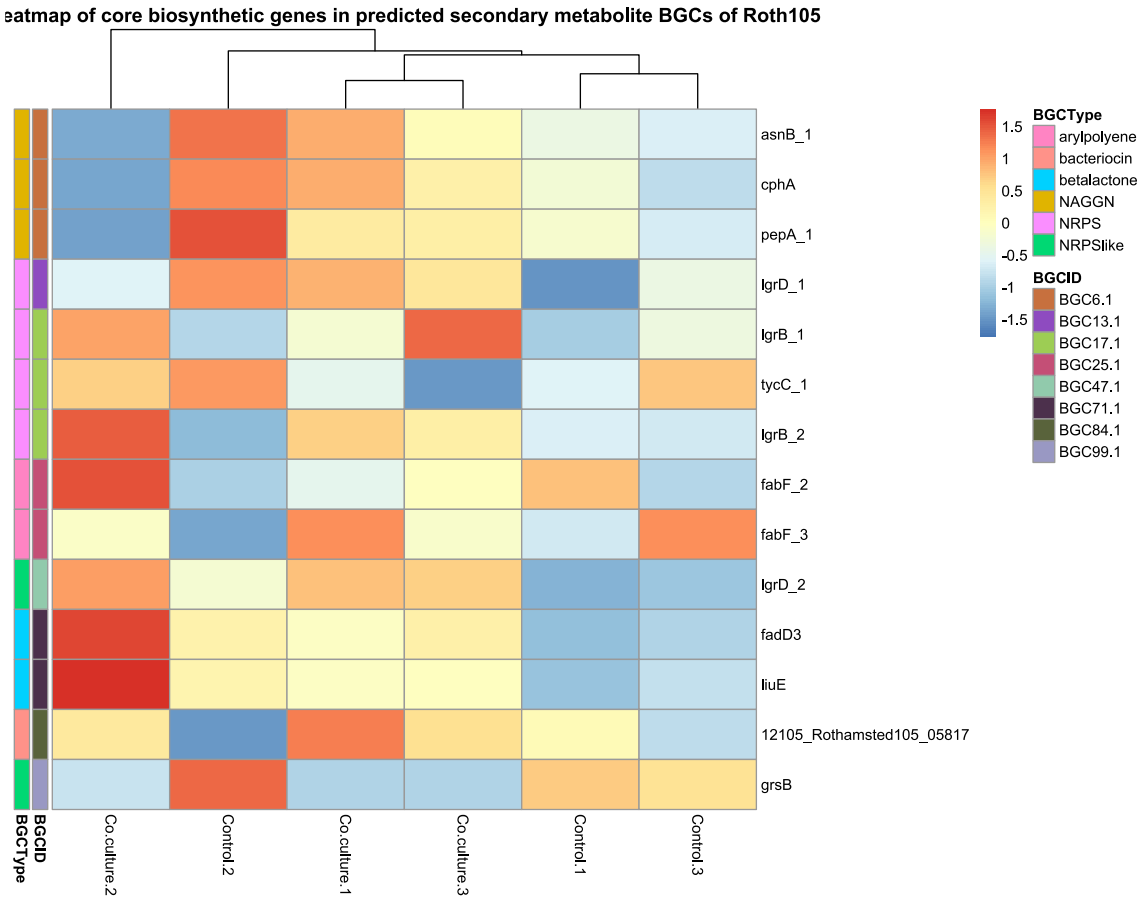


Figure 6.5 A heatmap indicating expression of predicted secondary metabolite core biosynthesis genes for *Pseudomonas* isolate Roth 105 in confrontation with *Z. tritici* blastospores.

A heatmap indicating the expression levels of predicted secondary metabolite 'core-biosynthesis' genes of Roth 105, under control conditions and in confrontation with *Z. tritici* blastospores in liquid culture (n=3). The class of predicted BGC, and BGC ID from which the predicted core biosynthesis genes are derived, are indicated. Please note the differing order of treatments in Figure 6.6, based on clustering of treatments based on similarity.

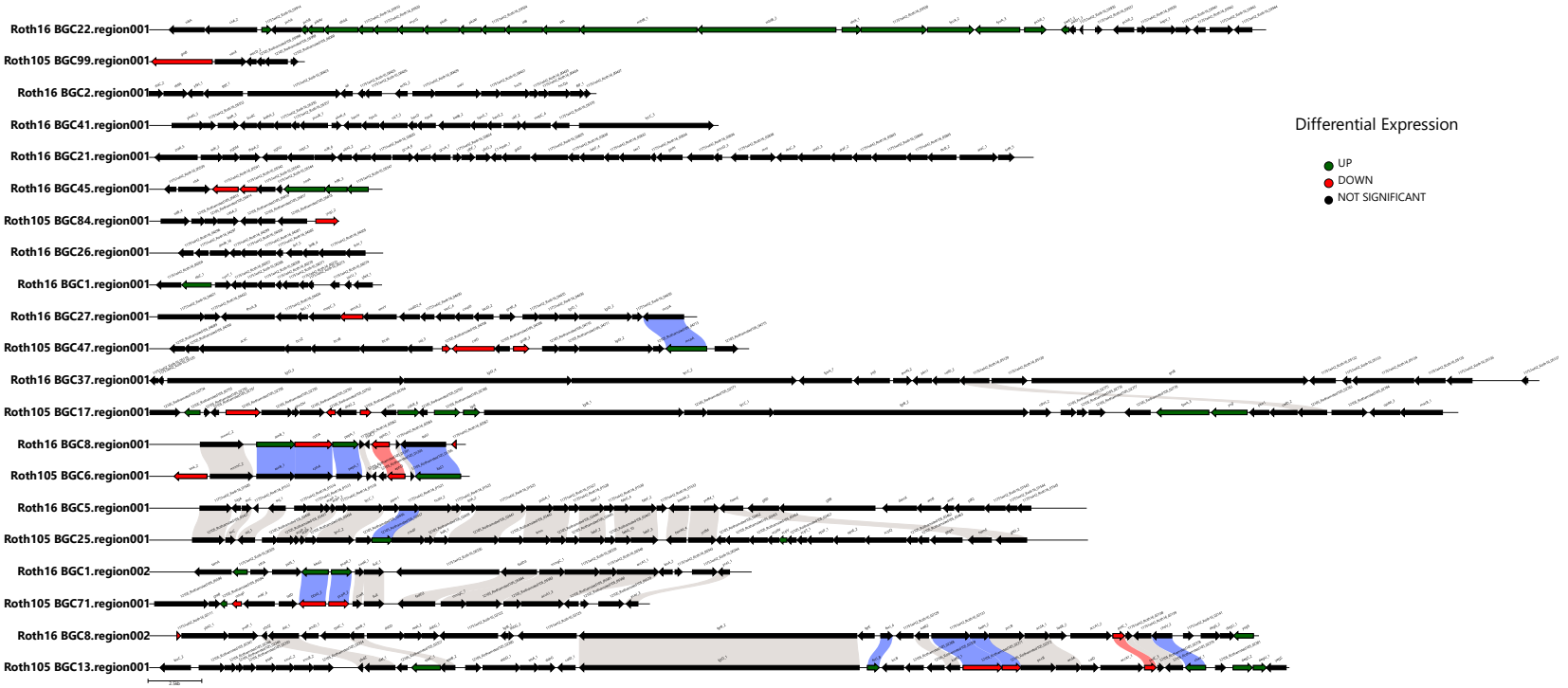


Figure 6.6 Amino acid alignments of *Pseudomonas* predicted secondary metabolite biosynthetic gene clusters annotated with differential expression data.

Amino acid alignments of secondary metabolite BGCs predicted using antiSMASH 5.2. were generated using clinker. Black genes indicate where no significant difference in expression was found (Padj > 0.05). Red genes were identified as significantly down-regulated in confrontation with *Z. tritici* compared to control (Padj > 0.05), and green genes were found to be up-regulated in confrontation with *Z. tritici* compared to control (Padj < 0.05). No fold-change threshold was used to define differential expression. Links indicate genes with high amino acid identity (> 80%), that are coloured to indicate concordant (red or green) and discordant (blue) differential expression changes between genes. This figure is a scalable graphics vector, with all detail visible if magnification is increased.

6.4. Discussion

This Chapter describes the use of a transcriptomic approach to confirm expression of predicted secondary metabolite BGCs and to identify yet undescribed candidate secondary metabolite BGCs. Some of these BGCs may be implicated in the antagonism of a fungal plant pathogen through expression changes (upregulation) during fungal confrontation by the *Pseudomonas* isolates.

The results described in this Chapter indicate observable transcriptomic responses of predicted secondary metabolite genes, for both antagonistic and non-antagonistic *Pseudomonas* isolates during confrontation with *Z. tritici* blastospores in liquid culture. These results confirm the transcription of all genes within predicted secondary metabolite BGCs under all observed conditions for both *Pseudomonas* isolates studied. Specifically, our results highlight a highly significant (Padj < 0.01) upregulation of a yet uncharacterised secondary metabolite BGC by antagonistic *Pseudomonas* isolate Roth16 in response to confrontation with *Z. tritici* blastospores in liquid culture. Our results also indicate conserved and different expression changes of predicted secondary metabolite genes in confrontation with *Z. tritici* blastospores in liquid culture between *Pseudomonas* isolates.

To my knowledge, this is the first study to combine predictive bioinformatics of bacterial secondary metabolism and global transcriptomics to investigate expression of secondary metabolite BGCs during fungal antagonism by bacterial isolates. More broadly, the combined approaches utilised in this Chapter could aid the prioritisation of candidate secondary metabolite BGCs underpinning phenotypes for further characterisation. The RNA sequencing reads originating from *Z. tritici* generated within this experiment will be analysed as part of a funded future project.

6.4.1. Common genes within predicted secondary metabolite BGCs from antagonistic and non-antagonistic *Pseudomonas* isolates undergo concordant and discordant regulatory changes in response to confrontation with *Z. tritici* blastospores in liquid culture

The results indicate statistically significant (Padj < 0.05) transcriptional responses of predicted secondary metabolite genes in both *Pseudomonas* isolates in confrontation with *Z. tritici* blastospores. These results indicate that significant transcriptional responses of *Pseudomonas* isolates to confrontation with *Z. tritici* blastospores are not solely found in *Pseudomonas* isolates observed to exhibit an antagonistic phenotype The results also indicate similarities and differences between the transcriptional responses in common (conserved) predicted secondary metabolism genes of *Pseudomonas* isolates during confrontation with *Z. tritici* blastospores *in vitro*.

Two genes were found to be significantly downregulated in response to *Z. tritici* confrontation between strains. Additional biosynthetic gene *epH* and 'other' gene *polC* were found to be significantly downregulated by both strains and are predicted to encode a putative oxidoreductase and a DNA polymerase III. Oxidoreductases are known to catalyse a vast range of chemical reactions with high specificity, the majority of which are nicotinamide cofactor-dependent enzymes which have a high preference for NAD or NADP (Younus, 2019) . DNA polymerase III enzymes are involved in the replication of bacterial genomes (McHenry, 2011; Timinskas et al., 2014) .

Differences in the transcriptomic response of genes within predicted secondary metabolite BGCs were also found between *Pseudomonas* strains. Roth 16 BGC 8.1 and Roth 105 BGC 6.1, whilst showing high levels of homology at the amino acid level between genes, undergo differing regulatory changes in response to confrontation with *Z. tritici* between *Pseudomonas* isolates. Differences in transcriptional response between strains could be seen for the 3 genes predicted

to be involved in the core biosynthesis of a secondary metabolite, predicted to be a currently unknown dipeptide N-acetylglutaminylglutamine amide (NAGGN), previously described as an osmolyte (Sagot et al., 2010). Genes *bbsG* and *pcpR*, both found within Roth 16 BGC 1.2 and Roth 105 BGC 71.1, are significantly upregulated in Roth 16, and significantly downregulated in Roth 105 in confrontation with *Z. tritici* compared to control, *bbsG* is predicted to have an additional biosynthetic function by antiSMASH 5.2 and has been shown to encode an enzyme involved in anaerobic toluene catabolism in *Thauera aromatica* (Leutwein and Heider, 2002). *pcpR* is predicted to have a regulatory function, a lysR family transcriptional regulator implicated in the regulation of pentachlorophenol degradation *Sphingobium chlorophenolicum* ATCC 39723 (Cai and Xun, 2002).

These observed commonalities and differences in the transcriptomic responses of *Pseudomonas* isolates to *Z. tritici* blastospore confrontation warrant further investigation into whether common or unique signal transduction pathways are present, what the elicitors of the observed transcriptional responses are, or if differences exist within gene promoter regions between isolates. It will be interesting to investigate if variation in the expression, or differences in transcriptomic changes in response to *Z. tritici* confrontation exist for *Pseudomonas* isolates with BGCs identified as having high levels of similarity in Chapter 3. These results potentially indicate differential regulatory mechanisms of secondary metabolite BGC expression by *Pseudomonas* isolates. It will be interesting to investigate the potential to alter the expression of these predicted BGCs, through the substitution of native promoter or regulatory sequences of predicted secondary metabolite BGCs, with promoters conferring higher or lower levels of expression. This approach could potentially be used alone, or in combination with the generation of loss-of-function mutants, to assist in the identification of the secondary metabolite products of these BGCs, through chemical analysis as well as *Z. tritici* confrontation screening of mutants.

A parallel study investigating the transcriptomic response of *P. fluorescens* isolate Pf0-1 to bacterial confrontation with *Pedobacter* sp. V48, *Brevundimonas* sp. V52, and *Bacillus* sp. V102, found evidence of a species-specific transcriptional and metabolic responses, alongside common differential gene expression across confrontation assays (Garbeva et al., 2011). Future experiments could investigate whether the transcriptional responses of *Pseudomonas* isolates identified within this Chapter, are also observed in confrontation with other fungal or bacterial species, or if the responses are wholly, or partly, due to a species-specific response to *Z. tritici*.

6.4.2. A unique BGC encoding an unknown secondary metabolite is significantly upregulated in response to *Z. tritici* confrontation by antagonistic *Pseudomonas* isolate Roth 16

These results indicate the highly significant (Padj < 0.01) upregulation of a currently uncharacterised NRPS-type secondary metabolite BGC (22.1) by antagonistic *Pseudomonas* isolate Roth16, when in confrontation with *Z. tritici* blastospores. The gene predictions of core biosynthesis genes within BGC 22.1 have previously been implicated in the biosynthesis of iron-scavenging siderophores. Genes *mbt_1* and *mbt_2* have previously been shown to be essential to the biosynthesis of mycobactin siderophores in *M. tuberculosis* (McMahon et al., 2012), which enable competition with the host for iron (De Voss et al., 2000). Gene *dhbE* has been implicated in the biosynthetic pathway of bacillibactin, a siderophore produced by *Bacillus subtilis* to acquire extracellular iron, under iron-limiting conditions (Rowland et al., 1996).

In the network analysis of predicted secondary metabolite BGCs described in Chapter 4, BGC 22.1 was found to form GCF network FAM_02208 based on sequence similarity, described in Chapter 4, with predicted secondary metabolite BGCs from antagonistic *Pseudomonas* isolate Roth 73 and non-antagonistic

Pseudomonas isolate Roth42. It will be interesting to examine whether the expression profiles of the predicted BGCs are the same across *Pseudomonas* isolates, or if expression profiles correlate with the antagonism phenotype.

These results could indicate the implication of a novel iron-chelating siderophore in the antagonism of *Z. tritici* blastospores by *Pseudomonas* isolates *in vitro*. This is an interesting possibility, as 'indirect' antagonism of *Z. tritici* blastospores through bacterial competition for rate-limiting essential micronutrients, such as iron, has not previously been described. More broadly, previous studies have identified the production of siderophores as a mechanism by *Pseudomonas* isolates antagonise plant pathogens.

Iron is often a limiting element in phyllosphere microbial communities (Legein et al., 2020). A number of *Pseudomonas* siderophores have previously been implicated in the suppression of fungal and oomycete pathogens. Pyrrolnitrin has previously been implicated in the antagonism of *Rhizoctonia solani* by a *P. fluorescens* isolates, and thioquinolobactin in the antagonism of *Pythium debaryanum*, an oomycete plant pathogen (Matthijs et al., 2007). Pyoverdine (Sass et al., 2018) and pyochelin (Sass et al., 2021), produced by *Pseudomonas aeruginosa*, have been shown to inhibit *Aspergillus fumigatus in vitro*. Siderophores produced by fluorescent pseudomonads have also previously been shown to play a role in the induction of systemic resistance (ISR) in *Arabidopsis thaliana* (Bakker et al., 2007) , and may similarly trigger wheat immunity, although more studies are needed on this topic to determine the potential effect on *Z. tritici* infection. Previous studies have described two putative siderophore clusters for *Z. tritici* IPO323 (Cairns and Meyer, 2017). Whilst siderophore production was shown not to be essential for filamentous growth *in vitro*, blastopore growth was shown to be disrupted on iron-depleted media in siderophore mutants (Derbyshire et al., 2018). It will be interesting to investigate the role and importance of *Z. tritici* siderophores as part of the natural lifecycle of the fungus during different life

stages. This could give further indications of which life stages potential control strategies limiting the availability of iron may be most effective to antagonise the *Z. tritici* in agricultural systems. The importance of *Z. tritici* siderophores for *in vitro* blastospore growth could be investigated through the confrontation of siderophore producing pseudomonads against IPO323 wild-type and siderophore mutants using the *in vitro* blastospore antagonism assay described in Chapter 5.

If the biosynthetic product of Roth 16 BCG 22.1 is indeed a siderophore, further investigation into the mechanism by which antagonism is achieved, (in direct or direct) will need to be conducted, alongside experiments testing the purified compound against the hyphal growth form of *Z. tritici in vitro* and *in planta*.

The biosynthesis of many siderophores have been shown to be induced under iron-limiting conditions (Vindeirinho et al., 2021). It will be interesting to investigate if a similar positive induction of expression of genes within Roth 16 BGC 22.1 is seen under iron-limiting conditions. This could prove useful in, as it may be possible to grow Roth 16 under iron-limiting conditions to generate enough compound for elucidation of the chemical structure of the biosynthetic product of Roth 16 BGC 21.1 through NMR.

Future studies could characterise BGC 22.1, through targeted disruption of core biosynthesis genes, and measure any differences in the *Z. tritici* blastospore antagonism phenotype of loss-of-function mutants. Comparative chemical analysis of agar extracts derived from *Z. tritici* blastospore confrontation assays, with wild-type *Pseudomonas* isolates and loss-of-function mutants in BGC biosynthesis, could also be employed to further investigate the secondary metabolite products of predicted BGCs.

A similar approach could be applied to BGC 45.1, shown to be significantly upregulated by antagonistic *Pseudomonas* isolate Roth16 in response to confrontation with *Z. tritici* blastospores, to ascertain if this BGC contributes to the

antagonism phenotype through the production of yet unknown antifungal secondary metabolites. Similarly, investigations into the products of predicted BGCs observed to be significantly down regulated (Benjamini-Hochberg adjusted p-value < 0.05) in Roth16 and Roth105 isolates in response to confrontation with *Z. tritici* blastospores (BGCs 8.1 and 99.1), could give further insights into their yet unknown function.

The *Z. tritici* blastospores antagonism phenotype of Roth16 could alternatively be caused by an expressed secondary metabolite BGC that is not differentially expressed after 4 hours of confrontation with *Z. tritici* blastospores in liquid culture. For this reason, the identification of the highly significant upregulation of core biosynthesis genes within a BGC simply facilitates the prioritisation of predicted BGCs for further characterisation, to elucidate BGCs underpinning the phenotype. It will be interesting to investigate if BGCs for which expression was detected, but differential expression after 4 hours of confrontation was not found, are differentially expressed after a longer confrontation with *Z. tritici*, or what the function of the biosynthetic products of the ubiquitously expressed BGCs identified in this study are. Longer confrontation times were not conducted within this project due to budgetary constraints.

6.5. Conclusions

Significant changes in predicted secondary metabolite gene expression were observed for antagonistic *Pseudomonas* isolate Roth16, and non-antagonistic *Pseudomonas* isolate Roth105, in response to 4 hours of confrontation with *Z. tritici* blastospores *in vitro*.

Expression of core biosynthetic genes associated with all predicted secondary metabolite BGCs was detected.

Highly significant upregulation of a predicted NRPS BGC of yet unknown function by antagonistic *Pseudomonas* isolate Roth16 was detected in response to confrontation with *Z. tritici* blastospores.

Transcriptional evidence for the involvement of secondary metabolite BGCs in the response of antagonistic *Pseudomonas* isolates to *Z. tritici* blastospores *in vitro* was found.

Chapter 7. General Discussion

This study investigated the antagonistic potential of *Pseudomonas* bacteria, effective against the fungal wheat pathogen *Z. tritici*, as a potential source of novel natural products for future crop protection. This study presents a combination of *in vitro* and in silico approaches, utilised to further understand possible mechanisms by which pseudomonads antagonise *Z. tritici in vitro*.

A high-throughput *in vitro* methodology was developed to screen *Pseudomonas* isolates for antagonism of *Z. tritici* blastospores (Chapter 2). Genome sequencing and comparative genomic approaches were employed to investigate the phylogenetic distribution of *Pseudomonas* isolates exhibiting an *Z. tritici* antagonistic phenotype (Chapter 3), and to investigate the potential implication of secondary metabolite BGCs through predictive bioinformatics (Chapter 4). Genetically diverse *Z. tritici* isolates were assessed for variation in sensitivity to antagonism by *Pseudomonas* isolates *in vitro* (Chapter 5). Finally, the transcriptomic responses, and expression profiles of predicted secondary metabolite BGCs, of antagonistic and non-antagonistic *Pseudomonas* isolates to confrontation with *Z. tritici* blastospores *in vitro*, were examined (Chapter 6).

The combined approaches described in this study can be utilised as a novel bio-prospecting pipeline for the discovery of bacterially derived antifungal compounds effective against *Z. tritici*, increasing the rate of discovery from widely used conventional approaches (Figure 7.1). Many of the approaches utilised in this pipeline are only possible due to recent advances in the fields of bacterial genome sequencing, comparative genomics, predictive bioinformatics, and transcriptomics.

7.1. The future challenges faced by fungicide resistant pathogens to agriculture

Fungal plant diseases constitute a major threat facing future agricultural systems, and food security, globally. Resistance to conventional chemical control strategies has arisen in many fungal plant pathogens (Fisher et al., 2018, 2012). This has led to the implementation of resistance management strategies, consisting of the application of mixtures of fungicides with differing modes of action, to delay the complete loss of efficacy of chemical control. Few fungicides with differing modes of action exist, and as such, novel fungicides are urgently required. Application of novel compounds would delay the evolution of resistance to chemical control strategies by plant pathogenic fungi, and the associated yield losses of staple crops, such as wheat, in light of a rapidly rising global population.

7.2. The selection of *Zymoseptoria tritici* as the initial target for the discovery pipeline

Z. tritici is an attractive pathosystem to utilise in a bioprospecting pipeline for bacterially derived antifungal compounds partly since it can be grown as a confluent lawn of cells, in its blastospore form, which facilitates high throughput screening. In addition, over the last 40 years, *Z. tritici* has become insensitive to every class of fungicides currently available to farmers. Therefore, novel antifungal products generated from a discovery pipeline involving *Z. tritici* is of immediate agricultural relevance, particularly in Western Europe, where Septoria tritici blotch is a major cause of yield loss in wheat. Fungicides are the main control strategy employed by farmers for the suppression of *Z. tritici*, as control through durable host genetic resistance is not possible (Torriani, 2015). This is due to natural *Z. tritici* populations having high genetic diversity compared to other fungal plant pathogens, partly due to a sexual reproductive cycle alongside asexual sporulation and high genomic instability (Möller et al., 2018). There remains an urgent need to

increase the speed at which novel fungicides effective against *Z. tritici* are discovered. The reliance on chemical fungicides for control, and rapid evolution of fungicide insensitivity in *Z. tritici*, make this fungus a priority target in many industrial fungicide discovery programmes. The environmentally regulated growth dimorphism, and more specifically, the inducible yeast-like growth of blastospores *in vitro*, make *Z. tritici* an extremely tractable fungal plant pathogen to employ in *in vitro* studies. The availability of high quality genome sequences (Goodwin et al., 2011), coupled with ease of mutagenesis through *Agrobacterium* and UV mediated approaches, could facilitate downstream investigations into the genetic targets of antagonism by bacterial antagonists such as *Pseudomonas*, or their isolated derived chemistry. These factors also highlight the potential use of *Z. tritici* as a potential model organism in investigation into bacterial-fungal interactions.

Zymoseptoria tritici blastospores were used throughout this study. *Zymoseptoria tritici* blastospores are commonly used as initial *in planta* inoculum in disease progression studies and used to quantify fungicide sensitivity of *Z. tritici* in field populations *in vitro* (Blake et al., 2018; Cools and Fraaije, 2012). Furthermore, other spore types of *Z. tritici*, such as ascospores (the main source of primary inoculum in a field setting), are technically infeasible to screen for antagonism *in vitro*, and in any case differentiate to form blastospores on rich media, or germinate to form hyphae under nutrient poor media (Morais et al., 2015; Steinberg, 2015; Suffert et al., 2011).

Zymoseptoria tritici blastospores are morphologically and transcriptomically identical to macropycnidiospores (the main source of secondary inoculum in a field setting), with both referred to as macropycnidiospores (Steinberg, 2015), prior to Francisco et al in 2019 (Francisco et al., 2019). Macropycnidiospores form a major part of the natural *Z. tritici* infection cycle, being dispersed by rain splash from pycnidia- the fruiting bodies of *Z. tritici*, before germinating to form hyphae on the leaf surface (Steinberg, 2015; Wiese, 1987).

Screening of *Pseudomonas* isolates against the hyphal growth form of *Z. tritici* in Chapter 2 found that all *Pseudomonas* isolates tested appeared to inhibit the growth of *Z. tritici* hyphae *in vitro*. This observation could be due to repression of hyphal extension caused by an in increase nutrient availability from neighbouring *Pseudomonas* inducing repression of the hyphal growth form of the fungus, alongside direct antagonism of hyphal growth by the *Pseudomonas* isolates. The inability to distinguish between repression of hyphal extension due to altered environmental conditions, and direct antagonism of the fungus by *Pseudomonas* isolates makes it difficult to justify the use of hyphal growth suppression screens to identify environmental microbial isolates with the biosynthetic potential to antagonise *Z. tritici*. Screening isolated candidate natural products against *Z. tritici* hyphae both *in vitro* and *in planta*, as opposed to live bacterial isolates may prove more fruitful, as environmental factors can be controlled solely conducive to hyphal growth of *Z. tritici*.

7.3. Bacteria as an underexploited source of novel fungicides?

Bacteria offer a potentially untapped source of novel antifungal compounds that could be utilised in future crop protection. A fungicide derived from natural compounds produced by *Streptomyces* spp. has recently become available to cereal growers to control Septoria tritici blotch (Jørgensen et al., 2017). Bacterially derived antifungal compounds could offer alternatives to conventional fungicides that are less harmful to human health. Chemical analogues of antifungal secondary metabolite 2,4-DAPG, produced by *Pseudomonas* species, have been shown to be less toxic to human lung epithelial and kidney cells compared to albesilate, a commonly used fungicide utilised to control post-harvest decay in citrus fruits (Gong et al., 2016) . The chemically synthesised 2,4-DAPG analogue was shown to have higher antifungal activity against *Penicillium digitatum* and *Penicillium italicum* than 2,4-DAPG *in vitro*, and significantly inhibited the development of decay in harvested mandarin *in vivo*, indicating the potential of naturally derived

antifungal compounds acting as templates for the development or tailoring of novel fungicides.

7.4. How to identify novel natural products with potential antifungal activities?

Previous efforts to derive effective antifungal compounds for the control of *Z. tritici* from bacterial isolates have mainly utilised analytical chemistry approaches, and targeted small numbers of bacterial isolates due to limitations in throughput. The reducing cost of bacterial genome sequencing and rise of predictive bioinformatic approaches have brought about a step-change in the ability to conduct high-throughput screening and comparative approaches involving bacterial isolates, shifting emphasis towards *in silico* approaches.

Many recent studies searching for novel bacterial secondary metabolites utilising predictive bioinformatics, have focussed on *Streptomyces* species, mainly due to a large body of work describing diverse secondary metabolic potential, and the comparatively high number of average secondary metabolite gene clusters found, relative to genome size. Studies have shown that, unlike most bacterial species including *Pseudomonas*, *Streptomyces* genomes contain around 40-60 secondary metabolite BGCs, whereas a *Pseudomonas* genome of comparable size would be predicted to contain 6-8 BGCs (Cimermancic et al., 2014).I predict that lower secondary metabolite BGC complexity in *Pseudomonas* spp. could be advantageous in the elucidation of candidate antifungal BGCs, where transcriptomic approaches, as described in Chapter 6, do not indicate differential expression of clear antifungal candidate BGCs. The discrepancy between research effort between *Streptomyces* spp. and pseudomonads is highlighted by the MiBIG repository currently containing 636 entries for BGCs originating from *Streptomyces* spp., compared to only 68 BGC entries derived from *Pseudomonas* spp. (https://mibig.secondarymetabolites.org/stats).

Pseudomonas bacteria are similarly an attractive model organism to utilise in the search for natural antifungal compounds, owing to a highly diverse secondary metabolism (Gross and Loper, 2009), and well documented biocontrol ability (Couillerot et al., 2011; Duffy and Défago, 1997; Huang et al., 2004; Keel et al., 1992), including some previously described ability to antagonise *Z. tritici in vitro* (Flaishman et al., 1990; Levy et al., 1992b, 1989). *Pseudomonas* bacteria are aerobic, and amenable to culture under the same conditions required for the growth of many fungal plant pathogens *in vitro*. Well described genetic transformation protocols of *Pseudomonas* isolates could assist in the characterisation of secondary metabolite BGCs to phenotypes, through the generation of loss-of-function mutants.

Previous efforts to derive effective antifungal compounds for the control of plant pathogens from *Pseudomonas* isolates have mainly utilised analytical chemistry approaches, and targeted small numbers of bacterial isolates due to limitations in throughput (Levy et al., 1992). Modern approaches, involving predictive bioinformatics of secondary metabolism and comparative genomics, have not been applied to interactions between *Pseudomonas* bacteria and *Z. tritici at scale*. This study highlights that *Pseudomonas* bacteria remain an underutilised resource of secondary metabolites that may form a basis for future crop protection products effective against *Z. tritici*.

7.5. The search for microbial natural products versus biological control agents

A clear distinction should be made between efforts to identify novel natural products effective against *Z. tritici* from microbial sources, from efforts to identify effective biological control agents for deployment against *Z. tritici in planta*.

This project aimed to identify microbes with the biosynthetic ability to antagonise *Z. tritici in vitro* for natural product discovery, as opposed to the identification of biocontrol agents to be deployed as a biofungicide *in planta*.

In vitro antagonism ability did not translate to effective biological control activity *in planta* for the *Pseudomonas* isolates tested in this study, indicating that the *Pseudomonas* isolates screened may not be effective biological control agents against *Z. tritici*. Microbes unable to antagonise *Z. tritici in planta* may nevertheless possess the biosynthetic ability to produce antifungal secondary metabolites that are antagonistic towards *Z. tritici*. The mechanisms by which *in vitro* antagonism is achieved could still prove useful for *Z. tritici* control, both to increase our fundamental understanding of microbial interactions, and as part of conventional chemical control strategies as novel antifungal active ingredients effective against *Z. tritici*.

The assessment of the *in planta* biocontrol potential of environmental *Pseudomonas* isolates within this study should be considered preliminary, with significant scope for further optimisation or development of the methodology. It would be useful as part of future *in planta* assessments to include a *Pseudomonas* isolate with previously documented biocontrol ability against *Z. tritici* from previous publications as a positive control treatment. The absence of *in planta* disease suppression by blastospore antagonistic *Pseudomonas* isolates applied to the wheat leaf surface could be due to a number of factors (outlined in 2.4.4).

Within this thesis, *Pseudomonas* culture collections were derived from wheat rhizosphere, endosphere and bulk soil samples from agricultural fields. It is possible that the *Pseudomonas* isolates screened within the *in planta* disease suppression assay lack phyllosphere colonisation ability, or the ability to persist within the phyllosphere environment. This could potentially be due to the *Pseudomonas* isolates being outcompeted or antagonised themselves by members of the resident phyllosphere microbiome. Phyllosphere competence, or

the persistence of the *Pseudomonas* isolates within the phyllosphere throughput *Z. tritici* disease progression was not assessed as part of this study. Fluorescent pseudomonads have previously been shown to commonly exist within the phyllosphere of wheat, and potentially contributed to natural plant protection against *Fusarium* and *Alternaria* species through the production of 2,4-DAPG (Müller et al., 2018, 2016) . Future projects seeking to identify *Z. tritici* biological control agents may benefit from isolating *Pseudomonas* isolates directly from the phyllosphere, to ensure phyllosphere competence. Parallel studies have sought to identify biological control agents and mechanisms of antagonism of soil-dwelling fungal pathogens through the characterisation of disease suppressive soils (Mendes et al., 2011; Tracanna et al., 2021). However, a disease suppressive phyllosphere of wheat, effective against *Z. tritici* has not been described previously in literature. For this reason, screening microbes from diverse microbiomes for antifungal secondary metabolites effective against *Z. tritici*, as opposed to the phyllosphere, may result in the identification of more antagonistic microbes *in vitro*.

The *Z. tritici* blastospore antagonism assay is conducted on high dextrose and rich nutrient agar *in vitro*. This environment differs significantly from the from the wheat phyllosphere which is a comparatively nutrient poor environment, lower in available nutrients and sugars (Vorholt, 2012). For this reason, *in vitro* antagonism due to the production of secondary metabolites that are environmentally regulated may not carry through to effective biocontrol *in planta*. The production of some secondary metabolites has been linked to availability of carbon (Shanahan et al., 1992) and iron (Lim et al., 2012). This may mean that *Pseudomonas* isolates have different secondary metabolite expression profiles between the two experimental systems. A transcriptomic study to investigate differential expression of *Pseudomonas* BGCs in high and low nutrient conditions could be conducted to test this hypothesis. This issue can effectively be decoupled from the *in planta* assay if isolated molecules of interest, or authentic chemical standards are screened

against *Z. tritici in planta*, as opposed to the application of living *Pseudomonas* cells.

Other potential limitations in the *in planta* study include the timing of the application of *Pseudomonas* bacteria to the leaf surface, and the formulation of *Pseudomonas* inoculum used. Whilst viability of the *Pseudomonas* inoculum was superficially tested after formulation (Supplementary Figure 1.), one concentration of *Pseudomonas* inoculum was tested in this study, applied at a single time point prior to *Z. tritici* infection.

A single wheat cultivar, Riband, was utilised in this study to assess *Z. tritici* disease progression *in planta*, as previous studies have used this cultivar for *in planta* disease progression assessment, based on (Saintenac et al., 2018). Previous studies have indicated variation in the efficacy of biocontrol agents applied to different wheat cultivars in both greenhouse and field conditions (Kildea et al., 2008; Lynch et al., 2016). For this reason, microbial inoculant and wheat cultivar interactions could play a role in the outcomes of *Z. tritici* biocontrol agents.

Similar limitations of *in planta* biocontrol by *Pseudomonas* isolates are applicable to the use of *Pseudomonas*, and other bacterial biocontrol agents more broadly. Inconsistent field performance of *Pseudomonas* biocontrol agents due to poor adaptation to environmental conditions, suboptimal formulation, and host-specific responses to microorganisms are potentially a reason for few *Pseudomonas* biocontrol strains being commercialised (Höfte, 2021). If successfully implemented as a control strategy, biocontrol bacteria could potentially antagonise *Z. tritici* in several ways, (1) directly, through the production of antifungal compounds, and (2 and 3) indirectly, through either competition for essential micro and macronutrients or through priming plant defences to subsequent attack (Köhl et al., 2019). These mechanisms could offer advantages in resistance management over the sole use of isolated chemistries, as many described fungicide resistance mechanisms could reduce the fitness of pathogens in competition for resources, such as reduced

metabolism and overexpression of efflux pumps. I believe that further investigation and understanding of the complex interactions between microorganisms within the phyllosphere environment will be required before any biocontrol strategies could offer comparable efficacy to chemical *Z. tritici* control strategies. This is particularly true for field environments, where conditions for bacterial establishment may be more difficult than in simplified *in planta* experimental systems.

Further characterisation of secondary metabolite BGCs implicated in antagonism of *Z. tritici* by *Pseudomonas* isolates and their respective natural products will be required before knowledge generated from this pipeline could be utilised as a crop protection product. This could be achieved through the generation of loss-of-function mutants or mutant wild-type restoration through complementation coupled with chemical analyses, as previously described.

Once the chemical structure of the secondary metabolite product has been elucidated, the route of production of the compound would depend upon its complexity. For simple structures, the compound could potentially be produced using conventional chemical synthesis. For more complex and larger compounds, a synthetic biology approach involving microbial fermentation may be more effective. *Pseudomonas* bacteria are considered a preferred microorganism for use in the industrial scale production of natural products (Zhao et al., 2019), which could further justify the investigation into their untapped metabolic potential.

I believe that chemical control strategies will continue to be the main method of control employed against *Z. tritici* for the foreseeable future, where the addition of novel natural antifungal compounds to the environment is likely to provide a more robust and efficacious delivery of fungal pathogen suppression as opposed to biological control, for the reasons described above.

7.6. Applications of natural product discovery pipelines beyond this study

The combination of approaches outlined in this study could be applied to other high throughput functional screens, such as antibiotic activity and iron solubilization, to investigate the implication of bacterial secondary metabolites in observable phenotypes, through a comparative-predictive bioinformatic approach. This study targeted the antifungal activity of *Pseudomonas* bacteria, yet the pipeline could easily be applied to other culturable bacterial species such as *Streptomyces* and *Bacillus*. With the present low cost of short-read 'whole genome' sequencing of bacterial isolates allowing for cost-effective comparative genomic studies at scale, I believe that these approaches, or similar, will become more widely used as sequencing costs reduce further. The application of these approaches to large bacterial culture collections, such as 'The UK Crop Microbiome CryoBank', could generate a significant number of candidate antifungal compounds for further investigation as future crop protection products. I believe that the exploitation of largescale bacterial resources for natural products will become an essential component of future programmes to uncover novel antifungal compounds, and antimicrobials more widely.

Similarly, the described *Pseudomonas-Zymoseptoria* interaction system could be further exploited as a potential 'stepping-stone' for the identification of broad spectrum antifungal secondary metabolites or compounds effective against other fungal plant pathogens, that are less amenable to high-throughput *in vitro* screening. Further characterisation of antagonistic *Pseudomonas* strains, identified through this pipeline, against fungal pathogens more broadly, such as medically important fungal species such as *Aspergillus* and *Candida*, could potentially reveal broad spectrum antifungal compounds that could be utilised in medical applications.

To conclude, *Pseudomonas* bacteria show great potential as sources of novel natural antifungal compounds that could be utilised in future crop protection

strategies against *Z. tritici*. The work within this thesis describes the development of an integrated antifungal discovery pipeline utilising *Z. tritici* and *Pseudomonas* bacteria, using a combination of modern approaches. I believe that the application of these methodologies and approaches will be essential to drive natural product discovery from bacterial sources.

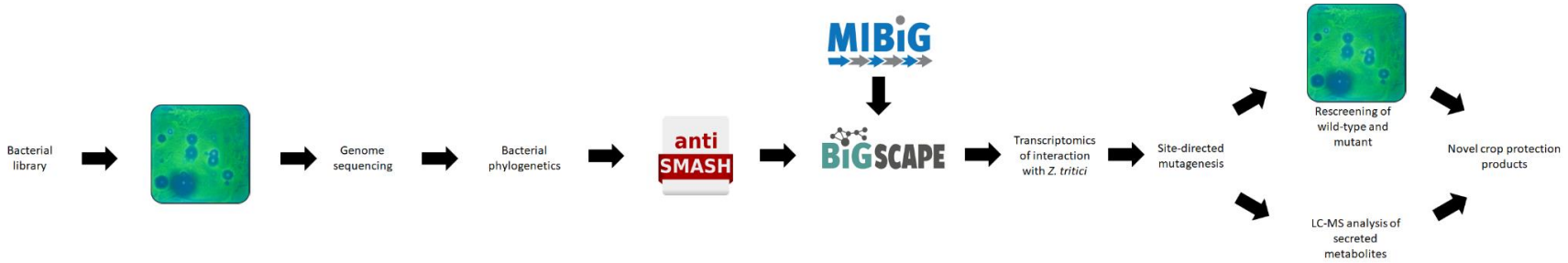


Figure 7.1 An overview of the bio-prospecting pipeline for naturally derived antifungal compounds generated by this project.

Bibliography

Allioui, N., Driss, F., Dhouib, H., Jlail, L., Tounsi, S., Frikha-Gargouri, O., 2021. Two Novel Bacillus Strains (subtilis and simplex Species) with Promising Potential for the Biocontrol of Zymoseptoria tritici, the Causal Agent of Septoria Tritici Blotch of Wheat. BioMed Res. Int. 2021, 1–10. https://doi.org/10.1155/2021/6611657

Almario, J., Bruto, M., Vacheron, J., Prigent-Combaret, C., Moënne-Loccoz, Y., Muller, D., 2017. Distribution of 2,4-Diacetylphloroglucinol Biosynthetic Genes among the Pseudomonas spp. Reveals Unexpected Polyphyletism. Front. Microbiol. 8, 1218. https://doi.org/10.3389/fmicb.2017.01218

Amos, G.C.A., Awakawa, T., Tuttle, R.N., Letzel, A.-C., Kim, M.C., Kudo, Y., Fenical, W., S. Moore, B., Jensen, P.R., 2017. Comparative transcriptomics as a guide to natural product discovery and biosynthetic gene cluster functionality. Proc. Natl. Acad. Sci. 114, E11121–E11130. https://doi.org/10.1073/pnas.1714381115

Arkin, A.P., Cottingham, R.W., Henry, C.S., Harris, N.L., Stevens, R.L., Maslov, S., Dehal, P., Ware, D., Perez, F., Canon, S., Sneddon, M.W., Henderson, M.L., Riehl, W.J., Murphy-Olson, D., Chan, S.Y., Kamimura, R.T., Kumari, S., Drake, M.M., Brettin, T.S., Glass, E.M., Chivian, D., Gunter, D., Weston, D.J., Allen, B.H., Baumohl, J., Best, A.A., Bowen, B., Brenner, S.E., Bun, C.C., Chandonia, J.-M., Chia, J.-M., Colasanti, R., Conrad, N., Davis, J.J., Davison, B.H., DeJongh, M., Devoid, S., Dietrich, E., Dubchak, I., Edirisinghe, J.N., Fang, G., Faria, J.P., Frybarger, P.M., Gerlach, W., Gerstein, M., Greiner, A., Gurtowski, J., Haun, H.L., He, F., Jain, R., Joachimiak, M.P., Keegan, K.P., Kondo, S., Kumar, V., Land, M.L., Meyer, F., Mills, M., Novichkov, P.S., Oh, T., Olsen, G.J., Olson, R., Parrello, B., Pasternak, S., Pearson, E., Poon, S.S., Price, G.A., Ramakrishnan, S., Ranjan, P., Ronald, P.C., Schatz, M.C., Seaver, S.M.D., Shukla, M., Sutormin, R.A., Syed, M.H., Thomason, J., Tintle, N.L., Wang, D., Xia, F., Yoo, H., Yoo, S., Yu, D., 2018. KBase: The United States Department of Energy Systems Biology Knowledgebase. Nat. Biotechnol. 36, 566–569. https://doi.org/10.1038/nbt.4163

Augostine, C.R., Avery, S.V., 2022. Discovery of Natural Products With Antifungal Potential Through Combinatorial Synergy. Front. Microbiol. 13, 866840. https://doi.org/10.3389/fmicb.2022.866840

Bakker, P.A.H.M., Pieterse, C.M.J., van Loon, L.C., 2007. Induced Systemic Resistance by Fluorescent *Pseudomonas* spp. Phytopathology® 97, 239–243. https://doi.org/10.1094/PHYTO-97-2-0239

Bangera, M.G., Thomashow, L.S., 1999. Identification and Characterization of a Gene Cluster for Synthesis of the Polyketide Antibiotic 2,4-Diacetylphloroglucinol from Pseudomonas fluorescens Q2-87. J. Bacteriol. 181, 3155–3163. https://doi.org/10.1128/JB.181.10.3155-3163.1999

Baum, L.E., Petrie, T., 1966. Statistical Inference for Probabilistic Functions of Finite State Markov Chains. Ann. Math. Stat. 37, 1554–1563. https://doi.org/10.1214/aoms/1177699147

Behrendt, U., Ulrich, A., Schumann, P., Meyer, J.-M., Spröer, C., 2007. Pseudomonas lurida sp. nov., a fluorescent species associated with the phyllosphere of grasses. Int. J. Syst. Evol. Microbiol. 57, 979–985. https://doi.org/10.1099/ijs.0.64793-0

Berry, C., 2010. Lipopeptides are essential for Pseudomonas sp. DF41 biocontrol of Sclerotinia sclerotiorum. Biol. Control 9.

Blake, J.J., Gosling, P., Fraaije, B.A., Burnett, F.J., Knight, S.M., Kildea, S., Paveley, N.D., 2018. Changes in field dose-response curves for demethylation inhibitor (DMI) and quinone outside inhibitor (QoI) fungicides against *Zymoseptoria tritici* , related to laboratory sensitivity phenotyping and genotyping assays: Fungicide efficacy related to *in vitro* sensitivity assays. Pest Manag. Sci. 74, 302–313. https://doi.org/10.1002/ps.4725

Blin, K., Shaw, S., Steinke, K., Villebro, R., Ziemert, N., Lee, S.Y., Medema, M.H., Weber, T., 2019. antiSMASH 5.0: updates to the secondary metabolite genome mining pipeline. Nucleic Acids Res. 47, W81–W87. https://doi.org/10.1093/nar/gkz310

Bolyen, E., Rideout, J.R., Dillon, M.R., Bokulich, N.A., Abnet, C.C., Al-Ghalith, G.A., Alexander, H., Alm, E.J., Arumugam, M., Asnicar, F., Bai, Y., Bisanz, J.E., Bittinger, K., Brejnrod, A., Brislawn, C.J., Brown, C.T., Callahan, B.J., Caraballo-Rodríguez, A.M., Chase, J., Cope, E.K., Da Silva, R., Diener, C., Dorrestein, P.C., Douglas, G.M., Durall, D.M., Duvallet, C., Edwardson, C.F., Ernst, M., Estaki, M., Fouquier, J., Gauglitz, J.M., Gibbons, S.M., Gibson, D.L., Gonzalez, A., Gorlick, K., Guo, J., Hillmann, B., Holmes, S., Holste, H., Huttenhower, C., Huttley, G.A., Janssen, S., Jarmusch, A.K., Jiang, L., Kaehler, B.D., Kang, K.B., Keefe, C.R., Keim, P., Kelley, S.T., Knights, D., Koester, I., Kosciolek, T., Kreps, J., Langille, M.G.I., Lee, J., Ley, R., Liu, Y.-X., Loftfield, E., Lozupone, C., Maher, M., Marotz, C., Martin, B.D., McDonald, D., McIver, L.J., Melnik, A.V., Metcalf, J.L., Morgan, S.C.,

Morton, J.T., Naimey, A.T., Navas-Molina, J.A., Nothias, L.F., Orchanian, S.B., Pearson, T., Peoples, S.L., Petras, D., Preuss, M.L., Pruesse, E., Rasmussen, L.B., Rivers, A., Robeson, M.S., Rosenthal, P., Segata, N., Shaffer, M., Shiffer, A., Sinha, R., Song, S.J., Spear, J.R., Swafford, A.D., Thompson, L.R., Torres, P.J., Trinh, P., Tripathi, A., Turnbaugh, P.J., Ul-Hasan, S., van der Hooft, J.J.J., Vargas, F., Vázquez-Baeza, Y., Vogtmann, E., von Hippel, M., Walters, W., Wan, Y., Wang, M., Warren, J., Weber, K.C., Williamson, C.H.D., Willis, A.D., Xu, Z.Z., Zaneveld, J.R., Zhang, Y., Zhu, Q., Knight, R., Caporaso, J.G., 2019. Reproducible, interactive, scalable and extensible microbiome data science using QIIME 2. Nat. Biotechnol. 37, 852–857. https://doi.org/10.1038/s41587-019-0209-9

Bonneau, A., Roche, B., Schalk, I.J., 2020. Iron acquisition in Pseudomonas aeruginosa by the siderophore pyoverdine: an intricate interacting network including periplasmic and membrane proteins. Sci. Rep. 10, 120. https://doi.org/10.1038/s41598-019-56913-x

Boosalis, M.G., 1964. Hyperparasitism 15.

Brown, J.K.M., Chartrain, L., Lasserre-Zuber, P., Saintenac, C., 2015. Genetics of resistance to Zymoseptoria tritici and applications to wheat breeding. Fungal Genet. Biol. 79, 33–41. https://doi.org/10.1016/j.fgb.2015.04.017

Brynildsrud, O., Bohlin, J., Scheffer, L., Eldholm, V., 2016. Rapid scoring of genes in microbial pan-genome-wide association studies with Scoary. Genome Biol. 17, 238. https://doi.org/10.1186/s13059-016-1108-8

Bubici, G., 2019. Biological Control Agents Against Fusarium Wilt of Banana. Front. Microbiol. 10, 34.

Buijs, Y., Isbrandt, T., Zhang, S.-D., Larsen, T.O., Gram, L., 2020. The Antibiotic Andrimid Produced by Vibrio coralliilyticus Increases Expression of Biosynthetic Gene Clusters and Antibiotic Production in Photobacterium galatheae. Front. Microbiol. 11, 622055. https://doi.org/10.3389/fmicb.2020.622055

Cai, M., Xun, L., 2002. Organization and Regulation of Pentachlorophenol-Degrading Genes in *Sphingobium chlorophenolicum* ATCC 39723. J. Bacteriol. 184, 4672–4680. https://doi.org/10.1128/JB.184.17.4672-4680.2002

Cairns, T., Meyer, V., 2017. In silico prediction and characterization of secondary metabolite biosynthetic gene clusters in the wheat pathogen Zymoseptoria tritici. BMC Genomics 18, 631. https://doi.org/10.1186/s12864-017-3969-y

Ceresini, P.C., Castroagudín, V.L., Rodrigues, F.Á., Rios, J.A., Eduardo Aucique-Pérez, C., Moreira, S.I., Alves, E., Croll, D., Maciel, J.L.N., 2018. Wheat Blast: Past, Present, and Future. Annu. Rev. Phytopathol. 56, 427–456. https://doi.org/10.1146/annurev-phyto-080417-050036

Chen, H., King, R., Smith, D., Bayon, C., Ashfield, T., Torriani, S., Kanyuka, K., Hammond-Kosack, K.E., Bieri, S., Rudd, J.J., 2022. Combined pangenomics and transcriptomics reveal core and redundant virulence processes in a rapidly evolving fungal plant pathogen. BMC Biol. Manuscr. Revis.

Chen, R.-S., McDonald, B.A., 1996. Sexual Reproduction Plays a Major Role in the Genetic Structure of Populations of the Fungus *Mycosphaerella graminicola*. Genetics 142, 1119–1127. https://doi.org/10.1093/genetics/142.4.1119

Cheval, P., Siah, A., Bomble, M., Popper, A.D., Reignault, P., Halama, P., 2017. Evolution of QoI resistance of the wheat pathogen Zymoseptoria tritici in Northern France. Crop Prot. 92, 131–133. https://doi.org/10.1016/j.cropro.2016.10.017

Choudhary, D.K., Prakash, A., Johri, B.N., 2007. Induced systemic resistance (ISR) in plants: mechanism of action. Indian J. Microbiol. 47, 289–297. https://doi.org/10.1007/s12088-007-0054-2

Cimermancic, P., Medema, M.H., Claesen, J., Kurita, K., Wieland Brown, L.C., Mavrommatis, K., Pati, A., Godfrey, P.A., Koehrsen, M., Clardy, J., Birren, B.W., Takano, E., Sali, A., Linington, R.G., Fischbach, M.A., 2014. Insights into Secondary Metabolism from a Global Analysis of Prokaryotic Biosynthetic Gene Clusters. Cell 158, 412–421. https://doi.org/10.1016/j.cell.2014.06.034

Clough, S.E., Jousset, A., Elphinstone, J.G., Friman, V., 2022. Combining in vitro and in vivo screening to identify efficient *Pseudomonas* biocontrol strains against the phytopathogenic bacterium *Ralstonia solanacearum*. MicrobiologyOpen 11. https://doi.org/10.1002/mbo3.1283

Colwell, R.R., Citarella, R.V., Ryman, I., 1965. Deoxyribonucleic acid base composition and Adansonian analysis of heterotrophic aerobic pseudomonads. J. Bacteriol. 90, 1148–1149. https://doi.org/10.1128/jb.90.4.1148-1149.1965

Cools, H.J., Bayon, C., Atkins, S., Lucas, J.A., Fraaije, B.A., 2012. Overexpression of the sterol 14α-demethylase gene (MgCYP51) in Mycosphaerella

graminicola isolates confers a novel azole fungicide sensitivity phenotype. Pest Manag. Sci. 68, 1034–1040. https://doi.org/10.1002/ps.3263

Cools, H.J., Fraaije, B.A., 2012. Update on mechanisms of azole resistance in Mycosphaerella graminicola and implications for future control. Pest Manag Sci 6.

Cools, H.J., Hawkins, N.J., Fraaije, B.A., 2013. Constraints on the evolution of azole resistance in plant pathogenic fungi. Plant Pathol. 62, 36–42. https://doi.org/10.1111/ppa.12128

Cotterill, P.J., Sivasithamparam, K., 1988. Inoculum of the take-all fungus in rotations of wheat and pasture: Relationships to disease and yield of wheat. Trans. Br. Mycol. Soc. 91, 63–72. https://doi.org/10.1016/S0007-1536(88)80007-X

Couillerot, O., Combes-Meynet, E., Pothier, J.F., Bellvert, F., Challita, E., Poirier, M.-A., Rohr, R., Comte, G., Moënne-Loccoz, Y., Prigent-Combaret, C., 2011. The role of the antimicrobial compound 2,4-diacetylphloroglucinol in the impact of biocontrol Pseudomonas fluorescens F113 on Azospirillum brasilense phytostimulators. Microbiology 157, 1694–1705. https://doi.org/10.1099/mic.0.043943-0

De Voss, J.J., Rutter, K., Schroeder, B.G., Su, H., Zhu, Y., Barry, C.E., 2000. The salicylate-derived mycobactin siderophores of Mycobacterium tuberculosis are essential for growth in macrophages. Proc. Natl. Acad. Sci. 97, 1252–1257. https://doi.org/10.1073/pnas.97.3.1252

Dean, R., Van Kan, J.A.L., Pretorius, Z.A., Hammond-Kosack, K.E., Di Pietro, A., Spanu, P.D., Rudd, J.J., Dickman, M., Kahmann, R., Ellis, J., Foster, G.D., 2012. The Top 10 fungal pathogens in molecular plant pathology: Top 10 fungal pathogens. Mol. Plant Pathol. 13, 414–430. https://doi.org/10.1111/j.1364-3703.2011.00783.x

Den Dooren de Jong, L.E., 1926. Bijdrage tot de kennis van het mineralisatieproces (urn:NBN:nl:ui:24-uuid:3b39333c-4e9a-4bd4-a30d-7835a2cc8771).

Derbyshire, M.C., Gohari, A.M., Mehrabi, R., Kilaru, S., Steinberg, G., Ali, S., Bailey, A., Hammond-Kosack, K., Kema, G.H.J., Rudd, J.J., 2018. Phosphopantetheinyl transferase (Ppt)-mediated biosynthesis of lysine, but not siderophores or DHN melanin, is required for virulence of Zymoseptoria tritici on wheat. Sci. Rep. 8, 17069. https://doi.org/10.1038/s41598-018-35223-8

Duffy, B.K., Défago, G., 1999. Environmental Factors Modulating Antibiotic and Siderophore Biosynthesis by Pseudomonas fluorescens Biocontrol Strains. Appl. Environ. Microbiol. 65, 2429–2438. https://doi.org/10.1128/AEM.65.6.2429-2438.1999

Duffy, B.K., Défago, G., 1997. Zinc Improves Biocontrol of Fusarium Crown and Root Rot of Tomato by *Pseudomonas fluorescens* and Represses the Production of Pathogen Metabolites Inhibitory to Bacterial Antibiotic Biosynthesis. Phytopathology® 87, 1250–1257. https://doi.org/10.1094/PHYTO.1997.87.12.1250

Elad, Y., 2003. Biocontrol of foliar pathogens: mechanisms and application. Commun. Agric. Appl. Biol. Sci. 68, 17–24.

Eyal, Z., Scharen, A.L., Prescott, J.M., Ginkel, M.V. (Eds.), 1987. The Septoria diseases of wheat: concepts and methods of disease management. CIMMYT, Mexico, D.F.

Fagundes, W.C., Haueisen, J., Stukenbrock, E.H., 2020. Dissecting the Biology of the Fungal Wheat Pathogen *Zymoseptoria tritici* : A Laboratory Workflow. Curr. Protoc. Microbiol. 59. https://doi.org/10.1002/cpmc.128

Fantozzi, E., Kilaru, S., Gurr, S.J., Steinberg, G., 2021. Asynchronous development of Zymoseptoria tritici infection in wheat. Fungal Genet. Biol. 146, 103504. https://doi.org/10.1016/j.fgb.2020.103504

Figlan, S., Ntushelo, K., Mwadzingeni, L., Terefe, T., Tsilo, T.J., Shimelis, H., 2020. Breeding Wheat for Durable Leaf Rust Resistance in Southern Africa: Variability, Distribution, Current Control Strategies, Challenges and Future Prospects. Front. Plant Sci. 11, 549. https://doi.org/10.3389/fpls.2020.00549

Fisher, M.C., Hawkins, N.J., Sanglard, D., Gurr, S.J., 2018. Worldwide emergence of resistance to antifungal drugs challenges human health and food security. Science 360, 739–742. https://doi.org/10.1126/science.aap7999

Fisher, M.C., Henk, Daniel.A., Briggs, C.J., Brownstein, J.S., Madoff, L.C., McCraw, S.L., Gurr, S.J., 2012. Emerging fungal threats to animal, plant and ecosystem health. Nature 484, 186–194. https://doi.org/10.1038/nature10947

Flaishman, M., Eyal, Z., Voisard, C., Haas, D., 1990. Suppression ofSeptoria tritici by Phenazine- or Siderophore-deficient mutants ofPseudomonas. Curr. Microbiol. 20, 121–124. https://doi.org/10.1007/BF02092884

Flaishman, M.A., 1996. Suppression of Septoria tritici Blotch and Leaf Rust of Wheat by Recombinant Cyanide-Producing Strains of *Pseudomonas putida*. Mol. Plant. Microbe Interact. 9, 642. https://doi.org/10.1094/MPMI-9-0642

Fones, H., Gurr, S., 2015. The impact of Septoria tritici Blotch disease on wheat: An EU perspective. Fungal Genet. Biol. 79, 3–7. https://doi.org/10.1016/j.fgb.2015.04.004

Francisco, C.S., Ma, X., Zwyssig, M.M., McDonald, B.A., Palma-Guerrero, J., 2019. Morphological changes in response to environmental stresses in the fungal plant pathogen Zymoseptoria tritici. Sci. Rep. 9, 9642. https://doi.org/10.1038/s41598-019-45994-3

Garbeva, P., Silby, M.W., Raaijmakers, J.M., Levy, S.B., Boer, W. de, 2011. Transcriptional and antagonistic responses of Pseudomonas fluorescens Pf0-1 to phylogenetically different bacterial competitors. ISME J. 5, 973–985. https://doi.org/10.1038/ismej.2010.196

Garrido-Sanz, D., Arrebola, E., Martínez-Granero, F., García-Méndez, S., Muriel, C., Blanco-Romero, E., Martín, M., Rivilla, R., Redondo-Nieto, M., 2017. Classification of Isolates from the Pseudomonas fluorescens Complex into Phylogenomic Groups Based in Group-Specific Markers. Front. Microbiol. 8. https://doi.org/10.3389/fmicb.2017.00413

Garrido-Sanz, D., Meier-Kolthoff, J.P., Göker, M., Martín, M., Rivilla, R., Redondo-Nieto, M., 2016. Genomic and Genetic Diversity within the Pseudomonas fluorescens Complex. PLOS ONE 30.

Geudens, N., Martins, J.C., 2018. Cyclic Lipodepsipeptides From Pseudomonas spp. – Biological Swiss-Army Knives. Front. Microbiol. 9, 1867. https://doi.org/10.3389/fmicb.2018.01867

Gilchrist, C.L.M., Chooi, Y.-H., 2021. clinker & clustermap.js: automatic generation of gene cluster comparison figures. Bioinformatics 37, 2473–2475. https://doi.org/10.1093/bioinformatics/btab007

Gomila, M., PeÃ±a, A., Mulet, M., Lalucat, J., GarcÃ-a-ValdÃ©s, E., 2015. Phylogenomics and systematics in Pseudomonas. Front. Microbiol. 6. https://doi.org/10.3389/fmicb.2015.00214

Gong, L., Tan, H., Chen, F., Li, T., Zhu, J., Jian, Q., Yuan, D., Xu, L., Hu, W., Jiang, Y., Duan, X., 2016. Novel synthesized 2, 4-DAPG analogues: antifungal activity, mechanism and toxicology. Sci. Rep. 6, 32266. https://doi.org/10.1038/srep32266

Goodwin, S.B., Ben M'Barek, S., Dhillon, B., Wittenberg, A.H.J., Crane, C.F., Hane, J.K., Foster, A.J., Van der Lee, T.A.J., Grimwood, J., Aerts, A., Antoniw, J., Bailey, A., Bluhm, B., Bowler, J., Bristow, J., van der Burgt, A., Canto-Canché, B., Churchill, A.C.L., Conde-Ferràez, L., Cools, H.J., Coutinho, P.M., Csukai, M., Dehal, P., De Wit, P., Donzelli, B., van de Geest, H.C., van Ham, R.C.H.J., Hammond-Kosack, K.E., Henrissat, B., Kilian, A., Kobayashi, A.K., Koopmann, E., Kourmpetis, Y., Kuzniar, A., Lindquist, E., Lombard, V., Maliepaard, C., Martins, N., Mehrabi, R., Nap, J.P.H., Ponomarenko, A., Rudd, J.J., Salamov, A., Schmutz, J., Schouten, H.J., Shapiro, H., Stergiopoulos, I., Torriani, S.F.F., Tu, H., de Vries, R.P., Waalwijk, C., Ware, S.B., Wiebenga, A., Zwiers, L.-H., Oliver, R.P., Grigoriev, I.V., Kema, G.H.J., 2011. Finished Genome of the Fungal Wheat Pathogen Mycosphaerella graminicola Reveals Dispensome Structure, Chromosome Plasticity, and Stealth Pathogenesis. PLoS Genet. 7, e1002070. https://doi.org/10.1371/journal.pgen.1002070

Götze, S., Herbst-Irmer, R., Klapper, M., Görls, H., Schneider, K.R.A., Barnett, R., Burks, T., Neu, U., Stallforth, P., 2017. Structure, Biosynthesis, and Biological Activity of the Cyclic Lipopeptide Anikasin. ACS Chem. Biol. 12, 2498–2502. https://doi.org/10.1021/acschembio.7b00589

Gross, H., Loper, J.E., 2009. Genomics of secondary metabolite production by Pseudomonas spp. Nat. Prod. Rep. 26, 1408. https://doi.org/10.1039/b817075b

Gu, Y., Ma, Y., Wang, J., Xia, Z., Wei, H., 2020. Genomic insights into a plant growth-promoting *Pseudomonas koreensis* strain with cyclic lipopeptide-mediated antifungal activity. MicrobiologyOpen 9. https://doi.org/10.1002/mbo3.1092

Guo, W., Li, F., Xia, J., Wang, W., 2021. Complete genome sequence of a marine-derived bacterium Pseudomonas sp. SXM-1 and characterization of its siderophore through antiSMASH analysis and with mass spectroscopic method. Mar. Genomics 55, 100802. https://doi.org/10.1016/j.margen.2020.100802

Hall, D., Tegstrom, C., Ingvarsson, P.K., 2010. Using association mapping to dissect the genetic basis of complex traits in plants. Brief. Funct. Genomics 9, 157–165. https://doi.org/10.1093/bfgp/elp048

Hansen, M.L., He, Z., Wibowo, M., Jelsbak, L., 2021. A Whole-Cell Biosensor for Detection of 2,4-Diacetylphloroglucinol (DAPG)-Producing Bacteria from Grassland Soil. Appl. Environ. Microbiol. 87, e01400-20. https://doi.org/10.1128/AEM.01400-20

Heick, T.M., Justesen, A.F., Jørgensen, L.N., 2017. Anti-resistance strategies for fungicides against wheat pathogen Zymoseptoria tritici with focus on DMI fungicides. Crop Prot. 99, 108–117. https://doi.org/10.1016/j.cropro.2017.05.009

Höfte, M., 2021. The use of Pseudomonas spp. as bacterial biocontrol agents to control plant diseases, in: Wageningen University & Research, The Netherlands, Köhl, J. (Eds.), Burleigh Dodds Series in Agricultural Science. Burleigh Dodds Science Publishing, pp. 301–374. https://doi.org/10.19103/AS.2021.0093.11

Howell, R., Stipamnovic, R.D., 1979. Control of Rhizoctonia solani on Cotton Seedlings with Pseudomonas fluorescens and With an Antibiotic Produced by the Bacterium. Phytopathology 69, 480–482.

Huang, Z., Bonsall, R.F., Mavrodi, D.V., Weller, D.M., Thomashow, L.S., 2004. Transformation of Pseudomonas fluorescens with genes for biosynthesis of phenazine-1-carboxylic acid improves biocontrol of rhizoctonia root rot and in situ antibiotic production. FEMS Microbiol. Ecol. 49, 243–251. https://doi.org/10.1016/j.femsec.2004.03.010

Hunter, M.C., Smith, R.G., Schipanski, M.E., Atwood, L.W., Mortensen, D.A., 2017. Agriculture in 2050: Recalibrating Targets for Sustainable Intensification. BioScience 67, 386–391. https://doi.org/10.1093/biosci/bix010

Ionescu, R., Măruţescu, L., Tănase, A.-M., Chiciudean, I., Csutak, O., Pelinescu, D., Vassu, T., Stoica, I., 2015. Flow Cytometry Based Method for Evaluation of Biodegradative Potential of Pseudomonas fluorescens. Agric. Agric. Sci. Procedia 6, 567–578. https://doi.org/10.1016/j.aaspro.2015.08.088

Johnson, J.L., Palleroni, N.J., 1989. Deoxyribonucleic Acid Similarities among Pseudomonas Species. Int. J. Syst. Bacteriol. 39, 230–235. https://doi.org/10.1099/00207713-39-3-230

Jørgensen, L.N., Maumene, C., Leader, A., 2017. INATREQ^{TM} ACTIVE – a new fungicide for control of Septoria tritici blotch (Zymoseptoria tritici). Presented at the Conference: 12th EFPP, Conference: 12th EFPP, Dunkerque, France.

Kautsar, S.A., Blin, K., Shaw, S., Navarro-Muñoz, J.C., Terlouw, B.R., van der Hooft, J.J.J., van Santen, J.A., Tracanna, V., Suarez Duran, H.G., Pascal Andreu, V., Selem-Mojica, N., Alanjary, M., Robinson, S.L., Lund, G., Epstein, S.C., Sisto, A.C., Charkoudian, L.K., Collemare, J., Linington, R.G., Weber, T., Medema, M.H., 2019. MIBiG 2.0: a repository for

biosynthetic gene clusters of known function. Nucleic Acids Res. gkz882. https://doi.org/10.1093/nar/gkz882

Kautsar, S.A., Blin, K., Shaw, S., Weber, T., Medema, M.H., 2021. BiG-FAM: the biosynthetic gene cluster families database. Nucleic Acids Res. 49, D490–D497. https://doi.org/10.1093/nar/gkaa812

Keel, C., Schnider-Keel, U., Maurhofer, M., Voisard, C., Laville, J., Burger, U., Wirthner, P., Haas, D., Defago, G., 1992. Suppression of Root Diseases by *Pseudomonas fluorescens* CHA0: Importance of the Bacterial Secondary Metabolite 2,4-Diacetylphloroglucinol. Mol. Plant. Microbe Interact. 5, 4. https://doi.org/10.1094/MPMI-5-004

Kema, G., Yu, D., Rijkenberg, F.H.J., Shaw, M.W., Baayen, R.P., 1996. Histology of the Pathogenesis of *Mycosphaerella graminicola* in Wheat. Phytopathology 86, 777. https://doi.org/10.1094/Phyto-86-777

Keon, J., Antoniw, J., Carzaniga, R., Deller, S., Ward, J.L., Baker, J.M., Beale, M.H., Hammond-Kosack, K., Rudd, J.J., 2007. Transcriptional Adaptation of *Mycosphaerella graminicola* to Programmed Cell Death (PCD) of Its Susceptible Wheat Host. Mol. Plant-Microbe Interactions® 20, 178–193. https://doi.org/10.1094/MPMI-20-2-0178

Kerr, K.G., Snelling, A.M., 2009. Pseudomonas aeruginosa: a formidable and ever-present adversary. J. Hosp. Infect. 73, 338–344. https://doi.org/10.1016/j.jhin.2009.04.020

Kettles, G.J., Kanyuka, K., 2016. Dissecting the Molecular Interactions between Wheat and the Fungal Pathogen Zymoseptoria tritici. Front. Plant Sci. 7. https://doi.org/10.3389/fpls.2016.00508

Kildea, S., Marten-Heick, T., Grant, J., Mehenni-Ciz, J., Dooley, H., 2019. A combination of target-site alterations, overexpression and enhanced efflux activity contribute to reduced azole sensitivity present in the Irish Zymoseptoria tritici population. Eur. J. Plant Pathol. 154, 529–540. https://doi.org/10.1007/s10658-019-01676-4

Kildea, S., Ransbotyn, V., Khan, M.R., Fagan, B., Leonard, G., Mullins, E., Doohan, F.M., 2008. Bacillus megaterium shows potential for the biocontrol of septoria tritici blotch of wheat. Biol. Control 9.

Kim, D., Paggi, J.M., Park, C., Bennett, C., Salzberg, S.L., 2019. Graph-based genome alignment and genotyping with HISAT2 and HISAT-genotype. Nat. Biotechnol. 37, 907–915. https://doi.org/10.1038/s41587-019-0201-4

King, R., Urban, M., Lauder, R.P., Hawkins, N., Evans, M., Plummer, A., Halsey, K., Lovegrove, A., Hammond-Kosack, K., Rudd, J.J., 2017. A conserved fungal glycosyltransferase facilitates pathogenesis of plants by enabling hyphal growth on solid surfaces. PLOS Pathog. 13, e1006672. https://doi.org/10.1371/journal.ppat.1006672

Kjeldgaard, B., Neves, A.R., Fonseca, C., Kovács, Á.T., Domínguez-Cuevas, P., 2022. Quantitative High-Throughput Screening Methods Designed for Identification of Bacterial Biocontrol Strains with Antifungal Properties. Microbiol. Spectr. 10, e01433-21. https://doi.org/10.1128/spectrum.01433-21

Köhl, J., Kolnaar, R., Ravensberg, W.J., 2019. Mode of Action of Microbial Biological Control Agents Against Plant Diseases: Relevance Beyond Efficacy. Front. Plant Sci. 10, 845. https://doi.org/10.3389/fpls.2019.00845

Kwon, S.W., Kim, J.S., Park, I.C., Yoon, S.H., Park, D.H., Lim, C.K., Go, S.J., 2003. Pseudomonas koreensis sp. nov., Pseudomonas umsongensis sp. nov. and Pseudomonas jinjuensis sp. nov., novel species from farm soils in Korea. Int. J. Syst. Evol. Microbiol. 53, 21–27. https://doi.org/10.1099/ijs.0.02326-0

Legein, M., Smets, W., Vandenheuvel, D., Eilers, T., Muyshondt, B., Prinsen, E., Samson, R., Lebeer, S., 2020. Modes of Action of Microbial Biocontrol in the Phyllosphere. Front. Microbiol. 11, 1619. https://doi.org/10.3389/fmicb.2020.01619

Lendenmann, M.H., Croll, D., McDonald, B.A., 2015. QTL mapping of fungicide sensitivity reveals novel genes and pleiotropy with melanization in the pathogen Zymoseptoria tritici. Fungal Genet. Biol. 80, 53–67. https://doi.org/10.1016/j.fgb.2015.05.001

Lendenmann, M.H., Croll, D., Palma-Guerrero, J., Stewart, E.L., McDonald, B.A., 2016. QTL mapping of temperature sensitivity reveals candidate genes for thermal adaptation and growth morphology in the plant pathogenic fungus Zymoseptoria tritici. Heredity 116, 384–394. https://doi.org/10.1038/hdy.2015.111

Letunic, I., Bork, P., 2019. Interactive Tree Of Life (iTOL) v4: recent updates and new developments. Nucleic Acids Res. 47, W256–W259. https://doi.org/10.1093/nar/gkz239

Leutwein, C., Heider, J., 2002. (R)-Benzylsuccinyl-CoA dehydrogenase of Thauera aromatica , an enzyme of the anaerobic toluene catabolic pathway. Arch. Microbiol. 178, 517–524. https://doi.org/10.1007/s00203-002-0484-5

Levy, E., Eyal, Z., Carmely, S., Kashman, Y., Chet, I., 1989. Suppression of Septoria tritici and Puccinia recondita of wheat by an antibiotic-producing fluorescent pseudomonad. Plant Pathol. 38, 564–570. https://doi.org/10.1111/j.1365-3059.1989.tb01452.x

Levy, E., Eyal, Z., Chet, I., 1988. Suppression of septoria tritici blotch and leaf rust on wheat seedling leaves by pseudomonads. Plant Pathol. 37, 551–557. https://doi.org/10.1111/j.1365-3059.1988.tb02114.x

Levy, E., Eyal, Z., Chet, I., Hochman, A., 1992a. Resistance mechanisms of Septoria tritici to antifungal products of Pseudomonas. Physiol. Mol. Plant Pathol. 40, 163–171. https://doi.org/10.1016/0885-5765(92)90057-3

Levy, E., Gough, F.J., Berlin, K.D., Guiana, P.W., Smith, J.T., 1992b. Inhibition of Septoria tritici and other phytopathogenic fungi and bacteria by Pseudomonas fluorescens and its antibiotics. Plant Pathol. 41, 335–341. https://doi.org/10.1111/j.1365-3059.1992.tb02355.x

Liao, Y., Smyth, G.K., Shi, W., 2014. featureCounts: an efficient general purpose program for assigning sequence reads to genomic features. Bioinformatics 30, 923–930. https://doi.org/10.1093/bioinformatics/btt656

Ligon, J.M., Hill, D.S., Hammer, P.E., Torkewitz, N.R., Hofmann, D., Kempf, H.-J., van Pee, K.-H., 2000. Natural products with antifungal activity from Pseudomonas biocontrol bacteria. Pest Manag Sci 8.

Lim, C.K., Hassan, K.A., Tetu, S.G., Loper, J.E., Paulsen, I.T., 2012. The Effect of Iron Limitation on the Transcriptome and Proteome of Pseudomonas fluorescens Pf-5. PLoS ONE 7, e39139. https://doi.org/10.1371/journal.pone.0039139

Lindberg, G.D., Larkin, J.M., Whaley, H.A., 1980. Production of Tropolone by A Pseudomonas. J. Nat. Prod. 43, 592–594. https://doi.org/10.1021/np50011a011

Linde, C.C., Zhan, J., McDonald, B.A., 2002. Population Structure of *Mycosphaerella graminicola*: From Lesions to Continents. Phytopathology® 92, 946–955. https://doi.org/10.1094/PHYTO.2002.92.9.946

Love, M.I., Huber, W., Anders, S., 2014. Moderated estimation of fold change and dispersion for RNA-seq data with DESeq2. Genome Biol. 15, 550. https://doi.org/10.1186/s13059-014-0550-8

Lucas, J.A., Bowyer, P., Anderson, H.M. (Eds.), 1999. Septoria on cereals: a study of pathosystems. CABI Pub, Wallingford, Oxon ; New York, NY.

Lucas, J.A., Fraaije, B.A., 2008. The final straw: crop archives and the recent history of cereal pathosystems, in: BSPP Presidential Meeting 2008 Proceedings. Home Grown Cereals Authority (HGCA) London, pp. 103–115.

Lucas, J.A., Hawkins, N.J., Fraaije, B.A., 2015. The Evolution of Fungicide Resistance, in: Advances in Applied Microbiology. Elsevier, pp. 29–92. https://doi.org/10.1016/bs.aambs.2014.09.001

Lynch, K.M., Zannini, E., Guo, J., Axel, C., Arendt, E.K., Kildea, S., Coffey, A., 2016. Control of Zymoseptoria tritici cause of septoria tritici blotch of wheat using antifungal Lactobacillus strains. J. Appl. Microbiol. 10.

Mac Nish, G., Dodman, R., Flentje, N., 1973. Bioassay of Undisturbed Soil Cores for the Presence of Gaeumannomyces Graminis Var. Tritici. Aust. J. Biol. Sci. 26, 1267. https://doi.org/10.1071/BI9731267

Matthijs, S., Tehrani, K.A., Laus, G., Jackson, R.W., Cooper, R.M., Cornelis, P., 2007. Thioquinolobactin, a Pseudomonas siderophore with antifungal and anti-Pythium activity. Environ. Microbiol. 9, 425–434. https://doi.org/10.1111/j.1462-2920.2006.01154.x

Mauchline, T.H., Chedom-Fotso, D., Chandra, G., Samuels, T., Greenaway, N., Backhaus, A., McMillan, V., Canning, G., Powers, S.J., Hammond-Kosack, K.E., Hirsch, P.R., Clark, I.M., Mehrabi, Z., Roworth, J., Burnell, J., Malone, J.G., 2015. An analysis of *P seudomonas* genomic diversity in take-all infected wheat fields reveals the lasting impact of wheat cultivars on the soil microbiota: *Pseudomonas* genome diversity in wheat rhizospheres. Environ. Microbiol. 17, 4764–4778. https://doi.org/10.1111/1462-2920.13038

Mazzola, M., Zhao, X., Cohen, M.F., Raaijmakers, J.M., 2007. Cyclic Lipopeptide Surfactant Production by *Pseudomonas fluorescens* SS101 Is Not Required for Suppression of Complex *Pythium* spp. Populations. Phytopathology® 97, 1348–1355. https://doi.org/10.1094/PHYTO-97-10-1348

McHenry, C.S., 2011. DNA Replicases from a Bacterial Perspective. Annu. Rev. Biochem. 80, 403–436. https://doi.org/10.1146/annurev-biochem-061208-091655

McIntosh, J.A., Donia, M.S., Schmidt, E.W., 2009. Ribosomal peptide natural products: bridging the ribosomal and nonribosomal worlds. Nat. Prod. Rep. 26, 537. https://doi.org/10.1039/b714132g

McMahon, M.D., Rush, J.S., Thomas, M.G., 2012. Analyses of MbtB, MbtE, and MbtF Suggest Revisions to the Mycobactin Biosynthesis Pathway in Mycobacterium tuberculosis. J. Bacteriol. 194, 2809–2818. https://doi.org/10.1128/JB.00088-12

Medema, M.H., Kottmann, R., Yilmaz, P., Cummings, M., Biggins, J.B., Blin, K., de Bruijn, I., Chooi, Y.H., Claesen, J., Coates, R.C., Cruz-Morales, P., Duddela, S., Düsterhus, S., Edwards, D.J., Fewer, D.P., Garg, N., Geiger, C., Gomez-Escribano, J.P., Greule, A., Hadjithomas, M., Haines, A.S., Helfrich, E.J.N., Hillwig, M.L., Ishida, K., Jones, A.C., Jones, C.S., Jungmann, K., Kegler, C., Kim, H.U., Kötter, P., Krug, D., Masschelein, J., Melnik, A.V., Mantovani, S.M., Monroe, E.A., Moore, M., Moss, N., Nützmann, H.-W., Pan, G., Pati, A., Petras, D., Reen, F.J., Rosconi, F., Rui, Z., Tian, Z., Tobias, N.J., Tsunematsu, Y., Wiemann, P., Wyckoff, E., Yan, X., Yim, G., Yu, F., Xie, Y., Aigle, B., Apel, A.K., Balibar, C.J., Balskus, E.P., Barona-Gómez, F., Bechthold, A., Bode, H.B., Borriss, R., Brady, S.F., Brakhage, A.A., Caffrey, P., Cheng, Y.-Q., Clardy, J., Cox, R.J., De Mot, R., Donadio, S., Donia, M.S., van der Donk, W.A., Dorrestein, P.C., Doyle, S., Driessen, A.J.M., Ehling-Schulz, M., Entian, K.-D., Fischbach, M.A., Gerwick, L., Gerwick, W.H., Gross, H., Gust, B., Hertweck, C., Höfte, M., Jensen, S.E., Ju, J., Katz, L., Kaysser, L., Klassen, J.L., Keller, N.P., Kormanec, J., Kuipers, O.P., Kuzuyama, T., Kyrpides, N.C., Kwon, H.-J., Lautru, S., Lavigne, R., Lee, C.Y., Linquan, B., Liu, X., Liu, W., Luzhetskyy, A., Mahmud, T., Mast, Y., Méndez, C., Metsä-Ketelä, M., Micklefield, J., Mitchell, D.A., Moore, B.S., Moreira, L.M., Müller, R., Neilan, B.A., Nett, M., Nielsen, J., O'Gara, F., Oikawa, H., Osbourn, A., Osburne, M.S., Ostash, B., Payne, S.M., Pernodet, J.-L., Petricek, M., Piel, J., Ploux, O., Raaijmakers, J.M., Salas, J.A., Schmitt, E.K., Scott, B., Seipke, R.F., Shen, B., Sherman, D.H., Sivonen, K., Smanski, M.J., Sosio, M., Stegmann, E., Süssmuth, R.D., Tahlan, K., Thomas, C.M., Tang, Y., Truman, A.W., Viaud, M., Walton, J.D., Walsh, C.T., Weber, T., van Wezel, G.P., Wilkinson, B., Willey, J.M., Wohlleben, W., Wright, G.D., Ziemert, N., Zhang, C., Zotchev, S.B., Breitling, R., Takano, E., Glöckner, F.O., 2015. Minimum Information about a Biosynthetic Gene cluster. Nat. Chem. Biol. 11, 625–631. https://doi.org/10.1038/nchembio.1890

Medina, A., Lambert, R.J.W., Magan, N., 2012. Rapid throughput analysis of filamentous fungal growth using turbidimetric measurements with the Bioscreen C: a tool for screening antifungal compounds. Fungal Biol. 116, 161–169. https://doi.org/10.1016/j.funbio.2011.11.001

Mehrabi, R., Kema, G.H.J., 2006. Protein kinase A subunits of the ascomycete pathogen Mycosphaerella graminicola regulate asexual fructification, filamentation, melanization and osmosensing. Mol. Plant Pathol. 7, 565–577. https://doi.org/10.1111/j.1364-3703.2006.00361.x

Mejri, S., Siah, A., Coutte, F., Magnin-Robert, M., Randoux, B., Tisserant, B., Krier, F., Jacques, P., Reignault, P., Halama, P., 2018. Biocontrol of the wheat pathogen Zymoseptoria tritici using cyclic lipopeptides from Bacillus subtilis. Environ. Sci. Pollut. Res. 25, 29822–29833. https://doi.org/10.1007/s11356-017-9241-9

Mendes, R., Kruijt, M., de Bruijn, I., Dekkers, E., van der Voort, M., Schneider, J.H.M., Piceno, Y.M., DeSantis, T.Z., Andersen, G.L., Bakker, P.A.H.M., Raaijmakers, J.M., 2011. Deciphering the Rhizosphere Microbiome for Disease-Suppressive Bacteria. Science 332, 1097–1100. https://doi.org/10.1126/science.1203980

Mercier, J., Lindow, S.E., 2000. Role of Leaf Surface Sugars in Colonization of Plants by Bacterial Epiphytes. Appl. Environ. Microbiol. 66, 369–374. https://doi.org/10.1128/AEM.66.1.369-374.2000

Mohr, K.I., Volz, C., Jansen, R., Wray, V., Hoffmann, J., Bernecker, S., Wink, J., Gerth, K., Stadler, M., Müller, R., 2015. Pinensins: The First Antifungal Lantibiotics. Angew. Chem. Int. Ed. 54, 11254–11258. https://doi.org/10.1002/anie.201500927

Möller, M., Habig, M., Freitag, M., Stukenbrock, E.H., 2018. Extraordinary Genome Instability and Widespread Chromosome Rearrangements During Vegetative Growth. Genetics 210, 517–529. https://doi.org/10.1534/genetics.118.301050

Morais, D., Laval, V., Sache, I., Suffert, F., 2015. Comparative pathogenicity of sexual and asexual spores of *Zymoseptoria tritici* (septoria tritici blotch) on wheat leaves. Plant Pathol. 64, 1429–1439. https://doi.org/10.1111/ppa.12372

Morris, C.E., Monteil, C.L., Berge, O., 2013. The Life History of *Pseudomonas syringae* : Linking Agriculture to Earth System Processes. Annu. Rev. Phytopathol. 51, 85–104. https://doi.org/10.1146/annurev-phyto-082712-102402

Motteram, J., Lovegrove, A., Pirie, E., Marsh, J., Devonshire, J., van de Meene, A., Hammond-Kosack, K., Rudd, J.J., 2011. Aberrant protein N-glycosylation impacts upon infection-related growth transitions of the haploid plant-pathogenic fungus Mycosphaerella graminicola: M.

graminicola yeast to hyphal morphogenesis. Mol. Microbiol. 81, 415–433. https://doi.org/10.1111/j.1365-2958.2011.07701.x

Moynihan, J.A., Morrissey, J.P., Coppoolse, E.R., Stiekema, W.J., O'Gara, F., Boyd, E.F., 2009. Evolutionary History of the *phl* Gene Cluster in the Plant-Associated Bacterium *Pseudomonas fluorescens*. Appl. Environ. Microbiol. 75, 2122–2131. https://doi.org/10.1128/AEM.02052-08

Mulet, M., Lalucat, J., García-Valdés, E., 2010. DNA sequence-based analysis of the *Pseudomonas* species. Environ. Microbiol. https://doi.org/10.1111/j.1462-2920.2010.02181.x

Müller, T., Behrendt, U., Ruppel, S., von der Waydbrink, G., Müller, M.E.H., 2016. Fluorescent Pseudomonads in the Phyllosphere of Wheat: Potential Antagonists Against Fungal Phytopathogens. Curr. Microbiol. 72, 383–389. https://doi.org/10.1007/s00284-015-0966-8

Müller, T., Ruppel, S., Behrendt, U., Lentzsch, P., Müller, M.E.H., 2018. Antagonistic Potential of Fluorescent Pseudomonads Colonizing Wheat Heads Against Mycotoxin Producing Alternaria and Fusaria. Front. Microbiol. 9, 2124. https://doi.org/10.3389/fmicb.2018.02124

Mullins, A.J., Webster, G., Kim, H.J., Zhao, J., Petrova, Y.D., Ramming, C.E., Jenner, M., Murray, J.A.H., Connor, T.R., Hertweck, C., Challis, G.L., Mahenthiralingam, E., 2021. Discovery of the Pseudomonas Polyyne Protegencin by a Phylogeny-Guided Study of Polyyne Biosynthetic Gene Cluster Diversity. mBio 12, e00715-21. https://doi.org/10.1128/mBio.00715-21

Nakagawa, S., 2004. A farewell to Bonferroni: the problems of low statistical power and publication bias. Behav. Ecol. 15, 1044–1045. https://doi.org/10.1093/beheco/arh107

Navarro-Muñoz, J.C., Selem-Mojica, N., Mullowney, M.W., Kautsar, S.A., Tryon, J.H., Parkinson, E.I., De Los Santos, E.L.C., Yeong, M., Cruz-Morales, P., Abubucker, S., Roeters, A., Lokhorst, W., Fernandez-Guerra, A., Cappelini, L.T.D., Goering, A.W., Thomson, R.J., Metcalf, W.W., Kelleher, N.L., Barona-Gomez, F., Medema, M.H., 2020. A computational framework to explore large-scale biosynthetic diversity. Nat. Chem. Biol. 16, 60–68. https://doi.org/10.1038/s41589-019-0400-9

Nelson, L.R., Marshall, D., 1990. Breeding Wheat for Resistance to Septoria nodorum and Septoria tritici, in: Advances in Agronomy. Elsevier, pp. 257–277. https://doi.org/10.1016/S0065-2113(08)60824-X

O'Driscoll, A., Kildea, S., Doohan, F., Spink, J., Mullins, E., 2014. The wheat–Septoria conflict: a new front opening up? Trends Plant Sci. 19, 602–610. https://doi.org/10.1016/j.tplants.2014.04.011

Ogier, J.-C., Pagès, S., Galan, M., Barret, M., Gaudriault, S., 2019. rpoB, a promising marker for analyzing the diversity of bacterial communities by amplicon sequencing. BMC Microbiol. 19, 171. https://doi.org/10.1186/s12866-019-1546-z

Omoboye, O.O., Geudens, N., Duban, M., Chevalier, M., Flahaut, C., Martins, J.C., Leclère, V., Oni, F.E., Höfte, M., 2019. Pseudomonas sp. COW3 Produces New Bananamide-Type Cyclic Lipopeptides with Antimicrobial Activity against Pythium myriotylum and Pyricularia oryzae. Molecules 24, 4170. https://doi.org/10.3390/molecules24224170

Omrane, S., Sghyer, H., Audéon, C., Lanen, C., Duplaix, C., Walker, A.-S., Fillinger, S., 2015. Fungicide efflux and the MgMFS1 transporter contribute to the multidrug resistance phenotype in *Z ymoseptoria tritici* field isolates: Fungicide efflux & *MgMFS 1* contribute to MDR in *Z. tritici*. Environ. Microbiol. 17, 2805–2823. https://doi.org/10.1111/1462-2920.12781

Orton, E.S., Deller, S., Brown, J.K.M., 2011. Mycosphaerella graminicola: from genomics to disease control. Mol. PLANT Pathol. 12.

Orton, E.S., Rudd, J.J., Brown, J.K.M., 2017. Early molecular signatures of responses of wheat to *Zymoseptoria tritici* in compatible and incompatible interactions. Plant Pathol. 66, 450–459. https://doi.org/10.1111/ppa.12633

Pacheco-Moreno, A., Stefanato, F.L., Ford, J.J., Trippel, C., Uszkoreit, S., Ferrafiat, L., Grenga, L., Dickens, R., Kelly, N., Kingdon, A.D., Ambrosetti, L., Nepogodiev, S.A., Findlay, K.C., Cheema, J., Trick, M., Chandra, G., Tomalin, G., Malone, J.G., Truman, A.W., 2021. Pan-genome analysis identifies intersecting roles for Pseudomonas specialized metabolites in potato pathogen inhibition. eLife 10, e71900. https://doi.org/10.7554/eLife.71900

Palmer, C.-L., Skinner, W., 2002. *Mycosphaerella graminicola* : latent infection, crop devastation and genomics: *M. GRAMINICOLA* : LATENT INFECTION, CROP DEVASTATION AND GENOMICS. Mol. Plant Pathol. 3, 63–70. https://doi.org/10.1046/j.1464-6722.2002.00100.x

Parte, A.C., 2014. LPSN—list of prokaryotic names with standing in nomenclature. Nucleic Acids Res. 42, D613–D616. https://doi.org/10.1093/nar/gkt1111

Peix, A., Ramírez-Bahena, M.-H., Velázquez, E., 2018. The current status on the taxonomy of Pseudomonas revisited: An update. Infect. Genet. Evol. 57, 106–116. https://doi.org/10.1016/j.meegid.2017.10.026

Perelló, A.E., Moreno, M.V., Mónaco, C., Simón, M.R., Cordo, C., 2009. Biological control of Septoria tritici blotch on wheat by Trichoderma spp. under field conditions in Argentina. BioControl 54, 113–122. https://doi.org/10.1007/s10526-008-9159-8

Pfender, W.F., Kraus, J., Loper, J.E., 1993. A Genomic Region from *Pseudomonas fluorescens* Pf-5 Required for Pyrrolnitrin Production and Inhibition of *Pyrenophora tritici-repentis* in Wheat Straw. Phytopathology 83, 1223. https://doi.org/10.1094/Phyto-83-1223

Price, M.N., Dehal, P.S., Arkin, A.P., 2010. FastTree 2 – Approximately Maximum-Likelihood Trees for Large Alignments. PLoS ONE 5, e9490. https://doi.org/10.1371/journal.pone.0009490

Raaijmakers, J.M., Vlami, M., de Souza, J.T., 2002. Antibiotic production by bacterial biocontrol agents 11.

Raaijmakers, J.M., Weller, D.M., 2001. Exploiting Genotypic Diversity of 2,4-Diacetylphloroglucinol-Producing *Pseudomonas* spp.: Characterization of Superior Root-Colonizing *P. fluorescens* Strain Q8r1-96. Appl. Environ. Microbiol. 67, 2545–2554. https://doi.org/10.1128/AEM.67.6.2545-2554.2001

Raaijmakers, J.M., Weller, D.M., 1998. Natural Plant Protection by 2,4-Diacetylphloroglucinol-Producing *Pseudomonas* spp. in Take-All Decline Soils. Mol. Plant-Microbe Interactions® 11, 144–152. https://doi.org/10.1094/MPMI.1998.11.2.144

Richter, M., Rosselló-Móra, R., 2009. Shifting the genomic gold standard for the prokaryotic species definition. Proc. Natl. Acad. Sci. 106, 19126–19131. https://doi.org/10.1073/pnas.0906412106

Rowland, B.M., Grossman, T.H., Osburne, M.S., Taber, H.W., 1996. Sequence and genetic organization of a Bacillus subtilis operon encoding 2,3-dihydroxybenzoate biosynthetic enzymes. Gene 178, 119–123. https://doi.org/10.1016/0378-1119(96)00349-6

Rudd, J.J., 2015. Previous bottlenecks and future solutions to dissecting the Zymoseptoria tritici –wheat host-pathogen interaction. Fungal Genet. Biol. 79, 24–28. https://doi.org/10.1016/j.fgb.2015.04.005

Sagot, B., Gaysinski, M., Mehiri, M., Guigonis, J.-M., Le Rudulier, D., Alloing, G., 2010. Osmotically induced synthesis of the dipeptide N-acetylglutaminylglutamine amide is mediated by a new pathway conserved among bacteria. Proc. Natl. Acad. Sci. 107, 12652–12657. https://doi.org/10.1073/pnas.1003063107

Saintenac, C., Lee, W.-S., Cambon, F., Rudd, J.J., King, R.C., Marande, W., Powers, S.J., Bergès, H., Phillips, A.L., Uauy, C., Hammond-Kosack, K.E., Langin, T., Kanyuka, K., 2018. Wheat receptor-kinase-like protein Stb6 controls gene-for-gene resistance to fungal pathogen Zymoseptoria tritici. Nat. Genet. 50, 368–374. https://doi.org/10.1038/s41588-018-0051-x

Samain, E., van Tuinen, D., Jeandet, P., Aussenac, T., Selim, S., 2017. Biological control of septoria leaf blotch and growth promotion in wheat by Paenibacillus sp. strain B2 and Curtobacterium plantarum strain EDS. Biol. Control 114, 87–96. https://doi.org/10.1016/j.biocontrol.2017.07.012

Sanderson, F.R., Scharen, A.L., Scott, P.R., 1985. Sources and importance of primary infection and identities of associated propagules.

Sass, G., Nazik, H., Chatterjee, P., Shrestha, P., Groleau, M.-C., Déziel, E., Stevens, D.A., 2021. Altered Pseudomonas Strategies to Inhibit Surface Aspergillus Colonies. Front. Cell. Infect. Microbiol. 11, 734296. https://doi.org/10.3389/fcimb.2021.734296

Sass, G., Nazik, H., Penner, J., Shah, H., Ansari, S.R., Clemons, K.V., Groleau, M.-C., Dietl, A.-M., Visca, P., Haas, H., Déziel, E., Stevens, D.A., 2019. *Aspergillus-Pseudomonas* interaction, relevant to competition in airways. Med. Mycol. 57, S228–S232. https://doi.org/10.1093/mmy/myy087

Sass, G., Nazik, H., Penner, J., Shah, H., Ansari, S.R., Clemons, K.V., Groleau, M.-C., Dietl, A.-M., Visca, P., Haas, H., Déziel, E., Stevens, D.A., 2018. Studies of Pseudomonas aeruginosa Mutants Indicate Pyoverdine as the Central Factor in Inhibition of Aspergillus fumigatus Biofilm. J. Bacteriol. 200, 24.

Savary, S., Willocquet, L., Pethybridge, S.J., Esker, P., McRoberts, N., Nelson, A., 2019. The global burden of pathogens and pests on major food crops. Nat. Ecol. Evol. 3, 430–439. https://doi.org/10.1038/s41559-018-0793-y

Scarpellini, M., Franzetti, L., Galli, A., 2004. Development of PCR assay to identify Pseudomonas fluorescens and its biotype. FEMS Microbiol. Lett. 236, 257–260. https://doi.org/10.1111/j.1574-6968.2004.tb09655.x

Schauberger, B., Ben-Ari, T., Makowski, D., Kato, T., Kato, H., Ciais, P., 2018. Yield trends, variability and stagnation analysis of major crops in France over more than a century. Sci. Rep. 8, 16865. https://doi.org/10.1038/s41598-018-35351-1

Schmidt, R., Cordovez, V., de Boer, W., Raaijmakers, J., Garbeva, P., 2015. Volatile affairs in microbial interactions. ISME J. 9, 2329–2335. https://doi.org/10.1038/ismej.2015.42

Schmidt, R., Etalo, D.W., de Jager, V., Gerards, S., Zweers, H., de Boer, W., Garbeva, P., 2016. Microbial Small Talk: Volatiles in Fungal–Bacterial Interactions. Front. Microbiol. 6. https://doi.org/10.3389/fmicb.2015.01495

Schnider-Keel, U., Seematter, A., Maurhofer, M., Blumer, C., Duffy, B., Gigot-Bonnefoy, C., Reimmann, C., Notz, R., Défago, G., Haas, D., Keel, C., 2000. Autoinduction of 2,4-Diacetylphloroglucinol Biosynthesis in the Biocontrol Agent Pseudomonas fluorescens CHA0 and Repression by the Bacterial Metabolites Salicylate and Pyoluteorin. J. Bacteriol. 182, 1215–1225. https://doi.org/10.1128/JB.182.5.1215-1225.2000

Shanahan, P., O'Sullivan, D.J., Simpson, P., Glennon, J.D., O'Gara, F., 1992. Isolation of 2,4-Diacetylphloroglucinol from a Fluorescent Pseudomonad and Investigation of Physiological Parameters Influencing Its Production. Appl. Environ. Microbiol. 58, 353–358. https://doi.org/10.1128/AEM.58.1.353-358.1992

Shaw, M.W., 1991. Interacting effects of interrupted humid periods and light on infection of wheat leaves by Mycosphaerella graminicola (Septoria tritici). Plant Pathol. 40, 14.

Shetty, N.P., Mehrabi, R., Lütken, H., Haldrup, A., Kema, G.H.J., Collinge, D.B., Jørgensen, H.J.L., 2007. Role of hydrogen peroxide during the interaction between the hemibiotrophic fungal pathogen Septoria tritici and wheat. New Phytol. 174, 637–647. https://doi.org/10.1111/j.1469-8137.2007.02026.x

Shiferaw, B., Smale, M., Braun, H.-J., Duveiller, E., Reynolds, M., Muricho, G., 2013. Crops that feed the world 10. Past successes and future challenges to the role played by wheat in global food security. Food Secur. 5, 291–317. https://doi.org/10.1007/s12571-013-0263-y

Simão, F.A., Waterhouse, R.M., Ioannidis, P., Kriventseva, E.V., Zdobnov, E.M., 2015. BUSCO: assessing genome assembly and annotation completeness with single-copy orthologs. Bioinformatics 31, 3210–3212. https://doi.org/10.1093/bioinformatics/btv351

Simón, M.R., Börner, A., Struik, P.C., 2021. Editorial: Fungal Wheat Diseases: Etiology, Breeding, and Integrated Management. Front. Plant Sci. 12, 671060. https://doi.org/10.3389/fpls.2021.671060

Spiers, A.J., Buckling, A., Rainey, P.B., 2000. The causes of Pseudomonas diversity. Microbiology 146, 2345–2350. https://doi.org/10.1099/00221287-146-10-2345

Stanbridge, L.H., Board, R.G., 1994. A modification of the Pseudomonas selective medium, CFC, that allows differentiation between meat pseudomonads and Enterobacteriaceae. Lett. Appl. Microbiol. 18, 327–328. https://doi.org/10.1111/j.1472-765X.1994.tb00880.x

Steinberg, G., 2015. Cell biology of Zymoseptoria tritici: Pathogen cell organization and wheat infection. Fungal Genet. Biol. 7.

Stephens, C., Ölmez, F., Blyth, H., McDonald, M., Bansal, A., Turgay, E.B., Hahn, F., Saintenac, C., Nekrasov, V., Solomon, P., Milgate, A., Fraaije, B., Rudd, J., Kanyuka, K., 2021. Remarkable recent changes in the genetic diversity of the avirulence gene *AvrStb6* in global populations of the wheat pathogen *Zymoseptoria tritici*. Mol. Plant Pathol. 22, 1121–1133. https://doi.org/10.1111/mpp.13101

Suffert, F., Sache, I., Lannou, C., 2011. Early stages of septoria tritici blotch epidemics of winter wheat: build-up, overseasoning, and release of primary inoculum: Primary inoculum of Mycosphaerella graminicola. Plant Pathol. 60, 166–177. https://doi.org/10.1111/j.1365-3059.2010.02369.x

Süssmuth, R.D., Mainz, A., 2017. Nonribosomal Peptide Synthesis-Principles and Prospects. Angew. Chem. Int. Ed. 56, 3770–3821. https://doi.org/10.1002/anie.201609079

Tatusov, R.L., 2001. The COG database: new developments in phylogenetic classification of proteins from complete genomes. Nucleic Acids Res. 29, 22–28. https://doi.org/10.1093/nar/29.1.22

Testa, A., Oliver, R., Hane, J., 2015. Overview of genomic and bioinformatic resources for Zymoseptoria tritici. Fungal Genet. Biol. 79, 13–16. https://doi.org/10.1016/j.fgb.2015.04.011

Thomassen, G.M.B., Reiche, T., Tennfjord, C.E., Mehli, L., 2022. Antibiotic Resistance Properties among Pseudomonas spp. Associated with Salmon Processing Environments. Microorganisms 10, 1420. https://doi.org/10.3390/microorganisms10071420

Timinskas, K., Balvočiūtė, M., Timinskas, A., Venclovas, Č., 2014. Comprehensive analysis of DNA polymerase III α subunits and their homologs in bacterial genomes. Nucleic Acids Res. 42, 1393–1413. https://doi.org/10.1093/nar/gkt900

Torriani, S.F.F., 2015. Zymoseptoria tritici: A major threat to wheat production, integrated approaches to control. Fungal Genet. Biol. 5.

Tracanna, V., Ossowicki, A., Petrus, M.L.C., Overduin, S., Terlouw, B.R., Lund, G., Robinson, S.L., Warris, S., Schijlen, E.G.W.M., van Wezel, G.P., Raaijmakers, J.M., Garbeva, P., Medema, M.H., 2021. Dissecting Disease-Suppressive Rhizosphere Microbiomes by Functional Amplicon Sequencing and 10× Metagenomics. mSystems 6. https://doi.org/10.1128/mSystems.01116-20

Tran, H., Ficke, A., Asiimwe, T., Höfte, M., Raaijmakers, J.M., 2007. Role of the cyclic lipopeptide massetolide A in biological control of Phytophthora infestans and in colonization of tomato plants by Pseudomonas fluorescens. New Phytol. 175, 731–742. https://doi.org/10.1111/j.1469-8137.2007.02138.x

Trnka, M., Feng, S., Semenov, M.A., Olesen, J.E., Kersebaum, K.C., Rötter, R.P., Semerádová, D., Klem, K., Huang, W., Ruiz-Ramos, M., Hlavinka, P., Meitner, J., Balek, J., Havlík, P., Büntgen, U., 2019. Mitigation efforts will not fully alleviate the increase in water scarcity occurrence probability in wheat-producing areas. Sci. Adv. 5, eaau2406. https://doi.org/10.1126/sciadv.aau2406

Troppens, D.M., Dmitriev, R.I., Papkovsky, D.B., O'Gara, F., Morrissey, J.P., 2013. Genome-wide investigation of cellular targets and mode of action of the antifungal bacterial metabolite 2,4-diacetylphloroglucinol in *Saccharomyces cerevisiae*. FEMS Yeast Res. 13, 322–334. https://doi.org/10.1111/1567-1364.12037

United Nations Department of Economic and Social Affairs Population Division, 2019. World population prospects Highlights, 2019 revision.

van Loon, L.C., Bakker, P.A.H.M., Pieterse, C.M.J., 1998. SYSTEMIC RESISTANCE INDUCED BY RHIZOSPHERE BACTERIA. Annu. Rev. Phytopathol. 36, 453–483. https://doi.org/10.1146/annurev.phyto.36.1.453

Varivarn, K., Champa, L.A., Silby, M.W., Robleto, E.A., 2013. Colonization strategies of Pseudomonas fluorescens Pf0-1: activation of soil-specific genes important for diverse and specific environments. BMC Microbiol. 13, 92. https://doi.org/10.1186/1471-2180-13-92

Vincent, M.N., Harrison, L.A., Brackin, J.M., Kovacevich, P.A., Mukerji, P., Weller, D.M., Pierson, E.A., 1991. Genetic analysis of the antifungal activity of a soilborne Pseudomonas aureofaciens strain. Appl. Environ. Microbiol. 57, 2928–2934. https://doi.org/10.1128/AEM.57.10.2928-2934.1991

Vindeirinho, J.M., Soares, H.M.V.M., Soares, E.V., 2021. Modulation of Siderophore Production by Pseudomonas fluorescens Through the Manipulation of the Culture Medium Composition. Appl. Biochem. Biotechnol. 193, 607–618. https://doi.org/10.1007/s12010-020-03349-z

Vorholt, J.A., 2012. Microbial life in the phyllosphere. Nat. Rev. Microbiol. 10, 828–840. https://doi.org/10.1038/nrmicro2910

Wells, J.S., Trejo, W.H., Principe, P.A., Sykes, R.B., 1984. Obafluorin, a novel .BETA.-lactone produced by Pseudomonas fluorescens. Taxonomy, fermentation and biological properties. J. Antibiot. (Tokyo) 37, 802–803. https://doi.org/10.7164/antibiotics.37.802

Weng, J.-K., Noel, J.P., 2012. Structure–Function Analyses of Plant Type III Polyketide Synthases, in: Methods in Enzymology. Elsevier, pp. 317–335. https://doi.org/10.1016/B978-0-12-394290-6.00014-8

Wiese, M.V., 1987. Compendium of wheat diseases, 2nd ed. ed, The Disease compendium series of the American Phytopathological Society. APS Press, St. Paul, Minn.

Wiik, L., 2009. Control of fungal diseases in winter wheat. Swedish University of Agricultural Sciences, Alnarp.

Williams, C., 2020. Developing synthetic consortia of Pseudomonas spp. for the biological control of Zymoseptoria tritici. University of Sheffield.

Wood, D.E., Salzberg, S.L., 2014. Kraken: ultrafast metagenomic sequence classification using exact alignments. Genome Biol. 15, R46. https://doi.org/10.1186/gb-2014-15-3-r46

Wu, D.-Q., Ye, J., Ou, H.-Y., Wei, X., Huang, X., He, Y.-W., Xu, Y., 2011. Genomic analysis and temperature-dependent transcriptome profiles of the rhizosphere originating strain Pseudomonas aeruginosa M18. BMC Genomics 12, 438. https://doi.org/10.1186/1471-2164-12-438

Xu, T., Li, Y., Zeng, X., Yang, X., Yang, Y., Yuan, S., Hu, X., Zeng, J., Wang, Z., Liu, Q., Liu, Y., Liao, H., Tong, C., Liu, X., Zhu, Y., 2017. Isolation and evaluation of endophytic *Streptomyces endus* OsiSh-2 with potential application for biocontrol of rice blast disease: Evaluation of endophytic *S.*

endus OsiSh-2. J. Sci. Food Agric. 97, 1149–1157. https://doi.org/10.1002/jsfa.7841

Yang, F., Cao, Y., 2012. Biosynthesis of phloroglucinol compounds in microorganisms—review. Appl. Microbiol. Biotechnol. 93, 487–495. https://doi.org/10.1007/s00253-011-3712-6

Yang, F., Jacobsen, S., Jørgensen, H.J.L., Collinge, D.B., Svensson, B., Finnie, C., 2013. Fusarium graminearum and Its Interactions with Cereal Heads: Studies in the Proteomics Era. Front. Plant Sci. 4. https://doi.org/10.3389/fpls.2013.00037

Younus, H., 2019. Oxidoreductases: Overview and Practical Applications, in: Husain, Q., Ullah, M.F. (Eds.), Biocatalysis. Springer International Publishing, Cham, pp. 39–55. https://doi.org/10.1007/978-3-030-25023-2_3

Zetzsche, H., Friedt, W., Ordon, F., 2020. Breeding progress for pathogen resistance is a second major driver for yield increase in German winter wheat at contrasting N levels. Sci. Rep. 10, 20374. https://doi.org/10.1038/s41598-020-77200-0

Zhan, J., Pettway, R.E., McDonald, B.A., 2003. The global genetic structure of the wheat pathogen Mycosphaerella graminicola is characterized by high nuclear diversity, low mitochondrial diversity, regular recombination, and gene flow. Fungal Genet. Biol. 38, 286–297. https://doi.org/10.1016/S1087-1845(02)00538-8

Zhao, X., Park, S.Y., Yang, D., Lee, S.Y., 2019. Synthetic Biology for Natural Compounds. Biochemistry 58, 1454–1456. https://doi.org/10.1021/acs.biochem.8b00569

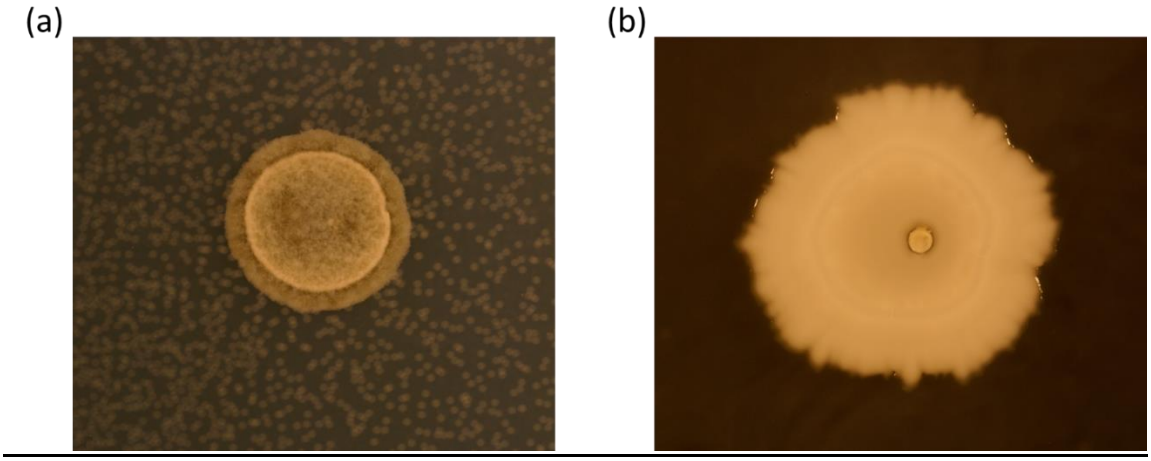
Zwiers, L.-H., Stergiopoulos, I., Gielkens, M.M.C., Goodall, S.D., De Waard, M.A., 2003. ABC transporters of the wheat pathogen Mycosphaerella graminicola function as protectants against biotic and xenobiotic toxic compounds. Mol. Genet. Genomics 269, 499–507. https://doi.org/10.1007/s00438-003-0855-x

Appendix

Supplementary Figures



Supplementary Figure 1. Assessment to determine the viability of *Pseudomonas* inoculum prepared as described in Methods.
Left. An LB agar plate inoculated with Tween-20 solution by aerosol spray. Right. An LB agar plate inoculated with prepared *Pseudomonas* inoculum of isolate Roth 16 by aerosol spray.



Supplementary Figure 2. Images of control plates of the hyphal *Z. tritici in vitro* antagonism assay.
(a) *Z. tritici* isolate IPO323 after 21 days of growth. Successful hyphal extension can be observed from the edge of the colony in all directions. **(b)** *Pseudomonas* isolate Roth 16 after 21 days of growth. Swarming motility can be observed.

Supplementary Tables

Supplementary Table 1. Inhibition data (1 or a 0) for environmental bacterial isolates that were screened using the *in vitro Z. tritici* blastospore assay, alongside the field conditions and niche from which they were isolated.
Inhibition was defined as the presence of a zone of clearing around the *Pseudomonas* colony, on a confluent lawn of *Z. tritici* blastospores.

***Pseudomonas* isolate**	**Antagonism phenotype**	**Isolation source**	**Field type**
1E_1	1	Endosphere	Take-all experiment
1E_11	0	Endosphere	Take-all experiment
1E_12	0	Endosphere	Take-all experiment
1E_13	0	Endosphere	Take-all experiment
1E_14	0	Endosphere	Take-all experiment
1E_15	0	Endosphere	Take-all experiment
1E_16	0	Endosphere	Take-all experiment
1E_2	1	Endosphere	Take-all experiment
1E_3	0	Endosphere	Take-all experiment
1E_4	0	Endosphere	Take-all experiment
1E_7	0	Endosphere	Take-all experiment
1E_8	0	Endosphere	Take-all experiment
1E_9	0	Endosphere	Take-all experiment
1R_1	0	Rhizosphere	Take-all experiment
1R_10	0	Rhizosphere	Take-all experiment
1R_11	0	Rhizosphere	Take-all experiment
1R_12	0	Rhizosphere	Take-all experiment

Pseudomonas isolate	Antagonism phenotype	Isolation source	Field type
1R_13	0	Rhizosphere	Take-all experiment
1R_14	0	Rhizosphere	Take-all experiment
1R_15	0	Rhizosphere	Take-all experiment
1R_16	0	Rhizosphere	Take-all experiment
1R_2	0	Rhizosphere	Take-all experiment
1R_3	1	Rhizosphere	Take-all experiment
1R_5	0	Rhizosphere	Take-all experiment
1R_6	0	Rhizosphere	Take-all experiment
1R_7	0	Rhizosphere	Take-all experiment
1R_8	0	Rhizosphere	Take-all experiment
1R_9	0	Rhizosphere	Take-all experiment
22E_1	0	Endosphere	Take-all experiment
22E_11	0	Endosphere	Take-all experiment
22E_12	0	Endosphere	Take-all experiment
22E_14	0	Endosphere	Take-all experiment
22E_15	0	Endosphere	Take-all experiment
22E_16	0	Endosphere	Take-all experiment
22E_2	0	Endosphere	Take-all experiment
22E_4	0	Endosphere	Take-all experiment
22E_6	1	Endosphere	Take-all experiment
22E_7	0	Endosphere	Take-all experiment
22E_8	0	Endosphere	Take-all experiment
22E_9	0	Endosphere	Take-all experiment
22R_1	0	Rhizosphere	Take-all experiment
22R_10	0	Rhizosphere	Take-all experiment

Pseudomonas isolate	Antagonism phenotype	Isolation source	Field type
22R_11	0	Rhizosphere	Take-all experiment
22R_12	0	Rhizosphere	Take-all experiment
22R_13	0	Rhizosphere	Take-all experiment
22R_14	0	Rhizosphere	Take-all experiment
22R_15	0	Rhizosphere	Take-all experiment
22R_16	0	Rhizosphere	Take-all experiment
22R_2	0	Rhizosphere	Take-all experiment
22R_3	0	Rhizosphere	Take-all experiment
22R_4	0	Rhizosphere	Take-all experiment
22R_5	0	Rhizosphere	Take-all experiment
22R_6	0	Rhizosphere	Take-all experiment
22R_7	0	Rhizosphere	Take-all experiment
22R_8	0	Rhizosphere	Take-all experiment
22R_9	0	Rhizosphere	Take-all experiment
24E_1	0	Endosphere	Take-all experiment
24E_10	1	Endosphere	Take-all experiment
24E_12	0	Endosphere	Take-all experiment
24E_13	0	Endosphere	Take-all experiment
24E_15	0	Endosphere	Take-all experiment
24E_16	0	Endosphere	Take-all experiment
24E_2	0	Endosphere	Take-all experiment
24E_3	0	Endosphere	Take-all experiment
24E_4	0	Endosphere	Take-all experiment
24E_5	0	Endosphere	Take-all experiment
24E_6	0	Endosphere	Take-all experiment

Pseudomonas isolate	Antagonism phenotype	Isolation source	Field type
24E_7	0	Endosphere	Take-all experiment
24E_8	0	Endosphere	Take-all experiment
24E_9	0	Endosphere	Take-all experiment
24R_1	0	Rhizosphere	Take-all experiment
24R_10	0	Rhizosphere	Take-all experiment
24R_11	0	Rhizosphere	Take-all experiment
24R_12	0	Rhizosphere	Take-all experiment
24R_13	0	Rhizosphere	Take-all experiment
24R_14	0	Rhizosphere	Take-all experiment
24R_15	0	Rhizosphere	Take-all experiment
24R_2	0	Rhizosphere	Take-all experiment
24R_3	0	Rhizosphere	Take-all experiment
24R_4	0	Rhizosphere	Take-all experiment
24R_5	1	Rhizosphere	Take-all experiment
24R_6	0	Rhizosphere	Take-all experiment
24R_7	0	Rhizosphere	Take-all experiment
24R_8	0	Rhizosphere	Take-all experiment
24R_9	0	Rhizosphere	Take-all experiment
25E_1	0	Endosphere	Take-all experiment
25E_10	0	Endosphere	Take-all experiment
25E_11	0	Endosphere	Take-all experiment
25E_12	0	Endosphere	Take-all experiment
25E_13	0	Endosphere	Take-all experiment
25E_14	0	Endosphere	Take-all experiment
25E_15	0	Endosphere	Take-all experiment

Pseudomonas isolate	Antagonism phenotype	Isolation source	Field type
25E_16	0	Endosphere	Take-all experiment
25E_2	0	Endosphere	Take-all experiment
25E_3	0	Endosphere	Take-all experiment
25E_4	0	Endosphere	Take-all experiment
25E_6	0	Endosphere	Take-all experiment
25E_7	0	Endosphere	Take-all experiment
25E_8	0	Endosphere	Take-all experiment
25E_9	0	Endosphere	Take-all experiment
25R_1	0	Rhizosphere	Take-all experiment
25R_10	0	Rhizosphere	Take-all experiment
25R_11	0	Rhizosphere	Take-all experiment
25R_12	0	Rhizosphere	Take-all experiment
25R_13	0	Rhizosphere	Take-all experiment
25R_14	0	Rhizosphere	Take-all experiment
25R_15	0	Rhizosphere	Take-all experiment
25R_16	0	Rhizosphere	Take-all experiment
25R_2	0	Rhizosphere	Take-all experiment
25R_3	0	Rhizosphere	Take-all experiment
25R_5	0	Rhizosphere	Take-all experiment
25R_6	0	Rhizosphere	Take-all experiment
25R_7	0	Rhizosphere	Take-all experiment
25R_8	0	Rhizosphere	Take-all experiment
25R_9	0	Rhizosphere	Take-all experiment
28E_1	0	Endosphere	Take-all experiment
28E_11	0	Endosphere	Take-all experiment

Pseudomonas isolate	Antagonism phenotype	Isolation source	Field type
28E_12	0	Endosphere	Take-all experiment
28E_13	0	Endosphere	Take-all experiment
28E_14	1	Endosphere	Take-all experiment
28E_15	1	Endosphere	Take-all experiment
28E_2	0	Endosphere	Take-all experiment
28E_3	0	Endosphere	Take-all experiment
28E_4	0	Endosphere	Take-all experiment
28E_5	0	Endosphere	Take-all experiment
28E_6	0	Endosphere	Take-all experiment
28E_7	0	Endosphere	Take-all experiment
28E_9	0	Endosphere	Take-all experiment
28R_1	0	Rhizosphere	Take-all experiment
28R_10	0	Rhizosphere	Take-all experiment
28R_11	1	Rhizosphere	Take-all experiment
28R_13	0	Rhizosphere	Take-all experiment
28R_14	0	Rhizosphere	Take-all experiment
28R_15	0	Rhizosphere	Take-all experiment
28R_2	1	Rhizosphere	Take-all experiment
28R_4	0	Rhizosphere	Take-all experiment
28R_5	0	Rhizosphere	Take-all experiment
28R_7	1	Rhizosphere	Take-all experiment
28R_8	0	Rhizosphere	Take-all experiment
30E_1	0	Endosphere	Take-all experiment
30E_10	0	Endosphere	Take-all experiment
30E_11	0	Endosphere	Take-all experiment

Pseudomonas isolate	Antagonism phenotype	Isolation source	Field type
30E_12	0	Endosphere	Take-all experiment
30E_13	0	Endosphere	Take-all experiment
30E_15	0	Endosphere	Take-all experiment
30E_16	0	Endosphere	Take-all experiment
30E_2	0	Endosphere	Take-all experiment
30E_3	0	Endosphere	Take-all experiment
30E_4	0	Endosphere	Take-all experiment
30E_5	0	Endosphere	Take-all experiment
30E_6	0	Endosphere	Take-all experiment
30E_7	0	Endosphere	Take-all experiment
30E_8	0	Endosphere	Take-all experiment
30R_1	0	Rhizosphere	Take-all experiment
30R_10	0	Rhizosphere	Take-all experiment
30R_12	0	Rhizosphere	Take-all experiment
30R_13	0	Rhizosphere	Take-all experiment
30R_14	1	Rhizosphere	Take-all experiment
30R_15	0	Rhizosphere	Take-all experiment
30R_16	1	Rhizosphere	Take-all experiment
30R_2	1	Rhizosphere	Take-all experiment
30R_3	0	Rhizosphere	Take-all experiment
30R_4	0	Rhizosphere	Take-all experiment
30R_5	0	Rhizosphere	Take-all experiment
30R_6	0	Rhizosphere	Take-all experiment
30R_7	0	Rhizosphere	Take-all experiment
30R_8	1	Rhizosphere	Take-all experiment

Pseudomonas isolate	Antagonism phenotype	Isolation source	Field type
30R_9	0	Rhizosphere	Take-all experiment
31E_1	0	Rhizosphere	Take-all experiment
31E_10	0	Rhizosphere	Take-all experiment
31E_11	1	Rhizosphere	Take-all experiment
31E_12	0	Rhizosphere	Take-all experiment
31E_13	0	Rhizosphere	Take-all experiment
31E_14	0	Rhizosphere	Take-all experiment
31E_15	0	Rhizosphere	Take-all experiment
31E_16	0	Rhizosphere	Take-all experiment
31E_2	0	Rhizosphere	Take-all experiment
31E_3	0	Rhizosphere	Take-all experiment
31E_4	0	Rhizosphere	Take-all experiment
31E_5	0	Rhizosphere	Take-all experiment
31E_6	0	Rhizosphere	Take-all experiment
31E_8	0	Rhizosphere	Take-all experiment
31E_9	0	Rhizosphere	Take-all experiment
31R_1	0	Rhizosphere	Take-all experiment
31R_10	0	Rhizosphere	Take-all experiment
31R_11	0	Rhizosphere	Take-all experiment
31R_12	0	Rhizosphere	Take-all experiment
31R_13	0	Rhizosphere	Take-all experiment
31R_14	1	Rhizosphere	Take-all experiment
31R_16	0	Rhizosphere	Take-all experiment
31R_2	0	Rhizosphere	Take-all experiment
31R_3	0	Rhizosphere	Take-all experiment

Pseudomonas isolate	Antagonism phenotype	Isolation source	Field type
31R_4	0	Rhizosphere	Take-all experiment
31R_5	0	Rhizosphere	Take-all experiment
31R_7	0	Rhizosphere	Take-all experiment
31R_8	0	Rhizosphere	Take-all experiment
31R_9	0	Rhizosphere	Take-all experiment
32E_1	0	Endosphere	Take-all experiment
32E_10	0	Endosphere	Take-all experiment
32E_11	0	Endosphere	Take-all experiment
32E_13	0	Endosphere	Take-all experiment
32E_14	0	Endosphere	Take-all experiment
32E_15	0	Endosphere	Take-all experiment
32E_16	0	Endosphere	Take-all experiment
32E_2	0	Endosphere	Take-all experiment
32E_3	0	Endosphere	Take-all experiment
32E_4	0	Endosphere	Take-all experiment
32E_7	0	Endosphere	Take-all experiment
32E_8	0	Endosphere	Take-all experiment
32E_9	0	Endosphere	Take-all experiment
34E_1	0	Rhizosphere	Take-all experiment
34E_11	0	Rhizosphere	Take-all experiment
34E_12	0	Rhizosphere	Take-all experiment
34E_14	0	Rhizosphere	Take-all experiment
34E_15	0	Rhizosphere	Take-all experiment
34E_16	0	Rhizosphere	Take-all experiment
34E_2	0	Rhizosphere	Take-all experiment

Pseudomonas isolate	Antagonism phenotype	Isolation source	Field type
34E_3	0	Rhizosphere	Take-all experiment
34E_4	0	Rhizosphere	Take-all experiment
34E_5	0	Rhizosphere	Take-all experiment
34E_6	0	Rhizosphere	Take-all experiment
34E_7	0	Rhizosphere	Take-all experiment
34E_8	0	Rhizosphere	Take-all experiment
34E_9	0	Rhizosphere	Take-all experiment
34R_1	0	Rhizosphere	Take-all experiment
34R_12	0	Rhizosphere	Take-all experiment
34R_13	0	Rhizosphere	Take-all experiment
34R_14	0	Rhizosphere	Take-all experiment
34R_15	0	Rhizosphere	Take-all experiment
34R_16	0	Rhizosphere	Take-all experiment
34R_2	0	Rhizosphere	Take-all experiment
34R_4	0	Rhizosphere	Take-all experiment
34R_5	0	Rhizosphere	Take-all experiment
34R_6	0	Rhizosphere	Take-all experiment
34R_7	0	Rhizosphere	Take-all experiment
34R_8	0	Rhizosphere	Take-all experiment
35E_1	0	Endosphere	Take-all experiment
35E_10	0	Endosphere	Take-all experiment
35E_11	0	Endosphere	Take-all experiment
35E_12	0	Endosphere	Take-all experiment
35E_13	0	Endosphere	Take-all experiment
35E_14	0	Endosphere	Take-all experiment

Pseudomonas isolate	Antagonism phenotype	Isolation source	Field type
35E_15	0	Endosphere	Take-all experiment
35E_2	0	Endosphere	Take-all experiment
35E_3	1	Endosphere	Take-all experiment
35E_5	0	Endosphere	Take-all experiment
35E_6	0	Endosphere	Take-all experiment
35E_7	0	Endosphere	Take-all experiment
35E_8	0	Endosphere	Take-all experiment
35E_9	0	Endosphere	Take-all experiment
35R_1	0	Rhizosphere	Take-all experiment
35R_10	0	Rhizosphere	Take-all experiment
35R_12	0	Rhizosphere	Take-all experiment
35R_13	0	Rhizosphere	Take-all experiment
35R_14	0	Rhizosphere	Take-all experiment
35R_15	0	Rhizosphere	Take-all experiment
35R_16	0	Rhizosphere	Take-all experiment
35R_3	0	Rhizosphere	Take-all experiment
35R_4	0	Rhizosphere	Take-all experiment
35R_5	0	Rhizosphere	Take-all experiment
35R_6	0	Rhizosphere	Take-all experiment
35R_7	0	Rhizosphere	Take-all experiment
35R_8	0	Rhizosphere	Take-all experiment
35R_9	0	Rhizosphere	Take-all experiment
37R_1	0	Rhizosphere	Take-all experiment
37R_10	0	Rhizosphere	Take-all experiment
37R_11	0	Rhizosphere	Take-all experiment

Pseudomonas isolate	Antagonism phenotype	Isolation source	Field type
37R_12	0	Rhizosphere	Take-all experiment
37R_16	1	Rhizosphere	Take-all experiment
37R_2	0	Rhizosphere	Take-all experiment
37R_3	0	Rhizosphere	Take-all experiment
37R_4	0	Rhizosphere	Take-all experiment
37R_5	0	Rhizosphere	Take-all experiment
37R_6	1	Rhizosphere	Take-all experiment
37R_7	1	Rhizosphere	Take-all experiment
37R_8	1	Rhizosphere	Take-all experiment
37R_9	0	Rhizosphere	Take-all experiment
44E_1	0	Endosphere	Take-all experiment
44E_10	0	Endosphere	Take-all experiment
44E_11	0	Endosphere	Take-all experiment
44E_12	0	Endosphere	Take-all experiment
44E_13	0	Endosphere	Take-all experiment
44E_15	0	Endosphere	Take-all experiment
44E_16	0	Endosphere	Take-all experiment
44E_2	0	Endosphere	Take-all experiment
44E_3	0	Endosphere	Take-all experiment
44E_4	0	Endosphere	Take-all experiment
44E_5	0	Endosphere	Take-all experiment
44E_6	0	Endosphere	Take-all experiment
44E_7	0	Endosphere	Take-all experiment
44E_8	0	Endosphere	Take-all experiment
44E_9	0	Endosphere	Take-all experiment

Pseudomonas isolate	Antagonism phenotype	Isolation source	Field type
44R_1	0	Rhizosphere	Take-all experiment
44R_10	0	Rhizosphere	Take-all experiment
44R_11	0	Rhizosphere	Take-all experiment
44R_12	0	Rhizosphere	Take-all experiment
44R_13	0	Rhizosphere	Take-all experiment
44R_14	0	Rhizosphere	Take-all experiment
44R_15	0	Rhizosphere	Take-all experiment
44R_16	0	Rhizosphere	Take-all experiment
44R_2	0	Rhizosphere	Take-all experiment
44R_3	0	Rhizosphere	Take-all experiment
44R_4	0	Rhizosphere	Take-all experiment
44R_5	0	Rhizosphere	Take-all experiment
44R_6	0	Rhizosphere	Take-all experiment
44R_7	0	Rhizosphere	Take-all experiment
44R_8	0	Rhizosphere	Take-all experiment
44R_9	0	Rhizosphere	Take-all experiment
46E_10	0	Endosphere	Take-all experiment
46E_11	0	Endosphere	Take-all experiment
46E_12	0	Endosphere	Take-all experiment
46E_13	0	Endosphere	Take-all experiment
46E_14	0	Endosphere	Take-all experiment
46E_15	0	Endosphere	Take-all experiment
46E_16	0	Endosphere	Take-all experiment
46E_2	0	Endosphere	Take-all experiment
46E_3	0	Endosphere	Take-all experiment

Pseudomonas isolate	Antagonism phenotype	Isolation source	Field type
46E_4	0	Endosphere	Take-all experiment
46E_5	0	Endosphere	Take-all experiment
46E_6	0	Endosphere	Take-all experiment
46E_7	0	Endosphere	Take-all experiment
46E_8	0	Endosphere	Take-all experiment
46E_9	0	Endosphere	Take-all experiment
46R_1	0	Rhizosphere	Take-all experiment
46R_10	0	Rhizosphere	Take-all experiment
46R_11	0	Rhizosphere	Take-all experiment
46R_12	0	Rhizosphere	Take-all experiment
46R_13	0	Rhizosphere	Take-all experiment
46R_14	0	Rhizosphere	Take-all experiment
46R_15	0	Rhizosphere	Take-all experiment
46R_16	0	Rhizosphere	Take-all experiment
46R_2	0	Rhizosphere	Take-all experiment
46R_3	0	Rhizosphere	Take-all experiment
46R_4	0	Rhizosphere	Take-all experiment
46R_5	0	Rhizosphere	Take-all experiment
46R_6	0	Rhizosphere	Take-all experiment
46R_7	0	Rhizosphere	Take-all experiment
46R_8	0	Rhizosphere	Take-all experiment
46R_9	0	Rhizosphere	Take-all experiment
52E_1	0	Rhizosphere	Take-all experiment
52E_10	0	Rhizosphere	Take-all experiment
52E_11	0	Rhizosphere	Take-all experiment

Pseudomonas isolate	Antagonism phenotype	Isolation source	Field type
52E_12	0	Rhizosphere	Take-all experiment
52E_13	0	Rhizosphere	Take-all experiment
52E_14	0	Rhizosphere	Take-all experiment
52E_15	0	Rhizosphere	Take-all experiment
52E_16	0	Rhizosphere	Take-all experiment
52E_2	0	Rhizosphere	Take-all experiment
52E_3	0	Rhizosphere	Take-all experiment
52E_4	0	Rhizosphere	Take-all experiment
52E_5	0	Rhizosphere	Take-all experiment
52E_6	0	Rhizosphere	Take-all experiment
52E_7	0	Rhizosphere	Take-all experiment
52E_8	0	Rhizosphere	Take-all experiment
52R_1	0	Rhizosphere	Take-all experiment
52R_10	0	Rhizosphere	Take-all experiment
52R_11	0	Rhizosphere	Take-all experiment
52R_12	0	Rhizosphere	Take-all experiment
52R_14	0	Rhizosphere	Take-all experiment
52R_15	0	Rhizosphere	Take-all experiment
52R_16	0	Rhizosphere	Take-all experiment
52R_2	0	Rhizosphere	Take-all experiment
52R_3	0	Rhizosphere	Take-all experiment
52R_4	0	Rhizosphere	Take-all experiment
52R_5	0	Rhizosphere	Take-all experiment
52R_6	0	Rhizosphere	Take-all experiment
52R_7	0	Rhizosphere	Take-all experiment

Pseudomonas isolate	Antagonism phenotype	Isolation source	Field type
52R_8	0	Rhizosphere	Take-all experiment
52R_9	0	Rhizosphere	Take-all experiment
58E_1	0	Endosphere	Take-all experiment
58E_10	0	Endosphere	Take-all experiment
58E_11	0	Endosphere	Take-all experiment
58E_12	1	Endosphere	Take-all experiment
58E_13	1	Endosphere	Take-all experiment
58E_14	0	Endosphere	Take-all experiment
58E_15	0	Endosphere	Take-all experiment
58E_16	0	Endosphere	Take-all experiment
58E_4	0	Endosphere	Take-all experiment
58E_7	0	Endosphere	Take-all experiment
58E_8	0	Endosphere	Take-all experiment
58R_1	1	Rhizosphere	Take-all experiment
58R_11	0	Rhizosphere	Take-all experiment
58R_12	0	Rhizosphere	Take-all experiment
58R_13	0	Rhizosphere	Take-all experiment
58R_14	0	Rhizosphere	Take-all experiment
58R_15	0	Rhizosphere	Take-all experiment
58R_16	0	Rhizosphere	Take-all experiment
58R_2	1	Rhizosphere	Take-all experiment
58R_3	0	Rhizosphere	Take-all experiment
58R_4	0	Rhizosphere	Take-all experiment
58R_6	0	Rhizosphere	Take-all experiment
58R_7	0	Rhizosphere	Take-all experiment

Pseudomonas isolate	Antagonism phenotype	Isolation source	Field type
58R_8	0	Rhizosphere	Take-all experiment
8E_1	1	Endosphere	Take-all experiment
8E_10	0	Endosphere	Take-all experiment
8E_11	0	Endosphere	Take-all experiment
8E_12	0	Endosphere	Take-all experiment
8E_14	0	Endosphere	Take-all experiment
8E_15	0	Endosphere	Take-all experiment
8E_16	0	Endosphere	Take-all experiment
8E_2	0	Endosphere	Take-all experiment
8E_3	0	Endosphere	Take-all experiment
8E_5	0	Endosphere	Take-all experiment
8E_6	0	Endosphere	Take-all experiment
8E_7	0	Endosphere	Take-all experiment
8E_8	0	Endosphere	Take-all experiment
8E_9	0	Endosphere	Take-all experiment
8R_1	0	Rhizosphere	Take-all experiment
8R_10	0	Rhizosphere	Take-all experiment
8R_11	0	Rhizosphere	Take-all experiment
8R_13	0	Rhizosphere	Take-all experiment
8R_14	0	Rhizosphere	Take-all experiment
8R_16	0	Rhizosphere	Take-all experiment
8R_2	0	Rhizosphere	Take-all experiment
8R_3	0	Rhizosphere	Take-all experiment
8R_4	0	Rhizosphere	Take-all experiment
8R_5	0	Rhizosphere	Take-all experiment

Pseudomonas isolate	Antagonism phenotype	Isolation source	Field type
8R_6	0	Rhizosphere	Take-all experiment
8R_7	0	Rhizosphere	Take-all experiment
8R_8	0	Rhizosphere	Take-all experiment
8R_9	0	Rhizosphere	Take-all experiment
A-B-20	0	Bulk soil	Arable
A-B-25	0	Bulk soil	Arable
A-R-20	0	Rhizosphere	Arable
A-R-25	0	Rhizosphere	Arable
A-RE-20	0	Root Endosphere	Arable
A-RE-25	0	Root Endosphere	Arable
BF-B-20	1	Bulk soil	Bare Fallow
BF-B-25	0	Bulk soil	Bare Fallow
BF-R-20	1	Rhizosphere	Bare Fallow
BF-R-25	0	Rhizosphere	Bare Fallow
BF-RE-20	0	Root Endosphere	Bare Fallow
BF-RE-25	0	Root Endosphere	Bare Fallow
GL-B-20	0	Bulk soil	Grassland
GL-B-25	0	Bulk soil	Grassland
GL-R-20	0	Rhizosphere	Grassland
GL-R-25	0	Rhizosphere	Grassland
GL-RE-20	0	Root Endosphere	Grassland
GL-RE-25	0	Bulk soil	Grassland
Roth1	0	Endosphere	Take-all experiment
Roth100	0	Bulk soil	Bare Fallow
Roth101	0	Rhizosphere	Bare Fallow

Pseudomonas isolate	Antagonism phenotype	Isolation source	Field type
Roth102	0	Rhizosphere	Bare Fallow
Roth103	1	Rhizosphere	Bare Fallow
Roth104	1	Rhizosphere	Bare Fallow
Roth105	0	Root Endosphere	Bare Fallow
Roth106	0	Root Endosphere	Bare Fallow
Roth107	1	Root Endosphere	Bare Fallow
Roth108	0	Root Endosphere	Bare Fallow
Roth109	0	Root Endosphere	Bare Fallow
Roth11	0	Endosphere	Take-all experiment
Roth110	0	Root Endosphere	Bare Fallow
Roth111	1	Root Endosphere	Arable
Roth112	1	Root Endosphere	Arable
Roth113	0	Root Endosphere	Grassland
Roth12	1	Endosphere	Take-all experiment
Roth13	0	Rhizosphere	Take-all experiment
Roth14	0	Rhizosphere	Take-all experiment
Roth15	0	Endosphere	Take-all experiment
Roth16	1	Rhizosphere	Take-all experiment
Roth17	0	Rhizosphere	Take-all experiment
Roth18	0	Endosphere	Take-all experiment
Roth2	0	Endosphere	Take-all experiment
Roth20	1	Rhizosphere	Take-all experiment
Roth21	1	Endosphere	Take-all experiment
Roth23	0	Rhizosphere	Take-all experiment
Roth25	0	Endosphere	Take-all experiment

Pseudomonas isolate	Antagonism phenotype	Isolation source	Field type
Roth26	1	Endosphere	Take-all experiment
Roth27	0	Endosphere	Take-all experiment
Roth28	0	Endosphere	Take-all experiment
Roth29	0	Rhizosphere	Take-all experiment
Roth3	0	Rhizosphere	Take-all experiment
Roth30	0	Endosphere	Take-all experiment
Roth31	0	Rhizosphere	Take-all experiment
Roth34	0	Endosphere	Take-all experiment
Roth35	0	Endosphere	Take-all experiment
Roth37	0	Rhizosphere	Take-all experiment
Roth39	0	Endosphere	Take-all experiment
Roth4	1	Rhizosphere	Take-all experiment
Roth40	1	Rhizosphere	Take-all experiment
Roth41	0	Rhizosphere	Take-all experiment
Roth42	0	Endosphere	Take-all experiment
Roth43	0	Endosphere	Take-all experiment
Roth44	0	Rhizosphere	Take-all experiment
Roth45	0	Rhizosphere	Take-all experiment
Roth46	0	Rhizosphere	Take-all experiment
Roth48	0	Rhizosphere	Take-all experiment
Roth5	0	Endosphere	Take-all experiment
Roth50	0	Endosphere	Take-all experiment
Roth51	0	Rhizosphere	Take-all experiment
Roth52	0	Rhizosphere	Take-all experiment
Roth53	0	Rhizosphere	Take-all experiment

Pseudomonas isolate	Antagonism phenotype	Isolation source	Field type
Roth54	1	Endosphere	Take-all experiment
Roth56	1	Rhizosphere	Take-all experiment
Roth58	1	Rhizosphere	Take-all experiment
Roth6	0	Endosphere	Take-all experiment
Roth62	0	Endosphere	Take-all experiment
Roth63	0	Rhizosphere	Take-all experiment
Roth64	1	Rhizosphere	Take-all experiment
Roth65	1	Rhizosphere	Take-all experiment
Roth66	0	Rhizosphere	Take-all experiment
Roth67	0	Rhizosphere	Take-all experiment
Roth69	0	Rhizosphere	Take-all experiment
Roth7	0	Endosphere	Take-all experiment
Roth70	1	Rhizosphere	Take-all experiment
Roth71	0	Endosphere	Take-all experiment
Roth72	0	Rhizosphere	Take-all experiment
Roth73	1	Endosphere	Take-all experiment
Roth74	0	Endosphere	Take-all experiment
Roth75	0	Endosphere	Take-all experiment
Roth76	0	Endosphere	Take-all experiment
Roth77	0	Endosphere	Take-all experiment
Roth78	0	Bulk soil	Grassland
Roth79	1	Bulk soil	Grassland
Roth80	0	Root Endosphere	Grassland
Roth81	1	Root Endosphere	Arable
Roth82	1	Root Endosphere	Arable

***Pseudomonas* isolate**	**Antagonism phenotype**	**Isolation source**	**Field type**
Roth83	1	Root Endosphere	Arable
Roth84	0	Root Endosphere	Arable
Roth85	0	Bulk soil	Bare Fallow
Roth86	0	Bulk soil	Bare Fallow
Roth87	0	Rhizosphere	Bare Fallow
Roth88	0	Rhizosphere	Bare Fallow
Roth89	0	Rhizosphere	Bare Fallow
Roth90	0	Rhizosphere	Bare Fallow
Roth91	0	Root Endosphere	Bare Fallow
Roth92	0	Root Endosphere	Bare Fallow
Roth93	0	Root Endosphere	Bare Fallow
Roth94	0	Root Endosphere	Bare Fallow
Roth95	0	Root Endosphere	Bare Fallow
Roth96	0	Root Endosphere	Bare Fallow
Roth97	1	Bulk soil	Bare Fallow
Roth98	0	Bulk soil	Bare Fallow
Roth99	0	Bulk soil	Bare Fallow

Supplementary Table 2. One-way Analysis of Variance of recovered pycnidiospore count data after treatment with *Pseudomonas* inoculum.

	Df	Sum Sq	Mean Sq	*F* value	Pr(>*F*)	
Treatment	5	14755	2951	2.6388	0.05856	.
Residuals	18	20130	1118.3			

Significance codes: 0 '***' 0.001 '**' 0.01 '*' 0.05 '.' 0.1 ' ' 1

Supplementary Table 3. Genome assembly information, taxonomic prediction, gyrB copy status, and BUSCO scores of 129 bacterial isolates.

Genome assemblies of 129 bacterial isolates (38 antagonistic and 91 non-antagonistic towards *Z. tritici* blastospores *in vitro*), with assembly length (in base pairs) and predicted most frequent family and the respective percentage of total reads mapping to this family were calculated by MicrobesNG using Kraken. gyrB copy number and BUSCO scores for all genome assemblies are also indicated.

***Pseudomonas* isolate**	***Z. tritici* blastospore antagonism phenotype**	**Total length of genome assembly (bp)**	**Most frequent family prediction**	**Percentage of total reads classified as most frequent Family (%)**	***gyrB* copy number**	***BUSCO score***
A-B-20	0	6477144	Pseudomonadaceae	65	1	100.00
A-B-25	0	6515109	Pseudomonadaceae	75.11	1	99.19
A-R-20	0	6302608	Pseudomonadaceae	79.96	1	98.39
A-R-25	0	7022807	Pseudomonadaceae	80.61	1	99.19
A-RE-20	0	5937628	Pseudomonadaceae	76.88	1	100.00
A-RE-25	0	6310608	Pseudomonadaceae	69.8	1	99.19
BF-B-20	1	6741353	Pseudomonadaceae	64.03	1	99.19
BF-B-25	0	6598486	Pseudomonadaceae	77.46	1	98.39
BF-R-20	1	6572573	Pseudomonadaceae	67.88	1	100.00
BF-R-25	0	6858872	Pseudomonadaceae	70.59	1	98.39
BF-RE-20	0	6415110	Pseudomonadaceae	63.94	1	100.00
BF-RE-25	0	6225560	Pseudomonadaceae	76.83	1	98.39
GL-B-20	0	6541118	Pseudomonadaceae	67.79	1	99.19

***Pseudomonas* isolate**	***Z. tritici* blastospore antagonism phenotype**	**Total length of genome assembly (bp)**	**Most frequent family prediction**	**Percentage of total reads classified as most frequent Family (%)**	***gyrB* copy number**	***BUSCO score***
GL-B-25	0	6524961	Pseudomonadaceae	55.67	1	100.00
GL-R-20	0	6430994	Pseudomonadaceae	77.8	1	99.19
GL-R-25	0	6502109	Pseudomonadaceae	76.81	1	98.39
GL-RE-20	0	6432708	Pseudomonadaceae	80.95	1	98.39
GL-RE-25	0	6861571	Pseudomonadaceae	79.39	1	99.19
Roth1	0	6793674	Pseudomonadaceae	75.58	1	96.77
Roth100	0	6299446	Pseudomonadaceae	80.85	1	98.39
Roth101	0	6263437	Pseudomonadaceae	83.14	1	98.39
Roth102	0	6222099	Pseudomonadaceae	84.47	1	98.39
Roth103	1	6503295	Pseudomonadaceae	69.51	1	100.00
Roth104	1	6356205	Pseudomonadaceae	81.83	1	97.58
Roth105	0	6706620	Pseudomonadaceae	68.29	1	100.00
Roth106	0	6520010	Pseudomonadaceae	65.19	1	100.00
Roth107	1	6623522	Pseudomonadaceae	96.7	1	100.00
Roth108	0	6371407	Pseudomonadaceae	69.02	1	100.00
Roth109	0	6589166	Pseudomonadaceae	77.77	1	97.58
Roth11	1	12502584	Pseudomonadaceae	72.91	2	27.42
Roth110	0	6445740	Pseudomonadaceae	80.17	1	98.39
Roth111	1	6787619	Pseudomonadaceae	93.58	1	100.00

***Pseudomonas* isolate**	***Z. tritici* blastospore antagonism phenotype**	**Total length of genome assembly (bp)**	**Most frequent family prediction**	**Percentage of total reads classified as most frequent Family (%)**	***gyrB* copy number**	***BUSCO score***
Roth112	1	6905894	Pseudomonadaceae	94.16	1	100.00
Roth113	0	6374364	Pseudomonadaceae	67.39	1	100.00
Roth12	1	6111043	Pseudomonadaceae	70.36	1	100.00
Roth13	0	6108378	Pseudomonadaceae	73.35	1	100.00
Roth14	0	6341204	Pseudomonadaceae	76.13	1	100.00
Roth15	1	5577285	Enterobacteriaceae	89.87	1	97.58
Roth16	1	6395403	Pseudomonadaceae	72.28	1	100.00
Roth17	0	6208635	Pseudomonadaceae	75.47	1	99.19
Roth18	0	6526026	Pseudomonadaceae	72.22	1	100.00
Roth19	0	6254765	Pseudomonadaceae	74.88	1	100.00
Roth2	1	5984681	Pseudomonadaceae	71.2	2	99.19
Roth20	0	6525667	Pseudomonadaceae	69.15	1	99.19
Roth21	0	6214739	Pseudomonadaceae	74.42	1	100.00
Roth22	0	6949394	Pseudomonadaceae	71.66	1	99.19
Roth23	0	6266813	Pseudomonadaceae	76.12	1	100.00
Roth24	0	6608752	Pseudomonadaceae	66.03	1	100.00
Roth25	1	11250108	Enterobacteriaceae	83.04	2	21.77
Roth26	1	11770484	Pseudomonadaceae	44.29	2	8.87
Roth27	0	11137874	Pseudomonadaceae	62.51	2	22.58

***Pseudomonas* isolate**	***Z. tritici* blastospore antagonism phenotype**	**Total length of genome assembly (bp)**	**Most frequent family prediction**	**Percentage of total reads classified as most frequent Family (%)**	***gyrB* copy number**	***BUSCO score***
Roth28	1	12849141	Pseudomonadaceae	73.11	2	18.55
Roth29	0	6431726	Pseudomonadaceae	67.89	1	100.00
Roth3	0	6612047	Pseudomonadaceae	65.74	2	100.00
Roth30	0	11913973	Pseudomonadaceae	75.52	2	56.45
Roth31	0	12589761	Enterobacteriaceae	61	3	8.06
Roth32	0	6782549	Pseudomonadaceae	71.54	1	98.39
Roth33	0	11075660	Pseudomonadaceae	66.6	2	19.35
Roth34	0	13169963	Pseudomonadaceae	64.9	2	54.84
Roth35	1	6674211	Pseudomonadaceae	96.09	2	100.00
Roth36	1	5423965	Enterobacteriaceae	91.72	1	100.00
Roth37	0	16154250	Pseudomonadaceae	75.68	3	36.29
Roth38	0	12720872	Pseudomonadaceae	90.61	2	31.45
Roth39	0	6127477	Pseudomonadaceae	70.39	1	99.19
Roth4	0	6271520	Pseudomonadaceae	67.23	2	99.19
Roth40	1	6000889	Pseudomonadaceae	73.98	1	100.00
Roth41	0	6107422	Pseudomonadaceae	74.27	1	99.19
Roth42	0	6378138	Pseudomonadaceae	72.95	1	100.00
Roth43	0	6392746	Pseudomonadaceae	74.85	1	100.00
Roth44	0	6874621	Pseudomonadaceae	73.85	1	98.39

***Pseudomonas* isolate**	***Z. tritici* blastospore antagonism phenotype**	**Total length of genome assembly (bp)**	**Most frequent family prediction**	**Percentage of total reads classified as most frequent Family (%)**	***gyrB* copy number**	***BUSCO score***
Roth45	0	6217825	Pseudomonadaceae	78.86	1	100.00
Roth46	0	12202445	Pseudomonadaceae	76.45	2	21.77
Roth47	1	11691951	Enterobacteriaceae	62.58	2	8.06
Roth48	0	6859391	Pseudomonadaceae	76.28	1	99.19
Roth49	0	6779422	Pseudomonadaceae	76.74	1	99.19
Roth5	0	6449530	Pseudomonadaceae	63.12	1	100.00
Roth50	0	6592124	Pseudomonadaceae	66.55	1	100.00
Roth51	0	6198881	Pseudomonadaceae	78.43	1	100.00
Roth52	1	8084713	Enterobacteriaceae	91.36	2	68.55
Roth53	0	12691075	Enterobacteriaceae	78.9	3	9.68
Roth54	1	7991605	Enterobacteriaceae	91.78	1	75.81
Roth55	1	10262868	Enterobacteriaceae	89.76	2	44.35
Roth56	0	12426412	Pseudomonadaceae	76.34	2	25.00
Roth57	1	11657523	Enterobacteriaceae	55.9	1	8.06
Roth58	1	5560249	Enterobacteriaceae	92.71	1	97.58
Roth59	1	11577219	Enterobacteriaceae	78.61	2	14.52
Roth6	1	10678200	Pseudomonadaceae	75.69	2	83.87
Roth61	1	12317711	Pseudomonadaceae	74.48	2	26.61
Roth62	0	8119296	Pseudomonadaceae	78.61	1	84.68

***Pseudomonas* isolate**	***Z. tritici* blastospore antagonism phenotype**	**Total length of genome assembly (bp)**	**Most frequent family prediction**	**Percentage of total reads classified as most frequent Family (%)**	***gyrB* copy number**	***BUSCO score***
Roth63	1	6420133	Pseudomonadaceae	72.84	2	99.19
Roth64	0	6383496	Enterobacteriaceae	90.22	2	85.48
Roth65	0	11154158	Enterobacteriaceae	86.6	1	18.55
Roth66	1	6360740	Pseudomonadaceae	78.09	1	100.00
Roth67	0	6190763	Pseudomonadaceae	77.54	1	99.19
Roth68	1	6123932	Pseudomonadaceae	73.65	1	100.00
Roth69	0	11726015	Enterobacteriaceae	72.67	2	8.06
Roth7	0	6108595	Pseudomonadaceae	69.75	1	99.19
Roth70	1	11011569	Enterobacteriaceae	83.57	2	20.97
Roth71	0	12331482	Pseudomonadaceae	73.77	2	54.84
Roth72	0	6206908	Pseudomonadaceae	75.63	1	100.00
Roth73	0	8834331	Pseudomonadaceae	77.02	1	97.58
Roth74	1	11528504	Enterobacteriaceae	57.36	2	8.06
Roth75	1	12100170	Enterobacteriaceae	81.99	2	13.71
Roth76	0	6737293	Pseudomonadaceae	71.84	1	99.19
Roth77	0	5972385	Pseudomonadaceae	66.46	1	100.00
Roth78	0	6732597	Pseudomonadaceae	76.76	1	99.19
Roth79	1	7043887	Pseudomonadaceae	71.39	1	99.19
Roth8	0	12173415	Pseudomonadaceae	70.57	2	39.52

***Pseudomonas* isolate**	***Z. tritici* blastospore antagonism phenotype**	**Total length of genome assembly (bp)**	**Most frequent family prediction**	**Percentage of total reads classified as most frequent Family (%)**	***gyrB* copy number**	***BUSCO score***
Roth80	0	6866768	Pseudomonadaceae	74.34	1	100.00
Roth81	1	6773838	Pseudomonadaceae	92.41	1	100.00
Roth82	1	6773754	Pseudomonadaceae	92.44	1	100.00
Roth83	1	6778653	Pseudomonadaceae	92.61	1	100.00
Roth84	0	6768845	Pseudomonadaceae	93.34	1	100.00
Roth85	0	6456191	Pseudomonadaceae	66.94	2	100.00
Roth86	0	6701326	Pseudomonadaceae	65.51	1	100.00
Roth87	0	6806430	Pseudomonadaceae	63.23	1	100.00
Roth88	0	6306979	Pseudomonadaceae	77.95	1	98.39
Roth89	0	6384558	Pseudomonadaceae	65.58	1	100.00
Roth9	0	6869550	Pseudomonadaceae	77.1	1	98.39
Roth90	0	6488355	Pseudomonadaceae	66.55	1	100.00
Roth91	0	6356469	Pseudomonadaceae	69.55	1	100.00
Roth92	0	6350325	Pseudomonadaceae	67.41	1	100.00
Roth93	0	6693532	Pseudomonadaceae	64.22	1	100.00
Roth94	0	6370867	Pseudomonadaceae	67.53	1	100.00
Roth95	0	6368974	Pseudomonadaceae	68	1	100.00
Roth96	0	6702923	Pseudomonadaceae	66.13	1	100.00
Roth97	1	6511970	Pseudomonadaceae	78.42	1	99.19

***Pseudomonas* isolate**	***Z. tritici* blastospore antagonism phenotype**	**Total length of genome assembly (bp)**	**Most frequent family prediction**	**Percentage of total reads classified as most frequent Family (%)**	***gyrB* copy number**	***BUSCO score***
Roth98	0	6253214	Pseudomonadaceae	82.98	1	99.19
Roth99	0	6247948	Pseudomonadaceae	81.69	1	98.39

Supplementary Table 4. One-way Analysis of Variance of the radius of zones of inhibition produced by *Pseudomonas* isolate BFR20 in confrontation with genetically diverse *Z. tritici* isolates in the blastospore antagonism assay *in vitro*.
Measurements were log transformed to achieve approximate normality.

	Df	Sum Sq	Mean Sq	*F* value	Pr(>*F*)	
Z. tritici genotype	11	45.198	4.109	11.476	9.423E-09	***
Residuals	36	12.889	0.358			

Significance codes: 0 '***' 0.001 '**' 0.01 '*' 0.05 '.' 0.1 ' ' 1

Supplementary Table 5. Tukey's test for multiple comparisons at the 5% level of significance, comparing zones of inhibition produced by *Pseudomonas* isolate BFR20 in confrontation with different *Z. tritici* genotypes *in vitro*.
Measurements were log transformed to achieve approximate normality.

Comparison	Mean Difference	Lower Bound	Upper Bound	Padj
L951-IPO323	3.3892755	1.91250399	4.86604702	0.0000001
Zt10-IPO323	2.1189732	0.64220166	3.59574469	0.0007863
Zt114-IPO323	2.3035831	0.82681158	3.78035461	0.0002151
Zt116-IPO323	3.6951467	2.21837519	5.17191822	0
Zt118-IPO323	2.9357476	1.45897613	4.41251916	0.0000024
Zt120-IPO323	3.8555348	2.37876325	5.33230628	0
Zt36-IPO323	1.9692034	0.49243186	3.44597489	0.0022042
Zt55-IPO323	2.5081041	1.0313326	3.98487563	0.0000502
Zt74-IPO323	3.0945381	1.61776662	4.57130965	0.0000008
Zt80-IPO323	2.7117675	1.23499602	4.18853905	0.0000118
Zt92-IPO323	2.8210343	1.34426279	4.29780583	0.0000054
Zt10-L951	-1.2703023	-2.74707384	0.20646919	0.1494898
Zt114-L951	-1.0856924	-2.56246393	0.39107911	0.3348054
Zt116-L951	0.3058712	-1.17090032	1.78264272	0.9998325
Zt118-L951	-0.4535279	-1.93029938	1.02324365	0.9941461
Zt120-L951	0.4662593	-1.01051225	1.94303078	0.9926561
Zt36-L951	-1.4200721	-2.89684365	0.05669938	0.0686984
Zt55-L951	-0.8811714	-2.35794291	0.59560013	0.6372617
Zt74-L951	-0.2947374	-1.77150888	1.18203415	0.999883
Zt80-L951	-0.677508	-2.15427948	0.79926355	0.8974541
Zt92-L951	-0.5682412	-2.04501271	0.90853032	0.9669885
Zt114-Zt10	0.1846099	-1.2921616	1.66138143	0.999999
Zt116-Zt10	1.5761735	0.09940201	3.05294504	0.027913
Zt118-Zt10	0.8167745	-0.65999705	2.29354598	0.7334086

Comparison	Mean Difference	Lower Bound	Upper Bound	Padj
Zt120-Zt10	1.7365616	0.25979008	3.21333311	0.0102865
Zt36-Zt10	-0.1497698	-1.62654132	1.32700171	0.9999999
Zt55-Zt10	0.3891309	-1.08764058	1.86590245	0.9984292
Zt74-Zt10	0.975565	-0.50120655	2.45233648	0.4909093
Zt80-Zt10	0.5927944	-0.88397715	2.06956588	0.9558116
Zt92-Zt10	0.7020611	-0.77471038	2.17883265	0.8744014
Zt116-Zt114	1.3915636	-0.08520791	2.86833513	0.080234
Zt118-Zt114	0.6321645	-0.84460697	2.10893606	0.9326965
Zt120-Zt114	1.5519517	0.07518016	3.02872319	0.032264
Zt36-Zt114	-0.3343797	-1.81115124	1.14239179	0.9996084
Zt55-Zt114	0.204521	-1.2722505	1.68129254	0.9999971
Zt74-Zt114	0.790955	-0.68581647	2.26772656	0.7692799
Zt80-Zt114	0.4081844	-1.06858707	1.88495596	0.9976067
Zt92-Zt114	0.5174512	-0.9593203	1.99422273	0.9833483
Zt118-Zt116	-0.7593991	-2.23617058	0.71737245	0.8101745
Zt120-Zt116	0.1603881	-1.31638345	1.63715958	0.9999998
Zt36-Zt116	-1.7259433	-3.20271485	-0.24917182	0.0110099
Zt55-Zt116	-1.1870426	-2.66381411	0.28972893	0.2201155
Zt74-Zt116	-0.6006086	-2.07738008	0.87616295	0.9517499
Zt80-Zt116	-0.9833792	-2.46015068	0.49339235	0.47905
Zt92-Zt116	-0.8741124	-2.35088391	0.60265912	0.6481235
Zt120-Zt118	0.9197871	-0.55698439	2.39655864	0.5772292
Zt36-Zt118	-0.9665443	-2.44331579	0.51022725	0.5046965
Zt55-Zt118	-0.4276435	-1.90441504	1.04912799	0.9964248
Zt74-Zt118	0.1587905	-1.31798102	1.63556201	0.9999998
Zt80-Zt118	-0.2239801	-1.70075162	1.25279141	0.9999925
Zt92-Zt118	-0.1147133	-1.59148485	1.36205818	1
Zt36-Zt120	-1.8863314	-3.36310291	-0.40955988	0.0038541
Zt55-Zt120	-1.3474307	-2.82420217	0.12934086	0.1013749
Zt74-Zt120	-0.7609966	-2.23776815	0.71577488	0.8081911
Zt80-Zt120	-1.1437672	-2.62053875	0.33300428	0.2652239
Zt92-Zt120	-1.0345005	-2.51127197	0.44227106	0.4040227
Zt55-Zt36	0.5389007	-0.93787077	2.01567226	0.9774503
Zt74-Zt36	1.1253348	-0.35143675	2.60210628	0.2862063
Zt80-Zt36	0.7425642	-0.73420735	2.21933568	0.8304654
Zt92-Zt36	0.8518309	-0.62494058	2.32860245	0.681987
Zt74-Zt55	0.586434	-0.89033749	2.06320554	0.9589337
Zt80-Zt55	0.2036634	-1.27310809	1.68043494	0.9999972
Zt92-Zt55	0.3129302	-1.16384132	1.78970171	0.9997914

Comparison	Mean Difference	Lower Bound	Upper Bound	Padj
Zt80-Zt74	-0.3827706	-1.85954212	1.09400091	0.9986441
Zt92-Zt74	-0.2735038	-1.75027534	1.20326769	0.9999439
Zt92-Zt80	0.1092668	-1.36750474	1.58603829	1

Supplementary Table 6. One-way Analysis of Variance of the radius of zones of inhibition produced by *Pseudomonas* isolate BFB20 in confrontation with genetically diverse *Z. tritici* isolates in the blastospore antagonism assay *in vitro*.

	Df	Sum Sq	Mean Sq	*F* value	Pr(>*F*)	
Z. tritici genotype	11	11.846	1.0769	10.97	1.70E-08	***
Residuals	36	3.535	0.0982			

Significance codes: 0 '***' 0.001 '**' 0.01 '*' 0.05 '.' 0.1 ' ' 1

Supplementary Table 7. Tukey's test for multiple comparisons at the 5% level of significance, comparing zones of inhibition produced by *Pseudomonas* isolate BFB20 in confrontation with different *Z. tritici* genotypes *in vitro*.

Comparison	Mean Difference	Lower Bound	Upper Bound	Padj
L951-IPO323	0.87613032	0.10274959	1.649511048	0.0153963
Zt10-IPO323	1.27820922	0.50482849	2.051589949	0.0000812
Zt114-IPO323	1.11975177	0.34637104	1.893132502	0.0006879
Zt116-IPO323	0.12457004	-0.64881069	0.897950764	0.9999862
Zt118-IPO323	0.17792996	-0.59545076	0.951310693	0.9995452
Zt120-IPO323	0.67016844	-0.10321229	1.443549169	0.1427984
Zt36-IPO323	1.36719858	0.59381785	2.140579311	0.0000242
Zt55-IPO323	-0.10867021	-0.88205094	0.664710516	0.9999966
Zt74-IPO323	1.08843085	0.31505012	1.86181158	0.0010422
Zt80-IPO323	0.40976064	-0.36362009	1.183141367	0.78066
Zt92-IPO323	0.83261525	0.05923452	1.605995977	0.0256969
Zt10-L951	0.4020789	-0.37130183	1.175459629	0.7996747
Zt114-L951	0.24362145	-0.52975927	1.017002183	0.9927912
Zt116-L951	-0.75156028	-1.52494101	0.021820445	0.0632204
Zt118-L951	-0.69820035	-1.47158108	0.075180374	0.1091171
Zt120-L951	-0.20596188	-0.97934261	0.56741885	0.9982739
Zt36-L951	0.49106826	-0.28231247	1.264448991	0.5493102

Comparison	Mean Difference	Lower Bound	Upper Bound	Padj
Zt55-L951	-0.98480053	-1.75818126	-0.211419803	0.0040078
Zt74-L951	0.21230053	-0.5610802	0.985681261	0.9977461
Zt80-L951	-0.46636968	-1.23975041	0.307011048	0.6227831
Zt92-L951	-0.04351507	-0.8168958	0.729865658	1
Zt114-Zt10	-0.15845745	-0.93183818	0.614923282	0.9998491
Zt116-Zt10	-1.15363918	-1.92701991	-0.380258455	0.0004374
Zt118-Zt10	-1.10027926	-1.87365998	-0.326898526	0.000891
Zt120-Zt10	-0.60804078	-1.38142151	0.165339949	0.2465025
Zt36-Zt10	0.08898936	-0.68439137	0.862370091	0.9999996
Zt55-Zt10	-1.38687943	-2.16026016	-0.613498704	0.0000185
Zt74-Zt10	-0.18977837	-0.9631591	0.58360236	0.9991741
Zt80-Zt10	-0.86844858	-1.64182931	-0.095067853	0.0168749
Zt92-Zt10	-0.44559397	-1.2189747	0.327786757	0.6834417
Zt116-Zt114	-0.99518174	-1.76856247	-0.221801009	0.0035101
Zt118-Zt114	-0.94182181	-1.71520254	-0.16844108	0.0068922
Zt120-Zt114	-0.44958333	-1.22296406	0.323797396	0.6719591
Zt36-Zt114	0.24744681	-0.52593392	1.020827537	0.991822
Zt55-Zt114	-1.22842199	-2.00180271	-0.455041257	0.0001596
Zt74-Zt114	-0.03132092	-0.80470165	0.742059807	1
Zt80-Zt114	-0.70999114	-1.48337186	0.063389594	0.0970733
Zt92-Zt114	-0.28713653	-1.06051725	0.486244204	0.9744221
Zt118-Zt116	0.05335993	-0.7200208	0.826740658	1
Zt120-Zt116	0.5455984	-0.22778232	1.318979133	0.3937203
Zt36-Zt116	1.24262855	0.46924782	2.016009275	0.0001317
Zt55-Zt116	-0.23324025	-1.00662098	0.540140481	0.9949645
Zt74-Zt116	0.96386082	0.19048009	1.737241545	0.0052268
Zt80-Zt116	0.2851906	-0.48819013	1.058571332	0.9756552
Zt92-Zt116	0.70804521	-0.06533552	1.481425942	0.0989799
Zt120-Zt118	0.49223848	-0.28114225	1.265619204	0.545834
Zt36-Zt118	1.18926862	0.41588789	1.962649346	0.0002709
Zt55-Zt118	-0.28660018	-1.05998091	0.486780552	0.9747666
Zt74-Zt118	0.91050089	0.13712016	1.683881616	0.0101527
Zt80-Zt118	0.23183067	-0.54155006	1.005211403	0.9952131
Zt92-Zt118	0.65468528	-0.11869545	1.428066013	0.1647201
Zt36-Zt120	0.69703014	-0.07635059	1.470410871	0.1103778
Zt55-Zt120	-0.77883865	-1.55221938	-0.005457924	0.0471057
Zt74-Zt120	0.41826241	-0.35511832	1.19164314	0.7587653
Zt80-Zt120	-0.2604078	-1.03378853	0.512972927	0.9877408
Zt92-Zt120	0.16244681	-0.61093392	0.935827537	0.9998082

Comparison	Mean Difference	Lower Bound	Upper Bound	Padj
Zt55-Zt36	-1.47586879	-2.24924952	-0.702488066	0.0000055
Zt74-Zt36	-0.27876773	-1.05214846	0.494612998	0.9794097
Zt80-Zt36	-0.95743794	-1.73081867	-0.184057215	0.0056674
Zt92-Zt36	-0.53458333	-1.30796406	0.238797395	0.4236466
Zt74-Zt55	1.19710106	0.42372034	1.970481793	0.0002438
Zt80-Zt55	0.51843085	-0.25494988	1.29181158	0.4691538
Zt92-Zt55	0.94128546	0.16790473	1.71466619	0.0069385
Zt80-Zt74	-0.67867021	-1.45205094	0.094710516	0.1317931
Zt92-Zt74	-0.2558156	-1.02919633	0.517565126	0.9893376
Zt92-Zt80	0.42285461	-0.35052612	1.196235339	0.7465985

Supplementary Table 8. One-way Analysis of Variance of the radius of zones of inhibition produced by *Pseudomonas* isolate Roth 82 in confrontation with genetically diverse *Z. tritici* isolates in the blastospore antagonism assay *in vitro*.

	Df	Sum Sq	Mean Sq	*F* value	Pr(>*F*)	
Z. tritici genotype	11	20.65	1.8769	4.455	3.09E-04	***
Residuals	36	15.16	0.4213			

Significance codes: 0 '***' 0.001 '**' 0.01 '*' 0.05 '.' 0.1 ' ' 1

Supplementary Table 9. Tukey's test for multiple comparisons at the 5% level of significance, comparing zones of inhibition produced by *Pseudomonas* isolate Roth 82 in confrontation with different *Z. tritici* genotypes *in vitro*.

Comparison	Mean Difference	Lower Bound	Upper Bound	Padj
L951-IPO323	-1.930474289	-3.5323385	-0.3286101	0.0077849
Zt10-IPO323	-1.235944148	-2.8378084	0.3659201	0.2700704
Zt114-IPO323	-1.158492905	-2.7603571	0.4433713	0.357921
Zt116-IPO323	-2.043147161	-3.6450114	-0.441283	0.0039252
Zt118-IPO323	-2.58317819	-4.1850424	-0.981314	0.0001238
Zt120-IPO323	-1.4358289	-3.0376931	0.1660353	0.1145686
Zt36-IPO323	-2.016143615	-3.6180078	-0.4142794	0.004633
Zt55-IPO323	-1.930917553	-3.5327818	-0.3290533	0.0077643
Zt74-IPO323	-2.34201241	-3.9438766	-0.7401482	0.0005943
Zt80-IPO323	-2.011981383	-3.6138456	-0.4101172	0.0047525

Comparison	Mean Difference	Lower Bound	Upper Bound	Padj
Zt92-IPO323	-1.993377658	-3.5952419	-0.3915135	0.0053238
Zt10-L951	0.694530141	-0.9073341	2.2963943	0.927074
Zt114-L951	0.771981383	-0.8298828	2.3738456	0.8646035
Zt116-L951	-0.112672873	-1.7145371	1.4891913	1
Zt118-L951	-0.652703902	-2.2545681	0.9491603	0.9511446
Zt120-L951	0.494645388	-1.1072188	2.0965096	0.9938759
Zt36-L951	-0.085669326	-1.6875335	1.5161949	1
Zt55-L951	-0.000443265	-1.6023075	1.6014209	1
Zt74-L951	-0.411538121	-2.0134023	1.1903261	0.9987476
Zt80-L951	-0.081507095	-1.6833713	1.5203571	1
Zt92-L951	-0.062903369	-1.6647676	1.5389608	1
Zt114-Zt10	0.077451243	-1.524413	1.6793154	1
Zt116-Zt10	-0.807203013	-2.4090672	0.7946612	0.8285826
Zt118-Zt10	-1.347234042	-2.9490982	0.2546302	0.1711614
Zt120-Zt10	-0.199884753	-1.801749	1.4019795	0.999999
Zt36-Zt10	-0.780199467	-2.3820637	0.8216647	0.8566073
Zt55-Zt10	-0.694973405	-2.2968376	0.9068908	0.9267834
Zt74-Zt10	-1.106068262	-2.7079325	0.4957959	0.4252301
Zt80-Zt10	-0.776037235	-2.3779014	0.825827	0.860689
Zt92-Zt10	-0.75743351	-2.3592977	0.8444307	0.8781279
Zt116-Zt114	-0.884654256	-2.4865185	0.71721	0.7351242
Zt118-Zt114	-1.424685285	-3.0265495	0.1771789	0.1207081
Zt120-Zt114	-0.277335995	-1.8792002	1.3245282	0.9999713
Zt36-Zt114	-0.857650709	-2.4595149	0.7442135	0.7696577
Zt55-Zt114	-0.772424648	-2.3742889	0.8294396	0.8641787
Zt74-Zt114	-1.183519504	-2.7853837	0.4183447	0.3279098
Zt80-Zt114	-0.853488478	-2.4553527	0.7483757	0.7748113
Zt92-Zt114	-0.834884753	-2.436749	0.7669795	0.7972338
Zt118-Zt116	-0.540031029	-2.1418952	1.0618332	0.9876231
Zt120-Zt116	0.607318261	-0.9945459	2.2091825	0.9702701
Zt36-Zt116	0.027003547	-1.5748607	1.6288678	1
Zt55-Zt116	0.112229608	-1.4896346	1.7140938	1
Zt74-Zt116	-0.298865249	-1.9007295	1.302999	0.9999396
Zt80-Zt116	0.031165778	-1.5706984	1.63303	1
Zt92-Zt116	0.049769503	-1.5520947	1.6516337	1
Zt120-Zt118	1.14734929	-0.4545149	2.7492135	0.3717485
Zt36-Zt118	0.567034576	-1.0348296	2.1688988	0.9820156
Zt55-Zt118	0.652260637	-0.9496036	2.2541248	0.9513652
Zt74-Zt118	0.241165781	-1.3606984	1.84303	0.9999931
Zt80-Zt118	0.571196807	-1.0306674	2.173061	0.9810012

Comparison	Mean Difference	Lower Bound	Upper Bound	Padj
Zt92-Zt118	0.589800532	-1.0120637	2.1916647	0.9759244
Zt36-Zt120	-0.580314714	-2.1821789	1.0215495	0.9786267
Zt55-Zt120	-0.495088653	-2.0969529	1.1067756	0.9938306
Zt74-Zt120	-0.906183509	-2.5080477	0.6956807	0.7063957
Zt80-Zt120	-0.576152483	-2.1780167	1.0257117	0.9797371
Zt92-Zt120	-0.557548758	-2.159413	1.0443154	0.9841718
Zt55-Zt36	0.085226062	-1.5166381	1.6870903	1
Zt74-Zt36	-0.325868795	-1.927733	1.2759954	0.9998592
Zt80-Zt36	0.004162232	-1.597702	1.6060264	1
Zt92-Zt36	0.022765957	-1.5790983	1.6246302	1
Zt74-Zt55	-0.411094857	-2.0129591	1.1907694	0.9987597
Zt80-Zt55	-0.08106383	-1.682928	1.5208004	1
Zt92-Zt55	-0.062460105	-1.6643243	1.5394041	1
Zt80-Zt74	0.330031027	-1.2718332	1.9318952	0.9998408
Zt92-Zt74	0.348634752	-1.2532295	1.950499	0.9997307
Zt92-Zt80	0.018603725	-1.5832605	1.6204679	1

Supplementary Table 10. One-way Analysis of Variance of the radius of zones of inhibition produced by *Pseudomonas* isolate Roth 107 in confrontation with genetically diverse *Z. tritici* isolates in the blastospore antagonism assay *in vitro*.

	Df	Sum Sq	Mean Sq	*F* value	Pr(>*F*)	
Z. tritici genotype	11	23.32	2.1203	5.567	3.94E-05	***
Residuals	36	13.71	0.3809			

Significance codes: 0 '***' 0.001 '**' 0.01 '*' 0.05 '.' 0.1 ' ' 1

Supplementary Table 11. Tukey's test for multiple comparisons at the 5% level of significance, comparing zones of inhibition produced by *Pseudomonas* isolate Roth 107 in confrontation with different *Z. tritici* genotypes *in vitro*.

Comparison	Mean Difference	Lower Bound	Upper Bound	Padj
L951-IPO323	-0.27970745	-1.802888542	1.24347365	0.9999484
Zt10-IPO323	-0.76655142	-2.289732514	0.75662968	0.8297251
Zt114-IPO323	1.24400709	-0.279174005	2.76718819	0.2020985
Zt116-IPO323	-1.09820035	-2.62138145	0.42498074	0.3623116

Comparison	Mean Difference	Lower Bound	Upper Bound	Padj
Zt118-IPO323	0.54451241	-0.978668684	2.06769351	0.9806394
Zt120-IPO323	0.25153369	-1.271647407	1.77471478	0.9999822
Zt36-IPO323	-1.18480496	-2.70798606	0.33837613	0.2597812
Zt55-IPO323	0.69613918	-0.827041911	2.21932028	0.8997142
Zt74-IPO323	0.09932181	-1.423859286	1.62250291	1
Zt80-IPO323	-0.25952571	-1.782706805	1.26365539	0.9999756
Zt92-IPO323	0.31906472	-1.204116379	1.84224581	0.9998132
Zt10-L951	-0.48684397	-2.010025068	1.03633712	0.99189
Zt114-L951	1.52371454	0.000533441	3.04689563	0.0498527
Zt116-L951	-0.81849291	-2.341674005	0.70468819	0.7657594
Zt118-L951	0.82421986	-0.698961238	2.34740095	0.7581682
Zt120-L951	0.53124113	-0.991939962	2.05442223	0.983925
Zt36-L951	-0.90509752	-2.428278614	0.61808358	0.6428864
Zt55-L951	0.97584663	-0.547334466	2.49902773	0.5362282
Zt74-L951	0.37902926	-1.144151841	1.90221035	0.9990618
Zt80-L951	0.02018174	-1.50299936	1.54336283	1
Zt92-L951	0.59877216	-0.924408933	2.12195326	0.9616884
Zt114-Zt10	2.01055851	0.487377413	3.53373961	0.0025229
Zt116-Zt10	-0.33164894	-1.854830033	1.19153216	0.9997296
Zt118-Zt10	1.31106383	-0.212117266	2.83424493	0.1488991
Zt120-Zt10	1.01808511	-0.50509599	2.5412662	0.4734858
Zt36-Zt10	-0.41825355	-1.941434642	1.10492755	0.9977402
Zt55-Zt10	1.4626906	-0.060490494	2.9858717	0.0694378
Zt74-Zt10	0.86587323	-0.657307869	2.38905432	0.7003882
Zt80-Zt10	0.50702571	-1.016155388	2.0302068	0.9887936
Zt92-Zt10	1.08561613	-0.437564962	2.60879723	0.3788678
Zt116-Zt114	-2.34220745	-3.865388542	-0.81902635	0.0002711
Zt118-Zt114	-0.69949468	-2.222675775	0.82368642	0.8968586
Zt120-Zt114	-0.9924734	-2.515654499	0.53070769	0.511317
Zt36-Zt114	-2.42881206	-3.951993151	-0.90563096	0.0001496
Zt55-Zt114	-0.54786791	-2.071049003	0.97531319	0.9797327
Zt74-Zt114	-1.14468528	-2.667866378	0.37849581	0.304686
Zt80-Zt114	-1.5035328	-3.026713897	0.0196483	0.0557038
Zt92-Zt114	-0.92494237	-2.448123471	0.59823872	0.6131166
Zt118-Zt116	1.64271277	0.119531671	3.16589386	0.0252676
Zt120-Zt116	1.34973404	-0.173447053	2.87291514	0.1236805
Zt36-Zt116	-0.08660461	-1.609785705	1.43657649	1
Zt55-Zt116	1.79433954	0.271158443	3.31752064	0.0100835
Zt74-Zt116	1.19752216	-0.325658932	2.72070326	0.2465233
Zt80-Zt116	0.83867465	-0.684506451	2.36185574	0.7385999
Zt92-Zt116	1.41726507	-0.105916025	2.94044617	0.0881062

Comparison	Mean Difference	Lower Bound	Upper Bound	Padj
Zt120-Zt118	-0.29297872	-1.81615982	1.23020237	0.9999185
Zt36-Zt118	-1.72931738	-3.252498472	-0.20613628	0.0150473
Zt55-Zt118	0.15162677	-1.371554324	1.67480787	0.9999999
Zt74-Zt118	-0.4451906	-1.968371699	1.07799049	0.9961317
Zt80-Zt118	-0.80403812	-2.327219218	0.71914297	0.7844774
Zt92-Zt118	-0.2254477	-1.748628791	1.2977334	0.9999942
Zt36-Zt120	-1.43633865	-2.959519748	0.08684244	0.0797977
Zt55-Zt120	0.4446055	-1.0785756	1.96778659	0.9961746
Zt74-Zt120	-0.15221188	-1.675392975	1.37096922	0.9999999
Zt80-Zt120	-0.5110594	-2.034240494	1.0121217	0.9880756
Zt92-Zt120	0.06753103	-1.455650068	1.59071212	1
Zt55-Zt36	1.88094415	0.357763052	3.40412524	0.0058415
Zt74-Zt36	1.28412677	-0.239054323	2.80730787	0.1687723
Zt80-Zt36	0.92527925	-0.597901842	2.44846035	0.6126089
Zt92-Zt36	1.50386968	-0.019311416	3.02705078	0.0556013
Zt74-Zt55	-0.59681737	-2.119998471	0.92636372	0.9625435
Zt80-Zt55	-0.95566489	-2.47884599	0.5675162	0.5666825
Zt92-Zt55	-0.37707447	-1.900255564	1.14610663	0.999105
Zt80-Zt74	-0.35884752	-1.882028615	1.16433358	0.9994327
Zt92-Zt74	0.21974291	-1.303438189	1.742924	0.9999955
Zt92-Zt80	0.57859043	-0.94459067	2.10177152	0.9698637

Supplementary Table 12. One-way Analysis of Variance of the radius of zones of inhibition produced by *Pseudomonas* isolate Roth 112 in confrontation with genetically diverse *Z. tritici* isolates in the blastospore antagonism assay *in vitro*.

	Df	Sum Sq	Mean Sq	*F* value	Pr(>*F*)	
Z. tritici genotype	11	63.63	5.785	8.11	6.92E-07	***
Residuals	36	25.68	0.713			

Significance codes: 0 '***' 0.001 '**' 0.01 '*' 0.05 '.' 0.1 ' ' 1

Supplementary Table 13. Tukey's test for multiple comparisons at the 5% level of significance, comparing zones of inhibition produced by *Pseudomonas* isolate Roth 112 in confrontation with different *Z. tritici* genotypes *in vitro*.

Comparison	Mean Difference	Lower Bound	Upper Bound	Padj
L951-IPO323	0.663989363	-1.4203954	2.7483741	0.9921064
Zt10-IPO323	-1.180443262	-3.264828	0.9039415	0.7050454
Zt114-IPO323	1.284955675	-0.7994291	3.3693404	0.5919036
Zt116-IPO323	-1.653439715	-3.7378245	0.4309451	0.2356942
Zt118-IPO323	1.950270389	-0.1341144	4.0346552	0.0845742
Zt120-IPO323	0.671023937	-1.4133608	2.7554087	0.9914071
Zt36-IPO323	-1.308847517	-3.3932323	0.7755373	0.5654938
Zt55-IPO323	-1.004388298	-3.0887731	1.0799965	0.8647011
Zt74-IPO323	-1.6191578	-3.7035426	0.465227	0.2614746
Zt80-IPO323	-1.004104609	-3.0884894	1.0802802	0.8649097
Zt92-IPO323	-0.415172872	-2.4995576	1.6692119	0.9998853
Zt10-L951	-1.844432625	-3.9288174	0.2399521	0.1248323
Zt114-L951	0.620966312	-1.4634185	2.7053511	0.9954551
Zt116-L951	-2.317429078	-4.4018138	-0.2330443	0.0186877
Zt118-L951	1.286281026	-0.7981037	3.3706658	0.5904391
Zt120-L951	0.007034574	-2.0773502	2.0914193	1
Zt36-L951	-1.97283688	-4.0572217	0.1115479	0.0776012
Zt55-L951	-1.668377661	-3.7527624	0.4160071	0.2250374
Zt74-L951	-2.283147163	-4.3675319	-0.1987624	0.0217046
Zt80-L951	-1.668093972	-3.7524787	0.4162908	0.2252366
Zt92-L951	-1.079162235	-3.163547	1.0052225	0.8037089
Zt114-Zt10	2.465398937	0.3810142	4.5497837	0.0096369
Zt116-Zt10	-0.472996453	-2.5573812	1.6113883	0.9996003
Zt118-Zt10	3.130713651	1.0463289	5.2150984	0.0003931
Zt120-Zt10	1.851467199	-0.2329176	3.935852	0.1217361
Zt36-Zt10	-0.128404255	-2.212789	1.9559805	1
Zt55-Zt10	0.176054964	-1.9083298	2.2604397	1
Zt74-Zt10	-0.438714539	-2.5230993	1.6456702	0.9998044
Zt80-Zt10	0.176338653	-1.9080461	2.2607234	1
Zt92-Zt10	0.76527039	-1.3191144	2.8496552	0.9764222
Zt116-Zt114	-2.93839539	-5.0227802	-0.8540106	0.0010174
Zt118-Zt114	0.665314714	-1.4190701	2.7496995	0.9919783
Zt120-Zt114	-0.613931738	-2.6983165	1.470453	0.9958709
Zt36-Zt114	-2.593803192	-4.678188	-0.5094184	0.0053245
Zt55-Zt114	-2.289343972	-4.3737287	-0.2049592	0.0211277
Zt74-Zt114	-2.904113475	-4.9884982	-0.8197287	0.0012034
Zt80-Zt114	-2.289060284	-4.3734451	-0.2046755	0.0211538
Zt92-Zt114	-1.700128547	-3.7845133	0.3842562	0.2035446

Comparison	Mean Difference	Lower Bound	Upper Bound	Padj
Zt118-Zt116	3.603710104	1.5193253	5.6880949	0.0000364
Zt120-Zt116	2.324463652	0.2400789	4.4088484	0.0181192
Zt36-Zt116	0.344592198	-1.7397926	2.428977	0.999982
Zt55-Zt116	0.649051418	-1.4353334	2.7334362	0.9934405
Zt74-Zt116	0.034281915	-2.0501029	2.1186667	1
Zt80-Zt116	0.649335106	-1.4350497	2.7337199	0.993417
Zt92-Zt116	1.238266843	-0.8461179	3.3226516	0.6432205
Zt120-Zt118	-1.279246452	-3.3636312	0.8051383	0.59821
Zt36-Zt118	-3.259117906	-5.3435027	-1.1747331	0.0002069
Zt55-Zt118	-2.954658687	-5.0390435	-0.8702739	0.0009394
Zt74-Zt118	-3.569428189	-5.653813	-1.4850434	0.0000433
Zt80-Zt118	-2.954374998	-5.0387598	-0.8699902	0.0009407
Zt92-Zt118	-2.365443261	-4.449828	-0.2810585	0.0151161
Zt36-Zt120	-1.979871454	-4.0642562	0.1045133	0.0755318
Zt55-Zt120	-1.675412234	-3.759797	0.4089725	0.22014
Zt74-Zt120	-2.290181737	-4.3745665	-0.205797	0.0210509
Zt80-Zt120	-1.675128546	-3.7595133	0.4092562	0.220336
Zt92-Zt120	-1.086196809	-3.1705816	0.998188	0.7973926
Zt55-Zt36	0.30445922	-1.7799256	2.388844	0.9999949
Zt74-Zt36	-0.310310283	-2.3946951	1.7740745	0.9999938
Zt80-Zt36	0.304742908	-1.7796419	2.3891277	0.9999949
Zt92-Zt36	0.893674645	-1.1907101	2.9780594	0.9320226
Zt74-Zt55	-0.614769503	-2.6991543	1.4696153	0.9958231
Zt80-Zt55	0.000283689	-2.0841011	2.0846685	1
Zt92-Zt55	0.589215426	-1.4951693	2.6736002	0.9970924
Zt80-Zt74	0.615053192	-1.4693316	2.699438	0.9958068
Zt92-Zt74	1.203984928	-0.8803998	3.2883697	0.6802073
Zt92-Zt80	0.588931737	-1.495453	2.6733165	0.9971044

Supplementary Table 14. Sequencing depth of coverage.
Sequencing depth of coverage and mapping percentage.

***Pseudomonas* isolate**	**Treatment condition**	**Replicate**	**Depth of coverage (x coverage)**	**% of total reads mapping (%)**
Roth 16	Control	1	514.793	97
Roth 16	Control	2	495.671	97.4
Roth 16	Control	3	350.299	96.5
Roth 16	*Z. tritici* confrontation	1	185.106	48
Roth 16	*Z. tritici* confrontation	2	233.362	40.7
Roth 16	*Z. tritici* confrontation	3	232.901	51.9
Roth 105	Control	1	492.41	96.1
Roth 105	Control	2	538.097	96.3
Roth 105	Control	3	547.272	96
Roth 105	*Z. tritici* confrontation	1	313.329	56.6
Roth 105	*Z. tritici* confrontation	2	244.943	52.4
Roth 105	*Z. tritici* confrontation	3	197.238	39.2

Supplementary Table 15. A table indicating the log2fold change and Benjamini-Hochberg adjusted p-values from differential expression analysis for genes within Roth 16 predicted secondary metabolite BGCs.
Benjamini-Hochberg adjusted p-values were used to determine significantly differentially expressed genes between *Z. tritici* confrontation treatment and control (Padj < 0.05).

Genetic locus	baseMean	log2FoldChange	lfcSE	stat	pvalue	Padj
drrA_1	1500.824988	7.234101142	0.280609721	25.77993776	1.4888E-146	8.6467E-143
pchR_1	3834.848307	4.760294481	0.19761736	24.08844279	3.3039E-128	6.3964E-125
fyuA_2	1631.665461	5.233092285	0.241592278	21.6608425	4.8037E-104	4.65E-101
11751wH2_Roth16_03930	3445.710633	5.682625402	0.282029798	20.14902481	2.74467E-90	2.2773E-87
irtA	661.4466723	4.635350078	0.269423079	17.20472536	2.44734E-66	1.42142E-63
11751wH2_Roth16_03924	450.2888403	4.972559262	0.290229909	17.13317305	8.39487E-66	4.43249E-63
dhbE	401.1811044	3.889923263	0.231065344	16.83473251	1.35801E-63	6.06716E-61
pksR	395.5335122	4.455451143	0.270280044	16.48457312	4.73628E-61	1.96488E-58
irtB	770.6175297	5.2230089	0.325555541	16.04337276	6.36043E-58	2.30883E-55
pksM	385.9850135	4.251050001	0.278656278	15.25553283	1.51255E-52	4.62363E-50
mbtB_2	2755.53078	4.718511937	0.316231331	14.92107666	2.40363E-50	6.98015E-48
mbtB_1	1538.958466	4.046138692	0.273559615	14.79070182	1.68191E-49	4.44024E-47
mycG	118.0533418	4.312174385	0.348308936	12.38031511	3.34029E-35	7.18533E-33
fyuA_3	763.8328636	3.077341099	0.313140463	9.827350546	8.58475E-23	1.34757E-20
pchB	82.15009502	3.11805298	0.317858012	9.809578067	1.02396E-22	1.52491E-20
pikAV	230.3102196	2.496039197	0.306527313	8.142958521	3.85734E-16	3.7972E-14
11751wH2_Roth16_03919	102.6402291	3.323707452	0.414774009	8.013297317	1.11673E-15	1.02952E-13
11751wH2_Roth16_05547	1268.960046	1.751131128	0.218873554	8.000651961	1.23762E-15	1.12314E-13
hflK_3	1396.793727	1.957819481	0.249459906	7.848233068	4.2194E-15	3.55163E-13
zosA	3127.904596	2.285699444	0.293541901	7.786620707	6.88252E-15	5.66338E-13
11751wH2_Roth16_03920	189.2218047	2.506282595	0.321901192	7.785875466	6.92321E-15	5.66338E-13

Genetic locus	baseMean	log2FoldChange	lfcSE	stat	pvalue	Padj
11751wH2_Roth16_05544	222.8494641	1.321270991	0.250654409	5.271285652	1.35471E-07	6.00625E-06
11751wH2_Roth16_05542	220.2713959	1.252234058	0.241183261	5.192043815	2.07998E-07	8.69103E-06
11751wH2_Roth16_02067	411.1104495	-1.02387674	0.22668065	-4.516824621	6.27739E-06	0.000206281
emrA_2	58.51616996	-1.465185102	0.330573786	-4.432248307	9.32555E-06	0.000292772
11751wH2_Roth16_00339	1345.99902	-1.769523871	0.440588056	-4.01627744	5.91246E-05	0.001553828
11751wH2_Roth16_05541	1117.955699	-0.920000382	0.229326606	-4.011747258	6.0271E-05	0.00157682
11751wH2_Roth16_00329	1948.567849	-1.154538556	0.293930852	-3.927925728	8.56817E-05	0.002078423
asnB_1	961.7382091	-1.093212723	0.292991883	-3.731204813	0.000190566	0.00411453
cphA	1084.723559	-1.263827562	0.348405263	-3.627464042	0.000286219	0.005852289
11751wH2_Roth16_00340	885.4696025	-1.764208974	0.492530654	-3.581927258	0.000341069	0.006783998
accA1_1	1576.422212	-1.640969146	0.479938823	-3.419121498	0.000628237	0.011227073
polC_1	635.1283548	-0.688279221	0.20204534	-3.406558253	0.000657875	0.011613795
ephD_1	367.4829044	-1.035971852	0.31861931	-3.251440886	0.001148217	0.018121852
11751wH2_Roth16_03914	564.0217574	-0.883624829	0.272739397	-3.239813674	0.001196078	0.018774016
11751wH2_Roth16_02111	54.17465882	1.211092421	0.381540866	3.17421416	0.001502428	0.02260648
11751wH2_Roth16_05543	192.3196254	0.739003066	0.234319776	3.153822867	0.001611469	0.023634873
pepA_1	797.1231042	-1.337927044	0.428295643	-3.123839961	0.001785075	0.025236233
ribZ_1	1280.373619	-0.850068525	0.277711099	-3.060981456	0.002206128	0.03014868
parE1_3	340.0419473	0.639974573	0.210793853	3.036021041	0.002397226	0.032304155
yegS	1301.649971	-0.570930022	0.1886289	-3.02673675	0.002472091	0.033006683
mmgC_1	559.4741988	-1.293588989	0.436194852	-2.965621859	0.003020716	0.039074212
bbsG	1093.130782	-0.840854989	0.289554285	-2.903963203	0.003684715	0.045826173
pcpR_1	663.1725162	-0.606917752	0.208981991	-2.904162931	0.003682365	0.045826173
11751wH2_Roth16_00274	1239.86199	-0.85174525	0.302296155	-2.817585456	0.004838624	0.057235695
11751wH2_Roth16_02065	1337.640589	-1.255300992	0.465335411	-2.69762619	0.006983581	0.072966686

Genetic locus	baseMean	log2FoldChange	lfcSE	stat	pvalue	Padj
gltD	999.221077	0.581743108	0.217060069	2.680101914	0.007359975	0.076053466
fadD3	301.9783746	-1.001323553	0.373826002	-2.678581875	0.007393465	0.076136963
mepC_4	5734.327417	0.558861205	0.230981247	2.419508997	0.015541476	0.130629369
pchA	580.8428165	0.458547132	0.194977512	2.351794965	0.01868307	0.150084746
yceJ_1	201.7048285	-0.577225567	0.247964107	-2.32785936	0.019919573	0.156978126
cueR_1	322.4143284	-0.757447195	0.331171808	-2.287172933	0.022185731	0.168275662
virF_2	441.9090172	0.707194992	0.310575889	2.277044088	0.022783593	0.171408171
lgrD_3	718.5237498	0.469762569	0.20879713	2.249851659	0.024458363	0.178909541
tamA	1220.472454	-0.43891516	0.203353444	-2.158385669	0.030897859	0.206033026
liuE_1	1299.514016	-0.617777171	0.287054991	-2.152121333	0.031387799	0.208105409
11751wH2_Roth16_02139	1164.546509	0.549340211	0.277465031	1.979853851	0.047719953	0.275369384
bdhA_2	185.3272207	-0.5816154	0.294202126	-1.976924529	0.048050162	0.276860455
11751wH2_Roth16_04439	184.7109754	0.50671579	0.259299611	1.954171039	0.050680993	0.287060775
cheV_2	2940.956254	0.526356932	0.271073574	1.941749337	0.052167453	0.291615559
tycC_1	432.1902705	0.522766047	0.29164704	1.792461349	0.073059095	0.353836804
11751wH2_Roth16_05357	99.87809911	-0.57922129	0.323877266	-1.78839749	0.073711901	0.356468544
ygbM	99.26010882	0.638645787	0.362970815	1.75949625	0.078493257	0.371244979
emrY	65.07983443	-0.531190513	0.303952475	-1.747610422	0.080531509	0.374851077
puuB_7	114.4648799	-0.516529801	0.295862634	-1.745843315	0.080838182	0.375306283
yfeX_1	150.4794258	-0.400498022	0.229727299	-1.743362777	0.081270266	0.375403635
purN_2	215.2227091	0.417333956	0.239272068	1.744181673	0.081127416	0.375403635
11751wH2_Roth16_01512	95.04866539	0.478308315	0.274211939	1.744301568	0.081106518	0.375403635
gltB	3899.47581	0.405532449	0.236012303	1.718268258	0.085747696	0.385466424
ynfM_1	360.1141085	0.514074666	0.308457277	1.666599244	0.095594119	0.411572012
11751wH2_Roth16_00264	677.9314014	-0.477425082	0.288941894	-1.652322117	0.098468903	0.41836678

Genetic locus	baseMean	log2FoldChange	lfcSE	stat	pvalue	Padj
qseB_1	841.3499242	-0.533568636	0.330886593	-1.612542327	0.106843977	0.437927595
idi	284.1548027	0.386389129	0.243556075	1.586448333	0.112637644	0.450240492
11751wH2_Roth16_00343	560.5844025	-0.370285293	0.238055707	-1.555456486	0.11983739	0.465562249
araF_2	80.7438751	-0.564852892	0.366019998	-1.543229591	0.12277508	0.470057788
11751wH2_Roth16_05137	510.3896782	-0.564402161	0.372573215	-1.514875838	0.12980385	0.487961659
11751wH2_Roth16_00270	21.88425231	-0.645928717	0.429149061	-1.505138366	0.132288507	0.492204771
mro	242.0065971	0.454161333	0.305315981	1.487512483	0.136879509	0.503623887
ttuB_2	73.7434174	0.566637424	0.381363081	1.485821393	0.13732637	0.504157306
lgrB_1	7.338427651	-1.033599364	0.701896821	-1.472580205	0.140864266	0.512618831
11751wH2_Roth16_01527	333.6213643	-0.390280574	0.26539962	-1.470539312	0.141415747	0.513339161
amnD_3	135.5310434	0.529376232	0.363239545	1.457375001	0.145012894	0.520497958
11751wH2_Roth16_05130	111.4805323	0.365389827	0.255130623	1.43216766	0.152095845	0.530366023
betB_2	132.7262397	0.461299681	0.323002412	1.428161721	0.153245316	0.533602394
11751wH2_Roth16_05120	223.6915453	-0.364594115	0.256659188	-1.420537946	0.155451129	0.539020991
ltaS1	2271.979259	0.273175977	0.193470217	1.411979479	0.157956003	0.54086222
lgrE	140.8261482	0.449448984	0.31827456	1.412142343	0.157908053	0.54086222
lgrD_1	496.0683739	0.426229125	0.310414438	1.373096971	0.169722203	0.558496631
11751wH2_Roth16_01514	125.1368159	0.470491829	0.343642592	1.369131302	0.170958235	0.560753142
11751wH2_Roth16_02062	122.6080666	-0.451974535	0.329962639	-1.369774882	0.170757185	0.560753142
damX	4666.033317	-0.31318614	0.232334213	-1.34799837	0.177658907	0.572292252
tauD_2	289.5703517	0.294438888	0.219491715	1.341457868	0.17977184	0.57495311
aroK	1315.732317	0.375699327	0.280803316	1.337944769	0.180914442	0.57797089
hpcD	34.65192957	0.506825077	0.38376555	1.3206633	0.186613656	0.585443271
11751wH2_Roth16_03944	892.9653296	0.314922998	0.240140093	1.311413659	0.189718047	0.589646764
mcpA	2527.774228	0.256708344	0.196978171	1.303232445	0.192495417	0.59335698

Genetic locus	baseMean	log2FoldChange	lfcSE	stat	pvalue	Padj
yfiH_1	489.8096672	0.328680436	0.263307699	1.248275068	0.211930341	0.620408983
11751wH2_Roth16_03844	77.53855905	0.34256735	0.276170184	1.240421199	0.214819644	0.625399746
11751wH2_Roth16_04435	68.90404067	0.38082466	0.310470367	1.226605503	0.2199709	0.635617407
fadH_2	133.3746613	-0.310769141	0.255982932	-1.2140229	0.22473898	0.643666735
11751wH2_Roth16_03836	578.8284415	0.426114792	0.35242972	1.209077352	0.226633129	0.645551844
tycC_2	999.6171459	0.266882471	0.224573973	1.188394487	0.234678027	0.654884195
11751wH2_Roth16_03845	72.17298583	0.366771373	0.310379777	1.181685795	0.237330397	0.656700783
pstS_1	1508.564581	0.306909318	0.260077755	1.180067545	0.237973351	0.657540069
araG_3	121.119284	-0.292240192	0.250401131	-1.167088146	0.243174774	0.661041008
rhtC_2	517.8381973	0.258102239	0.221691097	1.164242688	0.244325675	0.661381358
lgrB_2	624.6270898	0.229755238	0.200988112	1.143128493	0.252985246	0.673409209
11751wH2_Roth16_03843	175.4391401	-0.286502028	0.251851799	-1.137581818	0.255295142	0.675822327
gcvA_6	170.5234194	-0.282473919	0.249144481	-1.133775543	0.256888713	0.677878075
mepC_3	784.9660802	0.414524056	0.3727056	1.112202382	0.266051144	0.684518059
yfcG_3	145.9341787	0.309327884	0.280117601	1.104278639	0.269472286	0.687761777
11751wH2_Roth16_05129	127.4265533	0.262454055	0.239673622	1.095047729	0.273495727	0.690781913
11751wH2_Roth16_01543	243.1503006	0.262831775	0.239979963	1.095223833	0.273418587	0.690781913
11751wH2_Roth16_00269	90.30272389	0.282313337	0.26373738	1.070433537	0.28442421	0.705051564
11751wH2_Roth16_02138	1885.797438	-0.248838803	0.232929048	-1.06830301	0.285383851	0.705923939
degS_2	185.820977	0.26191833	0.245369488	1.067444581	0.285771126	0.706173037
pccB	205.6770688	-0.306709088	0.29363756	-1.044515859	0.296246786	0.714945099
11751wH2_Roth16_04300	100.3202426	0.357815613	0.347169072	1.030666732	0.302697131	0.719633621
pobA_1	803.6943601	-0.244361319	0.238508158	-1.024540717	0.305579949	0.721466807
11751wH2_Roth16_05356	184.2023159	-0.374166724	0.368674264	-1.014897867	0.310154515	0.722907546
hrcN	139.209002	0.293675383	0.29102831	1.009095586	0.312928795	0.723370868

Genetic locus	baseMean	log2FoldChange	lfcSE	stat	pvalue	Padj
11751wH2_Roth16_05370	3015.680289	0.287218289	0.28493405	1.008016731	0.31344643	0.72374506
fpvA_7	225.0542605	0.241625123	0.240366468	1.005236401	0.314783031	0.724853627
gntR_4	448.8249587	-0.225519718	0.22578908	-0.998807021	0.317888184	0.72832133
11751wH2_Roth16_01521	140.4845964	0.309105939	0.310721892	0.99479936	0.319833858	0.729566728
rclR_6	135.6929552	0.243240278	0.246189032	0.988022401	0.323141677	0.729768871
ppm1	139.1268295	0.239812206	0.243049927	0.986678783	0.323800134	0.729768871
11751wH2_Roth16_01509	1025.114303	-0.197520492	0.200719482	-0.984062386	0.32508484	0.7315386
lgrD_2	425.2493703	0.238094742	0.243271336	0.978720907	0.327717899	0.732736015
hutH_2	596.0445062	-0.187597207	0.191994035	-0.977099141	0.328520073	0.732736015
11751wH2_Roth16_03829	1099.937153	0.31588761	0.329965668	0.95733478	0.338398306	0.742507503
cynT_1	39.62370578	-0.324775438	0.339953834	-0.955351598	0.339399922	0.743862169
11751wH2_Roth16_00344	789.5183285	-0.224663461	0.246647427	-0.91086886	0.362364475	0.763679606
11751wH2_Roth16_04436	29.40057167	-0.408891545	0.452516294	-0.903595186	0.366210095	0.766179168
yghU	1916.148174	0.216487286	0.24343141	0.889315336	0.373833632	0.771621094
11751wH2_Roth16_01533	326.1069195	0.181330738	0.204790553	0.885444835	0.37591676	0.772584764
11751wH2_Roth16_01544	1554.408381	0.227345093	0.257151084	0.884091522	0.376646809	0.773064977
nepI_3	101.5078283	0.309389144	0.353573966	0.875033725	0.381555556	0.776055207
cirA_2	94.08471464	0.335184039	0.384205503	0.872408221	0.382985717	0.777066018
11751wH2_Roth16_02129	1803.812523	-0.21101373	0.247831802	-0.851439276	0.394525382	0.789119044
fadB_2	128.463272	-0.213049233	0.253802554	-0.839429036	0.401228596	0.79524067
iolX_2	44.88262986	0.260117215	0.31133776	0.835482385	0.403446161	0.796741007
11751wH2_Roth16_00425	82.96519646	-0.219264918	0.262640537	-0.834847968	0.403803314	0.797175271
11751wH2_Roth16_04424	94.73041503	-0.238755012	0.286663536	-0.832875416	0.404914996	0.797756717
dat_1	106.4717579	0.239486086	0.288925793	0.828884411	0.407169817	0.79974376
fecI_11	146.7522381	-0.311167793	0.39124007	-0.795337228	0.426417364	0.814949671

Genetic locus	baseMean	log2FoldChange	lfcSE	stat	pvalue	Padj
11751wH2_Roth16_00336	551.7410178	-0.200648897	0.254430238	-0.788620483	0.430333855	0.817339437
ssaV	405.4258037	0.195440269	0.248342044	0.786980189	0.431293463	0.817810132
11751wH2_Roth16_02131	421.6244682	0.192262082	0.244456724	0.78648719	0.431582121	0.817823477
11751wH2_Roth16_00272	48.72040526	-0.278108934	0.356432079	-0.780257869	0.435239106	0.820517723
proC_3	101.4495361	-0.269501117	0.347725387	-0.775040097	0.438315967	0.821535551
bacC_2	335.9053966	0.161726787	0.210176846	0.769479561	0.441608674	0.823518646
11751wH2_Roth16_00271	69.50342527	-0.216632227	0.28727941	-0.754081983	0.450799995	0.826529398
C1-hpah_1	132.5353155	0.216222415	0.28688003	0.753703261	0.451027423	0.826529398
araC_1	100.0461164	0.22098992	0.294050011	0.751538552	0.452328608	0.826529398
11751wH2_Roth16_04422	109.4194001	0.224320581	0.29600031	0.757839004	0.448547369	0.826529398
higA	143.5549702	0.195341098	0.260097304	0.751030843	0.452634094	0.826529398
11751wH2_Roth16_01528	116.5478875	-0.224757784	0.297466932	-0.755572333	0.449905649	0.826529398
11751wH2_Roth16_00433	14.38632513	0.42760774	0.581912797	0.734831306	0.462442238	0.832052206
11751wH2_Roth16_03824	273.1496868	0.211212978	0.290376915	0.727375238	0.466996119	0.835843902
fecI_4	594.7413551	0.16520205	0.227873275	0.724973342	0.468468385	0.837412102
11751wH2_Roth16_03820	38.93539941	-0.343269847	0.48477499	-0.708101396	0.478882293	0.841831106
11751wH2_Roth16_04302	11.21885018	-0.405953212	0.573847885	-0.707423035	0.479303626	0.841831106
fabF_1	473.6090877	-0.172225642	0.242451456	-0.71035103	0.477486482	0.841831106
11751wH2_Roth16_03838	100.6611278	0.222677226	0.316188842	0.704253904	0.481274667	0.842521739
aroB	2840.86695	-0.142725656	0.203774388	-0.70041018	0.483671181	0.843592257
yibF_1	458.7349257	-0.269461919	0.396573475	-0.679475395	0.496836692	0.854494376
11751wH2_Roth16_04305	319.1814665	-0.148835423	0.221299752	-0.672551242	0.50123283	0.857484617
11751wH2_Roth16_01525	570.4046777	0.196853813	0.298342986	0.659823835	0.509366886	0.862911237
11751wH2_Roth16_00267	27.99729294	-0.295300711	0.455179122	-0.648757152	0.516495357	0.864442283
11751wH2_Roth16_03937	725.0504851	0.157819809	0.243364454	0.648491617	0.516667031	0.864442283

Genetic locus	baseMean	log2FoldChange	lfcSE	stat	pvalue	Padj
11751wH2_Roth16_04301	65.30753707	0.234789077	0.361930628	0.648712926	0.516523948	0.864442283
dsbD	1940.933564	-0.197759822	0.301967653	-0.654903993	0.512529569	0.864442283
acdA_1	124.869994	-0.190646729	0.294572944	-0.647197012	0.517504445	0.864442283
11751wH2_Roth16_01523	145.2628433	0.172109283	0.267860303	0.642533744	0.520526687	0.865629684
thpA_2	27.93984222	0.259285224	0.404860614	0.64043084	0.521892538	0.86605123
11751wH2_Roth16_01515	164.022996	0.159826839	0.255771302	0.624881828	0.53204862	0.869237238
lptB_4	530.506491	-0.128750469	0.20696009	-0.622102883	0.533874219	0.870542859
yscU_1	19.72939881	0.277558622	0.44985691	0.616993128	0.537239258	0.870718704
cmpD	43.69579695	-0.267328056	0.430826714	-0.620500185	0.534928532	0.870718704
11751wH2_Roth16_05136	5091.035033	-0.172566817	0.293930641	-0.587100467	0.557136234	0.880023728
11751wH2_Roth16_03942	230.9280807	-0.149422898	0.25658751	-0.582346735	0.560333152	0.88109871
11751wH2_Roth16_05133	1347.048098	-0.24303385	0.416711016	-0.583219162	0.559745773	0.88109871
11751wH2_Roth16_02125	1467.407153	-0.111723505	0.195343305	-0.57193414	0.567366594	0.88433137
rbsC_4	41.27379356	-0.222283098	0.390954275	-0.568565462	0.569651069	0.884931603
11751wH2_Roth16_03941	46.05079991	0.210320116	0.376642435	0.558407912	0.576565871	0.886199673
yojI	77.99929657	0.166800145	0.299893545	0.55619785	0.578075609	0.886199673
zraR_5	952.1501159	0.155491425	0.28297543	0.549487373	0.582671028	0.888620617
11751wH2_Roth16_05135	6321.888062	-0.167233337	0.308403966	-0.54225417	0.587643423	0.889689153
lgrD_4	461.3371674	0.108842464	0.202029622	0.538745075	0.590062767	0.890309056
11751wH2_Roth16_03830	220.9499779	-0.234129682	0.43746773	-0.535193035	0.592516382	0.891066499
feaR_3	193.7225482	0.113355884	0.214593833	0.528234585	0.597336528	0.892962285
acpP_1	111.5661744	-0.158228603	0.305540285	-0.517864947	0.6045525	0.898190673
lexA_2	639.7876624	0.181288566	0.354971852	0.510712511	0.609552379	0.899843589
11751wH2_Roth16_04297	344.7258184	0.132692331	0.264198433	0.502244959	0.615495221	0.903016769
11751wH2_Roth16_00434	17.52630703	0.225675445	0.447872049	0.503883745	0.614343074	0.903016769

Genetic locus	baseMean	log2FoldChange	lfcSE	stat	pvalue	Padj
11751wH2_Roth16_00429	66.57578551	-0.147748029	0.302964392	-0.487674569	0.625780367	0.90546397
trxC	201.5175822	0.153298942	0.314332232	0.487697176	0.625764353	0.90546397
lolA_2	136.5804946	-0.131385451	0.283292128	-0.463780804	0.642804797	0.911173993
ohrR_4	65.78603343	-0.158677145	0.34777425	-0.456264789	0.648199581	0.914660633
fhuA_8	315.226453	0.119465001	0.268353271	0.445178107	0.656191047	0.915817046
dsbG_1	1155.431049	-0.16293311	0.361942783	-0.450162616	0.65259319	0.915817046
11751wH2_Roth16_02122	385.1057715	-0.092508093	0.208928187	-0.442774591	0.657928783	0.915817046
11751wH2_Roth16_00268	24.03259265	-0.176509626	0.406394509	-0.434330736	0.664048287	0.917873948
ybdZ	77.59989041	-0.148099923	0.346001642	-0.428032428	0.668627511	0.921107349
fabG_4	678.8559496	0.083376915	0.207981003	0.400887165	0.6885032	0.930392412
xthA	777.5450027	-0.073849394	0.186901384	-0.395124919	0.692750699	0.931580473
tycC_3	26260.48665	-0.112441907	0.285434499	-0.393932434	0.693630924	0.932332424
livH_7	261.5424579	-0.097394297	0.247885172	-0.392900858	0.694392708	0.932572554
htpX_1	131.7203742	0.142574826	0.365657348	0.389913745	0.696600329	0.933730605
fabF_2	693.7278518	-0.082391382	0.213922126	-0.385146613	0.700128794	0.935437782
hemE	670.1516315	0.085676337	0.223087574	0.384048001	0.700942871	0.93566449
ggt_1	1092.567421	0.084155014	0.242598922	0.346889479	0.728674351	0.943179435
yhdG_3	147.1327769	0.087923926	0.261704951	0.33596585	0.736896619	0.944703463
11751wH2_Roth16_01545	223.1920386	-0.093834215	0.275324785	-0.340812814	0.733244503	0.944703463
amiD_1	36.16844339	0.115315687	0.343273426	0.335929548	0.736923995	0.944703463
pkn1	54.65777294	0.112678509	0.339487632	0.331907552	0.739959067	0.946207636
hrcQa	129.6277995	0.081872609	0.248155816	0.329924199	0.741457238	0.946249976
dsbG_2	42.41072462	0.13055722	0.397609471	0.328355407	0.742642955	0.946930907
csrA_1	69.96708444	-0.095794552	0.299675694	-0.319660733	0.749225529	0.949902177
lutR_5	395.6104901	0.062713206	0.196876527	0.318540798	0.750074753	0.950210767

Genetic locus	baseMean	log2FoldChange	lfcSE	stat	pvalue	Padj
ybiO_1	1562.446169	0.068074441	0.213750124	0.318476733	0.750123341	0.950210767
dmlR_16	112.9408157	0.082935565	0.262339223	0.316138638	0.751897281	0.95142035
budC	135.5877218	-0.090117915	0.294255141	-0.306257743	0.759408411	0.953034583
11751wH2_Roth16_01518	50.0134714	0.107697757	0.359475512	0.299596923	0.764484632	0.954784871
qseC_1	1477.088855	-0.087963443	0.31405814	-0.280086494	0.779411146	0.957449226
clsA	830.689778	0.054479305	0.200461529	0.271769377	0.785799353	0.958700499
11751wH2_Roth16_04421	667.2651072	0.086485653	0.323279585	0.267525873	0.789064296	0.959266104
11751wH2_Roth16_03834	304.4767055	0.127766235	0.486115239	0.262831167	0.792680712	0.959509708
11751wH2_Roth16_03936	443.5661419	-0.077657447	0.296537783	-0.261880445	0.793413616	0.959509708
11751wH2_Roth16_04296	771.641737	0.05745736	0.223913596	0.256605053	0.797483674	0.961861925
11751wH2_Roth16_00437	7.913712878	0.164972824	0.675374642	0.244268609	0.807022794	0.962723741
11751wH2_Roth16_04299	73.38513791	-0.05964288	0.279187703	-0.21363004	0.830835571	0.970533588
grsB	47284.56619	0.060382754	0.284565622	0.212192724	0.831956683	0.970542772
parD1_3	377.6538046	-0.04760763	0.228730301	-0.208138713	0.83512066	0.970852841
nodD2_4	315.7998215	0.046659134	0.23169473	0.201381938	0.840399938	0.972683015
11751wH2_Roth16_00273	25.29399639	0.07247008	0.413457679	0.175278108	0.860861113	0.973270616
nikA	33.08505886	-0.08556062	0.457383492	-0.187065388	0.851609366	0.973270616
ecfG_2	508.809696	0.065011588	0.339794069	0.191326437	0.84826985	0.973270616
nicT_3	40.63032575	-0.066785162	0.349328875	-0.191181338	0.848383524	0.973270616
yxeP_1	1597.336105	-0.040582842	0.207270567	-0.195796453	0.844769486	0.973270616
kstR2	397.3913907	-0.043740952	0.248313707	-0.176151984	0.860174542	0.973270616
accA1_2	178.2627022	0.043653276	0.236595376	0.18450604	0.853616489	0.973270616
11751wH2_Roth16_02141	525.2077571	0.066267984	0.379831605	0.174466745	0.861498663	0.973270616
cefD_2	109.202057	0.050040305	0.295331829	0.16943756	0.865452482	0.973759786
livF_5	632.30323	-0.04465962	0.264967142	-0.168547766	0.866152369	0.973896142

Genetic locus	baseMean	log2FoldChange	lfcSE	stat	pvalue	Padj
hpcE_2	21.95823311	-0.070490424	0.434568277	-0.162207938	0.871142109	0.975277022
degU_1	362.9328344	0.039504254	0.246371402	0.160344317	0.872609851	0.975573163
11751wH2_Roth16_05119	287.2096818	-0.033283638	0.221539016	-0.150238269	0.880576635	0.977266571
11751wH2_Roth16_04430	790.5176842	0.031977546	0.224680839	0.142324314	0.886823842	0.979105536
acpP_2	62.7243919	0.049758785	0.358777334	0.138689879	0.889695216	0.979592382
11751wH2_Roth16_03939	84.52620773	0.043020613	0.322638658	0.133339922	0.893924556	0.981829392
hpcG	17.67271586	-0.072674367	0.567008545	-0.128171555	0.89801321	0.983539816
11751wH2_Roth16_05352	138.8728356	-0.034474283	0.277064716	-0.124426825	0.900977335	0.984919323
gabT	312.7828525	0.043618801	0.351824142	0.123978987	0.901331913	0.984936171
11751wH2_Roth16_00426	50.56746815	-0.034902069	0.304437841	-0.11464432	0.908727049	0.986125459
mnmC_2	383.4315023	-0.024764084	0.220917082	-0.112096737	0.910746704	0.986684734
11751wH2_Roth16_03943	468.6183326	-0.023285202	0.223845958	-0.104023329	0.917150835	0.987119329
11751wH2_Roth16_00431	75.65225105	-0.03258602	0.314358167	-0.103658895	0.917440048	0.987119329
11751wH2_Roth16_05132	7679.682971	-0.029232218	0.279311988	-0.104657944	0.916647235	0.987119329
hpcE_1	36.59590524	-0.035544983	0.358460477	-0.099160117	0.921011141	0.987119329
soj_1	3070.12861	-0.028890795	0.303182898	-0.095291637	0.924083185	0.987139073
gcvA_7	326.9143302	0.02060501	0.223806156	0.092066325	0.926645344	0.987277214
11751wH2_Roth16_03832	327.1624709	0.044374514	0.475853266	0.093252515	0.925702955	0.987277214
11751wH2_Roth16_05134	9293.311675	0.02585506	0.285713256	0.090493037	0.927895427	0.987277214
pilQ	287.2639055	0.020287044	0.238831573	0.084942891	0.932306793	0.988265421
gerN	260.7789895	0.037268912	0.457694606	0.081427465	0.935102008	0.989266386
fabF_4	254.292876	-0.031318847	0.431447153	-0.072590227	0.942132204	0.98988052
fliP_1	122.8071979	0.016374079	0.24090929	0.067967819	0.945811252	0.989944592
pchR_2	784.5532268	0.008519228	0.189380876	0.044984624	0.964119565	0.991887225
ubiG_2	212.4812035	0.013615764	0.317291592	0.042912464	0.965771313	0.99234785

Genetic locus	baseMean	log2FoldChange	lfcSE	stat	pvalue	Padj
hpcH	33.22798249	-0.016802184	0.392652014	-0.04279154	0.965867708	0.99234785
sauT	874.5436925	0.010838421	0.469240422	0.023097799	0.981572261	0.99753109
ssuC_4	89.30282881	-0.00429381	0.27696027	-0.015503344	0.987630617	0.99753109
ddlA	1154.226181	-0.005035793	0.281312245	-0.01790108	0.985717767	0.99753109
11751wH2_Roth16_00423	475.8040344	-0.002231193	0.192384805	-0.011597555	0.990746697	0.99753109
hpcB	106.3812623	0.0055661	0.2714001	0.020508837	0.983637463	0.99753109
11751wH2_Roth16_01530	182.188449	-0.005344019	0.256397945	-0.020842674	0.983371156	0.99753109
benM_2	104.0685984	0.002720697	0.259960642	0.010465802	0.991649651	0.99753109
resA_2	485.512638	0.007229599	0.283155287	0.025532276	0.979630404	0.99753109
11751wH2_Roth16_05539	1179.371971	0.001504057	0.204993785	0.007337085	0.994145906	0.998108179

Supplementary Table 16. A table indicating the log2fold change and Benjamini-Hochberg adjusted p-values from differential expression analysis for genes within Roth 105 predicted secondary metabolite BGCs.
Benjamini-Hochberg adjusted p-values were used to determine significantly differentially expressed genes between *Z. tritici* confrontation treatment and control (Padj < 0.05).

Genetic locus	baseMean	log2FoldChange	lfcSE	stat	pvalue	Padj
12105_Rothamsted105_02768	4673.823556	1.455050356	0.174806229	8.32379008	8.51944E-17	1.03885E-14
lgrE	321.1781135	0.979878227	0.156708682	6.252864946	4.02991E-10	1.45931E-08
grsB	2103.235609	-0.942655115	0.165639632	-5.690999818	1.26298E-08	3.09274E-07
fecI_8	241.8477265	1.272174846	0.226251532	5.62283417	1.8785E-08	4.36732E-07
ycgJ_2	633.8482246	-0.907854838	0.164678033	-5.512907966	3.52953E-08	7.53176E-07
polC_3	2322.151897	-0.656250045	0.121936695	-5.381891356	7.37072E-08	1.51862E-06
ephD	595.0619098	-0.960460867	0.196893203	-4.878080368	1.07123E-06	1.61632E-05

Genetic locus	baseMean	log2FoldChange	lfcSE	stat	pvalue	Padj
12105_Rothamsted105_05594	2617.895669	1.33246971	0.274910632	4.84691952	1.25393E-06	1.88247E-05
mcpA	2102.646657	0.612828144	0.134417472	4.559140524	5.13634E-06	6.57165E-05
gntR_3	2458.878388	-0.993372782	0.219221428	-4.531367176	5.86032E-06	7.41852E-05
bbsG_2	1046.046678	-0.800712706	0.178745486	-4.479624759	7.47744E-06	9.09933E-05
ltaS1	2516.837539	0.682647797	0.16728348	4.080784289	4.4884E-05	0.000431161
mhqP	1254.553435	-0.632862247	0.159149397	-3.976529335	6.99284E-05	0.000623615
pccB	449.6617855	-0.795152507	0.202656895	-3.923639049	8.72214E-05	0.000761912
pcpR_2	1001.782803	-0.553852649	0.141487103	-3.914509793	9.05881E-05	0.000789014
tmk_2	1645.287546	-0.658432724	0.170933587	-3.851979797	0.000117167	0.000990199
csrD	1037.69149	-0.570232406	0.153616444	-3.712053167	0.000205585	0.001605711
xcpV	99.33572936	0.811323178	0.221464381	3.663447707	0.000248843	0.001908648
cheV_1	1003.486748	0.497866387	0.139895374	3.558848105	0.000372485	0.002684677
12105_Rothamsted105_02371	596.1357582	-0.714917181	0.208147118	-3.434672501	0.00059327	0.003956239
12105_Rothamsted105_02372	379.9029625	-0.610463932	0.180606652	-3.380074455	0.000724662	0.00468599
12105_Rothamsted105_04706	457.7494175	-0.567980002	0.176618298	-3.215861605	0.001300535	0.007544368
fabG_10	456.569948	0.478115209	0.162791732	2.936974762	0.003314311	0.016245289
12105_Rothamsted105_02758	297.4151316	-0.548674895	0.187373039	-2.928248894	0.003408771	0.016640036
degS_2	595.2020191	0.411196975	0.140679756	2.922929267	0.003467553	0.016879892
cdhR_6	644.7779766	0.520434424	0.178519799	2.915275653	0.003553745	0.017207153
acdA	328.4149752	-0.576733678	0.205224113	-2.810262741	0.004950107	0.022491932
qseC_1	1914.328288	0.405234509	0.145649135	2.782265128	0.005398092	0.02412386
12105_Rothamsted105_02764	1602.323886	-0.463686755	0.171278649	-2.70720698	0.006785194	0.028978938
12105_Rothamsted105_05580	219.2431907	0.494334098	0.18330896	2.696726325	0.007002479	0.029747022
fpvA_3	371.0247318	0.42106778	0.160491031	2.623621874	0.008700031	0.035434688
12105_Rothamsted105_02762	54.24714768	-0.669012062	0.260978382	-2.563476932	0.010362959	0.040816531

Genetic locus	baseMean	log2FoldChange	lfcSE	stat	pvalue	Padj
degU_1	484.9991104	0.362228117	0.14209728	2.549155886	0.010798402	0.042253079
yojI	117.6311956	0.533168638	0.211654214	2.519055156	0.011767022	0.045098113
12105_Rothamsted105_02755	104.5346497	0.551534121	0.221047364	2.495094762	0.01259235	0.047559601
12105_Rothamsted105_03437	554.2625122	0.381944035	0.15372745	2.484553244	0.012971411	0.048516297
12105_Rothamsted105_04700	588.6226731	-0.430276682	0.175836421	-2.44702821	0.014403956	0.052597105
12105_Rothamsted105_05814	173.74917	-0.536843301	0.219439494	-2.446429727	0.014427892	0.052597105
12105_Rothamsted105_03427	779.1096092	-0.357849962	0.148565659	-2.408699045	0.016009494	0.056870823
trxC	266.3020102	-0.400169089	0.167646268	-2.386984764	0.016987195	0.059742382
12105_Rothamsted105_05579	2278.647944	-0.35960174	0.153179133	-2.347589608	0.018895328	0.064851802
accA1_1	411.6709483	-0.367030071	0.156579955	-2.344042516	0.019075997	0.065280115
soj_1	3123.525701	-0.375178969	0.160987681	-2.330482468	0.019780666	0.066895827
12105_Rothamsted105_03441	740.0189696	0.392401725	0.169606909	2.313595163	0.020689939	0.069372832
12105_Rothamsted105_03463	283.3492519	0.431962484	0.188166678	2.295637508	0.021696616	0.071821209
12105_Rothamsted105_02756	978.8765848	0.595838831	0.26109323	2.282092231	0.022483896	0.073854467
12105_Rothamsted105_02379	1878.893049	0.289110089	0.127520601	2.267163791	0.023380222	0.076212125
12105_Rothamsted105_03434	244.1570614	0.426011169	0.191497609	2.224629174	0.026106142	0.083235967
lgrD_2	480.7089758	0.326722538	0.14758784	2.213749713	0.026846001	0.085005223
fadD3	753.7285749	0.483878631	0.223665199	2.163405994	0.030509967	0.093919141
yceJ_3	311.8771065	-0.388412011	0.187315041	-2.073576199	0.038118688	0.110723947
12105_Rothamsted105_02759	131.1713618	-0.399137575	0.192872507	-2.069437378	0.038505062	0.111364931
12105_Rothamsted105_03430	349.9547092	0.349484901	0.170390249	2.051085095	0.040258661	0.115369543
12105_Rothamsted105_02347	101.4322405	0.415205415	0.203645459	2.038864095	0.041463593	0.11810103
dat_1	98.67390532	0.442691284	0.217173928	2.038418184	0.041508129	0.118156776
lgrB_2	1106.786737	0.270501563	0.134869422	2.005655241	0.044893044	0.125051718
leuC_2	120.054894	-0.452942172	0.225963017	-2.004496926	0.045016856	0.125163199

Genetic locus	baseMean	log2FoldChange	lfcSE	stat	pvalue	Padj
greB	1207.288962	0.279291236	0.144293815	1.935573162	0.05292	0.140719626
12105_Rothamsted105_04708	174.5605722	-0.365053841	0.189659522	-1.924785195	0.054256237	0.143506426
12105_Rothamsted105_02783	67.14093727	-0.466914543	0.243877634	-1.914544339	0.055550639	0.146153708
12105_Rothamsted105_02360	250.1580022	0.379995955	0.204632774	1.856965274	0.063316095	0.161603446
12105_Rothamsted105_02771	74.66403092	0.509486789	0.274577766	1.855528206	0.063520835	0.161987618
12105_Rothamsted105_03445	354.9741181	0.38224639	0.208664853	1.831867635	0.066971144	0.168912023
lgrB_1	510.3227048	0.282474507	0.155004633	1.822361705	0.068400121	0.171661404
xcpT_1	30.76428999	-0.799193014	0.440809464	-1.813012376	0.069829913	0.174428816
12105_Rothamsted105_05817	125.7108198	0.367361823	0.205173498	1.79049354	0.073374605	0.179853794
12105_Rothamsted105_03462	61.3982379	0.476891071	0.271137845	1.758851007	0.078602819	0.189496595
12105_Rothamsted105_05581	305.6640628	0.317564778	0.180706875	1.757347512	0.078858594	0.189991975
12105_Rothamsted105_04715	255.6093798	0.331089005	0.190371035	1.739177414	0.082003561	0.195831845
12105_Rothamsted105_02354	115.3278729	0.344256973	0.209224411	1.64539583	0.099888209	0.226072746
12105_Rothamsted105_02381	594.7821382	-0.34104134	0.207619617	-1.642625803	0.100460379	0.226743297
bcsB	1244.918743	0.32128369	0.196438984	1.635539363	0.10193603	0.2287149
kstR2_1	320.6149897	-0.267328088	0.168603519	-1.585542758	0.11284307	0.245177216
caiD	298.5287685	-0.270441539	0.176593601	-1.531434539	0.125662033	0.26398273
xcpQ	161.6664074	0.389730076	0.254845296	1.529281028	0.126194791	0.264632292
soj_3	1242.967773	0.322606973	0.215224393	1.498933131	0.13389098	0.276051969
tycC_2	1004.052456	0.235244071	0.157101604	1.497400824	0.134288994	0.27630053
12105_Rothamsted105_01291	374.7430403	-0.262242702	0.179069976	-1.464470525	0.143065431	0.289375744
cefD_2	38.14892959	-0.452701773	0.309177271	-1.464214272	0.143135412	0.28940488
12105_Rothamsted105_03439	124.5623789	-0.30741811	0.210755484	-1.458648209	0.144661957	0.291519459
12105_Rothamsted105_06000	98.04315892	0.376259941	0.258331729	1.45649914	0.145254687	0.292516601
kmo	592.661029	-0.247449811	0.173881235	-1.423096692	0.154708127	0.307205404

Genetic locus	baseMean	log2FoldChange	lfcSE	stat	pvalue	Padj
acpP_2	280.5001972	-0.280128406	0.200036948	-1.400383321	0.161398562	0.316286129
bcsZ	334.1041687	0.306954296	0.220469322	1.392276678	0.163838631	0.319287612
12105_Rothamsted105_03436	414.9079962	0.216591129	0.156399078	1.384861931	0.166094689	0.322736836
12105_Rothamsted105_01295	127.0713559	0.3449531	0.251531329	1.371412069	0.170246537	0.327495971
qseB_2	1792.368145	0.186787368	0.136857888	1.364827195	0.172307369	0.330085454
liuE	434.4648132	0.240943315	0.176698967	1.36358078	0.172699545	0.330624729
draG_2	349.4491015	-0.207586092	0.152594042	-1.360381377	0.173709269	0.331845051
12105_Rothamsted105_02761	104.0126377	-0.285653251	0.210387019	-1.357751315	0.174542608	0.332579842
12105_Rothamsted105_02754	82.58848589	0.292959912	0.22458155	1.304470079	0.192073355	0.35456178
12105_Rothamsted105_05584	1463.251047	0.424544393	0.328916025	1.290737943	0.196794563	0.360689421
oprM_3	54.75566873	0.398984159	0.312885597	1.275175854	0.202247006	0.367191084
12105_Rothamsted105_05596	1133.81972	0.166355827	0.132828355	1.25241201	0.210419772	0.376875941
catD_1	926.7186674	-0.246825533	0.200730399	-1.229637038	0.218833054	0.387856305
12105_Rothamsted105_04711	72.13245558	-0.298547182	0.245753782	-1.214822328	0.224433863	0.394757825
wecD_2	311.6738239	-0.196711802	0.165193147	-1.190798802	0.233732579	0.406683798
cueR	305.3140857	0.231941684	0.200446456	1.157125392	0.247221134	0.421319531
znuB_2	59.69591762	-0.313979361	0.272811695	-1.150901396	0.249772803	0.424188243
epsF_1	103.4378543	-0.247498909	0.221947804	-1.115122133	0.264798088	0.441207077
resA_1	486.2692474	-0.203910533	0.188472304	-1.081912453	0.279291431	0.458569185
12105_Rothamsted105_02368	913.1842454	0.164400452	0.156247092	1.052182477	0.292715838	0.473977542
vanX	796.297233	-0.164400614	0.15770613	-1.042449108	0.297203509	0.478005643
gbpA	194.85649	0.235213451	0.24356784	0.965699952	0.334194344	0.515867589
yegS	451.8746005	-0.235652988	0.248488965	-0.948343879	0.34295442	0.525423759
xcpW	11.32387935	-0.530042322	0.560441445	-0.945758609	0.344271721	0.527036519
ynfM	303.5766864	0.31906432	0.338467676	0.942672943	0.345848217	0.528202091

Genetic locus	baseMean	log2FoldChange	lfcSE	stat	pvalue	Padj
mnmC_2	1257.199825	0.140873246	0.150965081	0.933151196	0.350741909	0.53298141
12105_Rothamsted105_03442	296.848854	0.165477291	0.177708748	0.93117133	0.351764946	0.534128476
lolA_1	155.3486521	0.191152067	0.205563662	0.929892305	0.352426847	0.534590102
12105_Rothamsted105_04713	257.6423794	0.18437369	0.208449086	0.884502272	0.376425137	0.555069149
12105_Rothamsted105_02776	122.3760617	0.180824409	0.205889673	0.878258759	0.379803311	0.557641078
12105_Rothamsted105_02767	300.9562117	0.182220157	0.208727132	0.873006565	0.3826595	0.560433396
bcsA	686.006202	0.198901716	0.228468713	0.870586234	0.383980115	0.561202309
psaA	51.07990317	0.245571857	0.282863958	0.868162413	0.385305428	0.562538076
rstB_4	216.5836897	0.15026322	0.175178798	0.857770586	0.391019155	0.568729175
pepA_1	2361.122495	-0.209126951	0.263722583	-0.792980821	0.427788997	0.60298166
qhnDH	31.64951314	0.254062023	0.321749525	0.789626723	0.429745797	0.604204508
macB_1	105.5702499	0.154274998	0.212032879	0.727599411	0.466858841	0.638325303
12105_Rothamsted105_03453	92.5987184	0.168350743	0.232673089	0.723550557	0.469341705	0.640547439
csrA_1	266.97404	0.118601805	0.164688789	0.720157124	0.471428259	0.642075188
12105_Rothamsted105_05999	764.0589404	-0.128755705	0.180537728	-0.713178935	0.47573504	0.645052611
12105_Rothamsted105_02778	2327.300016	0.106126697	0.150106651	0.707008626	0.479561117	0.648422194
12105_Rothamsted105_05583	446.4116355	-0.236381003	0.347313525	-0.680598323	0.496125688	0.663165769
12105_Rothamsted105_02757	443.4753727	0.105706436	0.157117766	0.672784745	0.501084244	0.666661848
nlhH_2	83.43269262	-0.149691317	0.227633553	-0.65759777	0.510796628	0.676420623
iucB	163.5026139	0.120494897	0.188804256	0.63820011	0.523343426	0.685590215
mltF_4	1487.055356	0.116890909	0.183549951	0.636834324	0.524232766	0.68660473
epsE_2	66.68234078	0.175751753	0.279280823	0.629301186	0.529151895	0.6913804
12105_Rothamsted105_02357	89.30736866	0.150905439	0.240105645	0.628496004	0.529679064	0.691896559
ybdZ	104.1110606	0.147732461	0.2491267	0.593001317	0.553180271	0.712645994
acpP_3	219.2110855	-0.099584977	0.17256234	-0.577095656	0.563874839	0.720427483

Genetic locus	baseMean	log2FoldChange	lfcSE	stat	pvalue	Padj
12105_Rothamsted105_04699	536.006301	-0.087596809	0.160459607	-0.545911898	0.585126499	0.734790003
12105_Rothamsted105_02348	27.89184364	-0.204554386	0.375664354	-0.544513697	0.586088026	0.735657803
dsbG	1607.482298	0.081413337	0.152190574	0.53494336	0.592689024	0.741481766
12105_Rothamsted105_01293	122.7680043	-0.106531659	0.20217793	-0.526920316	0.598248925	0.745782877
12105_Rothamsted105_02784	68.55872503	0.132657933	0.25459468	0.521055402	0.602328177	0.749148805
12105_Rothamsted105_03457	38.38637817	-0.191635643	0.381483298	-0.50234347	0.615425936	0.757593293
cdsA_2	248.4200949	-0.096507189	0.192321704	-0.501800822	0.615807635	0.757868304
acsC	2632.708862	0.089329948	0.187196269	0.477199404	0.633220135	0.772072267
tycC_1	194.7656907	-0.082870197	0.175589799	-0.471953365	0.636960076	0.774705705
cmdF	699.0039853	-0.063727688	0.149938629	-0.425025145	0.670818345	0.803073454
12105_Rothamsted105_05816	50.20830344	0.120073052	0.285389415	0.420734075	0.673949276	0.805208343
12105_Rothamsted105_02350	39.53878499	-0.132093439	0.315361537	-0.418863505	0.67531589	0.806281434
inhA	58.46273401	-0.119935236	0.28652793	-0.418581309	0.675522152	0.806281434
gltD_2	1252.577685	-0.058481244	0.151871222	-0.385071266	0.700184616	0.822354837
12105_Rothamsted105_05813	292.4243488	-0.063230063	0.167212036	-0.378143011	0.705324358	0.825850096
fabF_2	347.0549802	0.057433011	0.154717687	0.371211669	0.710479883	0.827669584
dsbD_1	2235.352429	0.058099729	0.16052726	0.36193061	0.717403885	0.832652618
12105_Rothamsted105_03454	57.73148229	-0.088882114	0.246461448	-0.360632931	0.718373869	0.833453178
12105_Rothamsted105_03452	83.86966021	0.114543069	0.319443636	0.358570515	0.719916407	0.83508067
asnB_1	1322.936913	-0.106420264	0.301605285	-0.352846151	0.724203783	0.837939118
pkn1	31.31100307	-0.11674859	0.340812432	-0.342559657	0.731929757	0.842149104
lgrD_1	987.4241617	0.048303724	0.145081684	0.332941572	0.739178388	0.847293198
tatD	635.4403602	0.051442383	0.162460729	0.316645034	0.751512961	0.854479532
12105_Rothamsted105_05818	120.1218167	0.062796855	0.199510558	0.314754547	0.752948025	0.855460059
znuC_2	81.55000126	-0.07059668	0.229466569	-0.307655622	0.758344391	0.857975818

Genetic locus	baseMean	log2FoldChange	lfcSE	stat	pvalue	Padj
12105_Rothamsted105_05998	388.0262702	-0.062431919	0.206581588	-0.302214346	0.762488669	0.860084915
fabF_3	1177.587276	0.03090527	0.129524322	0.23860592	0.811411174	0.894993865
hemE	1178.152389	-0.025246719	0.126195766	-0.200059955	0.841433692	0.912532878
benM_4	170.6717991	-0.035382446	0.20724488	-0.170727721	0.864437865	0.926535154
12105_Rothamsted105_03447	72.53241257	0.038387045	0.233276	0.164556343	0.869293196	0.930162401
12105_Rothamsted105_02378	668.3522125	-0.027647925	0.171594498	-0.161123612	0.871996043	0.932117989
12105_Rothamsted105_03444	382.0352989	-0.024102727	0.15102337	-0.159596006	0.873199325	0.932617153
12105_Rothamsted105_02369	431.0427504	0.021335118	0.158096068	0.134950337	0.89265114	0.943601392
12105_Rothamsted105_02349	17.55023371	-0.057722336	0.446551174	-0.129262532	0.897149917	0.945159696
cphA	2362.559674	-0.031635419	0.280284447	-0.112868976	0.910134432	0.953304719
accA1_3	1109.948983	-0.033424989	0.313060855	-0.106768343	0.914972762	0.956264169
12105_Rothamsted105_04710	66.32391635	0.024855727	0.272898807	0.09108038	0.927428722	0.961045198
12105_Rothamsted105_03431	386.0346483	-0.007955082	0.174465546	-0.045596864	0.963631569	0.980727147
12105_Rothamsted105_02775	111.390441	0.008544751	0.227237735	0.037602692	0.970004462	0.983841403
mmgC_7	590.3345398	0.008072418	0.331161112	0.024376105	0.980552608	0.988994232
12105_Rothamsted105_02777	464.2735868	0.003367378	0.184548721	0.018246553	0.985442165	0.992250916

Supplementary Table 17. A table indicating the log2fold change and Benjamini-Hochberg adjusted p-values from differential expression analysis for core biosynthetic genes within Roth 16 predicted secondary metabolite BGCs. Benjamini-Hochberg adjusted p-values were used to determine significantly differentially expressed genes between *Z. tritici* confrontation treatment and control (Padj < 0.05).

BGC ID	BGC Type	Gene annotation	Gene description	log2foldchange	Padj
1.1	bacteriocin	11751wH2_Roth16_00269	hypothetical protein	0.2823133	0.7050516
1.2	betalactone	liuE_1	3-hydroxy-3-isohexenylglutaryl-CoA/hydroxy- methylglutaryl-CoA lyase	-0.617777171	0.208105409
1.2	betalactone	fadD3	3-[(3aS%2C4S%2C7aS)-7a-methyl-1%2C 5-dioxo-octahydro-1H-inden-4-yl]propanoyl:CoA ligase	-1.001323553	0.076136963
2.1	terpene	11751wH2_Roth16_00426	Germacrene A synthase	-0.03490207	0.9861255
5.1	arylpolyene	fabF_1	3-oxoacyl-[acyl-carrier-protein] synthase 2	-0.1722256	0.8418311
5.1	arylpolyene	fabF_2	3-oxoacyl-[acyl-carrier-protein] synthase 2	-0.08239138	0.9354378
8.1	NAGGN	asnB_1	Asparagine synthetase [glutamine-hydrolyzing] 1	-1.093212723	0.00411452996210568**
8.1	NAGGN	cphA	Cyanophycin synthetase	-1.263827562	0.00585228949513575**
8.1	NAGGN	pepA_1	Glutamyl aminopeptidase	-1.337927044	0.0252362329383732*

BGC ID	BGC Type	Gene annotation	Gene description	log2foldchange	Padj
8.2	NRPS	lgrB_2	Linear gramicidin synthase subunit B	0.2297552	0.6734092
21.1	arylpolyene	fabF_4	3-oxoacyl-[acyl-carrier-protein] synthase 2	-0.03131885	0.9898805
22.1	NRPS	dhbE	2%2C3-dihydroxybenzoate-AMP ligase	3.889923263	6.06715713753439E-61**
22.1	NRPS	mbtB_1	Phenyloxazoline synthase MbtB	4.046138692	4.44023877042504E-47**
22.1	NRPS	mbtB_2	Phenyloxazoline synthase MbtB	4.718511937	6.98015466309438E-48**
26.1	bacteriocin	11751wH2_Roth16_04301	hypothetical protein	0.2347891	0.8644423
27.1	NRPS-like	lgrD_2	Linear gramicidin synthase subunit D	0.2380947	0.732736
37.1	NRPS	lgrD_3	Linear gramicidin synthase subunit D	0.469762569	0.178909541
37.1	NRPS	lgrD_4	Linear gramicidin synthase subunit D	0.1088425	0.8903091
37.1	NRPS	tycC_2	Tyrocidine synthase 3	0.2668825	0.6548842
37.1	NRPS	grsB	Gramicidin S synthase 2	0.06038275	0.9705428
41.1	NRPS	tycC_3	Tyrocidine synthase 3	-0.1124419	0.9323324
45.1	bacteriocin	11751wH2_Roth16_05543	hypothetical protein	0.739003066	0.0236348733699807*

Supplementary Table 18. A table indicating the log2fold change and Benjamini-Hochberg adjusted p-values from differential expression analysis for core biosynthetic genes within Roth 105 predicted secondary metabolite BGCs. Benjamini-Hochberg adjusted p-values were used to determine significantly differentially expressed genes between *Z. tritici* confrontation treatment and control (Padj < 0.05).

BGC ID	BGC Type	Gene annotation	Gene description	log2foldchange	Padj
6.1	NAGGN	asnB_1	Asparagine synthetase [glutamine-hydrolyzing] 1	-0.1064203	0.8379391
6.1	NAGGN	cphA	Cyanophycin synthetase	-0.03163542	0.9533047
6.1	NAGGN	pepA_1	Glutamyl aminopeptidase	-0.209127	0.6029817
13.1	NRPS	lgrD_1	Linear gramicidin synthase subunit D	0.04830372	0.8472932
17.1	NRPS	lgrB_1	Linear gramicidin synthase subunit B	0.2824745	0.1716614
17.1	NRPS	tycC_1	Tyrocidine synthase 3	-0.0828702	0.7747057
17.1	NRPS	lgrB_2	Linear gramicidin synthase subunit B	0.2705016	0.1250517
25.1	arylpolyene	fabF_2	3-oxoacyl-[acyl-carrier-protein] synthase 2	0.05743301	0.8276696
25.1	arylpolyene	fabF_3	3-oxoacyl-[acyl-carrier-protein] synthase 2	0.03090527	0.8949939
47.1	NRPS-like	lgrD_2	Linear gramicidin synthase subunit D	0.326722538	0.085005223
71.1	betalactone	fadD3	3-[(3aS%2C4S%2C7aS)-7a-methyl-1%2C 5-dioxo-octahydro-1H-inden-4-yl]propanoyl:CoA ligase	0.483878631	0.093919141
71.1	betalactone	liuE	3-hydroxy-3-isohexenylglutaryl-CoA/hydroxy- methylglutaryl-CoA lyase	0.2409433	0.3306247
84.1	bacteriocin	12105_Rothamsted105_05817	hypothetical protein	0.3673618	0.1798538
99.1	NRPS-like	grsB	Gramicidin S synthase 2	-0.94265512	3.0927394042551 4E-07**